

**Who watches the watchmen: Molecular coordinators of homeostasis in regulatory cell-types**

Kristen Kelley Penberthy

Pelham, NY

B.A., New York University, 2009

A dissertation presented to the Graduate Faculty of the University of Virginia in  
Candidacy for the Degree of Doctor of Philosophy

Department of Microbiology, Immunology, and Cancer Biology

University of Virginia  
May 2017

---

---

---

---

---

---

---

## Abstract

The human body is exposed to a wide variety of stressors, both intrinsic and extrinsic, that can disrupt homeostasis. Unique subsets of cells have evolved to manage and mitigate these stresses. Here, I detail my findings regarding the molecular pathways that modulate the functions of two 'regulatory' cell-types: specialized phagocytes and peripheral T regulatory cells.

The first half of this dissertation looks at specialized phagocytes, which respond to the intrinsic stresses of cell death by clearing apoptotic corpses from tissues in a phosphatidylserine (PtdSer) dependent manner. Here, I demonstrate that PtdSer receptors have distinct functions, dependent on the tissue context. Specifically, I show that overexpression of one PtdSer receptor BAI1, in mice lacking a different PtdSer receptor, MerTK, rescues phagocytic defects in Sertoli cells but not in the retinal pigmented epithelium (RPE). I further demonstrate that MerTK is uniquely critical for RPE function as it regulates phagocytosis-independent processes including the visual cycle and transcription of genes related to metabolism and retinal disease.

In the second half of this dissertation, I present my findings on peripheral T regulatory cells, which suppress inflammatory responses to innocuous foreign antigens. Our data reveal that the phosphatase PP2A dephosphorylates the critical Treg transcription factor FoxO1. However, pharmacological inhibition of PP2A does not impair Treg function *ex vivo*, indicating that these *ex vivo* assays do not recapitulate *in vivo* assays of Treg function.

## Acknowledgements

First, I would like to thank my mentor Ravi for his guidance and boundless enthusiasm. Graduate school and the scientific process are both filled with hurdles and Ravi always had words of encouragement to keep me going. Ravi gave me a tremendous amount of freedom and allowed me to pursue the questions that truly interested me, even if it was a direction or method that was new to the lab. Ravi built a lab filled with brilliant and generous people with a love for science. Ravi's lab is one of collaboration and support and I am eternally grateful to Ravi for fostering that environment.

I would like to thank all the members of my committee: Drs, Loren Erickson, Tim Bender, Ulrike Lorenz, Ken Tung and Larry Borish. My committee has provided fantastic guidance on the many projects that I have pursued while in graduate school. My committee members always treated me as a colleague and their confidence in me contributed immensely to my growth as a scientist. I would also like to thank the MSTP director, Dean Kedes for all of his advice, insight and support. I would also like to thank Drs. Joel Ernst and Tyler Bold who mentored me at New York University and encouraged me to go down this path.

Next, there are a great many people that I need to thank from the Ravi lab. First, a huge thank you to Scott and Lisa for keeping the lab running; without their hard work and dedication the lab would likely have been destroyed by the students some years ago. I would like to thank Natxo Juncadella for taking me under his wing when I first joined and helping me find my footing and Ivan Poon

for being a consistent source of optimism and advice. I want to thank Sho Morioka for his advice, friendship and most importantly for always having a secret stash of reagents when things run out. I credit my recent sanity to Alexandra Bettina and our cathartic walks to Starbucks and I owe a tremendous debt to Laura for all the time she spent answering my many questions and doing microscopy with me. I remain incredibly grateful to Chris Medina for helping to maintain the sanity in bay 2 when the puns from bay 1 were getting too close. Lastly, I would like to thank Mike Raymond for being a patient rotation student while I learned to be a mentor.

There are four people from the Ravi lab that I need to thank in particular: Sanja Arandjelovic, Aaron Fond, Monica Buckley and Claudia Han. Thanks to them, the lab was always a place that I wanted to be; I never would have survived graduate school without them. They are some of my greatest friends and the best mentors I could have asked for. I credit the four of them with my forward momentum, especially when my project seemed determined to stand still. I was even lucky enough to be welcomed in to Claudia's family, as god-mother to her adorable son, Benson.

Most importantly, I would like to thank my family for their love and support. My parents Maria and Ned Penberthy have encouraged me every step of the way and they have never asked the question that every grad student dreads: "So, when are you going to graduate?" They fostered a love for science at a young age and I wouldn't be on this road if it weren't for them. My sister Liz

Penberthy is amazing and is always there when I need her, whether I need advice, a confidence boost, or a companion on a long-distance drive. She can always make me laugh after a hard day. My aunt, Robbie Munn and her daughter, Genevieve Hollingsworth have been a tremendous help to me here in Charlottesville. Robbie opened her home to me, my friends, and the rest of my family; Thanksgivings at her home are some of my fondest Charlottesville memories. She and Genevieve have both been a wonderful source of love and support.

## Table of Contents

<b>Abstract</b> .....	<b>ii</b>
<b>Acknowledgements</b> .....	<b>iii</b>
<b>List of Figures</b> .....	<b>xii</b>
<b>List of Tables</b> .....	<b>xv</b>
<b>List of Abbreviations</b> .....	<b>xvi</b>
<b>Chapter I Introduction</b> .....	<b>1</b>
<b>1.1 Overview of apoptotic cell clearance</b> .....	<b>1</b>
1.1.1 Consequences of apoptotic cell death .....	1
1.1.2 Apoptotic cells coordinate their own removal.....	2
1.1.3 Phosphatidylserine receptors.....	4
1.1.4 Signaling via the bipartite Rho-GEF ELMO and Dock180 .....	8
1.1.5 BAI1 signaling .....	12
1.1.6 MerTK signaling .....	12
<b>1.2 Specialized phagocytes support sensitive tissues</b> .....	<b>14</b>
1.2.1 Non-phagocytic functions of Sertoli cells: .....	18
1.2.2 Phagocytic function of Sertoli cells .....	20
1.2.3 Non-phagocytic functions of the retinal pigmented epithelium.....	21
1.2.4 Retinal pigmented epithelium as phagocytes .....	29
1.2.5 Deficits in RPE phagocytosis cause photoreceptor degeneration .....	30
<b>1.3 The role of T regulatory cells in allergic airway inflammation</b> .....	<b>33</b>
1.3.1 The transcription factor FoxO1.....	34
1.3.2 The phosphatase PP2A .....	36

1.3.3 Allergic airway inflammation.....	40
<b>1.4 Focus of this work and key hypotheses:.....</b>	<b>45</b>
1.4.1 Publications arising from this work:.....	45
 <b>Chapter II: Differential requirement for phosphatidylserine receptors</b>	
<b>MerTK and BAI1 in specialized phagocytes .....</b>	<b>47</b>
2.1 Summary.....	47
2.2 Introduction .....	49
2.3 Experimental Procedures.....	50
2.3.1 Mice.....	52
2.3.2 RPE isolation for culture and gene expression analyses .....	53
2.3.3 Immunoblotting.....	53
2.3.4 qRT-PCR.....	54
2.3.5 Eyecup dissection and ONL analysis.....	54
2.3.6 In situ rhodopsin analysis.....	55
2.3.7 Flat mount preparation and staining .....	55
2.3.8 Eyecup staining for HA.....	56
2.3.9 Ex vivo RPE phagocytosis assays .....	57
2.3.10 Testicular torsion.....	57
2.3.11 Sertoli cell isolation and staining.....	58
2.3.12 Retinoid analysis .....	59
2.3.13 RNAseq.....	60
2.3.14 Statistics.....	60
<b>2.4 Results .....</b>	<b>61</b>

2.4.1 BAI1-transgene can reduce corpse accumulation in the testes of <i>Mertk</i> <sup>-/-</sup> mice.....	61
2.4.2 RPE from <i>Mertk</i> <sup>-/-</sup> <i>Bai1</i> <sup>Tg</sup> mice express the <i>Bai1</i> <sup>Tg</sup> and BAI1 signaling pathway.....	68
2.4.3 <i>Mertk</i> -linked retinal degeneration is not rescued by BAI1.....	76
2.4.4 BAI1-transgene does not promote phagocytosis in the RPE.....	82
2.4.5 <i>Mertk</i> <sup>-/-</sup> mice exhibit diminished retinyl ester accumulation prior to the onset of degeneration.....	91
2.4.6 <i>Mertk</i> regulates the gene expression program in the RPE.....	95
<b>2.5 Discussion.....</b>	<b>102</b>
<b>2.6 Co-author contributions and acknowledgements.....</b>	<b>105</b>
<b>Chapter III: Ex vivo modulation of FoxO1 phosphorylation state does not lead to dysfunction of T regulatory cells.....</b>	<b>106</b>
<b>3.1 Summary.....</b>	<b>106</b>
<b>3.2 Introduction.....</b>	<b>108</b>
<b>3.3 Experimental Procedures.....</b>	<b>112</b>
3.3.1 Ethics Statement.....	112
3.3.2 Animals and primary cell culture.....	112
3.3.3 Mouse model of allergic airway inflammation.....	113
3.3.4 qRT-PCR.....	114
3.3.5 Flow cytometry.....	114
3.3.6 Protein isolation and Immunoblotting.....	115
3.3.7 Phosphatase assay.....	115
3.3.8 T cell proliferation and suppression assays.....	116

3.3.9 T regulatory cell differentiation .....	117
<b>3.4 Results .....</b>	<b>118</b>
3.4.1 Allergen-induced airway inflammation increases local Treg cell populations.....	118
3.4.2 Mice with HDM-induced inflammation do not exhibit increased IL-10 .....	119
3.4.3 Mediastinal lymph nodes from mice with allergic airway inflammation have decreased expression of the phosphatase PP2A .....	120
3.4.4 Phosphatase inhibitors increase FoxO1 phosphorylation and nuclear localization in total CD4 <sup>+</sup> Cells.....	124
3.4.5 Okadaic acid promotes FoxO1 phosphorylation in Treg cells.....	133
3.4.6 Okadaic acid does not impair Treg differentiation ex vivo .....	136
3.4.7 Okadaic acid does not affect the phenotype of Treg cells differentiated ex vivo .....	140
3.4.8 Okadaic acid treatment of Treg cells does not influence Treg suppression ex vivo.....	144
<b>3.5 Discussion.....</b>	<b>147</b>
<b>3.6 Acknowledgements and co-author contributions .....</b>	<b>151</b>
<b>Chapter IV: Summary and Future Directions.....</b>	<b>152</b>
<b>4.1 Summary.....</b>	<b>152</b>
<b>4.2 Future Directions .....</b>	<b>156</b>
4.2.1 Why doesn't BAI1 expression rescue defects in RPE phagocytosis? .....	156

4.2.2 Does phagocytosis by specialized phagocytes regulate their non-phagocytic functions? .....	167
4.2.3 What is the role of RPE-produced insulin? .....	177

## **Appendix I: Evaluation of *Tim4*<sup>-/-</sup> mice in pristane induced autoimmune disease .....**

<b>A1.1 Introduction .....</b>	<b>185</b>
<b>A1.2 Experimental procedures .....</b>	<b>188</b>
A1.2.1 Mice .....	188
A1.2.2 Autoantibody ELISA .....	188
A1.2.3. Glomerular measurement.....	189
<b>A1.3 Results .....</b>	<b>190</b>
A1.3.1 <i>Tim4</i> <sup>-/-</sup> mice do not exhibit exacerbated pristane-induced autoimmune disease relative to WT mice .....	190
A1.3.2 <i>Tim4</i> <sup>-/-</sup> mice have increased survival following pristane-administration.....	194
<b>A1.4 Discussion .....</b>	<b>197</b>

## **Appendix II: Characterization of colonic epithelial cells and inflammatory infiltrates from *Bai1*<sup>-/-</sup> and *Bai1*<sup>Tg</sup> mice with DSS-colitis.....**

<b>A2.1 Introduction .....</b>	<b>199</b>
<b>A2.2 Experimental Procedures .....</b>	<b>201</b>
A2.2.1 Mice and DSS-induced colitis.....	201
A2.2.2 Epithelial cell and lamina propria layer isolation.....	202
A2.2.3 Flow cytometric analysis of IEL and LPL populations .....	203
A2.2.4 Cytokine staining in LPL T cells.....	204

<b>A2.3 Results .....</b>	<b>205</b>
A2.3.1 Deletion of BAI1 does not influence the size of inflammatory infiltrate .....	205
A2.3.2 The <i>Bai1</i> <sup>Tg</sup> is expressed in macrophages from the LPL.....	208
A2.3.3 Colonic epithelial cells express multiple PtdSer receptors .....	211
<b>A2.4 Discussion .....</b>	<b>214</b>
<b>References .....</b>	<b>215</b>

## List of Figures

### Chapter I

<b>Figure 1.1:</b> Distinct Structural features of phosphatidylserine receptors .....	<b>6</b>
<b>Figure 1.2:</b> Multiple engulfment pathways utilize similar signaling components and influence each other .....	<b>10</b>
<b>Figure 1.3:</b> Schematic of specialized phagocyte function .....	<b>16</b>
<b>Figure 1.4:</b> Anatomy of the retina and retinal pigmented epithelium .....	<b>25</b>
<b>Figure 1.5:</b> Schematic of the visual cycle .....	<b>27</b>
<b>Figure 1.5:</b> Proposed PP2A-FoxO1 axis in CD4 cells .....	<b>38</b>
<b>Figure 1.6:</b> The inflammatory cascade in allergic airway inflammation .....	<b>43</b>

### Chapter II

<b>Figure 2.1:</b> <i>Bai1<sup>Tg</sup></i> rescues accumulation of apoptotic corpses post-torsion .....	<b>64</b>
<b>Figure 2.2:</b> Testicular cross sections .....	<b>66</b>
<b>Figure 2.3:</b> <i>Bai1<sup>Tg</sup></i> influences gene transcription in RPE despite the lack of endogenous <i>Bai1</i> .....	<b>71</b>
<b>Figure 2.4:</b> RPE express components of BAI1-signaling pathway and <i>Bai1<sup>Tg</sup></i> ...	<b>73</b>
<b>Figure 2.5:</b> <i>Bai1<sup>Tg</sup></i> does not reduce retinal degeneration in <i>Mertk<sup>-/-</sup></i> mice .....	<b>78</b>
<b>Figure 2.6:</b> <i>Mertk<sup>+/+</sup></i> and <i>Mertk<sup>+/-</sup></i> mice display no phenotypic differences in retinal degeneration and phagocytosis .....	<b>80</b>
<b>Figure 2.7:</b> <i>Bai1<sup>Tg</sup></i> does not enhance RPE phagocytosis .....	<b>85</b>
<b>Figure 2.8:</b> <i>Bai1<sup>Tg</sup></i> does not influence apical-basolateral localization of phagosomes .....	<b>87</b>

<b>Figure 2.9:</b> Ex vivo RPE phagocytosis assays do not recapitulate in vivo phenotypes .....	<b>89</b>
<b>Figure 2.10:</b> <i>Mertk</i> <sup>-/-</sup> mice have reduced retinyl ester accumulation .....	<b>93</b>
<b>Figure 2.11:</b> <i>MerTK</i> regulates multiple genes linked to phagocytosis and metabolism .....	<b>99</b>
<b>Chapter III</b>	
<b>Figure 3.1:</b> HDM potently induces allergic airway inflammation despite significant T regulatory cell recruitment.....	<b>122</b>
<b>Figure 3.2:</b> 3.2: Calyculin A increases FoxO1 phosphorylation and ubiquitylation .....	<b>127</b>
<b>Figure 3.3:</b> PP2A inhibition increases FoxO1 phosphorylation and cytosolic localization in CD4+ T cells .....	<b>129</b>
<b>Figure 3.4:</b> Phosphatase inhibitor LB100 enhances FoxO1 phosphorylation .	<b>131</b>
<b>Figure 3.5:</b> Okadaic acid increases phosphorylation and cytosolic localization of FoxO1 in T regulatory cells .....	<b>134</b>
<b>Figure 3.6:</b> Okadaic acid does not impair T regulatory cell differentiation in vitro .....	<b>138</b>
<b>Figure 3.7:</b> Okadaic acid does not induce a pro-inflammatory phenotype or affect lymph node homing signatures in Treg cells .....	<b>142</b>
<b>Figure 3.8:</b> Okadaic acid does not impair T regulatory cell mediated suppression of CD4 effector cells .....	<b>145</b>

## Chapter IV

<b>Figure 4.1:</b> Peritoneal macrophages over expressing BAI1 exhibit enhanced apoptotic cell clearance .....	<b>160</b>
<b>Figure 4.2:</b> Phagocytic pathways involve multiple small Rho GTPases .....	<b>165</b>
<b>Figure 4.3:</b> Genes related to cholesterol metabolism and vitamin A esterification are dysregulated in <i>Mertk</i> <sup>-/-</sup> RPE .....	<b>175</b>
<b>Figure 4.4:</b> RPE express insulin and multiple genes related to insulin release... ..	<b>183</b>

## Appendix I

<b>Figure A1.1:</b> <i>Tim4</i> <sup>-/-</sup> mice do not exhibit symptoms of autoimmune disease following pristane administration .....	<b>192</b>
<b>Figure A1.2:</b> <i>Tim4</i> <sup>-/-</sup> mice are resistant to death after pristane administration	<b>195</b>

## Appendix II

<b>Figure A2.1:</b> Loss of <i>Bai1</i> does not alter the inflammatory population in the lamia propria during DSS-colitis .....	<b>206</b>
<b>Figure A2.2:</b> <i>Bai1</i> <sup>Tg</sup> expression occurs in appropriate tissues .....	<b>209</b>
<b>Figure A2.3:</b> Colonic epithelial cells express multiple PtdSer receptors .....	<b>212</b>

## List of Tables

### Chapter II

<b>Table 2.1:</b> Genes dysregulated in <i>Mertk</i> <sup>-/-</sup> RPE with associations to retinal disease .....	<b>101</b>
--	------------

## List of Abbreviations

ABCA1: ATP Binding cassette transporter A1

Akt: Protein kinase B

ATP: Adenosine Triphosphate

BAI: brain angiogenesis inhibitor

BAL: Bronchoalveolar lavage fluid

Bcl2: B cell lymphoma 2

BRB: blood-retinal-barrier

BTB: Blood-testis-barrier

CC3: Cleaved caspase 3

CD4: Cluster of differentiation 4

CrkII: proto-oncogene c-Crk II

CTLA: Cytotoxic lymphocyte antigen

DerP1/2: House dust mite peptidase 1 / 2

DH: DBL homology domain

Dock180: Deducator of cytokinesis 1

DSS: dextran sodium sulfate

ELISA: Enzyme-linked immunosorbent assay

ELMO: engulfment and cell-motility protein

ERG: electroretinogram recording

EpCAM: Epithelial cell adhesion molecule

FACS: fluorescence-activated cell sorting

FasL: Fas ligand

FEEL: Fasciclin, EGF-like, laminin-type EGF-like, and link domain-containing scavenger receptor

FiSH: Fluorescence in situ hybridization

FMO: fluorescence-minus-one

FoxO1: Forkhead Box O1

FoxP3: Forkhead box P3

Gas6: Growth arrest specific 6

GAP: GTP hydrolysis-activating proteins

GDI: Guanine nucleotide dissociation inhibitors

GEF: Guanine nucleotide exchange factor

GLUT: Glucose transporter

GPCR: G-protein-coupled receptor

GTPase: Guanine triphosphatase

HDM: House dust mite

IEL: Intestinal epithelial layer

IFN $\gamma$ : Interferon gamma

IgE: Immunoglobulin E

IL-10: Interleukin-10

IP: intraperitoneal

LPL: lamina propria layer

MerTK: Mer tyrosine kinase

MFG-E8: Milk fat globule-EGF factor 8

MLN: mediastinal lymph node

MNU: N-methyl-N-nitrosurea

PBMCs: Peripheral blood mononuclear cells

PH: pleckstrin homology domain

PLC $\gamma$ 2: phospholipase C  $\gamma$ 2

POS: photoreceptor outer segments

PP2A: protein phosphatase 2A

PtdSer: phosphatidylserine

qRT-PCR: quantitative reverse transcriptase polymerase chain receptor

Rac1: Ras-related C3 botulinum toxin substrate 1

RCS: royal college of surgeons

RNAseq: Ribonucleic acid sequencing

RPE: retinal pigmented epithelium

RT: room temperature

S1pr1: Sphingosine 1 phosphate receptor 1

Ser: Serine

SLE: systemic lupus erythematosus

smRNP: Smith and ribonucleoprotein complex

TAM: Tyro3, Axl, MerTK

TCR: T cell receptor

Teff: Effector T cell

TGF $\beta$ : Transforming growth factor  $\beta$

Th2: T-helper type 2

Thr: Threonine

TIM: T cell immunoglobulin and mucin domain-containing protein

TLR: Toll-like receptor

TNF: Tumor necrosis factor

Treg: Regulatory T cell

TSLP: Thymic stromal lymphopoietin

TSR: thrombospondin repeats

ZO-1: Zona-occludens 1

# Chapter I

## Introduction

### 1.1 Overview of apoptotic cell clearance

Everyday, billions of cells in our body undergo the programmed cell death process known as apoptosis. The process of apoptotic cell death is crucial for normal tissue development as well as homeostasis within developed tissues. In fully developed tissues, aged and damaged members of the cellular community undergo apoptotic cell death [1]. Subsequently, these dying cells are cleared by phagocytes, and the engulfing phagocytes then actively limit or dampen local tissue inflammation [2-5].

During apoptosis, dying cells expose 'eat-me' signals so that phagocytes can recognize and distinguish them from healthy counterparts. The most classic and well-studied 'eat-me' signal is phosphatidylserine (PtdSer). Normally, PtdSer is sequestered on the inner leaflet of the plasma membrane, and during apoptosis PtdSer is exposed on the outer leaflet of the plasma membrane, where it can interact with PtdSer receptors on phagocytes [6-8]. Ligation of PtdSer receptors on phagocytes triggers phagocytic cup formation, which then facilitates the engulfment of the dying cell.

#### 1.1.1 Consequences of apoptotic cell death

Apoptotic cell death is often referred to as "immunologically silent" however the term 'silent' is a slight misnomer. While it is correct that apoptotic

cell removal does not elicit a pro-inflammatory response, apoptotic cell clearance also elicits potent anti-inflammatory signaling in phagocytes that recognize and clear apoptotic cells [4,5,9-11]. This signaling ultimately leads to anti-inflammatory cytokine production and secretion [4,5,12,13]. This anti-inflammatory signaling is very important for preventing a potentially devastating inflammatory cascade, as apoptotic cells are a repository of auto-antigens. Thus, the anti-inflammatory response to apoptotic cells helps to prevent autoimmune processes [14,15].

Failure to clear an apoptotic corpse results in secondary necrosis of the apoptotic cell [16,17]. Such secondarily necrotic cells, unlike apoptotic cells, often drive inflammatory responses by releasing damage associated molecular patterns while simultaneously releasing auto-antigens [18-20]. In fact, failure to clear apoptotic cells has been linked to the development of autoimmune diseases, including systemic lupus erythematosus [21-23]. To prevent the development of autoimmunity due to the accumulation of secondarily necrotic cells, apoptotic cells are efficiently cleared from tissues. In fact, apoptotic cells facilitate their own clearance by recruiting phagocytes and stimulating phagocytosis [24].

### **1.1.2 Apoptotic cells coordinate their own removal**

Apoptotic cell death can be triggered by extrinsic, receptor-mediated stimuli (e.g.  $\text{TNF}\alpha$ , FasL) or intracellular changes that lead to a loss of mitochondrial membrane potential [25,26]. Both the intrinsic and extrinsic

pathways of apoptosis converge by activating (by cleaving) the protease, caspase 3 [25,27-29]. Caspase 3 is the main executioner caspase in apoptosis and its cleavage is frequently used as a marker of cell death [30]. Cleavage of caspase 3 triggers the classic features of apoptosis: DNA degradation, chromatin condensation, phosphatidylserine exposure and apoptotic body formation [28,31]. While undergoing this process, the apoptotic cell simultaneously orchestrates its own removal.

First, the apoptotic cell releases 'find-me' signals to recruit near-by phagocytes. Some of the best-characterized find-me signals are nucleotides. Nucleotide release during apoptosis occurs via the pannexin 1 channel [32]. The pannexin 1 channel is opened when the C-terminal tail is cleaved by active caspase 3 [32,33]. Nucleotides released from the apoptotic cell function as a chemoattractant and elicit phagocyte migration by activating the P2Y2 receptor [34].

In addition to recruiting phagocytes, apoptotic cells also reveal themselves to phagocytes by exposing 'eat-me' signals on their surface. The most classic and well-studied 'eat-me' signal is the phospholipid phosphatidylserine (PtdSer). Normally, PtdSer is asymmetrically distributed on the plasma membrane and sequestered on the inner leaflet [35]. During apoptosis, caspase 3 cleaves and inactivates phospholipid flippases and simultaneously activates the scramblase Xkr8, which re-distributes PtdSer on the outer leaflet [36-38]. Phagocytes express multiple receptors that recognize PtdSer. Ligation of these receptors

subsequently elicits cytoskeletal rearrangement within the phagocyte and phagocytic removal of the apoptotic corpse.

### 1.1.3 Phosphatidylserine receptors

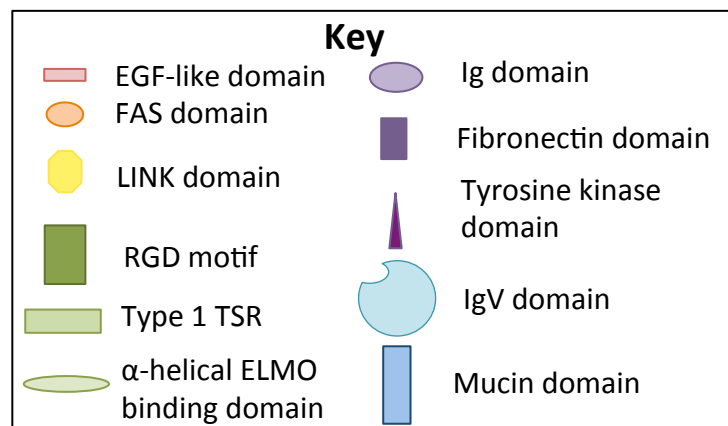
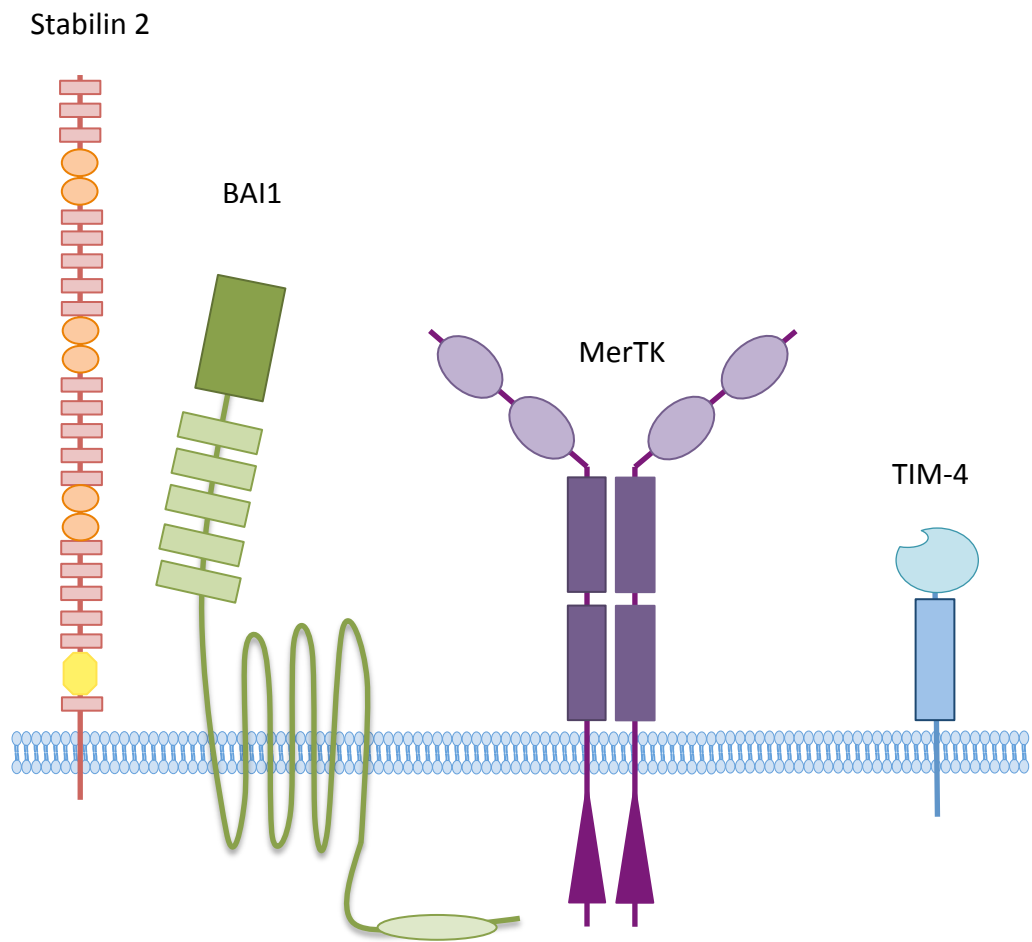
Phagocytes express a multitude of PtdSer receptors that recognize apoptotic cells and initiate phagocytosis. Interestingly, these PtdSer receptors do not fall in to a single family of proteins and do not share a common structure (**Figure 1.1**). Rather, PtdSer receptors come in a variety of different molecular formats, with the only commonality being their ability to recognize PtdSer. Many different PtdSer receptors have been identified such as the  $\alpha_v\beta_5$  and  $\alpha_v\beta_3$  integrins, the TAM family of receptor tyrosine kinases, the FEEL scavenger receptor family, the BAI family of GPCRs, and the TIM family [24,39-46] (**Figure 1.1**). Not all of these receptors are capable of binding to PtdSer directly.  $\alpha_v\beta_5$  and  $\alpha_v\beta_3$  integrins bind via the bridging molecule MFG-E8 [47-50]. And the TAM receptors bind via the bridging molecules Gas6, Protein S [51,52]. Importantly, regardless of whether these receptors recognize PtdSer directly or via soluble bridging proteins, all have been shown to promote apoptotic cell clearance.

Some PtdSer receptors, such as TIM4, are considered tethering receptors, as they are not capable of independent, downstream signaling [53]. However the majority of the identified PtdSer receptors are capable of signaling. When these receptors bind to PtdSer they initiate an evolutionarily conserved signaling cascade that converges on the small GTPase Rac1 [54-58]. Interestingly, several PtdSer receptors have signaling pathways that overlap

upstream of Rac1. Specifically, the bipartite Rho-GEF Dock180 and ELMO have been definitively linked to signaling downstream of BAI1 and the integrin  $\alpha_v\beta_5$  [42-44,59].

**Figure 1.1: Distinct Structural features of phosphatidylserine receptors**

Stabilin-2, TIM-4, and BAI1 bind PtdSer directly while MerTK recognizes phosphatidylserine indirectly. Their general structural domains and motifs are indicated. Stabilin-2 belongs to the scavenger receptor FEEL family, which also includes Stabilin-1 (FEEL1) that can also bind PtdSer. BAI1 represents the BAI family of 7-transmembrane PtdSer receptors that belong to the adhesion family of G-protein coupled receptors. MerTK is representative of the TAM family of PtdSer receptors, which utilize bridging molecules (Gas6 or Protein S) to bind PtdSer. TIM-4 is representative of the TIM family of proteins. TIM-1 and TIM-3 are also capable of binding PtdSer.



#### 1.1.4 Signaling via the bipartite Rho-GEF ELMO and Dock180

Rac1 is a small GTPase that belongs to the Rho family of GTPases. The rate-limiting step in activation of Rho GTPases is the exchange of GDP for GTP, which requires their progression through the nucleotide-free transition state. This activation step is regulated by proteins that control the nucleotide binding state of the GTPases: Rho guanine nucleotide dissociation inhibitors (GDIs), Rho GTP hydrolysis-activating proteins (GAPs), and guanine nucleotide exchange factors (GEFs) [60]. GEFs stabilize the Rho GTPases in the nucleotide-free state and thus are essential for controlling the rate of GTPase activity [61]. Prior to the discovery of the bipartite ELMO/Dock180 GEF, all GEFs for the Rho family of GTPases were thought to possess a DBL homology domain (DH) and a closely positioned pleckstrin-homology (PH) domain (often referred to as the DH-PH cassette) [61-64].

Though Dock180 was a known binding partner of Rac1 that promoted membrane ruffling, it did not possess the classic DH or PH domains [65]. In addition, Dock180 alone did not have RacGEF activity *in vitro* [66,67]. However, overexpression of Dock180 increased nucleotide exchange on Rac1 within cells, which suggested that there may be other missing players [65]. The mechanism of Dock180 function in Rac nucleotide exchange was revealed when ELMO1, an additional member of this engulfment pathway, was identified.

Mammalian ELMO1 was found to bind to Dock180 [66]. Though the ELMO/Dock180 complex could promote Rac activity *in vivo*, neither ELMO nor

Dock180 possessed the classic DH-PH domains found on other Rho-family GEFs. A series of deletion mutant studies of Dock180 suggested that truncation at residue 1472 on Dock180 abolished the increase in Rac activation observed when Dock180 is overexpressed [67]. This deleted region was found to be part of a larger domain, which was initially termed as 'Docker' (a Dock homology region involved in exchange on Rac) [67,68]. A series of studies revealed that ELMO1 and Dock180 form a bipartite GEF for Rac, as the expression of both proteins and their association was essential for *in vivo* GEF function[67,69].

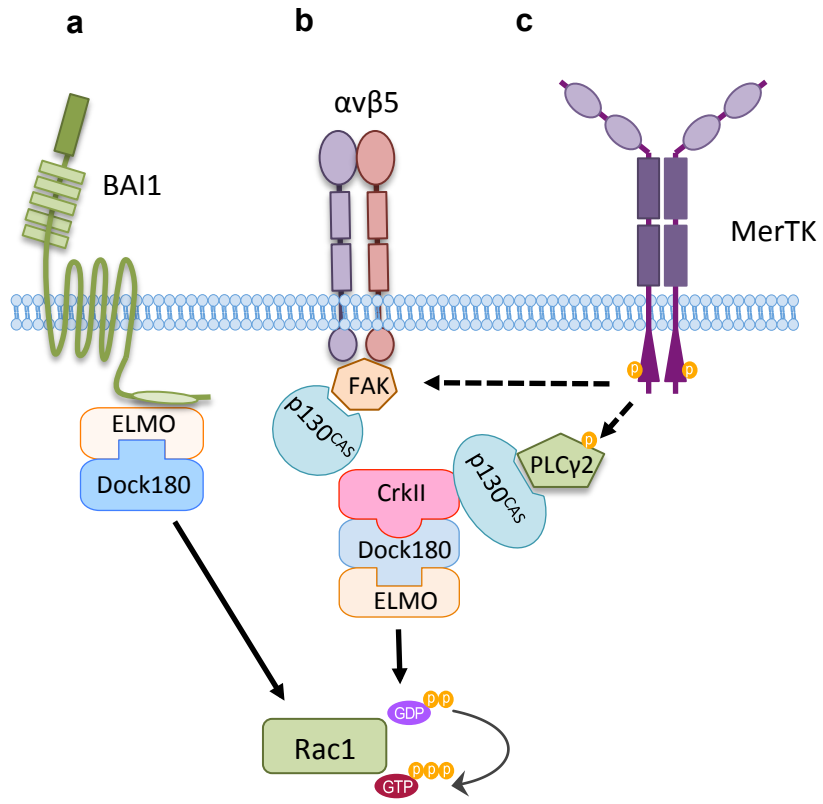
Dock180 and ELMO function downstream of BAI1,  $\alpha_v\beta_3$  integrin and it has been suggested that they are downstream of the TAM family of PtdSer receptors [42,70-72]. As BAI1 and the TAM receptor MerTK are discussed at length in this manuscript, the current knowledge regarding their signaling has been further detailed below (**Figure 1.2**):

**Figure 1.2: Multiple engulfment pathways utilize similar signaling components and influence each other**

(a) BAI1 engulfment pathway promotes ABCA1 transcription for cholesterol efflux at the cell membrane.

(b) Integrin mediated engulfment similarly relies on Dock180 and ELMO to elicit Rac1 activation. It is unclear whether this pathway also elicits ABCA1 transcription.

(c) MerTK is phosphorylated and recruits FAK. FAK can interact with p130<sup>CAS</sup> to elicit Rac1 activation via CrkII, Dock180 and ELMO.



### 1.1.5 BAI1 signaling

BAI1 belongs to the type II adhesion GPCR family (recently classified as ADGRB1) [73]. BAI1 has a large extracellular region, and a seven transmembrane domain, followed by a long intracellular tail ([74]). BAI1 interacts with PtdSer via 5, type-1 thrombospondin repeats in its extracellular domain [42]. Similarly, red blood cells exposing PtdSer can bind to thrombospondin in the endothelial matrix [75] [76]. Upon binding to PtdSer, the cytoplasmic tail of BAI1 interacts with ELMO, which subsequently recruits Dock180 [42,67,69]. ELMO1 and Dock180 drive nucleotide exchange on Rac, which then causes F-actin rearrangement [60] and phagocytic cup formation (**Figure 1.2a**).

### 1.1.6 MerTK signaling

The receptor tyrosine kinase MerTK binds to phosphatidylserine via bridging molecules that include Gas6, Protein S, and potentially Tubby and Tubby-like protein 1 [51,52,71,77]. Bridging elicits dimerization of MerTK and subsequent phosphorylation of the tyrosine kinase domain. While the signaling pathway from this point further is not fully resolved, it is known that activation of MerTK drives a series of phosphorylation reactions. Bridging of MerTK to PtdSer stimulates auto-phosphorylation of the tyrosine kinase domain in *trans* [78]. This subsequently is thought to drive the phosphorylation of phospholipase C $\gamma$  2 (PLC $\gamma$ 2) [78,79]. PLC $\gamma$ 2 can recruit p130<sup>CAS</sup> to the intracellular tail of  $\beta$ 5 integrin, which can activate the CrkII-ELMO-Dock180 module [71]. CrkII is not a necessary component of Dock180/ ELMO signaling but it was originally identified

as a promoter of engulfment within the Dock180, ELMO and Rac1 pathway [54,80]. CrkII is an adapter protein, and while CrkII is not essential for Rac1 activation, overexpression of CrkII boosts Rac activity [54,59,65,81]. Interestingly, co-expression of CrkII, Dock180 and ELMO further enhances Rac activation and increases the number of corpses that are engulfed [55,65,66,82-85]. Since BAI1 can activate Dock180 and ELMO directly, it is likely that overexpression of CrkII boosts engulfment by linking other PtdSer receptors (such as integrins and possibly MerTK) to the ELMO/Dock180/Rac pathway (**Figure 1.2b, 1.2c**).

Despite the signaling overlap between many PtdSer receptors, phagocytes express a variety of PtdSer receptors on their surface [71,86-90]. Importantly, this is not only true of professional phagocytes such as macrophages and dendritic cells, but also of the 'non-professional' stromal phagocytes such as colonic and bronchial epithelial cells [86,91] and 'specialized' phagocytes such as Sertoli cells and the retinal pigmented epithelium [52,92,93].

## **1.2 Specialized phagocytes support sensitive tissues**

Specialized phagocytes are epithelial-derived, mitotically-quiescent cells, that carry out routine phagocytic events for the entire life of an organism [94-97]. Currently, two examples of specialized phagocytes are the retinal pigmented epithelium (RPE) of the eye and the Sertoli cells of the testes [94]. Like non-professional stromal phagocytes, specialized phagocytes perform a multitude of supportive functions within a tissue. There are however two key differences that place 'specialized' phagocytes in a league of their own. First, non-professional phagocytes undergo regular apoptosis and renewal [98,99]. However, specialized phagocytes are mitotically quiescent and therefore must retain their phagocytic activity and resist the physiological stresses associated with phagocytosis for the entire life of an organism [100-102]. Second, non-professional phagocytes are rarely thought to engulf apoptotic cells under homeostatic conditions [86,103] while specialized phagocytes routinely phagocytose dead cells and debris [104,105].

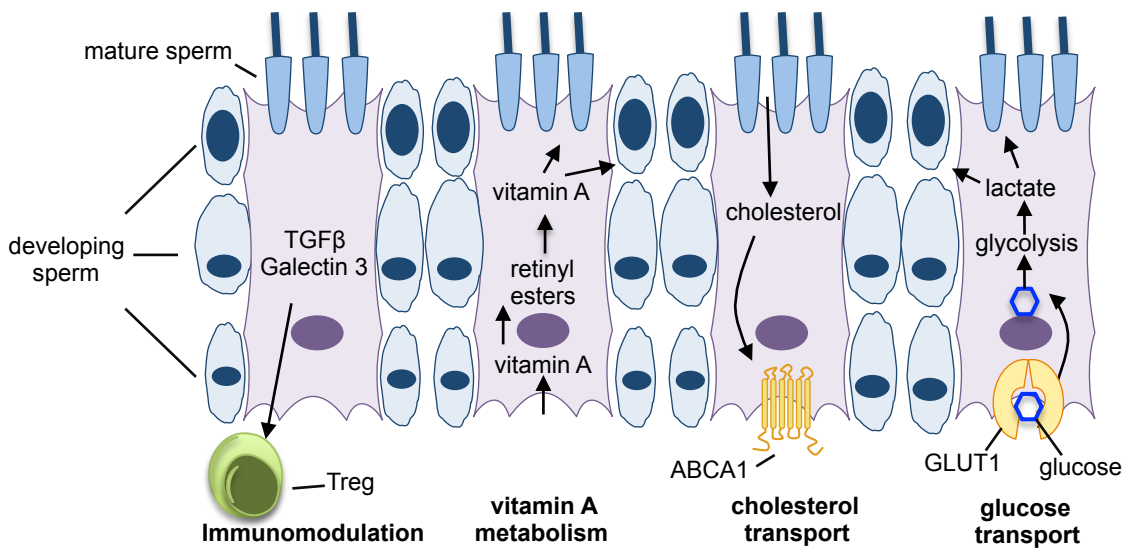
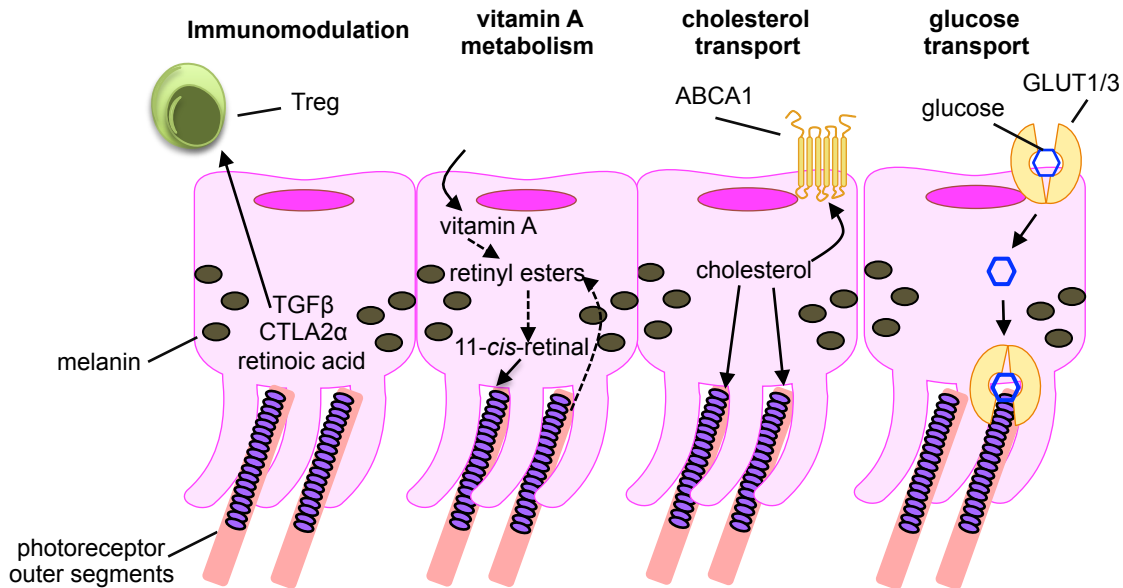
The Sertoli cells of the testes and RPE of the retina are highly differentiated and specialized cells, particularly suited to support their respective tissues. Interestingly, despite supporting tissues that are disparate in function, Sertoli cells and RPE share several key features, including: epithelial derivation, formation of a blood-tissue barrier, maintenance of immunological privilege, nutrient transport, vitamin A metabolism, cholesterol transport, and fluid transport

**(Figure 1.3).** A further review of Sertoli cell and RPE functions are detailed below.

**Figure 1.3: Schematic of specialized phagocyte function**

Specialized phagocytes have a multitude of functions within their respective tissues including immune regulation via promoting Treg differentiation, vitamin A metabolism and storage, cholesterol transport, and glucose / nutrient transport.

### RPE Cells



### Sertoli Cells

### **1.2.1 Non-phagocytic functions of Sertoli cells:**

Sertoli cells are a single layer of epithelial-derived cells that line the interior of the seminiferous tubules in the testes [95,106]. The Sertoli cells arise from the coelomic epithelium early in testicular development and are critical for early-sex determination [95]. The seminiferous tubules of the testes house the developing germ cells and the Sertoli cells support the developing sperm in a number of ways.

First, Sertoli cells are the primary mediators of testicular immune privilege. The seminiferous tubules are immunologically privileged to protect autoantigenic sperm from recognition by the immune system [107]. Break down of testicular immune privilege leads to autoimmune orchitis, a major cause of male infertility [108,109]. Sertoli cells provide an effective physical barrier known as the blood-testis-barrier (BTB) [110]. The Sertoli cells are tightly-joined by gap junctions, adherens junctions and zona-occludens junctions, making this barrier largely impermeable not only to invading cells but also to most large molecules [111,112]. However, some sperm autoantigens have recently been shown to egress from the seminiferous tubules and promote tolerogenic immune responses once they reach the periphery [113].

Sertoli cells are also immunomodulatory and promote immune privilege by actively suppressing immune responses. Sertoli cells produce TGF $\beta$  and JAGGED1, which induce the differentiation of regulatory T (Treg) cells [114,115]. Furthermore, in the setting of inflammation, Sertoli cells can function as

regulatory antigen presenting cells [116]. In fact, the immunosuppressive properties of Sertoli cells are so potent, that co-transplant of purified Sertoli cells and pancreatic  $\beta$  cells prevents graft rejection [117,118].

Due to their physical barrier function, Sertoli cells need to mediate extensive paracellular and transcellular transport in order to provide the developing sperm with necessary nutrients. One major nutrient provided by the Sertoli cells is iron. Sertoli cells produce transferrin, which facilitates transport of iron across the BTB [119]. Decreased transferrin production by the Sertoli cells leads to impaired spermatogenesis, indicating that iron is crucial for the developing germ cells [120]. Sertoli cells also provide developing sperm with vitamin A, which initiates meiosis [121,122]. Sertoli cells absorb vitamin A from the serum and store it in the form of retinyl esters for later use during spermatogenesis [121,123]. Yet another crucial metabolite provided by Sertoli cells is lactate [124,125]. Developing germ cells are dependent on lactate and Sertoli cells provide lactate to the germ cells by absorbing and metabolizing glucose [124,126-128]. Lastly, Sertoli cells produce seminiferous fluid, which bathes the germ cells as they undergo spermatogenesis [129].

In addition to secreting nutrients and fluid in to the lumen of the seminiferous tubules, Sertoli cells also absorb factors from the seminiferous tubules for excretion in to the blood stream. Interestingly, one critical compound that is exported by the Sertoli cells is cholesterol, and Sertoli cell cholesterol transport is mediated by ABCA1 [130]. The importance of ABCA1 is of particular

interest as phagocytosis positively regulates ABCA1 expression.

Furthermore, the PtdSer receptors MerTK and BAI1 have both been linked to ABCA1 upregulation [131,132] and both of these receptors promote Sertoli cell phagocytosis [52,86]. Loss of ABCA1 decreases spermatogenesis and reduces testosterone levels in mice, suggesting that reverse cholesterol transport from Sertoli cells, or other function(s) of ABCA1, are important for spermatogenesis [130].

### **1.2.2 Phagocytic function of Sertoli cells**

Sertoli cells perform two major phagocytic functions. First, Sertoli cells phagocytose the developing germ cells that undergo apoptosis. Second, in the final phase of spermatogenesis, the residual body of the sperm, which consists of excess cytoplasm, is phagocytosed by the Sertoli cell [133-135]. These phagocytic events are dependent upon PtdSer recognition and multiple PtdSer receptors contribute to Sertoli cell phagocytosis including Tyro3, Axl, MerTK (TAMs) and BAI1 [52,86,93,136].

Impaired Sertoli cell phagocytosis can lead to accumulation of apoptotic germ cells in the seminiferous tubules and potentially, loss of fertility [52,93]. These findings have been established by genetic experiments that deleted PtdSer receptors and by blocking PtdSer *in vivo* [52,86,93,136,137]. Importantly, loss of MerTK alone is sufficient to cause apoptotic germ cell accumulation, however *Mertk*<sup>-/-</sup> mice do not exhibit infertility [52]. Loss of all three TAM receptors leads to profound apoptotic corpse accumulation in the seminiferous

tubules and male infertility [93]. Interestingly, loss of all three TAM receptors also leads to anti-sperm antibody production and breakdown of the BTB [93,109]. The role of BAI1 and its downstream signaling partner, ELMO, were demonstrated using BAI1 and ELMO1 knockout mice. Similar to *Mertk*<sup>-/-</sup> mice, *Elmo1*<sup>-/-</sup> mice exhibit corpse accumulation at baseline. However, *Bai1*<sup>-/-</sup> mice only exhibit increased corpse accumulation following testicular torsion [86,136].

### **1.2.3 Non-phagocytic functions of the retinal pigmented epithelium**

The RPE are a single layer of pigmented epithelium that lies between the neural retina and the choroid (**Figure 1.4a, 1.4b**). Like the neuronal cells of the retina, the RPE are derived from the neuroectoderm and are therefore considered a true component of the retina [138]. The eye is an immunologically privileged site and the RPE contribute to this immunological privilege. As the outer blood-retinal barrier (BRB), the RPE function as a physical barrier to immune-cell infiltration [139]. The RPE are tightly associated by zona-occludens, adherens, and gap junctions, which prevent infiltration of immune cells and large molecules [140-142].

The RPE also possess immunoregulatory properties that limit inflammation within the retinal microenvironment. The immunosuppressive properties of the RPE have been extensively characterized *in vitro* and a few *in vivo* studies have been conducted which support these data. First, supernatants from cultured RPE cells suppress T effector (Teff) activation *in vitro* [143].

Second, RPE cell supernatants can also induce Treg cell differentiation *in vitro* [144]. The RPE capacity to influence Treg differentiation has been attributed to RPE production of TGF $\beta$ , retinoic acid and CTLA2 $\alpha$  [144-147]. Furthermore, Treg cells differentiated by RPE supernatants can inhibit inflammation in experimental autoimmune uveitis [145]. The importance of immune privilege in the eye is profoundly demonstrated by mouse models of experimental autoimmune uveitis and in human patients with autoimmune uveitis. In these individuals (and mice), autoimmune-mediated inflammation in the retina can lead to severe vision loss [148].

The barrier function of the RPE necessitates extensive paracellular and transcellular transport of fluid, ions, and nutrients, which support the sensitive cells of the neural retina. First, fluid (in the form of the aqueous humor) is continuously produced by the ciliary body [149]. Therefore, fluid export from the eye is essential to preventing a pathological increase in intraocular pressure [150]. Fluid removal is mediated by aquaporins on the RPE [151,152]. This continuous fluid transport is driven by simultaneous ion transport [153,154].

In addition to transporting fluid and ions, the RPE must also provide necessary metabolites to the neural retina and particularly the photoreceptors. The photoreceptors of the retina rely largely on aerobic glycolysis and have large metabolic demands; thus these cells require large amounts of glucose in order to maintain their functionality [155]. The RPE express high levels of the glucose transporters, GLUT1 and GLUT3 on both their apical and basolateral membranes

[156-158]. These glucose transporters ensure high levels of glucose are delivered to the photoreceptors. As a consequence of their rapid glycolytic metabolism, the photoreceptors also produce high levels of lactate. While photoreceptors are capable of further metabolizing lactate into amino acids, the RPE effluxes some of the lactate from the retina [127,159,160].

Another metabolite that requires delicate balance in the retina is cholesterol. The photoreceptors possess unique membrane-bound rhodopsin-containing organelles that initiate phototransduction. The photoreceptors generate new rhodopsin-discs daily and cholesterol constitutes 10% of the total lipid content of these discs [161]. While the retina is capable of *de novo* cholesterol synthesis, the RPE also transports considerable amounts of cholesterol from low-density lipoproteins in the blood stream to the photoreceptors [162,163]. However, too much cholesterol accumulation in the retina will lead to dysfunction, thus the RPE simultaneously effluxes cholesterol in order to prevent a toxic accumulation [161]. The significant cholesterol transport across the BRB is unique within the central nervous system. The blood-brain-barrier does not mediate cholesterol transport and thus the high cholesterol demand in the brain is satisfied purely by *de novo* synthesis [161].

In addition to its role in barrier function and nutrient transport, the RPE is also essential for phototransduction. While the RPE is not directly involved in phototransduction, it plays a key role in the visual cycle by re-generating the chromophore 11-*cis* retinal [164,165] (**Figure 1.5**). Phototransduction occurs

when light excites opsin-bound 11-*cis* retinal and converts it to all-*trans* retinal [166]. The opsins are a family of GPCRs that are activated upon 11-*cis* retinal conversion [166]. Following its conversion, all-*trans* retinal is rapidly released by the opsin and then converted to all-*trans* retinol by retinol dehydrogenase [167]. All-*trans* retinol is transferred from the RPE to the photoreceptor by retinoid binding proteins, where it is converted to retinyl esters by the enzyme lecithin retinol acyltransferase (LRAT) [168]. Retinyl esters are a form of stored vitamin A that accumulates in the RPE in lipid-droplet like structures called retinosomes [169,170]. The enzyme RPE65 then mediates the conversion of retinyl esters to 11-*cis* retinol, which is subsequently converted to the chromophore 11-*cis* retinal by 11-*cis* retinol dehydrogenase [171,172]. The chromophore is then transferred back to the photoreceptor by retinoid binding proteins for use in future phototransduction events. Perturbation of the visual cycle causes visual impairments due to decreased levels of the necessary chromophore [173].

## **Figure 1.4: Anatomy of the retina and retinal pigmented epithelium**

**(a)** The RPE is a single layer of pigmented epithelium that lies between the photoreceptors and the choroid. The outer segments of the photoreceptors are in direct contact with the RPE. Image is of a representative 20x H&E stained, WT eyecup. The outer nuclear layer (ONL) are the nuclei of the photoreceptors. The inner nuclear layer (INL) are the nuclei of the interneurons which transmit signal from the photoreceptors to the ganglion cell layer (GCL). The yellow box indicates RPE and photoreceptors.

**(b)** A schematic view of the RPE / Photoreceptor relationship. The outer segments of the photoreceptor are tightly associated with the long apical microvilli of the RPE.

**(c)** Transmission electron microscopy image of the RPE and photoreceptors (obtained from 21 day-old mice. Eye sections prepared with the assistance of the UVa advanced microscopy core). Outer segments are labeled with OS.  $\mu$ villi denote the apical microvilli of the RPE and \* denote outer segment-containing phagosomes.

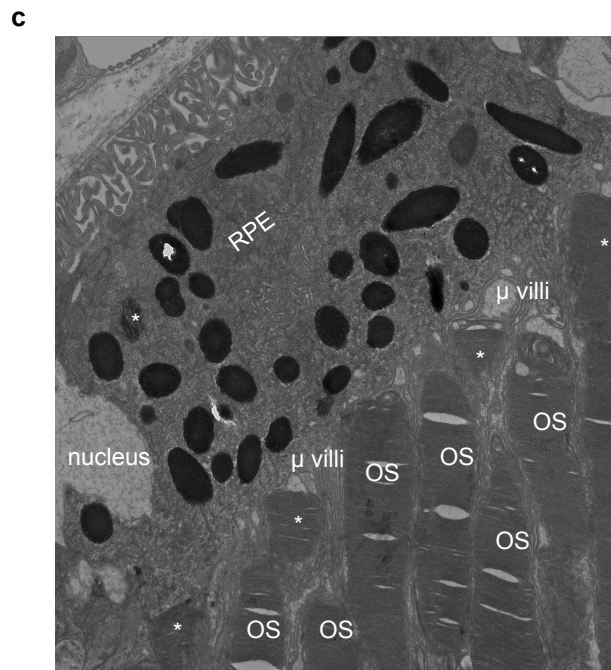
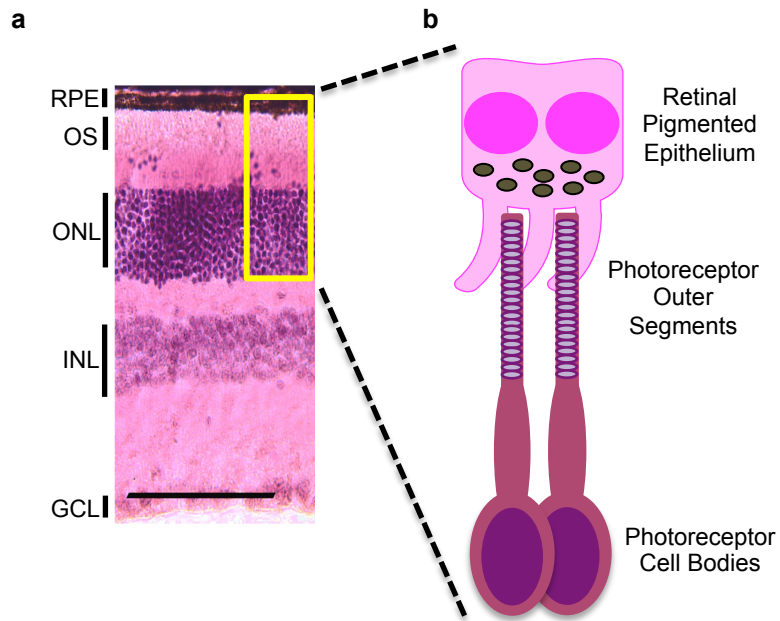
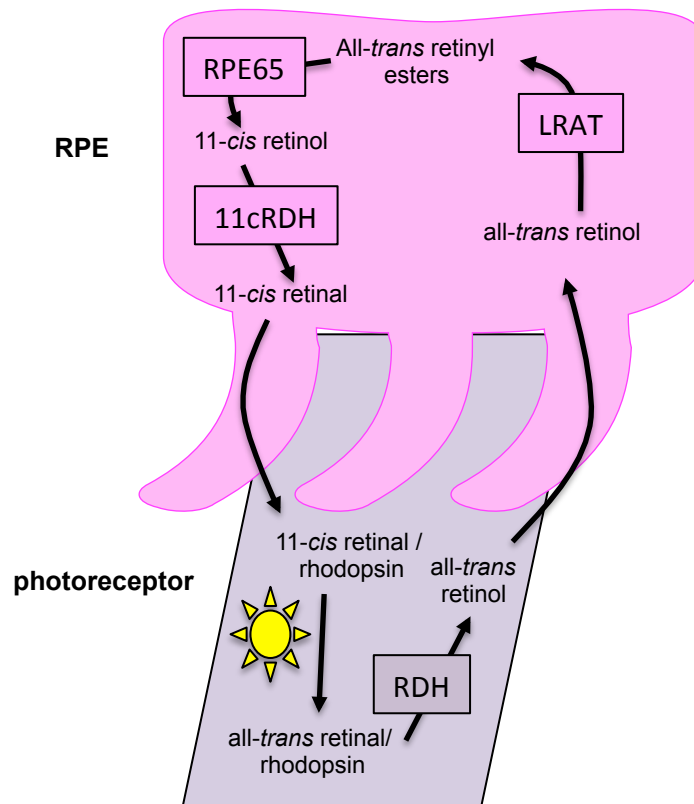


**Figure 1.5: Schematic of the visual cycle**

Photon-excitation converts 11-*cis*-retinal to all-*trans*-retinal. Following conversion to all-*trans*-retinal the retinoid goes through a series of enzymatic conversions in order to regenerate 11-*cis*-retinal. Enzyme abbreviations are in boxes and vitamin A intermediates have no surrounding box. RDH – retinol dehydrogenase; LRAT – lecithin retinyl acyl transferase; RPE65 – retinal pigmented epithelium 65; 11cRDH – 11-*cis*-retinal dehydrogenase.



#### 1.2.4 Retinal pigmented epithelium as phagocytes

Phototransduction produces many oxidative by-products that must be broken down in order to prevent photoreceptor death. However, the photoreceptors do not have the capacity to neutralize the photo-oxidative waste – instead this process of waste management is handled by the RPE [174]. In order to rid themselves of photo-oxidative waste, photoreceptors shed their distal-most (oldest) outer segments (POS) daily [105]. POS shedding is regulated by the circadian rhythm and occurs around the time of light onset [105,174]. To replenish the lost rhodopsin-discs, the photoreceptors renew daily and add fresh rhodopsin-discs at the base of the outer segment [175]. The RPE phagocytose the shed POS, safely removing the oxidative by-products from the milieu [176].

The role of PtdSer in RPE phagocytosis has been demonstrated in multiple ways. First, outer segments membranes were shown to contain high levels of PtdSer and PtdSer is exposed on outer segment tips in a diurnal fashion that is coincident with the time of phagocytosis [177,178]. Furthermore, blocking PtdSer with either an antibody or Annexin 5 inhibits RPE phagocytosis of POS *in vitro* [178].

RPE phagocytosis of POS is mediated by the apical microvilli [92,105,179] (**Figure 1.4b, 1.4c**). Multiple PtdSer receptors are expressed by the RPE and localize to the apical surface. These receptors include the class B scavenger receptor CD36,  $\alpha v \beta 5$  integrin, MerTK and Tyro3. Importantly, all of these receptors have been implicated in RPE phagocytosis. CD36 plays a role in POS

internalization but not in binding [180]. Interestingly, CD36 binding does not need to occur on the apical surface in order to promote phagocytosis, which suggests that signaling via CD36 indirectly supports POS phagocytosis [180]. Conversely,  $\alpha_v\beta_5$  mediates binding of the POS to RPE via MFG-E8 but is not required for internalization [180]. *In vivo*, MFG-E8 and  $\alpha_v\beta_5$  are essential for regulating the timing of phagocytosis [181,182]. *Mfge8*<sup>-/-</sup> and  $\beta_5$ <sup>-/-</sup> mice do not exhibit the typical burst of RPE phagocytosis that occurs around the time of light onset [181,182]. Interestingly, this loss of chronicity seems to be mediated at the level of the photoreceptor as photoreceptors of *Mfge8*<sup>-/-</sup> and  $\beta_5$ <sup>-/-</sup> mice do not exhibit diurnal exposure of PtdSer [178]. Despite *Mfge8*<sup>-/-</sup> and  $\beta_5$ <sup>-/-</sup> mice exhibiting similar phagocytic phenotypes, only  $\beta_5$ <sup>-/-</sup> mice exhibit age-related vision loss [182].

### **1.2.5 Deficits in RPE phagocytosis cause photoreceptor degeneration**

The role of MerTK in RPE phagocytosis was originally identified when it was discovered that the retinitis pigmentosa phenotype in the royal college of surgeons (RCS) rat was due to a mutation in *Mertk* [183]. Retinitis pigmentosa is a group of inherited diseases of photoreceptor degeneration [184] and the RCS rat model of retinitis pigmentosa was originally described in 1938 [185]. RCS rats were found to have an autosomal recessive degeneration of photoreceptors that began at 3 weeks of age [185]. In 1976, this phenotype was linked to dysfunction of the RPE by generating chimeric rat embryos with RCS and albino rats. As the RPE of albino rats lack pigment, the origin of a given RPE cell could readily be

distinguished. Using this system, they observed that photoreceptor degeneration only occurred in the patches adjacent to RCS-derived RPE [186]. Soon after, the RCS phenotype was linked to diminished POS clearance by the RPE [97,187].

Though the RCS rat was studied extensively as a model of retinitis pigmentosa, the causative mutation was unknown for more than 60 years following the rat's initial discovery. *Mertk* was ultimately determined to be the causative mutation by using a positional cloning screen, which revealed a deletion in the splice site upstream of the second exon in *Mertk*, resulting in a truncated transcript [183]. Importantly, *in vivo* delivery of *Mertk* to the RPE of RCS rats abrogated photoreceptor loss, demonstrating that this phenotype was due to the mutation in *Mertk* [188].

Since identifying the *Mertk* mutation in the RCS rat, the importance of MerTK in RPE phagocytosis has been confirmed in multiple species. *Mertk*<sup>-/-</sup> mice exhibit retinal degeneration that largely mimics the RCS rat [189]. In addition, loss of *Mertk* in humans causes early onset rod-cone dystrophies and retinitis pigmentosa [190,191]. Confirmation of retinal disease in *Mertk*<sup>-/-</sup> mice facilitated additional genetic studies as mice lacking all three TAM receptors were generated several years prior to the discovery of MerTK's role in the RCS rat [93]. It was subsequently reported that though the receptor Tyro3 is expressed in the RPE, loss of *Tyro3* does not cause retinal degeneration [192]. However, it was later determined that increased expression of *Tyro3* in *Mertk*<sup>-/-</sup> mice

abrogates retinal degeneration, suggesting that Tyro3 can in fact participate in RPE phagocytosis and that retinal degeneration due to the loss of *Mertk* is modifiable [92]. In keeping with early observations that the inherited photoreceptor degeneration in the RCS rat was autosomal recessive, one allele of *Mertk* is sufficient to prevent retinal degeneration in mice [192]. Lastly, it was confirmed that the retinal degeneration associated with loss of *Mertk* is due to impaired PtdSer recognition as loss of both bridging molecules, Protein S and Gas6, phenocopies the loss of MerTK [51]. Importantly, only one allele of one bridging molecule is necessary to prevent degeneration [51]. However, loss of Gas6 alone does lead to elongation of the POS, suggesting that phagocytosis was subtly altered in a way that leads to a new homeostatic set-point for outer segment length [51].

### **1.3 The role of T regulatory cells in allergic airway inflammation**

In a healthy state, immunogenic reactions to harmless, non-self antigens are dampened by peripheral tolerogenic responses [193,194]. Allergic airway inflammation occurs when the tolerogenic response is either absent or overpowered by an inappropriate inflammatory response to innocuous foreign antigens [195-198]. However, the mechanisms underlying this defective tolerogenic response are incompletely understood.

Tregs are one of the key mediators of immunologic tolerance [199-201]. Tregs maintain a tolerogenic milieu by secreting anti-inflammatory cytokines and expressing the negative regulator CTLA4 [201-203]. Treg expressed CTLA4 reduces MHCII expression and inflammatory cytokine production by antigen presenting cells. Treg cells can also act directly on Teff cells to induce cell death, decrease proliferation or dampen inflammation [204]. In fact, Treg functionality is typically measured by the ability of a Treg population to inhibit effector T cell proliferation and cytokine production [205]. The canonical anti-inflammatory cytokine produced by Treg cells is IL-10, which acts on APCs and lymphocytes to decrease inflammatory activity [202,206]. Treg cells and Treg-produced IL-10 are crucial for the induction of tolerance, particularly within the lung and at other environmental interfaces [207,208]. Interestingly, patients with asthma are known to have lower IL-10 in their airways, perhaps indicative of diminished Treg activity in these individuals [209,210].

The role of Treg cells in allergic airway inflammation and asthma has been extensively studied in the mouse. Multiple studies have shown that increasing the size of the Treg population can abrogate allergic airway inflammation [211-213]. Additional studies have examined the effect of the inflammatory milieu on Treg function and found that inflammatory mediators released in response to allergens reduce Treg function both in a mouse model and in Treg cells from human patients [214,215]. These studies have shown that Treg cells can be functionally suppressed in the setting of allergic airway inflammation. However, the intrinsic mechanism of Treg dysfunction in allergic airway inflammation and asthma remains unknown.

### **1.3.1 The transcription factor FoxO1**

FoxO1 is a regulator of numerous metabolic pathways and is commonly associated with glucose metabolism, tumor suppression and aging [216]. However, FoxO1 also plays an essential role in the immune system, specifically, in the development, homeostasis and function of Treg cells [217-220]. Treg differentiation occurs at the double positive stage in thymic development when FoxP3 transcription is initiated [221]. FoxO1 affects early Treg development by promoting FoxP3 expression in the thymus, but does not seem to play a greater role in overall thymic development [222]. *Cd4-cre Foxo1<sup>fl/fl</sup>* mice have fewer FoxP3<sup>+</sup> circulating CD4 cells in the periphery but show no obvious defect in other T cell populations [217,223]. Interestingly, the FoxP3<sup>+</sup> cells that do develop in *Cd4-cre Foxo1<sup>fl/fl</sup>* mice expressed lower levels of CD25 and CTLA4, both of which

play important roles in Treg suppressor function [223]. Accordingly, these mice have a greater proportion of activated T cells and eventually develop autoimmune disease [217].

FoxO1 is not only important during early Treg development, but is also critical for maintaining normal Treg function. Conditional deletion of FoxO1 in Treg cells (*Foxp3-cre Foxo<sup>fl/fl</sup>*) caused severe, spontaneous autoimmune disease that resulted in 100% mortality by day 30. Analysis of the lymphocyte populations showed that neither the size of the Treg population nor the expression of FoxP3 differed from control mice, however the Treg cells adopted a pro-inflammatory phenotype and expressed high levels of IFN $\gamma$  [218].

The transcriptional activity of FoxO1 is tightly regulated by post-translational modification, specifically phosphorylation. Dephosphorylated FoxO1 is active and localized to the nucleus while phosphorylated FoxO1 is sequestered in the cytosol [224]. FoxO1 is active in naïve and resting CD4<sup>+</sup> cells and promotes expression of genes essential for survival and immune surveillance [225], specifically, Bcl-2 and S1pr1, which inhibit apoptosis and permit egress from lymphoid organs, respectively [218,226,227].

FoxO1 is a negative regulator of several proteins that are essential for a typical inflammatory response, including SOCS3 and IFN $\gamma$  [218]. Accordingly, T cell activation necessitates a loss of FoxO1 activity. T cell receptor (TCR) stimulation activates Akt, which phosphorylates FoxO1 at three residues: Thr24, Ser256 and Ser319. The phosphorylation of FoxO1 results in its nuclear

exclusion and subsequent inactivation [224]. The stimulation-induced deactivation of FoxO1 is transient in all CD4<sup>+</sup> cells, but Treg cells restore FoxO1 nuclear localization more rapidly than Teff [218]. The rapid restoration of FoxO1 is crucial for normal Treg function as it prevents expression of inflammatory mediators. However, the mechanism that promotes the dephosphorylation of FoxO1 and its nuclear re-entry in T cells is unknown [218,228].

### **1.3.2 The phosphatase PP2A**

The majority of studies on FoxO1 regulation have focused on FoxO1 phosphorylation by Akt. However, the dephosphorylation of FoxO1 is equally important to its regulation. FoxO1 dephosphorylation has been studied in a B lymphocyte cell line and this study observed that the protein phosphatase 2A (PP2A) likely played a physiological role in dephosphorylating FoxO1 in this cell type (**Figure 1.6**) [229].

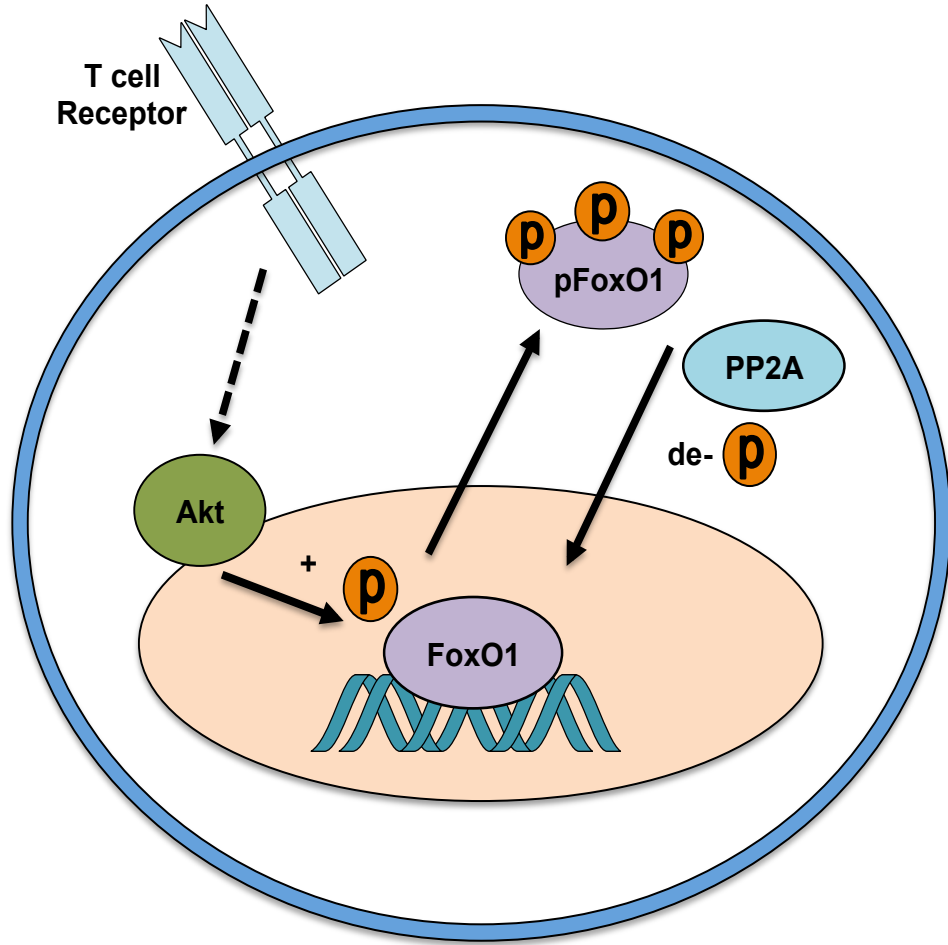
PP2A is not a single protein but rather a family of serine-threonine phosphatases that are ubiquitously expressed [230]. The PP2A family of holoenzymes consist of three sub-units: A, B and C. Sub-units A and B are regulatory sub-units while C is the catalytic component [231]. There are multiple isoforms of all the sub-units: A and C have two, highly similar isoforms ( $\alpha$  and  $\beta$ ) [230]; sub-unit B has 18 known isoforms and this sub-unit confers substrate specificity [231]. Therefore, studies that manipulate PP2A activity or function, target the A and/or C sub-units [229,232]. PP2A expression is tightly regulated by

a complex autoregulatory mechanism, making it uncommon to see any deviation in protein concentration [233].

Interestingly, a study found that patients with severe asthma had lower levels of PP2A protein in their peripheral blood monocytes (PBMCs) than healthy controls [234]. They further found that PP2A expression inversely correlated with disease severity and glucocorticoid sensitivity [234]. Lymphocytes partially comprise the PBMC fraction of blood and the decrease in PP2A expression prompted consideration that Treg cells in asthmatic patients might have decreased PP2A expression and decreased PP2A could result in decreased FoxO1 activity and subsequent Treg dysfunction.

**Figure 1.6: Proposed PP2A-FoxO1 axis in CD4 cells**

FoxO1 is localized to the nucleus in a dephosphorylated state. Following TCR stimulation, Akt phosphorylates FoxO1 leading to its cytosolic sequestration. Cytosolic FoxO1 is dephosphorylated by PP2A, exposing a nuclear localization sequence and permitting nuclear re-entry.



### 1.3.3 Allergic airway inflammation

Allergens are generally innocuous foreign antigens that, in most healthy individuals, elicit a protective, tolerogenic response [235,236]. However, the immune system can respond inappropriately to an allergen. Allergic inflammation occurs when the immune system develops an inflammatory response to an allergen [237].

One of the most common allergens and causes of allergic airway inflammation is house dust mite (HDM). HDM is one of the most potent allergens, as it has multiple allergenic components with different mechanisms of action. The HDM allergen DerP1 is a cysteine protease and the other major allergen, DerP2, binds to the pattern recognition receptor, TLR4 [238,239]. Additionally, HDM has endogenous endotoxin that can further activate TLR4 [240,241].

Upon exposure to HDM, DerP2 and endotoxin will bind to TLR4 and the protease activity of DerP1 disrupts the epithelial cell barrier [242]. The epithelial cells then produce IL-33 and TSLP, which activate dendritic cells and recruit innate lymphoid cells [243-245]. Activated dendritic cells migrate to the mediastinal lymph node (MLN), activate naïve T cells and drive the proliferation of allergen specific, Th2 cells [246]. Upon re-exposure to allergen, Th2 cells are recruited to the lung and produce IL-4, IL-13 and IL-5: the classic Th2 cytokines [247]. These cytokines drive IgE class switching, mucus hyper-secretion, smooth muscle reactivity and eosinophilia, which are all considered hallmarks of allergic

airway inflammation [248] (**Figure 1.7**). Chronic inflammation due to repeated exposure can ultimately cause allergic asthma [249].

In most individuals, this inflammatory cascade is suppressed by the regulatory components of the immune system, which elicit a complete tolerogenic response [208,250]. For reasons that are currently being investigated, allergic individuals do not develop tolerance, which allows the inflammatory response to propagate, seemingly unchecked by the regulatory components of the immune system [251].

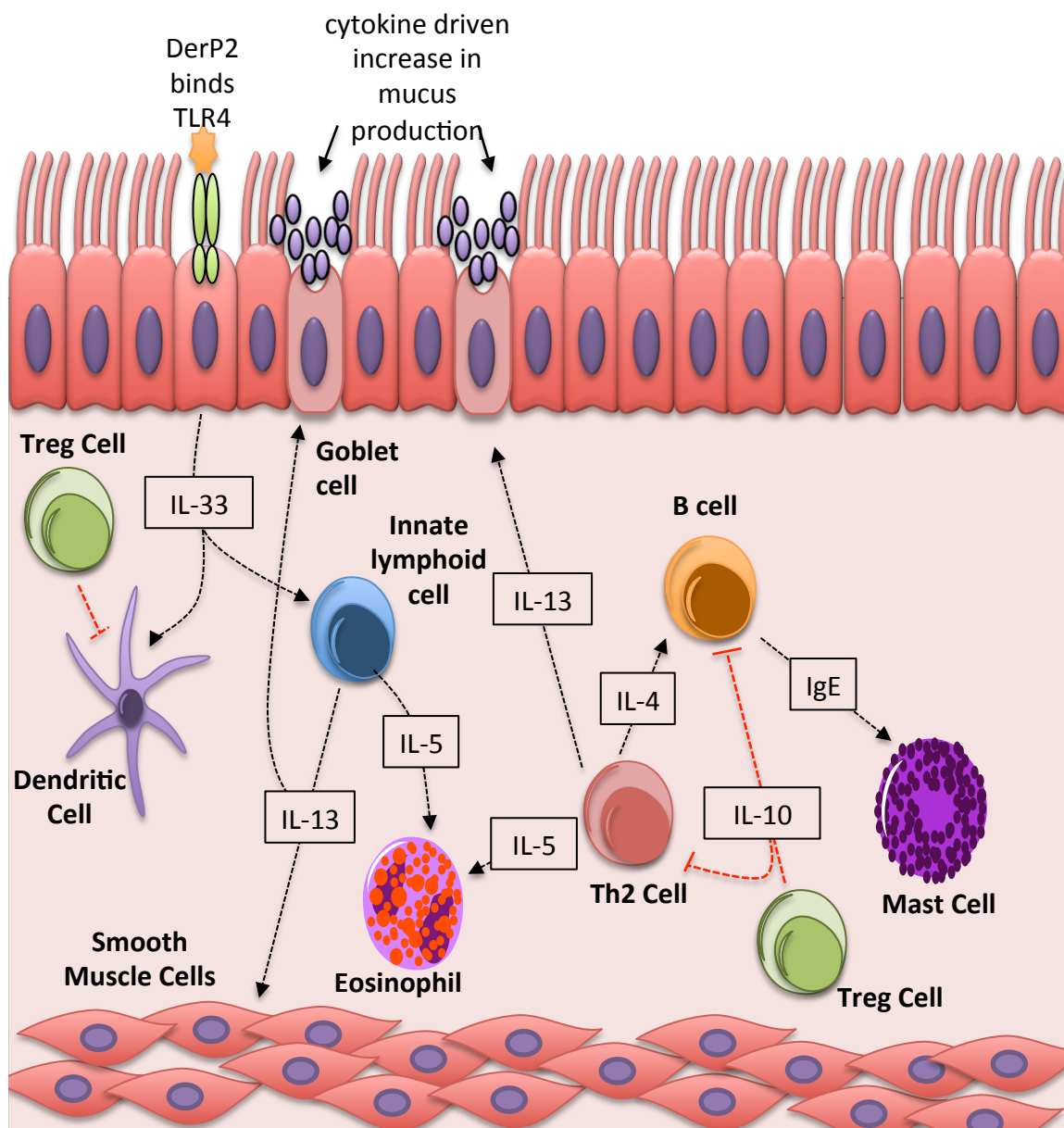
Thirty nine million people in the United States alone have been diagnosed with asthma and the prevalence is steadily increasing [252]. The rapid rise of asthma is thought to be critically linked to a simultaneous increase in the prevalence of allergy. At least 80% of asthmatics are predisposed to allergic hypersensitivity, and it is estimated that 50% of asthma attacks and asthma-related hospitalizations are caused by allergic reactions [253]. The common therapy for the control of asthma, beyond avoidance of any allergen or triggers, is dual treatment with a  $\beta$  agonist to promote bronchodilation and inhaled glucocorticoids to mediate local immune suppression [254]. However, the nearly 13 million patients suffering from asthma attacks each year, suggest that the control offered by these therapies is inadequate [252]. Some of the patients with recurrent attacks are characterized as glucocorticoid-resistant asthmatics. Interestingly, this subset of patients also exhibits dramatically impaired Treg function and decreased PP2A expression in their PBMCs, further establishing the

hypothesis that decreased PP2A expression might in fact cause Treg dysfunction [234,255,256].

**Figure 1.7: The inflammatory cascade in allergic airway inflammation**

The HDM allergen DerP2 binds to TLR4 expressed on the surface of airway epithelial cells, leading to release of inflammatory mediators that recruit innate lymphoid cells and activate dendritic cells. Activated dendritic cells drive Th2 differentiation in the lung-draining mediastinal lymph nodes. Th2 cells re-enter the lung upon re-exposure to allergen and promote IgE class switching on B cells, smooth muscle cell hyperreactivity and increased mucus production. Treg cells suppress this inflammatory cascade at multiple points.

## Pathways underlying allergic airway inflammation



## **1.4 Focus of this work and key hypotheses:**

This dissertation evaluates the molecular mediators that regulate the function of specialized phagocytes and Treg cells. Chapter II of this dissertation details our investigation into the role of PtdSer receptors MerTK and BAI1 in phagocytosis by both RPE and Sertoli cells. Specifically, we tested the hypothesis that PtdSer receptors might be redundant and can functionally compensate for one other. Indeed, we found that BAI1 is capable of compensating for MerTK in Sertoli cells, but not in the RPE, suggesting that PtdSer receptors function in tissue and context-specific manners. In Chapter III of this manuscript we tested the hypothesis that the phosphatase PP2A can regulate the activity of FoxO1 activity and, in turn, Treg cell functionality. We observed that while inhibition of PP2A leads to cytosolic sequestration of FoxO1 in Tregs, corresponding functional deficits in Treg cells were not seen after PP2A inhibition *ex vivo*. Since both FoxO1 and PP2A are linked to Treg function *in vivo*, our data suggest that *ex vivo* assays of Treg function do not always recapitulate *in vivo* phenotypes.

### **1.4.1 Publications arising from this work:**

**Penberthy KK;** Rival C; Shankman LS; Raymond MH; Zhang J; Perry JSA,<sup>†</sup> Han CZ; Lysiak JJ; Onengut-Gumuscu S; Palczewski K; Ravichandran KS. Differential requirement for phosphatidylserine receptors MerTK and BAI1 in specialized phagocytes. Manuscript submitted to Nature Communications.

Arandjelovic S; Perry JSA; **Penberthy KK**; Walk SF; Kim T; Chuang T;  
Cambré E; Onengut-Gomescu S; Gaultier A; Elewaut D; Kim M; Elliott MR;  
Ravichandran KS. Unexpected linkage of a cell clearance module to promoting  
inflammatory arthritis. Manuscript submitted to Science.

**Penberthy KK**; Buckley MW; Arandjelovic S; Ravichandran K. 2017. Ex vivo  
modulation of the FoxO1 phosphorylation state does not lead to dysfunction of  
regulatory T cells. PLoS ONE 12(3) e0173386

Lee CS; **Penberthy KK**; Wheeler KM; Juncadella IJ; Vandendabeele P; Lysiak  
JJ; Ravichandran KS. 2016. Boosting apoptotic cell clearance by colonic  
epithelial cells attenuates inflammation in vivo. 44(4) 807-820

**Penberthy KK**; Ravichandran KS. 2016. Apoptotic cell recognition receptors and  
scavenger receptors. Immunological Reviews. 269(1) 44-59

**Penberthy KK**; Juncadella IJ; Ravichandran KS. 2014. Apoptosis and  
engulfment by bronchial epithelial cells: implications for allergic airway  
inflammation. 11(S5) S259-62.

## Chapter II

### Context dependent compensation among phosphatidylserine recognition receptors

*This work has been submitted for review to Current Biology: Kristen K Penberthy, Claudia Rival, Laura S Shankman, Michael H Raymond, Jianye Zhang, Justin S A Perry, Claudia Z Han, Jeffrey J Lysiak, Suna Onengut-Gumuscu, Krzysztof Palczewski, Kodi S Ravichandran*

#### 2.1 Summary

Phagocytes typically express multiple receptors on their surface, which engage the lipid phosphatidylserine (PtdSer) that is exposed on apoptotic cells. A long-standing unanswered question is whether these receptors are interchangeable or if they play unique roles during cell clearance. Functional disruption or loss of the PtdSer receptor *Mertk* is associated with apoptotic corpse accumulation in the testes and degeneration of photoreceptors in the eye. Both of these phenotypes are linked to impaired phagocytosis by specialized phagocytes, the Sertoli cells of the testes and the retinal pigmented epithelium (RPE) of the eye. Here, we used a transgenic approach to overexpress the PtdSer receptor BAI1 in mice lacking MerTK (*Mertk<sup>-/-</sup>Bai1<sup>Tg</sup>*) to evaluate PtdSer receptor compensation *in vivo*. *Bai1* overexpression rescued Sertoli cell-mediated clearance of apoptotic germ cells in the testes of *Mertk<sup>-/-</sup>* mice. However, despite robust expression of BAI1 on the apical surface of the RPE in the *Mertk<sup>-/-</sup>* background, we observed no improvements in RPE phagocytosis or photoreceptor degeneration. To determine what makes MerTK critical to RPE function, we examined the visual cycle intermediates and

performed unbiased RNAseq analysis of RPE from *Mertk*<sup>+/+</sup> and *Mertk*<sup>-/-</sup> mice.

Prior to the onset of photoreceptor degeneration, *Mertk*<sup>-/-</sup> mice had less accumulation of retinyl esters (precursors of chromophore 11-*cis*-retinal) and dysregulation of a striking array of genes, including subsets related to phagocytosis, metabolism, and several linked to retinal disease in humans. Collectively, these genetic rescue experiments establish that not all phagocytic receptors are created equal, and that compensation among specific engulfment receptors is context and tissue dependent.

## 2.2 Introduction

Cell death is a crucial part of life. Each day, billions of cells in the human body undergo apoptotic cell death and must be cleared [24,39]. In many tissues, dying cells are cleared by phagocytes that engulf and digest the apoptotic corpse [24,94]. Impediments to apoptotic cell clearance can lead to chronic inflammation and autoimmunity [257,258]. Apoptotic cell clearance is stimulated upon apoptotic cell exposure of the 'eat-me' signal phosphatidylserine (PtdSer) and its subsequent recognition by PtdSer receptors on phagocytes [6,7]. Phagocytes express a multitude of PtdSer receptors, yet, despite extensive research on apoptotic cell recognition and clearance, it is unclear how these PtdSer receptors orchestrate cell clearance in a given phagocyte or tissue context [259].

PtdSer receptors include many different families of proteins including integrins, the BAI family of GPCRs, the TIM family, and the TAM family of receptor tyrosine kinases [24,39-44]. These protein families are structurally diverse and are related only by their shared ligand, PtdSer [24,94,259]. Given the importance of apoptotic cell clearance to health and homeostasis, it is not surprising that many different receptors have evolved. However, the loss of a single receptor often causes deficits in apoptotic cell clearance, suggesting that the presence of many receptors cannot be explained as a simple redundancy mechanism [41,42,52,257,258]. Thus, the question of whether PtdSer receptors are interchangeable or unique in cell clearance remains unclear. To address this question, we considered designing a mouse model in which one PtdSer receptor

is overexpressed in the absence of another in order to assess functional compensation *in vivo*.

In most tissues, evaluation of phagocytosis *in vivo* is complicated by the unpredictable timing of apoptosis and subsequent phagocytic events. Two exceptions to this rule are tissues where phagocytosis is mediated by 'specialized' phagocytes: the testes and the retina [94]. Specialized phagocytes are epithelial-derived, mitotically-quiescent cells [106,164]. Currently, two best known examples of specialized phagocytes are the retinal pigmented epithelium (RPE) of the eye and the Sertoli cells of the testes [94]. Sertoli cell phagocytosis is easily studied in the testes as apoptosis of developing germ cells occurs with sufficient regularity to quantify apoptotic corpse accumulation. Similarly, RPE phagocytosis is conducive to *in vivo* analysis as RPE phagocytosis is circadian-regulated and occurs daily around the time of light onset [134,181]. Furthermore, loss of a single PtdSer receptor, MerTK, leads to phagocytic defects in both Sertoli cells and the RPE [52]. *Mertk*<sup>-/-</sup> mice exhibit apoptotic corpse accumulation in the testes and profound retinal degeneration [52]. Thus, *Mertk*<sup>-/-</sup> mice are uniquely suited for *in vivo* evaluation of compensation among PtdSer receptors. Therefore, we overexpressed the PtdSer receptor BAI1 in *Mertk*<sup>-/-</sup> mice (*Mertk*<sup>-/-</sup>*Bai1*<sup>Tg</sup>).

Specialized phagocytes perform a multitude of supportive functions within the tissue. Though the testes and retina are highly disparate at first glance, Sertoli cells and RPE share several key features, including: epithelial derivation,

mitotic quiescence, formation of a blood-tissue barrier, maintenance of immunological privilege, and as stated above, phagocytosis [106,164]. As phagocytes, Sertoli cells are responsible for clearing germ cells that undergo apoptosis during spermatogenesis and the residual-body of cytoplasm that is removed from maturing sperm during spermiation [134,260]. RPE have a slightly different phagocytic function, unlike Sertoli cells which mediate corpse clearance, the RPE 'trim' the adjacent photoreceptors in a PtdSer dependent manner [174,178]. This RPE-mediated pruning of the photoreceptors occurs daily and is a waste-removal mechanism, removing the photo-oxidative byproducts that accumulate during phototransduction [174,189]. *Mertk*<sup>-/-</sup> mice are born with a full complement of photoreceptors but exhibit early-onset photoreceptor degeneration due to impaired phagocytosis (pruning) of photoreceptor outer segments (POS) [189,192].

Here, we show that BAI1 is capable of rescuing the phagocytic defects in *Mertk*<sup>-/-</sup> Sertoli cells. However, the phagocytic defect in *Mertk*<sup>-/-</sup> RPE is not compensated by transgenic overexpression of BAI1. When we evaluated the visual cycle (a function unique to RPE), we observed that MerTK expression impacted the visual cycle prior to the onset of retinal degeneration. In addition, we utilized the unbiased method of RNAseq to more broadly assess the role of MerTK in the RPE. Indeed, we observed that the expression of many genes, including those related to phagocytosis and metabolism and other forms of retinal disease, were dysregulated in *Mertk*<sup>-/-</sup> RPE prior to the onset of retinal

degeneration. Collectively, these findings suggest that PtdSer receptor functionality is contingent on tissue and context, and that while they can compensate for each other in certain contexts, they also have unique roles where they are not interchangeable.

## 2.3 Experimental Procedures

### 2.3.1 Mice

*Mertk*<sup>-/-</sup> mice were purchased from Jackson Laboratories (stock no: 011122 – B6;129-*Mertk*<sup>tm1Grl</sup>/J). *Bai1*<sup>Tg</sup> mice were previously generated by our lab on a C57Bl/6N background and then backcrossed with C57Bl/6J mice [86]. The *Bai1*<sup>Tg</sup> mice were screened for the RD8 mutation and were confirmed to be RD8 negative [261] *Mertk*<sup>-/-</sup> mice were crossed to *Bai1*<sup>Tg</sup> mice to generate the first generation of *Mertk*<sup>+/-</sup>*Bai1*<sup>Tg</sup> mice. Progeny from this initial cross were bred to the original *Mertk*<sup>-/-</sup> line from Jackson Laboratories. For line maintenance, *Mertk*<sup>+/-</sup>*Bai1*<sup>Tg</sup> progeny were crossed to the original *Mertk*<sup>-/-</sup> line from Jackson Laboratories. *Mertk*<sup>+/+</sup> and *Mertk*<sup>+/+</sup> *Bai1*<sup>Tg</sup> mice were generated by crossing *Mertk*<sup>+/-</sup> and *Mertk*<sup>+/-</sup> *Bai1*<sup>Tg</sup> siblings. Mice were maintained on a 14-10 h light-dark cycle. Animals for analysis were euthanized by CO<sub>2</sub> asphyxiation. All animal procedures were approved by and performed according to guidelines of the Institutional Animal Care and Use Committee (IACUC) at the University of Virginia.

### **2.3.2 RPE isolation for culture and gene expression analyses**

The RPE isolation protocol was previously described [262] Eyes were enucleated from P14 neonatal mice 2 hours after light onset. Globes were incubated in serum free DMEM (Corning) with 2% dispase (Worthington). Following incubation, eyes were washed 3 times in DMEM supplemented with 10% fetal bovine serum (FBS) (Gemini). Cornea, iris and lens were removed from each eyecup. The eyecups were incubated for 20 minutes at 37 °C in DMEM supplemented with 10% FBS. Following incubation, the neural retina was removed from each eyecup. The eyecup was tugged at opposite ends to release the RPE layer. RPE sheets were washed in  $\text{Ca}^{2+}$  /  $\text{Mg}^{2+}$  free HBSS (Gibco). RPE to be used for RT-PCR or RNAseq were lysed in 350  $\mu\text{L}$  of RLT buffer (Qiagen). RPE to be used for protein analysis were lysed in 40  $\mu\text{L}$  of RIPA buffer. Cultured primary RPE were re-suspended in DMEM supplemented with 10% FBS and non-essential amino acids (Corning) and plated on fibronectin coated chamber slides. RPE from both eyes were plated per well of 8-well chamber slides.

### **2.3.3 Immunoblotting**

Crude RPE lysates in RIPA buffer were sonicated 2 times for 10 s to shear DNA. Sonicated lysates were incubated at 37 °C in Laemmli sample buffer for 30 min.. Lysates were run on Any-kD stain free gels (Bio-Rad) and transferred to PVDF membranes. Membranes were blocked in Tris buffered saline with Tween 20 (TBS-T) with 5% milk for 1 h at room temperature. The following primary antibodies were used at 1:1000 dilution unless otherwise indicated: MerTK (R&D

#AF591), HA (Cell Signaling Technology, clone C29F4), Rac1 (Millipore, clone 23A8), Dock180 1:200 (Santa Cruz #6043 and #6167), ELMO2 (in-house[67]), and  $\beta$ -actin 1:100,000 (Sigma clone AC-15).

### 2.3.4 qRT-PCR

RNA was purified from cell lysates with RNeasy kit (Qiagen). cDNA was prepared with Superscript III kit (Thermo Fisher). The following Taqman probes (Thermo Fisher) were used for qPCR: *Bai1* (Mm00558144\_m1), *Bai1* human (Hs01105174\_m1), *Bai2* (Mm00557365\_m1), *Bai3* (Mm00657451\_m1), *Mertk* (Mm00434920\_m1), *Dock1* (Mm01269874\_m1), *Elmo2* (Mm01248046\_m1), *Elmo1* (Mm00519109\_m1), *Rac1* (Mm01201657\_m1), *Ano1* (Mm00724407\_m1), *Elovl1* (Mm01188316\_g1), *Acss2* (Mm00480101\_m1), *Fbln7* (Mm01336227\_m1),  *$\beta$ 2m* (Mm00437762\_m1), *Hprt* (Mm00446968\_m1), and *Slc4a4* (Mm01347935\_m1).

### 2.3.5 Eyecup dissection and ONL analysis

Central corneas of enucleated eyes were punctured with a 25-gauge needle. Eyes were submerged in Hartman's fixative (Sigma) and incubated for 1-3 h at room temperature. Following initial fixation, the cornea, iris and lens were removed. Eyecups were returned to fixative and incubated overnight at 4 °C. Eyecups were moved to 30% sucrose for cryo-protection and incubated at 4 °C until they sank. Eyecups were embedded in O.C.T. (Tissue-Tek) and flash frozen in an isobutane dry ice bath. Consistent orientation of the 'nasal-notch' during embedding was maintained to control eyecup orientation. Sagittal eyecup

sections were cut at 10  $\mu\text{m}$  thickness and sections transecting the optic cup were collected. Sections for ONL analysis were stained with Mayer's haematoxylin (Sigma) and eosin (Fisher) and tiled at 20x magnification on an Axio Imager.z1 (Zeiss) with Stereo Investigator software (MBF Biosciences). An image mask with 20 fixed measurement points was applied to eyecup images in Photoshop (Adobe). The ONL was measured at points indicated by the mask in ImageJ software (NIH).

### **2.3.6 In situ rhodopsin analysis**

P17-P21 mice were euthanized 1 h after light onset. Eyes were dissected, fixed and sectioned as described above. Eye sections were blocked in PBS (Corning) with 10% normal goat serum (Jackson ImmunoResearch) for 1 h at room temperature. Sections were stained overnight with rhodopsin antibody diluted 1:500 (Abcam clone Rho 4D2). AF647 conjugated secondary antibody was used to detect rhodopsin. Tiled images were acquired at 40x magnification on an Axio Observer.z1 microscope (Zeiss). The RPE layer was isolated in Photoshop (Adobe). Quantification of puncta was performed by automated particle count in ImageJ (NIH).

### **2.3.7 Flat mount preparation and staining**

Mice were euthanized between 4 and 6 weeks of age. Eyes were enucleated and the cornea, iris, lens and neural retina were removed. Eyes were cut at four points for flat mount 'clover' preparation and fixed for 1 h in PBS 4% paraformaldehyde (PFA) at room temperature. Flat mounts were blocked and

permeabilized in PBS 10% normal horse serum (Hyclone) and 0.1% Tween 20 then stained over night at 4 °C with anti-GFP antibody at 1:50 (Abcam #6673). Secondary antibody conjugated to AF488 was used to detect GFP staining. Flat mounts were then stained with anti-ZO-1 at 1:250 (Thermo Fisher #61-7300) for 1 h at room temperature. Secondary antibody conjugated to AF647 was used to detect ZO-1 staining. Images were acquired at 20x magnification on a confocal Axio Observer.z1 microscope (Zeiss).

### **2.3.8 Eyecup staining for HA**

Mice were euthanized between 4 and 6 weeks of age. Eyes were enucleated and the cornea, iris, lens, and neural retinas were removed. Eyecups were fixed for 1 h in PBS 4% PFA at room temperature then moved to 30% sucrose for cryo-protection and incubated at 4 °C until the eyecups sank. Eyes were embedded in O.C.T. Eyecups were sectioned at 10 µm and sections bisecting the optic cup were collected. Sections were blocked in PBS with 10% normal goat serum for 1 h at room temperature. Sections were stained overnight at 4 °C with anti-HA antibody 1:100 (Cell Signaling Technology clone C29F4). AF647 conjugated secondary antibody was used to detect staining (Thermo Fisher). Sections were then stained with biotin conjugated anti-ezrin antibody 1:100 (Thermo Fisher clone 3C12) overnight at 4 °C. AF488 conjugated streptavidin was used to detect ezrin staining (Thermo Fisher). Images were acquired on an Axio Imager.z2 microscope with Apotome (Zeiss).

### **2.3.9 Ex vivo RPE phagocytosis assays**

Primary RPE were isolated and cultured as described above on 8-well cover slips. *Ex vivo* phagocytosis assays were performed after 3-5 days in culture. Bovine photoreceptor outer segments (Invision Biosciences) were stained with CypHer 5e (GE Healthcare). Outer segments ( $1 \times 10^6$ ) were added to each well of RPE in a 300  $\mu$ L volume. An Axio Observer.z1 microscope with an incubation chamber was used to acquire images every 5 min. RPE were imaged for 3 h. 2 h still images were used to calculate phagocytic index, which was determined by the number of events per field. Phagocytic index was normalized to control in each experiment.

### **2.3.10 Testicular torsion**

Torsion surgery was performed as previously described [263]. The studies were performed in accordance with the 'Guiding Principles of the Care and Use of Research Animals' promulgated by the Society for the Study of Reproduction. The male mice were anesthetized with an intraperitoneal (IP) injection of a mixture of 6 mg /100 g of ketamine and 0.5 mg/100 g of xylazine. After the testes were exteriorized through a low ventral midline incision, the testes were released from the epididymo-testicular membrane through incising the gubernaculum. For torsion, the testis of right side was rotated 720° for 2 h, during which time it remained in the abdomen with a closed incision. For sham control, the testis was freed of the epididymo-testicular membrane and left in the abdomen. After 2 h, the incision was reopened, the testis was counter-rotated to the natural position,

the gubernaculum was rejoined, the testes were reinserted into the scrotum, and then the incision was closed. 24 h after operation, mice were euthanized. The testes were removed and fixed for 6 h in Bouin's fixative for paraffin embedding. Testicular cross sections were stained for cleaved caspase-3 at the University of Virginia Biorepository and Tissue Research Facility. Testicular cross sections were imaged at 20x with an Aperio Scanscope at the University of Virginia Biomolecular Analysis Facility and Shared Instrumentation Core. The number of apoptotic cells per tubule was determined for the entire cross section.

#### **2.3.11 Sertoli cell isolation and staining**

Testes from P11-P21 day-old mice were isolated and decapsulated. Tubules were dispersed in a solution of HBSS, 0.0625% Trypsin (Corning) 10  $\mu\text{g}/\text{mL}$  DNase (Sigma) for 20 min. at 37 °C then 0.00625% Soybean trypsin inhibitor (SBTI) (Sigma) was added and the supernatants were decanted. Tubules were re-suspended in HBSS with 1 M glycine, 2 mM EDTA, 0.0625% SBTI, and 10  $\mu\text{g}/\text{mL}$  DNase and incubated for 10 min. at room temperature. Suspensions were spun at 1000 RPM. Tubules were minced and re-suspended in HBSS with 1 mg/mL collagenase and 10  $\mu\text{g}/\text{mL}$  DNase in a shaking water bath at 37°C for 30 minutes. Tubule fragments were allowed to sediment at room temperature and re-suspended in HBSS with 15 U/mL hyaluronidase (Sigma) and 10  $\mu\text{g}/\text{mL}$  DNase and incubated in a shaking water bath at 37 °C for 30 min. Tubule fragments were centrifuged at 1000 RPM. Pellets are washed and re-

suspended in F12/DMEM (Corning) with 10% FBS, 1% PSQ 1% (Corning), sodium pyruvate (Corning), 10mM HEPES (Corning), 5  $\mu\text{g/mL}$  Transferrin (Sigma), 2.5 ng/mL epidermal growth factor (Gibco), 10  $\mu\text{g/mL}$  insulin (Gibco). Media was changed after 24 h of culture to remove floating germ cells. Sertoli cell cultures were passaged after 3-5 days to chamber slides for staining. Sertoli cells were fixed in PBS with 4% PFA for 30 min. at room temperature, blocked in PBS with 10% normal goat serum (Jackson Immunoresearch) and stained overnight in anti-BAI1 antibody 1:100 (R&D #AF4969).

### **2.3.12 Retinoid analysis**

P20-P21 mice were dark adapted overnight. Eyes were collected under dim red light and stored at  $-80\text{ }^{\circ}\text{C}$  until they were analyzed. Eyes were then homogenized in 10 mM sodium phosphate buffer, pH 8.0, containing 50% methanol (v/v) and 100 mM hydroxylamine. The resulting mixture was extracted twice with 4 ml of ethyl acetate. The combined organic layers were dried in vacuo, reconstituted in 400  $\mu\text{l}$  of hexanes, and 100  $\mu\text{l}$  of the extract was injected on to a normal-phase high-performance liquid chromatography (HPLC) (Agilent Sil, 5  $\mu\text{m}$ , 4.6  $\times$  250 mm; Agilent Technologies, Santa Clara, CA) in a stepwise gradient of ethyl acetate in hexanes (0–17 min, 0.6%; 17.01–42 min. 10%) at a flow rate of  $1.4\text{ ml}\cdot\text{min}^{-1}$ . Retinoids were detected by monitoring absorbance at 325 nm and quantified based on a standard curve representing the relationship between the amount of synthetic retinoid standard and the area under the corresponding chromatographic peak.

### **2.3.13 RNAseq**

RPE were isolated from littermate P14 mice 2 h after light onset. RNA was isolated with an RNeasy kit (Qiagen). An mRNA library was prepared using an Illumina TruSeq platform. The transcriptome was sequenced on a NextSeq 500 cartridge. The statistical software package R (version 3.3.2) was used for all analyses. The Bioconductor package DESeq2 was used for differential gene expression analysis of RNA-seq data. Heatmaps were created using the R package gplots via the heatmap.2 package. The R code used for bioinformatics analysis and heatmap generation is available upon request.

### **2.3.14 Statistics**

Statistics analysis was performed in GraphPad Prism 7.0. Statistical test used as indicated in the figure legends. A p-value  $<0.05$  was considered statistically significant.

## 2.4 Results

### 2.4.1 BAI1-transgene can reduce corpse accumulation in the testes of *Mertk*<sup>-/-</sup> mice

To determine whether distinct PtdSer receptors play unique roles in the process of engulfment, we designed a genetic approach to determine whether the overexpression of one receptor could rescue for the loss of another. We crossed MerTK null (*Mertk*<sup>-/-</sup>) and BAI1-overexpressing (*Bai1*<sup>Tg</sup>) mice to generate *Mertk*<sup>-/-</sup>*Bai1*<sup>Tg</sup> mice. The rationale for choosing *Mertk*<sup>-/-</sup> mice is that they have two *in vivo* phenotypes associated with impaired phagocytosis. First, *Mertk*<sup>-/-</sup> mice exhibit accumulation of apoptotic germ cells in the testes due to impaired Sertoli cell phagocytosis [52,93]. Second, these mice exhibit profound retinal degeneration due to failed clearance of POS by the RPE [24,39,189]. We elected to overexpress *Bai1* in an attempt to rescue the phenotypes in *Mertk*<sup>-/-</sup> mice, as BAI1 overexpression can enhance PtdSer-dependent apoptotic cell clearance by multiple phagocytes, including intestinal epithelial cells and Sertoli cells. Furthermore, *Bai1*<sup>Tg</sup> mice had been previously generated and characterized [24,42,86,94,131].

Sertoli cells are the specialized phagocytes of the testes and promote routine phagocytosis of apoptotic germ cells. Sertoli cells utilize both BAI1 and MerTK during the phagocytosis of apoptotic germ cells [52,86]. *Mertk*<sup>-/-</sup> mice exhibit accumulation of apoptotic corpses at baseline [52] and *Bai1*<sup>-/-</sup> mice exhibit apoptotic corpse accumulation following testicular torsion [86]. Furthermore,

*Bai1<sup>Tg</sup>* mice exhibit a decrease in corpse accumulation following torsion [86]. Given the endogenous role for MerTK and BAI1 in the testes, we initially tested PtdSer receptor compensation in *Mertk<sup>-/-</sup>Bai1<sup>Tg</sup>* mice in the context of Sertoli cells.

Prior to evaluating apoptotic cell accumulation in the testes, we confirmed that Sertoli cells endogenously express *Mertk*, *Bai1* and components of the BAI1 signaling pathway: *Elmo1*, *Dock180* and *Rac1* (**Figure 2.1a**) [259]. Importantly, expression of the BAI1 signaling pathway did not differ between *Mertk<sup>+/+</sup>* and *Mertk<sup>-/-</sup>* mice (**Figure 2.1a**). In addition, we confirmed that the *Bai1<sup>Tg</sup>* was expressed by Sertoli cells and that the BAI1-Tg properly localized to the surface of *Mertk<sup>-/-</sup>* Sertoli cells (**Figure 2.1b**). To determine whether *Bai1* overexpression could rescue phagocytic deficits in *Mertk<sup>-/-</sup>* Sertoli cells, we evaluated apoptotic corpse accumulation in testes that had undergone surgical torsion and those that underwent sham surgery [263,264]. Corpse accumulation was quantified by counting cleaved-caspase 3 positive cells in testicular cross-sections (**Figure 2.1c, 2.2**). As was previously reported, *Mertk<sup>-/-</sup>* mice exhibited a slight but significant increase in apoptotic corpse accumulation at baseline (**Figure 2.1c, 2.1d**) [52]. While the *Mertk<sup>-/-</sup>Bai1<sup>Tg</sup>* mice trended towards fewer apoptotic corpses at baseline, this was not statistically significant (**Figure 2.1d**). Analysis of injured testes revealed that *Mertk<sup>-/-</sup>* mice had substantially more apoptotic cell accumulation than control littermates (**Figure 2.1c, 2.1d**). Interestingly, corpse accumulation in *Mertk<sup>-/-</sup>Bai1<sup>Tg</sup>* mice was significantly decreased compared to

*Mertk*<sup>-/-</sup> mice. In fact, the corpse numbers in *Mertk*<sup>-/-</sup>*Bai1*<sup>Tg</sup> mice were reduced to the number in *Mertk*<sup>+/+</sup> mice (**Figure 2.1c, 2.1d**). These data suggest that *Bai1* overexpression can rescue phagocytic defects in *Mertk*<sup>-/-</sup> Sertoli cells.

**Figure 2.1: *Bai1*<sup>Tg</sup> rescues accumulation of apoptotic corpses post-torsion**

(a) Sertoli cell expression of *Bai1*, BAI1 signaling pathway genes, and *Mertk* were analyzed by quantitative RT-PCR. Sertoli cells were isolated from *Mertk*<sup>+/+</sup> (n=4) and *Mertk*<sup>-/-</sup> (n=2) mice and were cultured for 3 days to expand them prior to RNA isolation.

(b) Representative images of isolated Sertoli cells from *Mertk*<sup>-/-</sup> and *Mertk*<sup>-/-</sup> *Bai1*<sup>Tg</sup> mice were stained for BAI1 to confirm surface expression of the *Bai1*<sup>Tg</sup>.

(c) Mice (8-12 weeks-old) underwent testicular torsion surgery to induce ischemic injury. Testicular cross sections from sham and torsion testes were stained for cleaved caspase 3 (CC3) (black arrowheads). Images are of representative tubule cross sections from matched sham and torsion testes.

(d) The number of CC3 positive cells per tubule cross section was determined by analyzing the entire testicular cross section. Each mouse is represented by an individual data point within the bar. Statistical analysis was performed with a Wilcoxon rank-sum test. \* $p < 0.05$ , \*\*\* $p < 0.001$ .

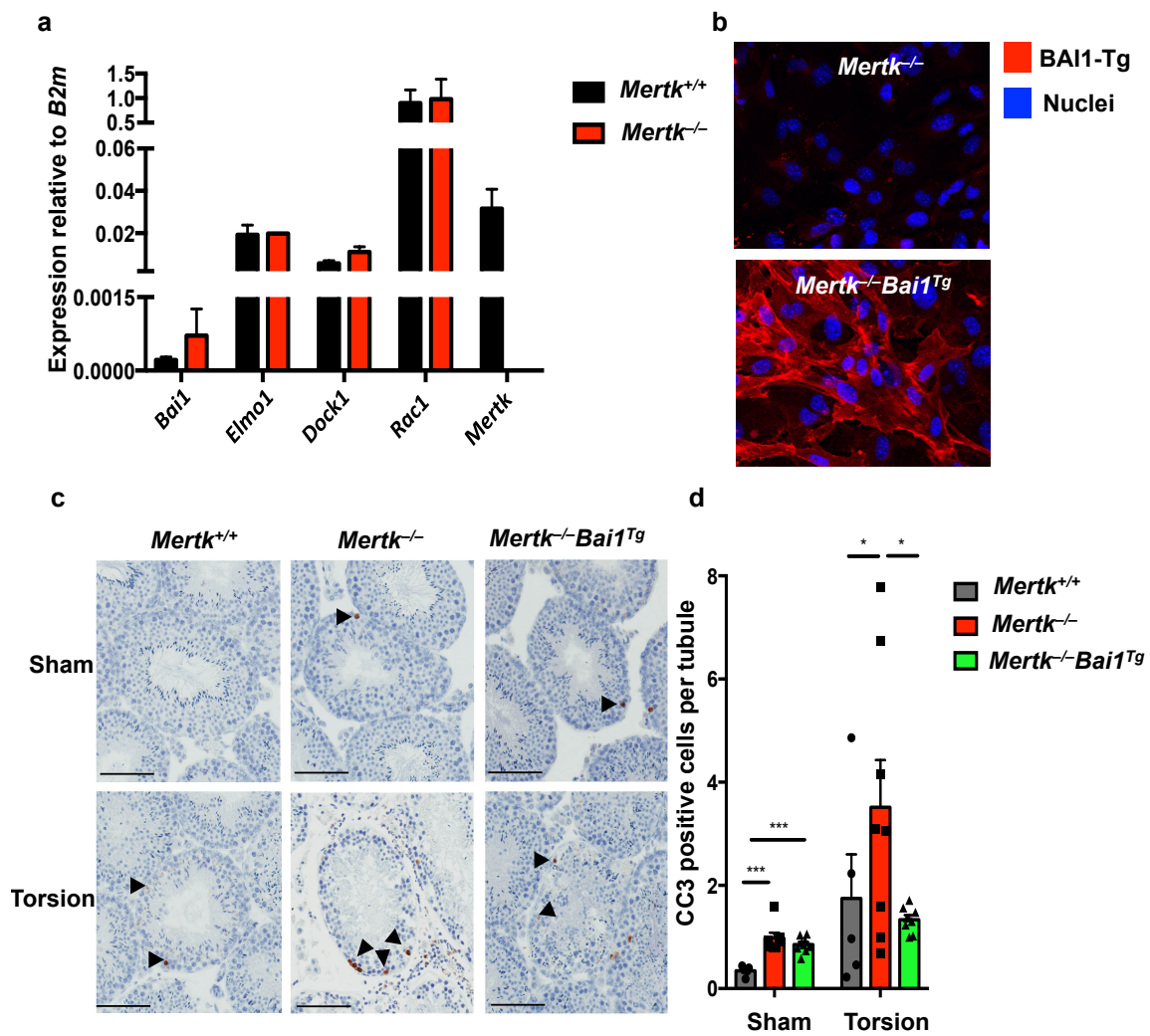
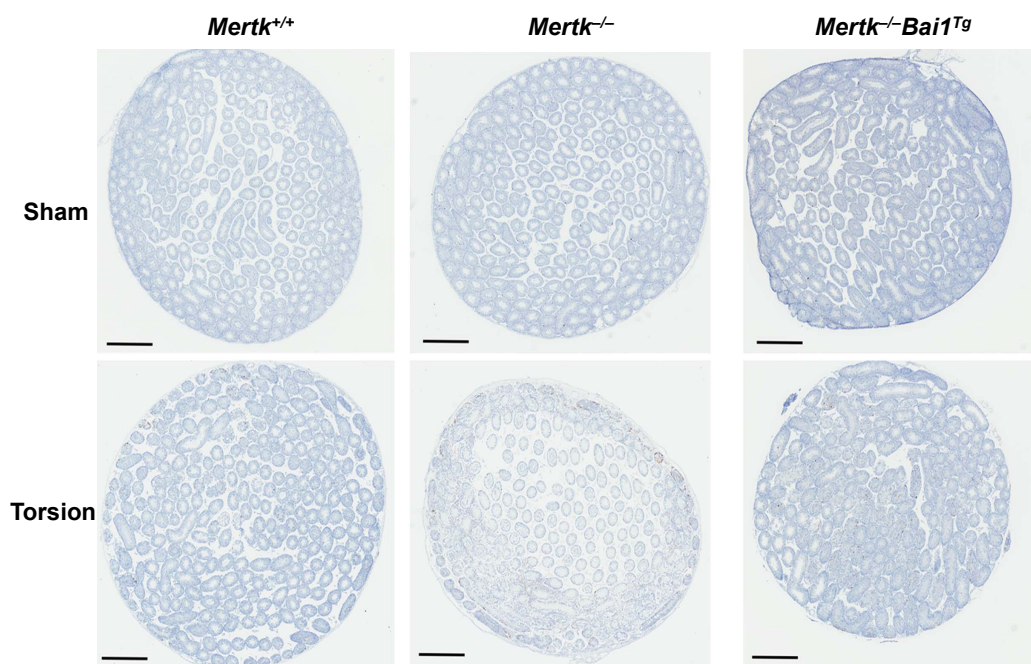


**Figure 2.2: Testicular cross sections**

Representative scans of testicular cross sections from sham and torsion testes.

Scans were magnified 20x and CC3+ cells were counted. Scale bar = 700  $\mu\text{m}$ .



### 2.4.2 RPE from *Mertk*<sup>-/-</sup>*Bai1*<sup>Tg</sup> mice express the *Bai1*<sup>Tg</sup> and BAI1 signaling pathway

*Mertk*<sup>-/-</sup> mice exhibit profound retinal degeneration that is the result of failed clearance of POS by the RPE [183,189]. Previous studies have established that POS expose PtdSer that is subsequently recognized by the RPE [178]. *Mertk* is highly expressed by the RPE and is crucial for POS clearance [183,189,192]. Since the RPE do not express BAI1 endogenously (**Figure 2.3a**), we tested whether the components of the BAI1 signaling pathway are present within the RPE. We isolated RPE from *Mertk*<sup>+/-</sup> and *Mertk*<sup>-/-</sup> mice and analyzed expression of the BAI1 signaling components ELMO, Dock180 and Rac1 by RT-PCR and immunoblotting (**Figure 2.4a, 2.4b**). Importantly, we found that ELMO2, Dock180 and Rac1 were all expressed. Furthermore, expression of BAI1 signaling components did not differ between RPE from *Mertk*<sup>+/-</sup> and *Mertk*<sup>-/-</sup> mice as assessed by both RNA and protein (**Figure 2.4a, 2.4b**), suggesting that BAI1 could theoretically function in the RPE.

We next assessed *Bai1*<sup>Tg</sup> expression and localization within the RPE. The *Bai1*<sup>Tg</sup> mouse construct contains three separate methods to detect expression in situ (**Figure 2.4c**). First, the *Bai1*<sup>Tg</sup> construct includes an IRES-driven GFP, which allows visualization of the transcriptional activity at the *Bai1*<sup>Tg</sup> locus. To assess GFP expression in RPE, we prepared RPE flat mounts from *Mertk*<sup>+/-</sup> *Bai1*<sup>Tg</sup> and *Mertk*<sup>-/-</sup> *Bai1*<sup>Tg</sup> mice and imaged GFP by confocal microscopy (**Figure 2.4d**). The GFP expression pattern appears uniform across the RPE layer in both

*Mertk*<sup>+/-</sup>*Bai1*<sup>Tg</sup> and *Mertk*<sup>-/-</sup>*Bai1*<sup>Tg</sup> mice. On average, 45% of the area in each 20x field is GFP positive (data not shown). Importantly, no GFP signal was detected in mice lacking the *Bai1*<sup>Tg</sup> (**Figure 2.4d**). Second, the *Bai1*<sup>Tg</sup> is derived from the human *Bai1* cDNA [86]. Despite being highly homologous to mouse BAI1 at the protein level and indistinguishable in functional assays [42,189], human *Bai1* transcript can be distinguished from the murine transcript by RT-PCR. Human *Bai1* was readily detected in the RPE of *Mertk*<sup>+/-</sup>*Bai1*<sup>Tg</sup> and *Mertk*<sup>-/-</sup>*Bai1*<sup>Tg</sup> but not littermate control mice (**Figure 2.4e**). Third, the *Bai1*<sup>Tg</sup> construct has an N-terminal HA-tag, which facilitates detection of the *Bai1*<sup>Tg</sup> protein. The HA-BAI1 protein was readily detected in the extracts of isolated RPE cells by immunoblotting (**Figure 2.4f**).

RPE cells are highly polarized and the apical microvilli mediate the phagocytosis of photoreceptor outer segments. Therefore, to assess whether the *Bai1*<sup>Tg</sup> protein was properly localized on the apical surface in a location similar to MerTK [192], we stained for the HA-tag in eyecup cross sections. HA-BAI1 showed apical localization and co-localized with ezrin, a cytoskeletal protein enriched in microvilli (**Figure 2.4g**). Furthermore, HA-BAI1 was detected on the apical RPE surface of both *Mertk*<sup>+/-</sup>*Bai1*<sup>Tg</sup> and *Mertk*<sup>-/-</sup>*Bai1*<sup>Tg</sup> mice. These data suggested that RPE cells in the *Mertk*<sup>-/-</sup>*Bai1*<sup>Tg</sup> mice express the *Bai1*<sup>Tg</sup>, and that the BAI1 protein localizes to the region of the RPE that mediates phagocytosis.

To examine whether there are signals initiated by the BAI1 transgene within the RPE, we performed RNAseq on *Mertk*<sup>+/+</sup> and *Mertk*<sup>+/+</sup>*Bai1*<sup>Tg</sup> mice to

identify genes likely altered by the *Bai1<sup>Tg</sup>*. Significant transcriptional changes were noted in 63 genes from the *Bai1<sup>Tg</sup>* mice. When we focused on genes previously associated with BAI1, such as cholesterol homeostasis, axonal growth and synaptogenesis [131,265,266], we identified 10 genes with functions that are associated with the aforementioned processes (**Figure 2.3b**). These data suggest that BAI1 is not only expressed by RPE cells at the correct location, but can also signal to induce transcriptional changes in RPE cells.

**Figure 2.3: *Bai1<sup>Tg</sup>* influences gene transcription in RPE despite the lack of endogenous *Bai1***

(a) RPE expression of *Bai1*, *Bai2* and *Bai3* was assessed by quantitative RT-PCR in *Mertk<sup>+/+</sup>* mice (n=2). *Mertk* expression was also evaluated for comparison. Cortex was used as a positive control for *Bai* family expression.

(b) RNAseq was performed on *Mertk<sup>+/+</sup>* and *Mertk<sup>+/+</sup>Bai1<sup>Tg</sup>* RPE. Genes related to different BAI1 functions were annotated in the heatmap and annotated gene function is noted on the right.

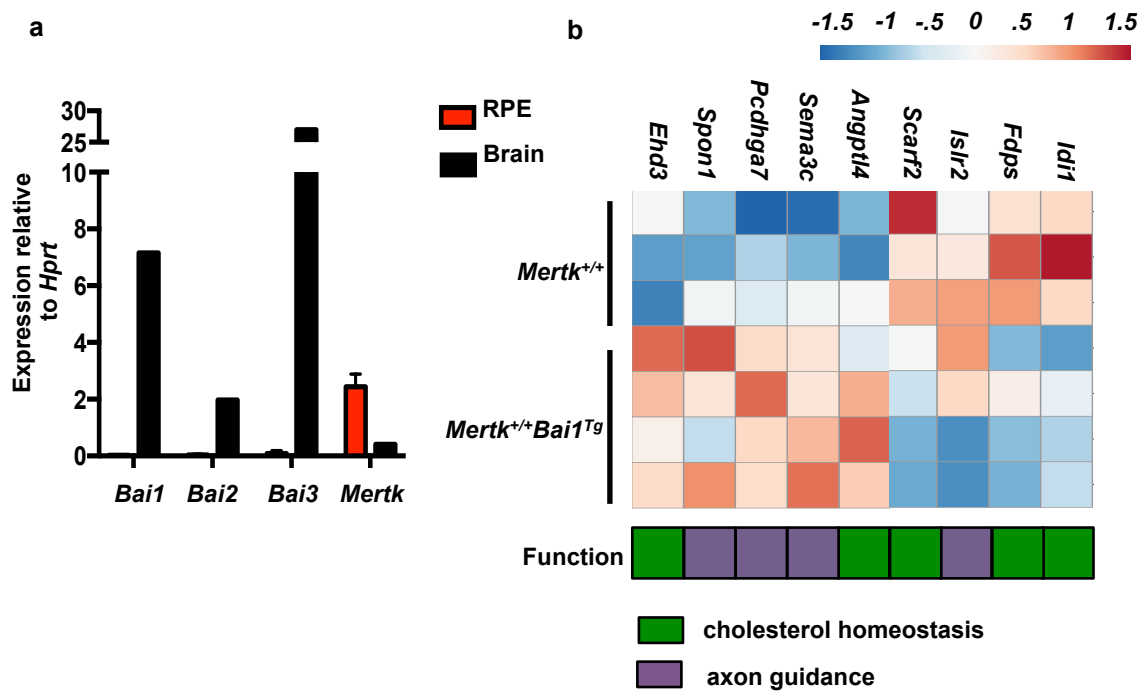


**Figure 2.4: RPE express components of BAI1-signaling pathway and *Bai1<sup>Tg</sup>***

(a) Expression of the BAI1 signaling pathway was analyzed by quantitative RT-PCR in RPE isolated from P14 *Mertk<sup>+/-</sup>* and *Mertk<sup>-/-</sup>* mice.

(b) Immunoblot analysis of BAI1 signaling pathway in RPE whole cell lysates isolated from P14 mice. Left panel shows representative immunoblots for Mer, Dock180, Elmo2 and Rac. Right panel shows combined densitometry analysis of immunoblots from n=3 mice per genotype. For densitometry analysis, band volumes were normalized to an actin loading control and band densities in *Mertk<sup>-/-</sup>* were then normalized to *Mertk<sup>+/-</sup>* for comparison across multiple blots.

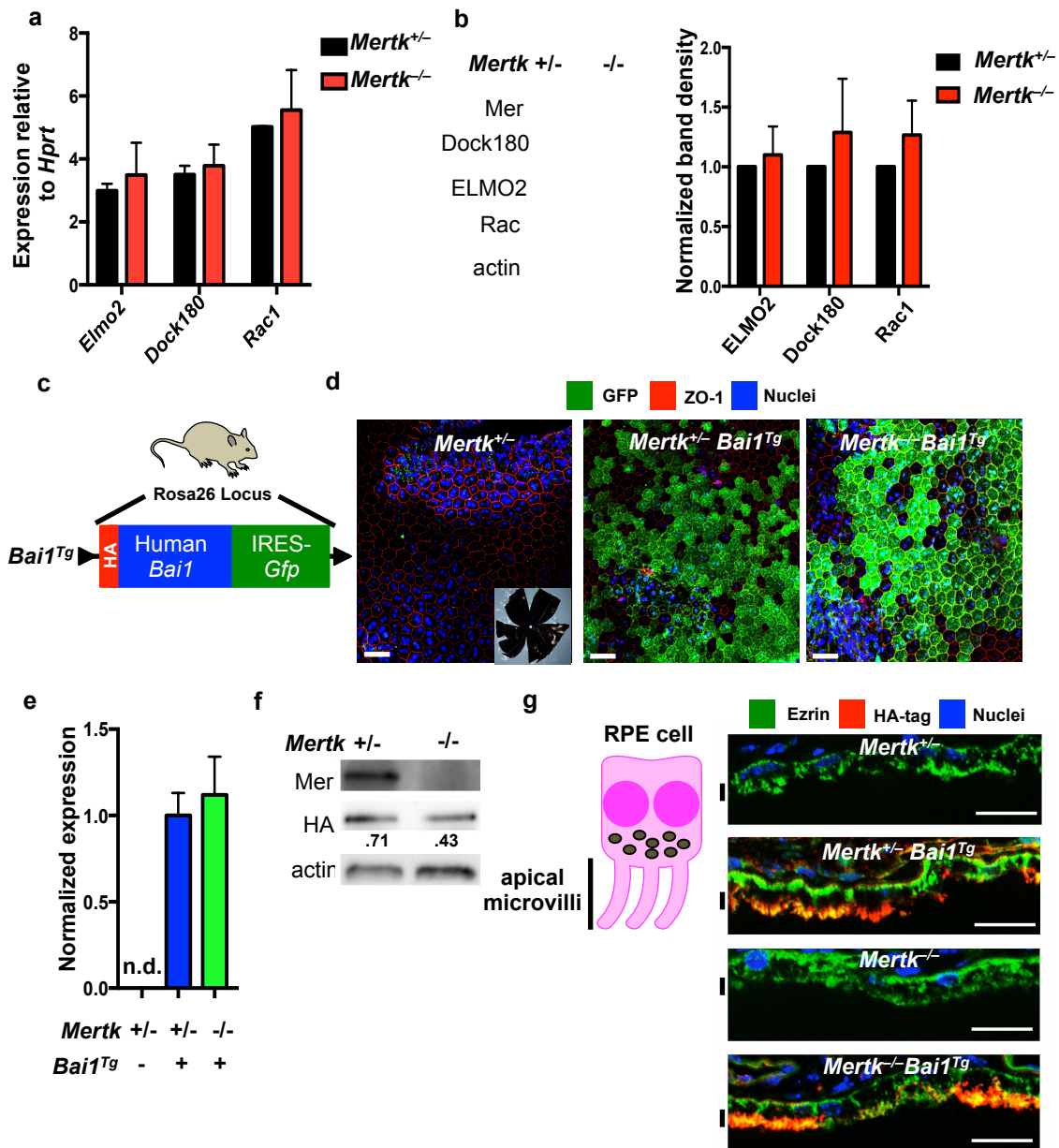
(c) Schematic of *Bai1<sup>Tg</sup>* insertion in the Rosa26 locus indicating the N-terminal HA-tag in red and IRES-GFP in green.

(d) GFP expression was analyzed in RPE flat mount preparations at 20x magnification. Inset image in the left panel shows a representative flat mount at 1.2x magnification. White scale bars in images are 50  $\mu$ m. Images are representative of n=2 mice per genotype.

(e) qRT-PCR analysis of *Bai1<sup>Tg</sup>* expression in *Mertk<sup>+/-</sup>Bai1<sup>Tg</sup>* (n=9) and *Mertk<sup>-/-</sup>Bai1<sup>Tg</sup>* (n=3) RPE isolated on P14. n.d. = not detected.

(f) Immunoblot analysis of HA-tag (*Bai1<sup>Tg</sup>*) in RPE whole cell lysates isolated from P13-P14 mice. Immunoblot shown is representative of n=2 experiments.

**(g)** HA staining and localization was analyzed in eyecups at 40x magnification. Neural retinas were removed prior to fixation and staining. Black lines next to the figure align with apical microvilli of RPE. Scale bars are 20  $\mu\text{m}$ .



### 2.4.3 *Mertk*-linked retinal degeneration is not rescued by BAI1

We next assessed the retinal degeneration in *Mertk*<sup>-/-</sup>*Bai1*<sup>Tg</sup> mice. Photoreceptors in *Mertk*<sup>-/-</sup> mice begin to show signs of overgrowth at post-natal day 17 and exhibit highly disorganized POS 35 days after birth [189,192]. Degeneration of the photoreceptor layer begins soon afterwards and previous reports have demonstrated that most photoreceptors are lost by 12 weeks of age [51,189,192]. To assess retinal degeneration, we collected sagittal sections of eyes that transect the optic cup (where the optic nerve meets the retina) (**Figure 2.5a, 2.5b**). Inspection of central retinas from 12 week-old *Mertk*<sup>-/-</sup> and *Mertk*<sup>-/-</sup>*Bai1*<sup>Tg</sup> revealed equivalent degeneration of the outer nuclear layer (ONL) consisting of photoreceptor nuclei. Importantly, *Mertk*<sup>+/-</sup>*Bai1*<sup>Tg</sup> retinal cross sections exhibited normal retinal architecture suggesting that the retinal structure was not adversely affected by transgenic *Bai1* expression (**Figure 2.4a**).

ONL thickness is not equivalent across the retina and degeneration is not necessarily homogeneous [51,92]. To standardize the measurement of ONL across the entire section, we adapted a previously described technique [51] and measured the ONL thickness at 20 standardized points across the 'inferior-superior' axis of the retinal section (**Figure 2.5b**). We measured ONL thickness in mice at 8 and 12 weeks of age (**Figure 2.5c**). At 8 weeks of age, both *Mertk*<sup>-/-</sup> and *Mertk*<sup>-/-</sup>*Bai1*<sup>Tg</sup> mice exhibited moderate degeneration across the entire inferior-superior axis (**Figure 2.5c**). By 12 weeks of age, retinal degeneration had progressed in both *Mertk*<sup>-/-</sup> and *Mertk*<sup>-/-</sup>*Bai1*<sup>Tg</sup> mice (**Figure 2.5c**). As

previously reported [51,92], degeneration was more severe in the superior than the inferior retina (**Figure 2.5d, 2.5e**). Importantly, degeneration was equivalent between *Mertk*<sup>-/-</sup> and *Mertk*<sup>-/-</sup>*Bai1*<sup>Tg</sup> animals. Collectively, these data indicate that overexpression of *Bai1* did not rescue retinal degeneration resulting from the loss of *Mertk*.

For analysis of ONL degeneration we facilitated littermate comparison by using *Mertk*<sup>+/-</sup> and *Mertk*<sup>-/-</sup> mice as previous studies demonstrated that the retinas of *Mertk*<sup>+/-</sup> mice are indistinguishable from *Mertk*<sup>+/+</sup> mice [51,192]. Importantly, we also confirmed that *Mertk*<sup>+/-</sup> mice exhibited no retinal degeneration as late as 16 weeks of age (**Figure 2.6a**), despite decreased expression of MerTK in *Mertk*<sup>+/-</sup> relative to *Mertk*<sup>+/+</sup> animals (**Figure 2.6b, 2.6c**).

## Figure 2.5: *Bai1<sup>Tg</sup>* does not reduce retinal degeneration in

### *Mertk<sup>-/-</sup>* mice

(a) H&E stained eyecup sections that transect the optic cup were imaged from the different genotypes at 20x magnification.

(b) An image mask was applied to the images in Photoshop marking the regions to be measured (white dashes overlaid on ONL). Image is a representative eyecup with the overlaid image mask. Scale bar is 500  $\mu\text{m}$ .

(c) ONL measurements were taken at the indicated points (according to the image mask) along the inferior-superior axis of the retina. The left panel includes measurements from 8 week-old *Mertk<sup>+/-</sup>* (n=3) *Mertk<sup>+/-</sup>Bai1<sup>Tg</sup>* (n=5), *Mertk<sup>-/-</sup>* (n=10) and *Mertk<sup>-/-</sup>Bai1<sup>Tg</sup>* (n=13) mice. Right panel shows measurements from 12 week-old *Mertk<sup>+/-</sup>* (n=6) *Mertk<sup>+/-</sup>Bai1<sup>Tg</sup>* (n=8), *Mertk<sup>-/-</sup>* (n=6) and *Mertk<sup>-/-</sup>Bai1<sup>Tg</sup>* (n=10) mice. Statistical analysis by 2-way ANOVA showed no difference between *Mertk<sup>+/-</sup>* and *Mertk<sup>+/-</sup>Bai1<sup>Tg</sup>* mice or *Mertk<sup>-/-</sup>* and *Mertk<sup>-/-</sup>Bai1<sup>Tg</sup>* mice at any time point. Asterisks indicate the difference between genotypes as measured by 2-way ANOVA. \*\*\*\*p<0.0001

(d) Images of the ONL in the inferior retina (25% measurement mark) and the superior retina (75% measurement mark) from representative mice.

(e) Quantification of the difference in ONL thickness in inferior retina (25% measurement mark) and the superior retina (75% measurement mark) at 12 weeks of age. Significance was determined using a Wilcoxon rank-sum test.

\*p<0.05, \*\*p<0.01, \*\*\*\*p<0.0001

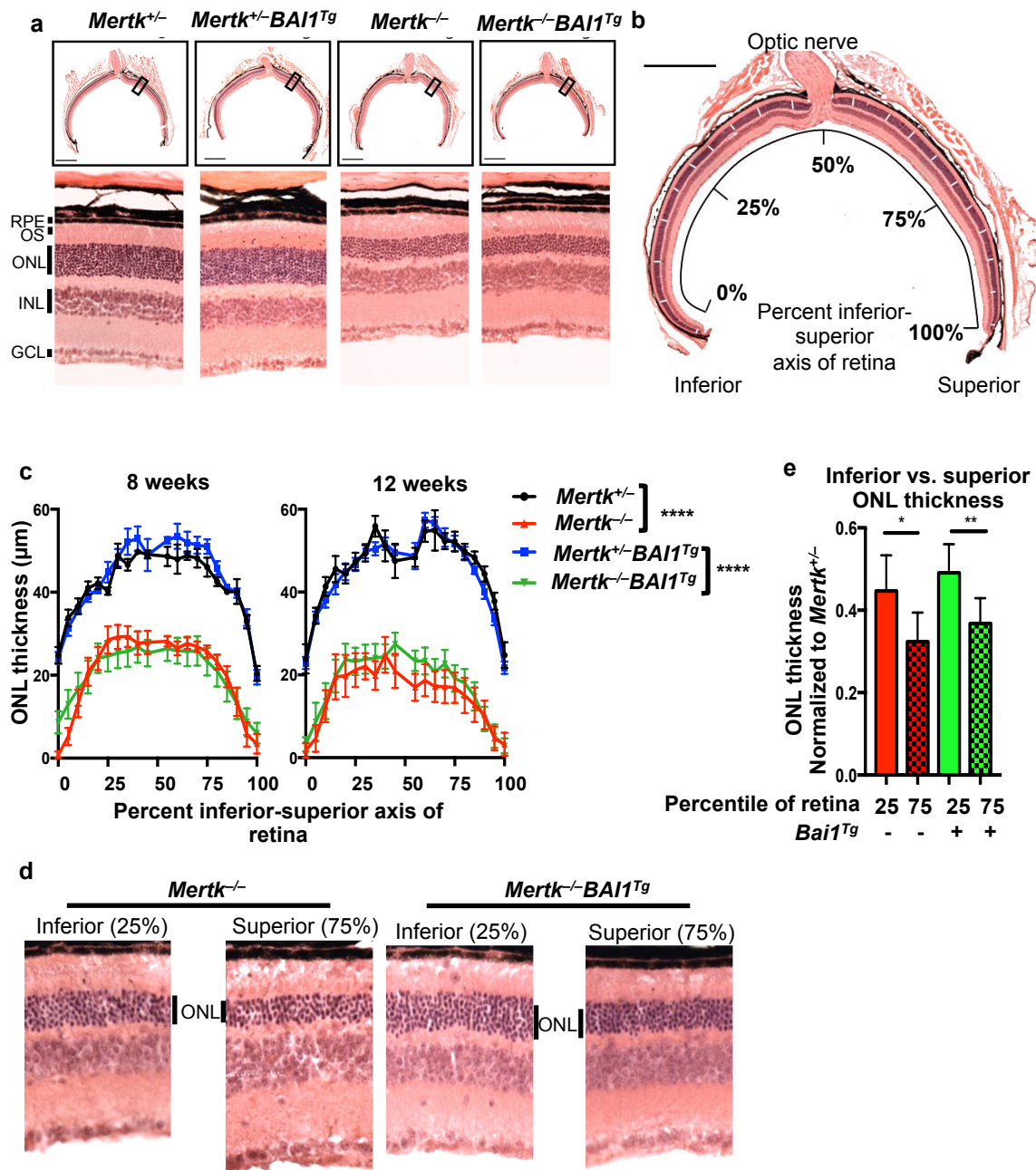


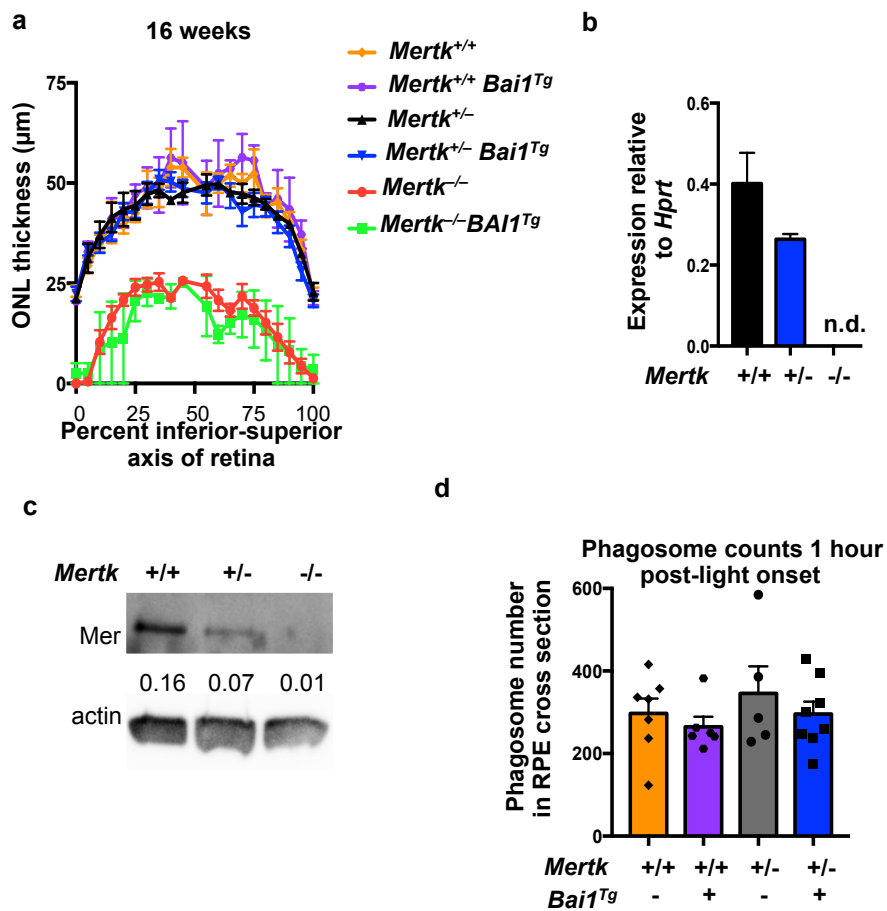
**Figure 2.6: *Mertk*<sup>+/+</sup> and *Mertk*<sup>+/-</sup> mice display no phenotypic differences in retinal degeneration and phagocytosis**

**(a)** ONL thickness was measured in *Mertk*<sup>+/+</sup> (n=3), *Mertk*<sup>+/+</sup>*Bai1*<sup>Tg</sup> (n=2), *Mertk*<sup>+/-</sup> (n=4), *Mertk*<sup>+/-</sup>*Bai1*<sup>Tg</sup> (n=7), *Mertk*<sup>-/-</sup> (n=4) and *Mertk*<sup>-/-</sup>*Bai1*<sup>Tg</sup> (n=2) mice at 4 months of age.

**(b)** *Mertk* expression in the RPE of *Mertk*<sup>+/+</sup> (n=2), *Mertk*<sup>+/-</sup> (n=2) and *Mertk*<sup>-/-</sup> (n=2) mice was evaluated by quantitative RT-PCR and

**(c)** immunoblotting. Immunoblot shown is representative of 2 experiments.

**(d)** Eyes from P17-P21 *Mertk*<sup>+/+</sup>, *Mertk*<sup>+/+</sup>*Bai1*<sup>Tg</sup>, *Mertk*<sup>+/-</sup>, *Mertk*<sup>+/-</sup>*Bai1*<sup>Tg</sup> mice were isolated at 1 h after light onset. Eyes were sectioned and stained for rhodopsin. Rhodopsin puncta in the RPE, referred to as phagosomes, were quantified by automated particle count in ImageJ. Symbols within the bars represent the average particle count from the left and right eyes of one mouse.



#### 2.4.4 BAI1-transgene does not promote phagocytosis in the RPE

Retinal degeneration in *Mertk*<sup>-/-</sup> mice is attributed to decreased phagocytosis of POS. Therefore, we analyzed RPE phagocytosis of POS in *Mertk*<sup>-/-</sup> and *Mertk*<sup>-/-</sup>*Bai1*<sup>Tg</sup> mice. Unlike most *in vivo* phagocytic events, RPE phagocytosis is readily analyzed due to its temporal regulation (around light onset) and because the content of the phagosomes (rhodopsin) can be visualized [189,267]. The rate and amount of phagocytosis is a dual function of phagocyte efficiency and the ratio of targets to phagocytes. Since *Mertk*<sup>-/-</sup> mice exhibit photoreceptor degeneration, the number of POS targets decreases as degeneration progresses. Therefore, decreases in RPE phagocytosis after the onset of degeneration could be due to the inefficient uptake by the RPE or a decreased target to phagocyte ratio. To ensure that any observed changes in phagocytosis were due to RPE phagocytic efficiency, we analyzed mice prior to the onset of retinal degeneration, at P17-P21 days of age. Importantly, analysis of ONL thickness at this age confirmed that degeneration in *Mertk*<sup>-/-</sup> and *Mertk*<sup>-/-</sup>*Bai1*<sup>Tg</sup> mice had not yet begun (**Figure 2.7a**).

To quantify phagocytosis, we harvested eyes 1 h after light onset and immunostained sagittal-eye sections for rhodopsin (**Figure 2.7b, white arrows**). Importantly, rhodopsin puncta are degraded over time and thus are mostly absent 8 h after light onset, suggesting that these puncta are not artifacts of sectioning or staining (**Figure 2.7b**). Quantification of puncta at 1 h post-light onset revealed a striking decrease in rhodopsin puncta in the RPE of *Mertk*<sup>-/-</sup>

mice relative to *Mertk*<sup>+/-</sup> mice. However, neither *Mertk*<sup>+/-</sup>*Bai1*<sup>Tg</sup> nor *Mertk*<sup>-/-</sup>*Bai1*<sup>Tg</sup> mice exhibited differences in the number of puncta compared to their respective controls (**Figure 2.7c**). Furthermore, neither the loss of *Mertk* nor overexpression of BAI1 affected phagosome trafficking in RPE, as indicated by basolateral localization of phagosomes (**Figure 2.8**). BAI1 overexpression was previously shown to enhance phagocytosis in WT epithelial cells (both *in vitro* and *in vivo*) [86]. However, BAI1 was unable to enhance phagocytosis in *Mertk*<sup>+/+</sup> mice and importantly, the number of puncta in *Mertk*<sup>+/+</sup> mice were equivalent to the number seen in *Mertk*<sup>+/-</sup> (**Figure 2.6d**). Collectively, these data suggest that *Bai1*<sup>Tg</sup> expression is unable to rescue the RPE phagocytic defect observed in *Mertk*<sup>-/-</sup> mice.

We attempted to dissect RPE phagocytosis further by using an *in vitro* culture system, which would allow better target ratio modifications and the use of pharmacological agents to test additional hypotheses. We developed an *in vitro* culture and phagocytosis system for primary RPE cells that would allow monitoring of phagocytosis by real-time imaging. Time-lapse microscopy at the appropriate resolution necessitated culturing RPE cells on cover glass. The cultured RPE cells exhibited hexagonal architecture with clear ZO-1 staining (indicative of tight junctions) at the cell boundaries. In addition, staining for the Na<sup>+</sup>/K<sup>+</sup> ATPase was apparent on the apical surface, suggesting that RPE cells were polarizing appropriately (**Figure 2.9a**). Bovine POS were labeled with the pH sensitive dye CypHer 5e and used as targets for phagocytosis by RPE.

These POS also exposed PtdSer, as indicated by annexin V staining (**Figure 2.9b**). Labeled POS were added to RPE cultures and phagocytosis was monitored in real-time. Within 15-30 min. of POS addition to RPE cultures, CypHer-positive phagocytosis events were apparent in the RPE (**Figure 2.9c**).

Although our *in vitro* assay system could detect changes in phagocytosis, it did not recapitulate well-established *in vivo* phenotypes. We were able to detect changes in phagocytosis when the number of POS were increased (data not shown), and with inhibition of the kinase ROCK (via the drug Y27632, a well-established means of enhancing cell clearance) [57,268] (**Figure 2.9d**). However, we surprisingly did not observe a phagocytic defect in *Mertk*<sup>-/-</sup> RPE, nor did we observe a significant phagocytic enhancement in RPE expressing the *Bai1*<sup>Tg</sup> (**Figure 2.9e**). Since this assay did not recapitulate the decreased phagocytosis in *Mertk*<sup>-/-</sup> RPE, we were unable to use it to assess MerTK-specific mechanisms of RPE phagocytosis.

**Figure 2.7: *Bai1*<sup>Tg</sup> does not enhance RPE phagocytosis**

(a) Eyes were isolated from P17-P21 mice 1 h after light onset. ONL measurements were completed as described above. Measurements were taken along the inferior-superior axis at the indicated points from *Mertk*<sup>+/-</sup> (n=2), *Mertk*<sup>+/-</sup>*Bai1*<sup>Tg</sup> (n=5), *Mertk*<sup>-/-</sup> (n=5), and *Mertk*<sup>-/-</sup>*Bai1*<sup>Tg</sup> (n=4) mice. No significant difference was found between any genotypes by 2-way ANOVA.

(b) Eyecups isolated 1 h after light onset (top panel) were stained for rhodopsin and nuclei (Hoechst). The entire eyecup was imaged at 40x (top panel, inset). Rhodopsin staining is robust in the outer segments (OS) of the photoreceptors. Rhodopsin puncta are apparent in the RPE layer (white arrowheads). Bottom panel shows representative staining from an eyecup isolated 8 h after light onset.

(c) Rhodopsin puncta in the RPE, referred to as phagosomes, were quantified in ImageJ by an automated particle count. Particle size was constrained from 0.5  $\mu\text{m}$  to  $\infty$  and minimum circularity was restricted to 0.2. Symbols within the bars represent the average particle count from the left and right eyes of one mouse. Significance was determined by one-way ANOVA. Multiple comparison analysis was corrected with a post-hoc Tukey's test.

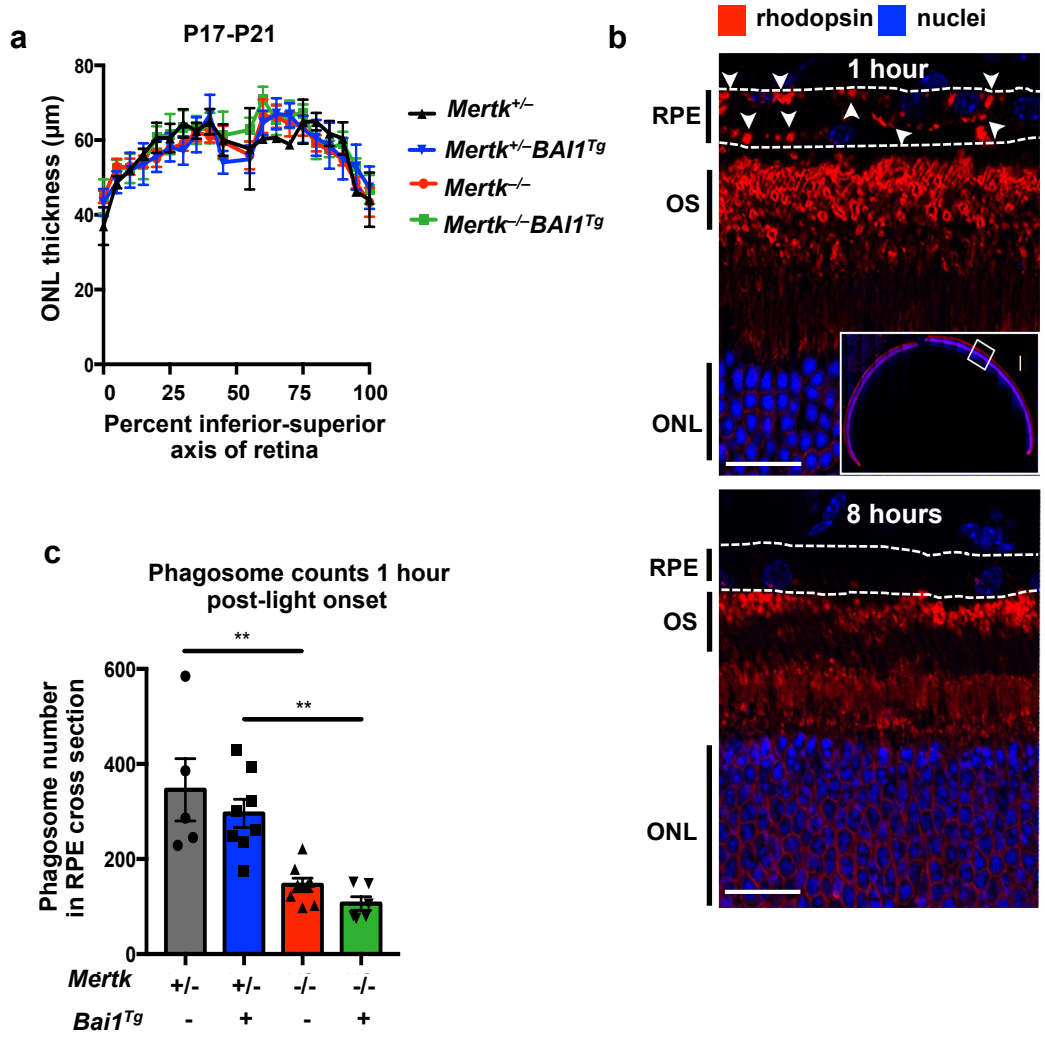


**Figure 2.8: *Bai1*<sup>Tg</sup> does not influence apical-basolateral localization of phagosomes**

Eyecups isolated at 1 hour and 8 h after light onset were stained for rhodopsin and nuclei. Entire eye cups were imaged at 40x and phagosome localization was compared. Representative images from the central retina are shown. Dotted lines indicate RPE boundaries. White scale bars are 20 $\mu$ M. Rhodopsin punctae are indicated by white arrowheads.

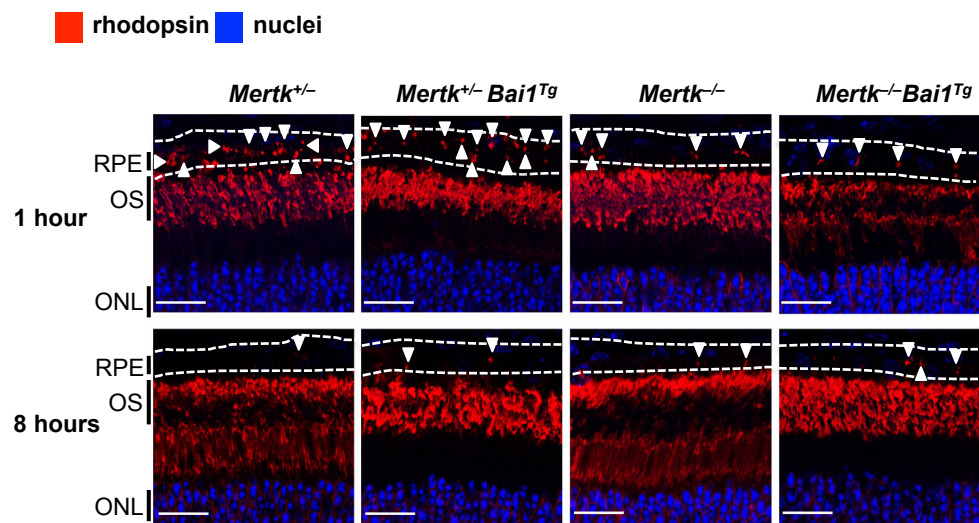


**Figure 2.9: Ex vivo RPE phagocytosis assays do not recapitulate in vivo phenotypes**

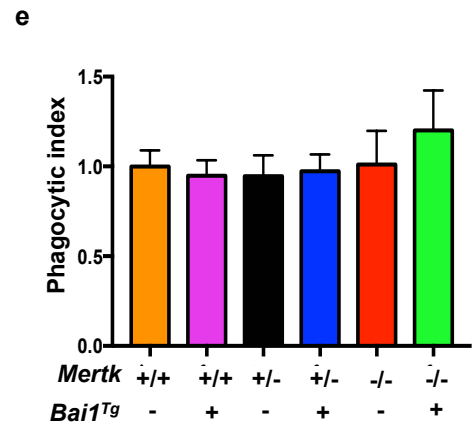
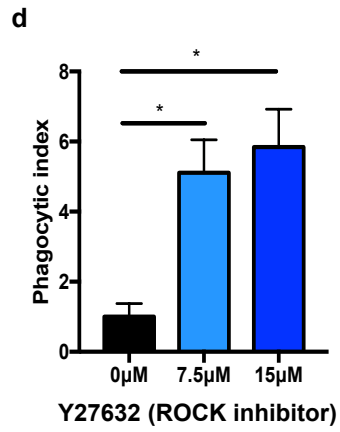
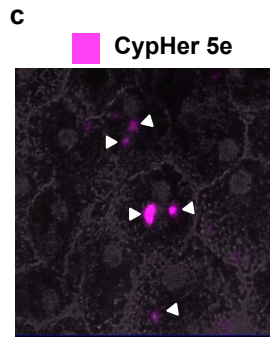
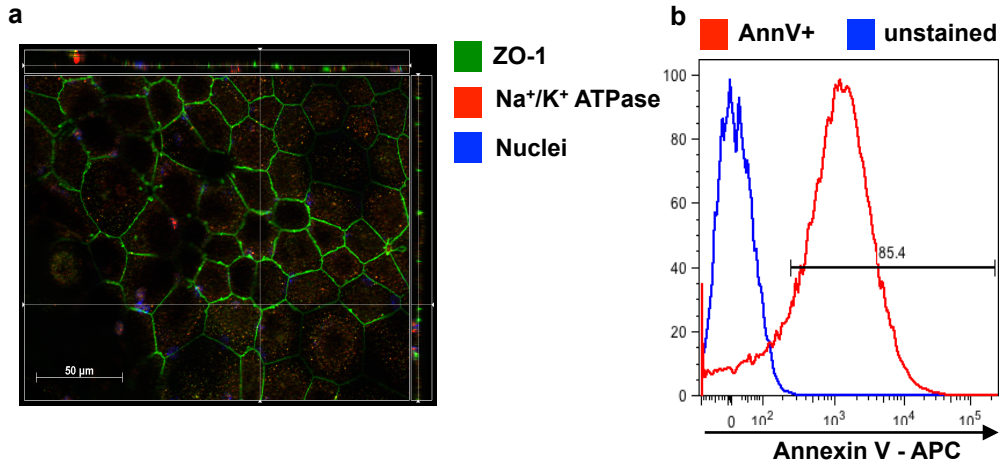
(a) RPE were isolated from P11-P14 mice and plated on coverglass for live imaging. RPE architecture and polarization were assessed by staining for the tight junction marker ZO-1 and the apical Na/K ATPase.

(b) Bovine POS were stained with annexin V to confirm PtdSer exposure.

(c) Representative field from phagocytosis assay at a 2 h time point. White arrowheads indicate CypHer 5e+ puncta.

(d) RPE cultures were pre-treated with ROCK inhibitor Y27632 for 2 hours prior to POS addition. ROCK inhibitor remained in culture for the duration of the phagocytosis assay. Phagocytic index was calculated based on the number of CypHer+ events per field at 2 hours and normalized to control. Data were compiled from 2 experiments with a total of n=2 mice per treatment. Data plotted are from all fields and bars show standard deviation. Significance determined by Wilcoxon rank-sum test. \* p<0.05

(e) Phagocytic index was calculated based on the number of CypHer+ events per field at 2 hours and normalized to WT. Data were compiled from 4 independent experiments with a minimum of n=3 mice per genotype.



#### 2.4.5 *Mertk*<sup>-/-</sup> mice exhibit diminished retinyl ester accumulation prior to the onset of degeneration

Because *Bai1*<sup>Tg</sup> expression could rescue phagocytic deficits in *Mertk*<sup>-/-</sup> Sertoli cells but not RPE, we asked whether MerTK influences RPE-specific functions beyond phagocytosis. One critical function of the RPE is recycling the inactive form of vitamin A (all-*trans*-retinol) to the light-reactive chromophore 11-*cis*-retinal. This process is known as the visual or retinoid cycle [269]. Failure to generate 11-*cis*-retinal leads to visual impairment due to decreased phototransduction [269]. It was previously reported that by the peak of retinal degeneration at 3 months, *Mertk*<sup>-/-</sup> mice have increased retinyl esters (stored form of vitamin A and precursors to 11-*cis*-retinal) and substantially decreased 11-*cis*-retinal [270]. As these results could be due to either the absence of MerTK or the ongoing retinal degeneration, we assessed whether the loss of *Mertk* affects the visual cycle prior to the onset of retinal degeneration (**Figure 2.10a**).

High-performance liquid chromatography was used in a blinded assay to quantify all-*trans*-retinyl esters and 11-*cis*-retinal in the eyes of dark-adapted mice at P21 (prior to degeneration but after significant retinal maturation) [189,192,271,272]. Retinyl esters are notoriously difficult to extract and quantify, thus we developed a novel procedure that allows extraction and quantification of the esters with more than 90 percent accuracy. Interestingly, we found that all-*trans*-retinyl ester levels were significantly lower in *Mertk*<sup>-/-</sup> relative to WT mice (**Figure 2.10b**). However, there was no difference in levels of the chromophore

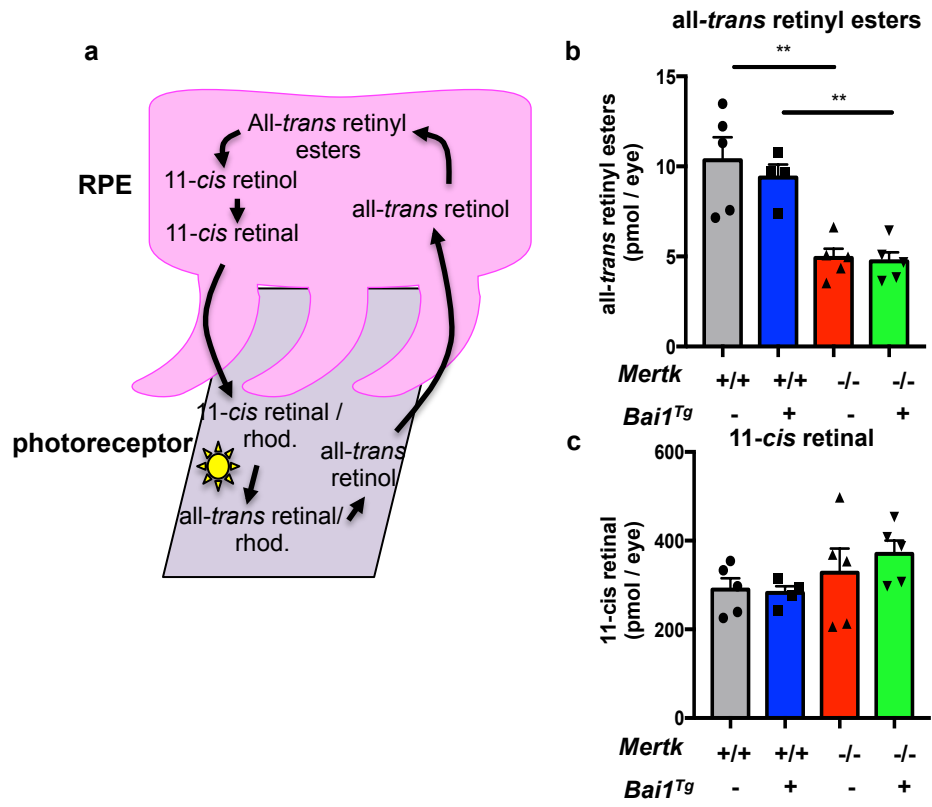
11-*cis*-retinal, likely reflecting the absence of retinal degeneration at this time point (**Figure 2.10c**). Retinyl esters are a form of stored vitamin A; esterification to fatty acids prevents their release into the serum and extracellular space [273,274]. Diminished retinyl ester levels in *Mertk*<sup>-/-</sup> mice prior to the loss of photoreceptors suggest that *Mertk* influences processes beyond phagocytosis, possibly by directly affecting the visual cycle enzymes or by altering the RPE metabolic profile in a manner that would decrease the availability of fatty acids for esterification. Interestingly, expression of the *Bai1*<sup>Tg</sup> did not elevate retinyl ester levels in *Mertk*<sup>-/-</sup> mice (**Figure 2.10b**).

**Figure 2.10: *Mertk*<sup>-/-</sup> mice have reduced retinyl ester accumulation**

**(a)** Schematic of the visual (retinoid) cycle that occurs in RPE (pink) and POS (gray).

**(b)** P20-P21 mice were dark adapted overnight and HPLC analysis was performed to quantify all-*trans*-retinyl esters and

**(c)** 11-*cis*-retinal. Individual points within bars are the average value for both eyes from one mouse. Statistical analysis was performed by one-way ANOVA. Multiple comparisons were corrected with a post-hoc Tukey's test. \*\*  $p < 0.01$ .



#### 2.4.6 *Mertk* regulates the gene expression program in the RPE

One of the first characterizations of *Mertk*<sup>-/-</sup> mice revealed that visual abnormalities measured by electroretinogram recordings manifest as early as P20 [189]. Deficits in phototransduction are due to impairments in generating and relaying the electrical response to light. The RPE contributes to phototransduction by regenerating the chromophore 11-*cis*-retinal, as the response to a photo-stimulus is initiated when the chromophore 11-*cis*-retinal is converted to all-*trans*-retinal, activating the visual pigmented rhodopsin [275]. As 11-*cis*-retinal levels were unaffected as late as P21 (when *Mertk*<sup>-/-</sup> mice are already reported to have deficits in phototransduction) we considered that MerTK might affect additional processes that could influence photoreceptor function.

To further explore how MerTK can influence RPE function, we chose an unbiased transcriptomics approach and performed RNAseq analysis of *Mertk*<sup>+/+</sup> and *Mertk*<sup>-/-</sup> RPE. The RPE was isolated at 14 days-of-age; at this time, mouse pups have opened their eyes but *Mertk*<sup>-/-</sup> mice do not yet exhibit photoreceptor overgrowth that could impact RPE gene expression [189,192].

Our RNAseq analysis identified 60 genes that were differentially regulated in *Mertk*<sup>-/-</sup> RPE (**Figure 2.11a**). Further analysis of this RNAseq dataset revealed 11 genes that have annotated functions related to either cytoskeletal rearrangement or endosomal maturation, two processes that are essential for phagocytosis (**Figure 2.11b**). The gene fibulin 7 (*Fbln7*), important for extracellular matrix adhesion and cytoskeletal rearrangement [276-278], has a

SNP associated with age-related macular degeneration and its expression is altered in patients with retinoschisis, a form of inherited retinal dystrophy [279,280]. qRT-PCR validation of the original library and an additional cohort of *Mertk*<sup>+/+</sup> and *Mertk*<sup>-/-</sup> mice confirmed that *Fbln7* is upregulated in *Mertk*<sup>-/-</sup> RPE (**Figure 2.11c**). We also selected the chloride channel anoctamin 1 (*Ano1*) and the bicarbonate transporter *Slc4a4* for further validation. Phagosome maturation culminates in acidification, which promotes the breakdown of the phagosome content [281]. Chloride flux across the lysosome membrane regulates lysosome acidification [282,283]. Although *Ano1* has yet to be implicated in the chloride flux across lysosomal membranes, it is a well-established calcium-activated chloride transporter [284] and RPE phagocytosis is accompanied by substantial calcium accumulation in the RPE [285]. *Slc4a4* is a bicarbonate transporter that is thought to regulate intracellular pH by electrogenic flux of H<sup>+</sup> and HCO<sub>3</sub><sup>-</sup> [286]. Interestingly, it has been proposed that these ion transporters work together in certain cellular processes [287]. We validated that *Slc4a4* and *Ano1* were reproducibly downregulated in both the original RPE samples as well as in an additional cohort of RPE (**Figure 2.11d**). These data suggest that MerTK can regulate the expression of various components of the phagocytic machinery.

Besides identifying a subset of genes with functions linked to phagocytosis, we identified an additional 11 genes related to cell metabolism (**Figure 2.11b**). Phagocytosis is a metabolically demanding process for the

phagocyte that requires significant ATP generation to mediate cytoskeletal rearrangement and digestion of cargo [288,289]. Though the genes we identified have yet to be directly linked to phagocytosis or phagocytic processes, we were intrigued by the sheer number of genes that were differentially regulated. We elected to further validate the fatty acid elongase, *Elovl1* and the acetyl CoA synthetase, *Acss2*. Indeed, the changes in *Elovl1* and *Acss2* were reproducible, in both the original library and a fresh cohort of *Mertk*<sup>+/+</sup> and *Mertk*<sup>-/-</sup> mice (**Figure 2.11e**). Interestingly, these changes might be reflected in the decreased retinyl ester accumulation in *Mertk*<sup>-/-</sup> RPE (**Figure 2.10b**). Overall, these data suggest that MerTK coordinates the phagocytic process at multiple levels from PtdSer binding to cytoskeletal reorganization and phagosome maturation, as well as coordinating metabolic changes that phagocytosis (and potentially the visual cycle) may require.

In addition to annotating the biochemical function of the genes identified in our RNAseq screen, we further assessed whether any were linked to retinal disease. Indeed, 9 genes identified in our RNAseq screen were linked to human retinal disease (**Table 2.1**). Five of these genes were also annotated under our metabolic subset (marked with \* in table) and three were annotated in our phagocytosis subset (marked with # in table) (**Figure 2.11b, Table 2.1**).

Two genes, *Gja1* and *Cyp27a1* have a striking monogenic association with oculodentodigital dysplasia and cerebrotendinous xanthomatosis respectively, both of which are associated with retinal abnormalities [290,291].

We also identified three genes with SNP associations to retinal disease:

*Ldlrad3*, *Fads2*, and *Fbln7* (**Table 2.1**). Five of the genes we annotated as being linked to retinal disease, were identified in the comparative toxicogenomics database, which infers gene-disease associations by examining curated associations between pharmacological agents, known diseases and the gene of interest [292,293]. These associations were further validated by experimental links to retinal disease or RPE function. Notably, *Slc4a4* has also been linked to retinitis pigmentosa (RP) type 17 and *Elovl1* is an endogenous inhibitor of the visual cycle enzyme RPE65, defects in which cause RP type 20 [173,294,295]. Overall, our findings suggest that the loss of MerTK (or possibly the resulting defect in phagocytosis) perturbs a multitude of genes, which might disrupt additional RPE functions.

**Figure 2.11: *MerTK* regulates multiple genes linked to phagocytosis and metabolism**

**(a)** RNAseq was performed on RPE isolated from P14 *Mertk*<sup>+/+</sup> (n=4) and *Mertk*<sup>-/-</sup> (n=4) mice 2 h after light-onset. DEseq2 analysis identified 60 genes that were differentially expressed according to p values adjusted for multiple comparisons. The log<sub>2</sub> fold change and -Log<sub>10</sub>padj values are plotted for all hits. Green dots represent genes that had a padj value <0.05. Blue dots indicate genes with a padj <0.05 and log<sub>2</sub> fold change >0.5.

**(b)** Further annotation of the differentially regulated genes revealed 11 linked to pathways important in phagocytosis and 11 linked to metabolic pathways. These genes and their expression changes are depicted in heat maps. Functional associations with regard to phagocytosis are indicated on the left.

**(c)** Genes related to cytoskeletal reorganization (graphs in green),

**(d)** genes related to phagosome maturation (graphs in yellow) and

**(e)** genes related to metabolism (graphs in purple) were selected for further validation by qRT-PCR. Validation studies were done with fresh RPE samples from P14 *Mertk*<sup>+/+</sup> (n=4) and *Mertk*<sup>-/-</sup> (n=4) and original library preparations. Significance was calculated by student's T-test. \*p<.05

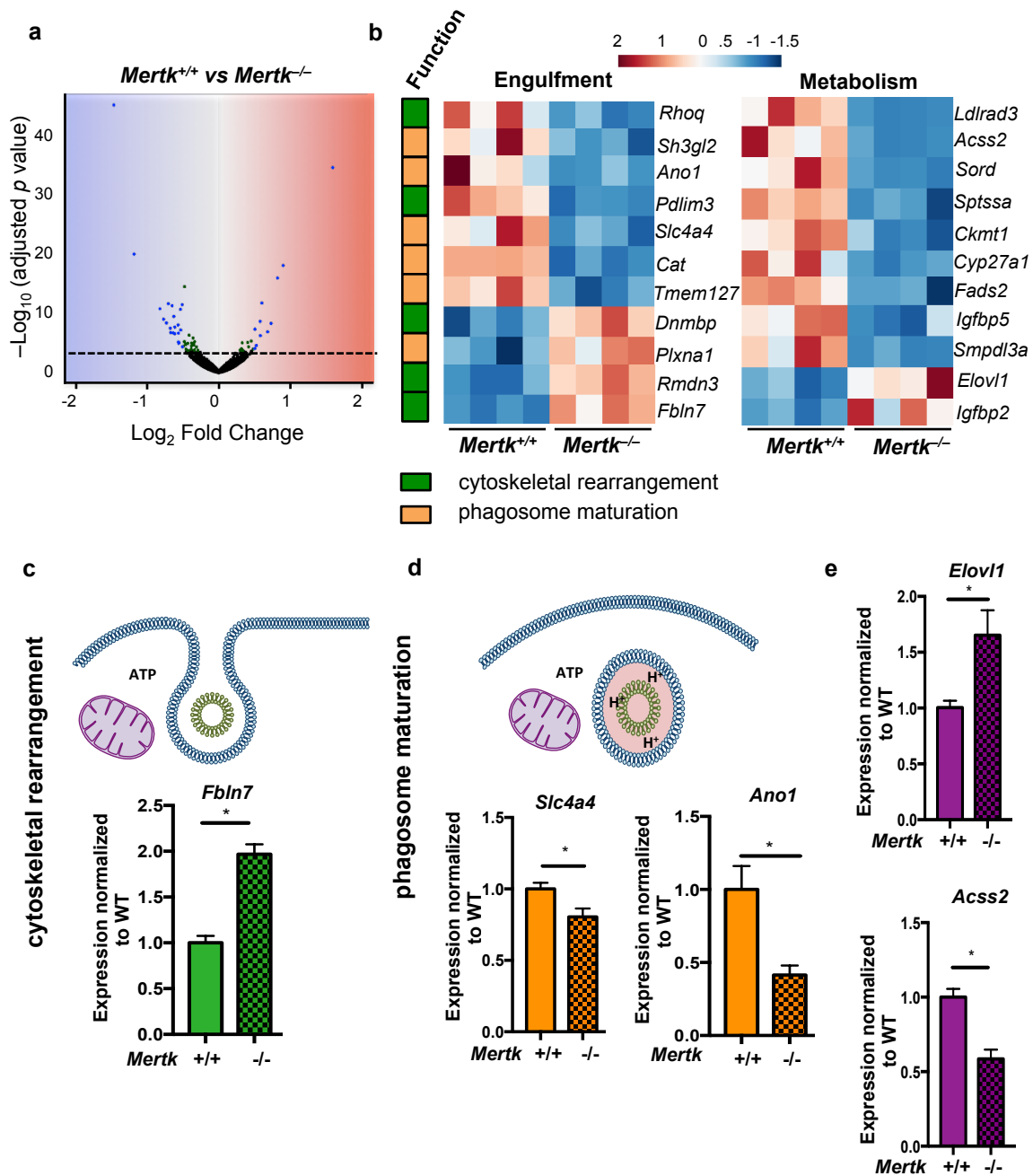


**Table 2.1: Genes dysregulated in *Mertk*<sup>-/-</sup> RPE with associations to retinal disease**

Gene	Log <sub>2</sub> fold change	Reported retinal disease association in humans	Experimental evidence
<b><i>Ldlrad3</i><sup>*</sup></b>	-1.08	SNP[296], inferred[292,293]	Intronic SNP associated with pathological myopia, a disease associated with degeneration of several eye structures including RPE[297-299]
<b><i>Gja1</i></b>	-0.54	Monogenic[291,300], inferred[292,293]	Mutations in <i>Gja1</i> have a monogenic association with oculodentodigital dysplasia, which has multiple manifestations including retinal dysplasia[291]. <i>Gja1</i> is also critical in RPE differentiation and communication between RPE cells[301,302].
<b><i>Cyp27a1</i><sup>*</sup></b>	-0.48	Monogenic[290], inferred[292,293]	Mutations in <i>Cyp27a1</i> have a monogenic association with cerebrotendinous xanthomatosis, which is associated with premature retinal senescence[290,303]. Mice with mutations in <i>Cyp27a1</i> exhibit abnormal retinal vascularization and cholesterol deposits in the RPE[304,305].
<b><i>Slc4a4</i><sup>#</sup></b>	-0.48	inferred[292-294,306]	Retinitis pigmentosa 17 (RP17) is characterized by mutations in <i>Ca4</i> [307,308]. Some variants of RP17 have <i>Ca4</i> mutations that prevent interaction and activation of <i>Slc4a4</i> [294].
<b><i>Cat</i><sup>#</sup></b>	-0.48	inferred[100,306,309,310]	Increased expression of <i>Cat</i> in RPE prevents oxidative damage to photoreceptors[310]. Age-related macular degeneration (AMD) is associated with decreased catalase activity in RPE[309].
<b><i>Fads2</i><sup>*</sup></b>	-0.36	SNP[311],inferred [292,293]	SNPs in intronic and regulatory regions of <i>Fads2</i> have been linked to AMD[311]. <i>Fads2</i> <sup>-/-</sup> mice exhibit structural changes in interphase between RPE and photoreceptors[312].
<b><i>Igfbp5</i><sup>*</sup></b>	-0.36	inferred[292,293]	Altered <i>Igfbp5</i> expression is associated with myofibroblastic changes in RPE[313].
<b><i>Elovl1</i><sup>*</sup></b>	0.45	inferred[292,293]	ELOVL1 is an endogenous inhibitor of the visual cycle enzyme, RPE65[295]. Mutations in <i>Rpe65</i> cause retinitis pigmentosa[173].
<b><i>Fbln7</i><sup>#</sup></b>	0.82	SNP [279],inferred [292,293]	Intronic SNP associated with reduced severity of AMD[279].

## 2.5 Discussion

Phagocytes express multiple PtdSer receptors and it has been unclear whether these receptors are functionally redundant or if they have tissue and context specific functions. In an attempt to determine if PtdSer receptors are functionally unique, we asked if PtdSer receptors are capable of compensating for one another in specialized phagocytes *in vivo*. Our analysis of the *Mertk*<sup>-/-</sup> *Bai1*<sup>Tg</sup> mice led to two major findings. First, *Bai1*<sup>Tg</sup> expression does in fact rescue phagocytic deficits in *Mertk*<sup>-/-</sup> Sertoli cells. Second, *Bai1*<sup>Tg</sup> expression was not able to preventing retinal degeneration or rescue phagocytic deficits in the *Mertk*<sup>-/-</sup> RPE. These findings provide the first evidence for functional compensation between two different PtdSer phagocytosis receptors from two distinct receptor families: The GPCR BAI1 and the receptor tyrosine kinase MerTK. Our results also suggest that the role of a given PtdSer receptor in cell clearance may differ depending on the tissue context. Overall, this indicates that PtdSer receptors are not fully interchangeable, which could, in part, explain why phagocytes express a variety of PtdSer receptors on their cell surface. It also suggests expression of MerTK is non-redundant in the eye/retina.

To understand why MerTK might be uniquely essential for RPE phagocytosis, we performed RNAseq on *Mertk*<sup>-/-</sup> and *Mertk*<sup>+/+</sup> RPE and identified 60 genes that were differentially expressed in *Mertk*<sup>-/-</sup> RPE cells. From those genes, three critical subsets were dysregulated: genes linked to retinal disease, phagocytosis, and metabolism. Genes linked to human retinal disease have

associations that are either monogenic, SNP, or inferred based on curated experimental and pharmacological data. Interestingly, 8 of the 9 genes associated with retinal disease were linked to either metabolic or phagocytic functions. We selected some genes for further validation and indeed, we found that the expression of these genes (*Fbln7*, *Slc4a4*, *Ano1*, *Acss2*, and *Elovl1*) was reproducibly altered. In addition to the genes discussed above, we also observed that *Tyro3* was downregulated in *Mertk*<sup>-/-</sup> mice relative to *Mertk*<sup>+/+</sup>. However, this difference in *Tyro3* expression was previously ascribed to a *cis*-enhancer element in *Tyro3* that co-segregates with the *Mertk*<sup>-/-</sup> allele [92,192].

Based on our findings, we propose that MerTK is uniquely important for RPE engulfment as it not only mediates PtdSer binding, but also regulates transcription of multiple genes implicated in phagocytosis, metabolism and retinal disease. These perturbations could explain why *Mertk*<sup>-/-</sup> mice exhibit visual defects (as measured by electroretinogram recordings) at P20, an age when defects in the 11-*cis*-retinal chromophore have yet to manifest [189]. Furthermore, the observed transcriptional changes may help to explain the decreased retinyl ester accumulation in *Mertk*<sup>-/-</sup> mice. Our data not only revealed significant changes in metabolic genes that could perturb the availability of fatty acids for esterification, but expression of the visual cycle enzyme lecithin retinol acyltransferase (which generates retinyl esters) was lower (but not significantly so) in *Mertk*<sup>-/-</sup> mice (data not shown).

The finding that *Bai1* overexpression can reduce apoptotic corpse clearance in the testes is intriguing. Though RPE phagocytosis of POS is PtdSer dependent, it is not 'traditional apoptotic corpse clearance' and could instead be analogous to the cell pruning observed in the nervous system. It is possible that the mechanism of action of BAI1 in phagocytosis is not conducive to pruning-type events, but rather that BAI1 is more suited for larger corpse uptake. Alternatively, BAI1-mediated phagocytosis could require an as-of-yet unidentified co-factor that RPE cells do not express. This might explain why the *Bai1<sup>Tg</sup>* can enhance phagocytosis in *Mertk<sup>-/-</sup>* Sertoli cells, where it is known to function endogenously [86,136].

Overall, this work suggests that the variety of PtdSer receptors did not evolve as a simple redundancy mechanism. Rather, these receptors likely play unique roles beyond PtdSer recognition, including the regulation of genes crucial to the process of phagocytosis and biological processes essential for general homeostasis and even specialized tissue functions. Overall, this suggests that PtdSer receptors should not be regarded as having homogenous functionality. Further research into the downstream functions of PtdSer receptors is critical to understanding how the phagocytic process is coordinated in different tissues and contexts.

## **2.6 Co-author contributions and acknowledgements**

### **Author Contributions:**

KKP performed most of the key experiments in this work with help in specific instances from others. KKP, CR, LSS, KP, SO, JL and KSR designed research. KKP, CR, MHR, JZ, CH, JL performed experiments. KKP and JSP analyzed and visualized data. KKP and KSR wrote the manuscript with input from all other authors.

### **Acknowledgements:**

We would like to acknowledge the support of the University of Virginia Research Histology Core and Biological Tissue Repository Facility for preparing testicular sections and cleaved-caspase 3 staining, respectively. We would like to thank the University of Virginia Genomics Core Facility and AnhThu Nguyen for her preparation of the cDNA libraries for RNAseq. We would like to thank Emily Farber for running the Illumina NextSeq analysis. We would like to thank Alex Koeppel and the University of Virginia Bioinformatics Core for performing the DESeq2 analysis of the raw RNAseq data.

## Chapter III

### ***Ex vivo* modulation of the FoxO1 phosphorylation state does not lead to dysfunction of T regulatory cells**

*This work has been published in PLoS ONE: Kristen Kelley Penberthy, Monica Weaver Buckley, Sanja Arandjelovic, Kodi S Ravichandran. Ex vivo modulation of the FoxO1 phosphorylation state does not lead to dysfunction of T regulatory cells. 2017 PLoS ONE. 12(3) e0173386.*

#### **3.1 Summary**

Peripheral regulatory CD4<sup>+</sup> T cells (Treg cells) prevent maladaptive inflammatory responses to innocuous foreign antigens. Treg cell dysfunction has been linked to many inflammatory diseases, including allergic airway inflammation. Glucocorticoids that are used to treat allergic airway inflammation and asthma are thought to work in part by promoting Treg cell differentiation; patients who are refractory to these drugs have defective induction of anti-inflammatory Treg cells. Previous observations suggest that Treg cells deficient in the transcription factor FoxO1 are pro-inflammatory, and that FoxO1 activity is regulated by its phosphorylation status and nuclear localization. Here, we asked whether altering the phosphorylation state of FoxO1 through modulation of a regulatory phosphatase might affect Treg cell function. In a mouse model of house dust mite-induced allergic airway inflammation, we observed robust recruitment of Treg cells to the lungs and lymph nodes of diseased mice, without an apparent increase in the Treg cytokine interleukin-10 in the airways.

Intriguingly, expression of PP2A, a serine/threonine phosphatase linked to the regulation of FoxO1 phosphorylation, was decreased in the mediastinal lymph nodes of HDM-treated mice, mirroring the decreased PP2A expression seen in peripheral blood monocytes of glucocorticoid-resistant asthmatic patients. When we asked whether modulation of PP2A activity alters Treg cell function via treatment with the PP2A inhibitor okadaic acid, we observed increased phosphorylation of FoxO1 and decreased nuclear localization. However, dysregulation of FoxO1 did not impair Treg cell differentiation *ex vivo* or cause Treg cells to adopt a pro-inflammatory phenotype. Moreover, inhibition of PP2A activity did not affect the suppressive function of Treg cells *ex vivo*. Collectively, these data suggest that modulation of the phosphorylation state of FoxO1 via PP2A inhibition does not modify Treg cell function *ex vivo*. Our data also highlight the caveat in using *ex vivo* assays of Treg cell differentiation and function, in that while these assays are useful, they may not fully recapitulate Treg cell phenotypes that are observed *in vivo*.

### 3.2 Introduction

Allergic airway inflammation is the result of maladaptive immune responses to generally innocuous foreign antigens or allergens [314-316]. One possible explanation for the development of this maladaptive inflammatory response is the functional insufficiency of the regulatory T cell (Treg) compartment [215,247,317-319]. Current evidences in the literature suggest that this functional insufficiency likely results from both decreased Treg cell numbers and Treg cell dysfunction [318-322].

Treg cells are a population of CD4<sup>+</sup> T cells that are typically characterized by their expression of the transcription factor FoxP3 [323,324]. In the context of allergic airway inflammation, Treg cells are thought to suppress airway inflammation to allergens by suppressing dendritic cell activation and by producing the anti-inflammatory cytokine interleukin-10 (IL-10) [207,325]. The hypothesis that asthmatic patients have a dysfunctional Treg cell compartment is supported by the finding that the airways of patients with allergic airway inflammation have decreased IL-10 [256,326]. Furthermore, glucocorticoids, a well-established treatment for allergy, are thought to work in part by promoting Treg cell differentiation, thereby suppressing the inappropriate inflammatory response to allergens [255].

While there are multiple reports of Treg cell dysfunction in patients with allergy and asthma, how Treg cells become dysregulated in this setting is less well understood [215,256,318,319]. In recent years, a substantial body of work

has emerged that indicates the transcription factor FoxO1 is crucial for both peripheral and thymic Treg cell differentiation and function. These studies utilized Treg and CD4<sup>+</sup> T cell specific deletion of FoxO1 to demonstrate that the absence of FoxO1 impairs Treg cell differentiation and that Treg cells deficient in FoxO1 (FoxO1 was deleted after Treg cell differentiation) are pro-inflammatory and produce interferon  $\gamma$  (IFN $\gamma$ ) [217,218,222,223]. While these studies utilize elegant genetic models of gene deletion, it is possible for FoxO1 activity to become acutely dysregulated as FoxO1's transcriptional activity is contingent on it being dephosphorylated [218,220,229]. Interestingly, the phosphatase PP2A has been shown to dephosphorylate FoxO1 in certain cell types, and patients with severe glucocorticoid-resistant asthma exhibit decreased expression of the serine-threonine phosphatase PP2A in their peripheral blood monocytes [229,234]. The significance of this finding is magnified by the observation that glucocorticoid-resistant asthmatics are also reported to have high levels of IFN $\gamma$  in their airways (the same cytokine that is increased in FoxO1 deficient Treg cells) and defective induction of IL-10 producing Treg cells [256,327,328].

The transcription factor FoxO1 is crucially involved in Treg cell development and function [217,218,329]. In the absence of FoxO1, the locus for another key Treg cell transcription factor, FoxP3, fails to open, thereby preventing Treg cell differentiation [223,330,331]. Furthermore, FoxO1 suppresses the production of pro-inflammatory mediators, including IFN $\gamma$  [217,220]. Under homeostatic conditions in Treg cells, FoxO1 is

dephosphorylated and has an exposed nuclear localization sequence, which permits FoxO1 to carry out its transcriptional functions [229]. However, upon T cell receptor stimulation, FoxO1 is phosphorylated, which masks the nuclear localization sequence, resulting in its extrusion from the nucleus [218,229,332]. In Treg cells, rapid dephosphorylation of FoxO1 permits it to re-enter the nucleus and resume its anti-inflammatory transcriptional program [218]. Treg cells that lack FoxO1 are pro-inflammatory, and mice with FoxO1-deficient Treg cells develop systemic autoimmune disease [218]. Similarly, mice with Treg cells lacking the alpha catalytic sub-unit of PP2A (PP2A $\alpha$ ) exhibit profound autoimmune disease [333].

The notion that changes in PP2A expression might influence Treg cell function in allergic airway inflammation is intriguing. However, PP2A regulates diverse cellular pathways making analysis of the role of PP2A in complex biological systems challenging [232,334-336]. In an attempt to create an *in vitro* system to assess the role of phosphatases in Treg function, we tested the pharmacologic phosphatase inhibitor, okadaic acid. Indeed, okadaic acid caused an increase in FoxO1 phosphorylation and cytosolic sequestration in Treg cells and CD4<sup>+</sup> T effector cells (Teff). However, okadaic acid did not cause Treg cells to produce IFN $\gamma$ . Furthermore, okadaic acid treatment did not recapitulate the findings from the recent study that utilized an *in vivo* model of PP2A catalytic sub-unit deletion in Treg cells [333]. Specifically, okadaic acid treated Treg cells did not produce IL-17 nor did they demonstrate impaired suppression of CD4<sup>+</sup>

effector proliferation. Collectively, these data suggest that *ex vivo* treatment of Treg cells with okadaic acid and the resultant modulation of PP2A activity and FoxO1 phosphorylation are not sufficient to modulate the functional activity of Treg cells. These findings also suggest a caution for others attempting to utilize *ex vivo* assays to assesses the effects of altering PP2A activity / FoxO1 phosphorylation status in Treg cells.

### **3.3 Experimental Procedures**

#### **3.3.1 Ethics Statement**

All animal experiments conducted in this study were carried out in strict accordance with protocols approved by the University of Virginia Animal Care and Use Committee (Protocol number: 2992). All experiments followed the recommendations in the Guide for the Care and Use of Laboratory Animals of the National Institutes of Health (OLAW/NIH, 2002) and followed the requirements of the Animal Welfare Act (Public Law 91-579). All efforts were made to minimize animal suffering including the use of anesthesia (isoflurane delivered at 5% for induction and 3% for maintenance in oxygen in a precision vaporizer) for the administration of house dust mite (HDM). Mice were monitored daily by vivarium staff and were euthanized at the experimental endpoint in a carbon dioxide chamber followed by confirmation via cervical dislocation. These methods are consistent with the recommendations of the Panel on Euthanasia and approved by the UVA Animal Care and Use Committee.

#### **3.3.2 Animals and primary cell culture**

Mice used in airway inflammation studies were C57Bl/6J purchased from Jackson Laboratories. For primary CD4<sup>+</sup> T cell cultures, total CD4<sup>+</sup> T cells were isolated from the lymph nodes and spleens of either C57Bl6/J mice or FoxP3-EGFP mice (Stock 016961 from Jackson Laboratories) by negative magnetic selection with the MACS CD4<sup>+</sup> T cell isolation kit (Miltenyi). Cells were cultured in RPMI (Cell Gro) supplemented with 10% FBS, 1% PSQ, 1% non-essential amino

acids, 1% Sodium Pyruvate, and 10mM HEPES (Gibco). For long-term assays, cell culture plates were coated with antibodies to CD3 and CD28 (eBiosciences - clones 17A2 and 37.51, respectively) to promote activation and proliferation. Short-term stimulation assays were performed using soluble CD3 and CD28, cross-linked with anti-hamster IgG (Jackson Immunolabs, 107-005-142). Cultures were treated with calyculin A (Calbiochem), okadaic acid (Sigma) or LB100 (Selleckchem).

### **3.3.3 Mouse model of allergic airway inflammation**

House dust mite extract was purchased from Greer laboratories (XPB82D3A2.5) and reconstituted in PBS such that the DerP1 concentration was 0.87 mg/mL. Mice were anesthetized by isoflurane and 17.4  $\mu$ g of DerP1 was administered intranasally in a 50  $\mu$ L volume on days 0, 2, and 4 for antigen priming. HDM was again administered on days 10, 12 and 14 as an antigen challenge. 50 $\mu$ L of PBS was administered to control mice at all time points. On day 15, mice were euthanized and the severity of airway inflammation was analyzed. Bronchoalveolar spaces were lavaged with 1 mL of PBS for analysis of T cell infiltration (T effectors: CD4<sup>+</sup>CD25<sup>+</sup>FoxP3<sup>-</sup>, T regulatory cells: CD4<sup>+</sup>CD25<sup>+</sup>FoxP3<sup>+</sup>) and eosinophilia (CD45<sup>+</sup>Siglec F<sup>+</sup>CD11b<sup>+</sup>CD11c<sup>-</sup>). The following antibodies were used at a dilution of 1:100 for flow cytometric analysis: CD4 (eBioscience GK1.5), CD25 (eBioscience PC61.5), FoxP3 (eBioscience FJK-16s), CD45 (eBioscience RA3-6B2), Siglec F (BD E50-2440), CD11b (M1/70 eBioscience), CD11c (eBioscience N148). Right lung lobes were

analyzed by histology and left lung lobes were analyzed by flow cytometry to assess tissue infiltrate. Mediastinal lymph nodes were collected and analyzed by flow cytometry and RT-PCR. Cell populations were quantified by flow cytometry via Spherotech counting beads (Spherotech ACBP-50-10).

### **3.3.4 qRT-PCR**

RNA was isolated with the RNeasy RNA isolation kit (Qiagen) and cDNA was prepared using the Quantitect kit (Qiagen). Expression of the PP2A catalytic subunit was assessed by RT-PCR with a Taqman probe (Mm00479816\_m1, Thermo Fisher). HPRT probe (Mm00446968\_m1, Thermo Fisher) was used to assess housekeeping gene expression for normalization.

### **3.3.5 Flow cytometry**

Single cell suspensions were generated from tissue by passing through a 70 $\mu$ m cell strainer (lungs were first digested and minced in 0.6 mg/mL type-2 collagenase (Worthington Biochemical) for 1 hour at 37° C to promote tissue breakdown). Cell suspensions were incubated with anti-CD16/32 antibodies (1:200 dilution; eBioscience clone 93) to block Fc interactions. Subsequent extracellular antibody labeling was performed on ice in PBS supplemented with 0.5% BSA (Roche). Viability staining was performed with 7-AAD (1:1000 dilution; BD Bioscience) for live-cell analysis, or an amine reactive fixable viability dye (1:1000 dilution; FVD eFluor780 eBioscience) when cells were to be fixed and permeabilized. For intracellular labeling, cells were fixed and permeabilized with either the FoxP3 fixation buffer kit or IC fixation buffer kit from eBioscience,

according to manufacturer recommendations. Intracellular antibody labeling was performed for 30 minutes on ice in permeabilization buffer (eBioscience). All flow cytometry was performed on BD FACS Canto I and Canto II. Flow cytometric data was analyzed in Flow Jo software version 887 (FlowJo LLC).

### **3.3.6 Protein isolation and Immunoblotting**

Whole cell lysates were prepared in RIPA buffer supplemented with a protease inhibitor cocktail (Calbiochem), 10mM NaF and 1mM NaVO<sub>3</sub> (Sigma). Nuclear and cytoplasmic extraction was performed with the NE-Per kit (Pierce). Lysates were analyzed by SDS-PAGE and immunoblotting. Antibody binding was detected by chemiluminescence on either film or a ChemiDoc Touch (Bio-Rad). Immunoblot band density analysis and normalization was performed using ImageJ for analysis of film or Image Lab (Bio-Rad) for analysis of ChemiDoc Touch images. The following primary antibodies were purchased from Cell Signaling Technologies and used at 1:1000 dilutions unless otherwise indicated: phospho-FoxO1 (Thr24) (#9464), FoxO1 (clone C29H4 - #2880), HDAC1 (#2062), phospho-Akt (ser473) (#4060S) Akt (1:2000; #9272). The antibody to  $\beta$ -actin was purchased from Sigma and used at 1:50,000 (clone AC-15, #A3854).

### **3.3.7 Phosphatase assay**

Total CD4<sup>+</sup> T cells were stimulated with 5 $\mu$ g/mL anti-CD3 and 1 $\mu$ g/mL anti-CD28 for 10 minutes to elicit FoxO1 phosphorylation. CD4<sup>+</sup> T cells were lysed in IP buffer (50mM Tris pH 7.6, 150mM NaCl, 1% Triton X-100, protease

inhibitor cocktail (Calbiochem), 10mM NaF, 1mM NaVO<sub>3</sub>) and incubated with anti-FoxO1 (clone C29H4 - #2880). Antibody bound FoxO1 was immunoprecipitated with Protein A conjugated sepharose beads. Beads were washed in the IP buffer without NaF and NaVO<sub>3</sub> to ensure irreversible phosphatase inhibitors would not inhibit the subsequent phosphatase reaction. Beads were then re-suspended in phosphatase assay buffer (50mM MOPS pH 7.5, 100mM NaCl, 10mM MgSO<sub>4</sub>, 1mM MnCl<sub>2</sub>, 1mM DTT, 1mM EDTA, 0.1% β mercaptoethanol, protease inhibitor cocktail (Calbiochem)) with purified PP2A +/- 100 nM okadaic acid. Purified (tested and validated) PP2A was generously provided by Dr. David Brautigan at the University of Virginia [337]. Phosphatase reactions were incubated for 1 hour at 30°C. Following incubation, beads were re-suspended in Laemmli buffer and boiled. Laemmli buffer was then loaded on an SDS-PAGE gel for immunoblot analysis.

### **3.3.8 T cell proliferation and suppression assays**

Total CD4<sup>+</sup> T cells were isolated from lymph nodes and spleens of naïve mice by negative magnetic selection. The positive fraction from the spleen was treated with mitomycin C (Sigma) to inhibit proliferation and used as antigen presenting cells. Treg cells were further isolated from the total CD4<sup>+</sup> T cell population by positive selection for CD25 expression. CD4<sup>+</sup> Teff cells constituted the negative fraction of this CD25 selection. Teff cells were labeled with 5μM Cell Trace Violet (Thermo Fisher). APCs and Teff cells were co-cultured at a 1:1 ratio with 0.15 μg/mL soluble anti-CD3 (eBiosciences 17A2) to elicit proliferation. For

suppression assays, Treg cells were added at the indicated ratios (Treg : Teff). Proliferation of Teff cells was analyzed by dye dilution on a BD Canto II flow cytometer after 96 hours of culture.

### **3.3.9 T regulatory cell differentiation**

Total CD4<sup>+</sup> T cells were isolated from lymph nodes of FoxP3 EGFP mice and cultured *ex vivo* in media supplemented with 20 nM retinoic acid (sigma), 5 or 10 ng/mL TGF $\beta$  (R&D systems) and recombinant IL-2 (R&D systems) at either 100 or 250U/mL. When assessing the effects of okadaic acid on Treg cell differentiation, the lower concentrations of TGF $\beta$  and IL-2 were used. The higher concentrations of TGF $\beta$  and IL-2 were used to generate maximum numbers of Tregs. Cells were plated on dishes coated with anti-CD3 and anti-CD28 (clones 17A2 and 37.51 respectively; eBiosciences). Cultures were incubated for 72 hours and flow cytometry was used to assess FoxP3 induction and CD25 expression. To assess cytokine production, GolgiPlug (BD Biosciences) was added to the culture for 5 hours prior to staining for IFN $\gamma$  (clone XMG1.2; eBioscience) and IL-17 staining (clone TC11-18H10; BD).

## 3.4 Results

### 3.4.1 Allergen-induced airway inflammation increases local Treg cell populations

Patients with severe, glucocorticoid-resistant allergic asthma are reported to have a dysfunctional Treg cell compartment [256,318]. Treg cell dysfunction is thought to underlie the defective tolerogenic response that leads to the development of allergy [338]. To test potential Treg cell dysfunction, we used a murine model of severe allergic airway inflammation. In this model, the common allergen house dust mite (HDM) is delivered to mice intranasally, which mimics the typical route of exposure to airborne allergens. We treated mice with three intranasal administrations of HDM on days 0, 2 and 4 to prime the immune system and subsequently challenged the mice intranasally with HDM on days 10, 12 and 14 (**Figure 3.1a**). The inflammatory response was assessed on day 15.

We initially assessed whether this model caused severe airway disease and whether Treg cells were recruited to the site of inflammation. HDM-treated mice exhibited classic signs of allergic airway inflammation. First, hematoxylin and eosin (H&E) staining of lung sections revealed marked cellular infiltration around the airways of HDM-treated mice (indicated with black asterisks) compared to mice that received the saline (PBS) vehicle control (**Figure 3.1b**, left panels). Second, Periodic acid-Schiff (PAS) stain, which detects mucus production, showed dramatically increased mucus production (marked by black arrowheads) in HDM-treated mice relative to PBS-treated controls (**Figure 3.1b**,

right panels). Additionally, analysis of bronchoalveolar lavage (BAL) fluid showed severe eosinophilia in HDM-treated animals relative to PBS-treated controls (**Figure 3.1c**).

Analysis of CD4<sup>+</sup> T cell populations of lungs from HDM-treated mice showed a significant increase in the number of Teff cells (CD4<sup>+</sup>CD25<sup>+</sup>FoxP3<sup>-</sup>) and Treg cells (CD4<sup>+</sup>CD25<sup>+</sup>FoxP3<sup>+</sup>), compared to PBS controls (**Figure 3.1d**). It should be noted that the ratio of Treg cells to Teff cells trended toward a decrease in HDM-treated mice relative to PBS controls (**Figure 3.1d**). We performed a similar analysis of CD4<sup>+</sup> T cell populations in the lung-draining, mediastinal lymph nodes (MLN), and observed a similar trend with more Teff cells and Treg cells in HDM-treated mice (**Figure 3.1e**). Additionally, the ratio of Treg cells to Teff cells was significantly decreased in the MLN of HDM-treated mice (**Figure 3.1e**). These data confirmed that this model of airway inflammation recapitulated key characteristics of allergic airway inflammation.

#### **3.4.2 Mice with HDM-induced inflammation do not exhibit increased IL-10**

Treg cells are major producers of IL-10, and IL-10 levels inversely correlate with airway inflammation [322,326,339,340]. Since Treg populations in the lung increased with HDM-induced airway inflammation, we asked whether IL-10 levels in the BAL fluid had a concomitant increase. HDM-treated mice did not exhibit increased IL-10 levels in their BAL fluid, despite the increase in Treg numbers (**Figure 3.1f**). This suggested a potential Treg dysfunction in this airway inflammation model, which we further explored, as detailed below.

### **3.4.3 Mediastinal lymph nodes from mice with allergic airway inflammation have decreased expression of the phosphatase PP2A**

FoxO1 transcriptional activity is tightly regulated by a series of phosphorylation and dephosphorylation reactions [341,342]. In a resting CD4<sup>+</sup> T cell, FoxO1 exists in a dephosphorylated state and localizes to the nucleus [218]. However, upon T cell receptor (TCR) stimulation, Akt phosphorylates FoxO1, which masks a nuclear localization sequence leading to cytosolic sequestration (**Figure 3.1g**) [218,224,314-316]. FoxO1 transcriptional activity is critical to proper Treg anti-inflammatory function, with Treg cells rapidly dephosphorylating FoxO1 to maintain their suppressive activity. Treg cells that lack FoxO1 upregulate expression of the pro-inflammatory cytokine interferon  $\gamma$  (IFN $\gamma$ ), the production of which is linked to severe, glucocorticoid-resistant asthma in humans [215,247,317-319,327,328]. We considered the possibility that FoxO1 might be dysregulated under conditions of allergic airway inflammation, thereby rendering Treg cells pro-inflammatory.

While the mediator of FoxO1 dephosphorylation in Treg cells was previously unexplored, PP2A has been shown to dephosphorylate FoxO1 in the hematopoietic cell line FL5.12 [229,318-322]. Since PP2A expression is down regulated in the peripheral blood monocytes of patients with severe, glucocorticoid-resistant asthma [234,323,324], the same group reported to have increased IFN $\gamma$  production, we hypothesized that decreased PP2A expression might promote dysregulation of FoxO1, subsequently causing aberrant IFN $\gamma$

production in Tregs cells and potentially greater overall dysfunction.

Expression of the PP2A catalytic sub-unit  $\alpha$  (PP2Ac $\alpha$ ) was decreased in the MLN of HDM-treated mice (**Figure 3.1h**) [207,234,325]. This prompted us to explore whether alterations in PP2A activity in Treg cells might perturb FoxO1 activity and thereby Treg cell function.

**Figure 3.1 HDM potently induces allergic airway inflammation despite significant T regulatory cell recruitment**

**(a)** Allergic airway inflammation was induced with three separate priming and challenge doses of house dust mite (HDM) over 14 days. Disease severity was assessed at day 15.

**(b)** Histological assessment of inflammation in lung sections of representative HDM-treated and PBS-treated mice. \* in H&E images indicates inflammatory infiltrate and arrowheads in PAS images indicate mucus.

**(c)** Eosinophils were quantified in the bronchoalveolar lavage (BAL) by flow cytometry ( $CD45^+Cd11b^+SiglecF^+CD11c^-$ ). Treg ( $CD4^+CD25^+FoxP3^+$ ) Teff ( $CD4^+CD25^+FoxP3^-$ ) populations in the lung parenchyma

**(d)** and mediastinal lymph nodes (MLN)

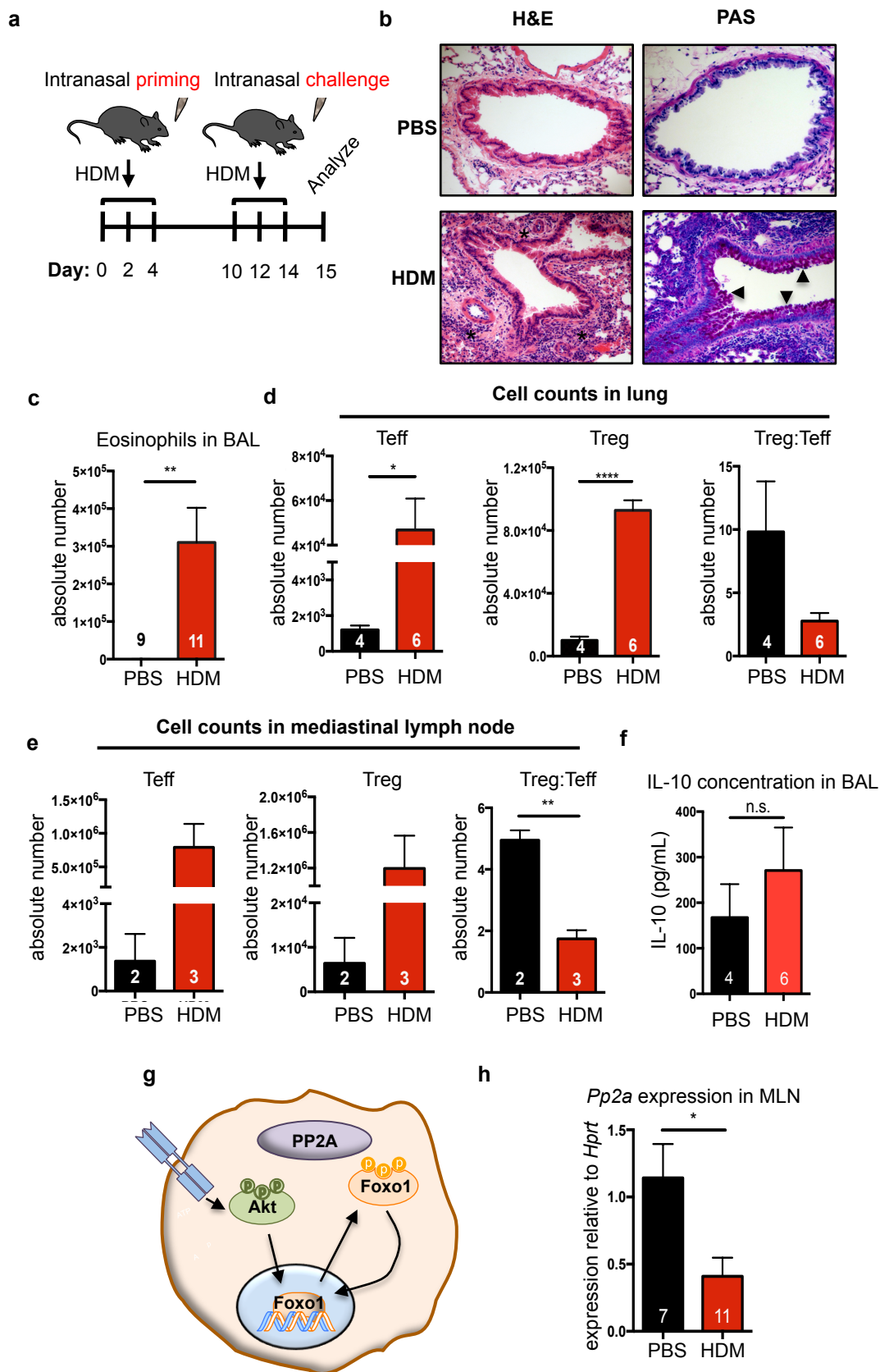
**(e)** were quantified by flow cytometry.

**(f)** IL-10 concentration in BAL was quantified by ELISA.

**(g)** Schematic of PP2A-FoxO1 axis.

**(h)** PP2A $\alpha$  sub-unit transcript levels were measured by RT-PCR. Transcript levels in HDM-treated mice were normalized to PBS-treated controls. Numbers in the bars of **c**, **d**, **e**, **f** and **h** represent the number of animals analyzed.

Significance in all panels was determined by two-tailed students' T-test: \* $<0.05$ ; \*\* $<0.01$ ; \*\*\*\* $<0.0001$ .



#### 3.4.4 Phosphatase inhibitors increase FoxO1 phosphorylation and nuclear localization in total CD4<sup>+</sup> Cells

Following TCR activation, FoxO1 is rapidly phosphorylated and extruded from the nucleus. To assess whether phosphatase inhibition would influence the kinetics and extent of FoxO1 phosphorylation following TCR stimulation, we utilized the pharmacologic inhibitor calyculin A, a fast-acting, broad phosphatase inhibitor [256,326,343]. Indeed, treatment of total CD4<sup>+</sup> T cells with calyculin A prior to TCR stimulation led to increased phosphorylation of FoxO1 (**Figure 3.2a and 3.2b**). Calyculin A treatment also led to an apparent increase in the molecular weight of FoxO1 and decreased FoxO1 expression. This appeared to result from calyculin A-dependent ubiquitylation and proteasomal degradation of FoxO1, as the decrease in FoxO1 expression, but not the apparent size change, was abrogated by proteasomal inhibition with lactacystin (**Figure 3.2c**).

Calyculin A has the benefit of rapid activity in culture however, it exhibits near-equal activity against PP1 and PP2A [255,343]. Therefore, we tested the phosphatase inhibitor okadaic acid, as this exhibits greater preference for PP2A than for PP1 (IC<sub>50</sub> for PP2A 0.1-0.3 nM, IC<sub>50</sub> for PP1 15-50 nM) [215,256,318,319,343]. Although okadaic acid can affect PP4, the expression of PP4 is lower than PP2A and PP1 in Treg cells [217,218,222,223,344]. Total CD4<sup>+</sup> T cells were isolated from the lymph nodes of naïve mice and treated *ex vivo* with increasing concentrations of okadaic acid for 48 hours (**Figure 3.3a**). We observed that concentrations of 10 and 25 nM were sufficient to induce Akt

and FoxO1 phosphorylation in total CD4<sup>+</sup> T cells (**Figure 3.3b**).

Furthermore, okadaic acid treatment of CD4<sup>+</sup> T cells led to increased cytosolic localization of FoxO1 (**Figure 3.3c**). For future experiments, we elected to use 10 nM okadaic acid as this concentration fell below the IC<sub>50</sub> for PP1 (15-50 nM) and 25 nM okadaic acid had some effects (albeit minimal) on cell viability after 48 hours (**Figure 3.3d**).

Since okadaic acid also increases Akt phosphorylation, it could be enhancing FoxO1 phosphorylation indirectly by enhancing Akt activity. To demonstrate that PP2A directly mediates the dephosphorylation of FoxO1, we assayed PP2A activity against purified FoxO1 *in vitro*. First, total CD4<sup>+</sup> T cells were stimulated with anti-CD3 and anti-CD28 to increase FoxO1 phosphorylation. These cells were subsequently lysed and FoxO1 was purified by immunoprecipitation. Immunoprecipitated FoxO1 was then treated with purified PP2A +/- 100nM okadaic acid. Treatment of FoxO1 with PP2A eliminated FoxO1 phosphorylation. This effect on phosphorylation was reversed by treatment with okadaic acid (**Figure 3.3e**). Collectively, these data suggest that phosphatase inhibition with okadaic acid promoted FoxO1 phosphorylation and subsequent cytosolic localization, likely through its effect on PP2A.

Though okadaic acid at the concentration used predominantly inhibits PP2A, it has the potential for off-target effects. Therefore, we tested LB100, a second PP2A inhibitor. LB100 is a derivative of norcantharidin with high specificity for PP2A (IC<sub>50</sub>≈0.4μM) over PP1 (IC<sub>50</sub>≈80μM) [218,220,229,345]. To

test the effect of LB100 on FoxO1 phosphorylation, we treated total CD4<sup>+</sup> T cells for 2 hours in the presence of 0, 0.25 $\mu$ M, or 2.5 $\mu$ M LB100. Following 2 hours of treatment, we collected whole cell lysates and assayed FoxO1 phosphorylation. We observed a dose-dependent augmentation of FoxO1 phosphorylation in the presence of LB100 (**Figure 3.4**). These data suggest that the changes in FoxO1 phosphorylation are not due to off-target effects of okadaic acid.

**Figure 3.2: Calyculin A increases FoxO1 phosphorylation and ubiquitylation**

(a) Total CD4<sup>+</sup> T cells were isolated from the lymph nodes of mice by magnetic cell sorting and treated with calyculin A or DMSO (vehicle control) for 30 minutes prior to stimulation with soluble, cross-linked anti-CD3 and anti-CD28.

(b) Cells were stimulated for the indicated amount of time and then lysed for analysis of FoxO1 phosphorylation at Thr24. Arrows point to higher molecular weight forms of FoxO1.

(c) Following isolation, CD4<sup>+</sup> T cells were treated with Calyculin A and/or the proteasomal inhibitor lactacystin. Data are representative of 2 independent experiments.

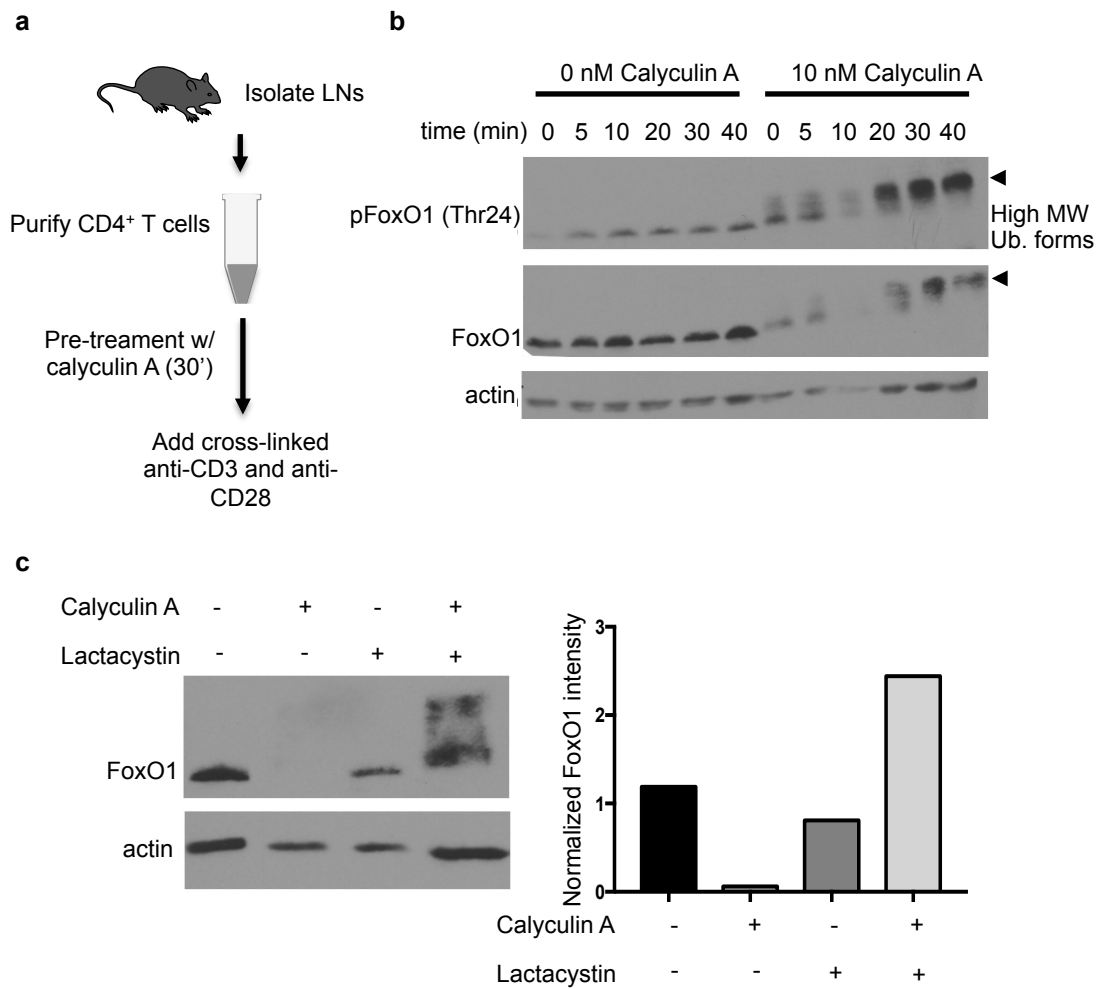


**Figure 3.3: PP2A inhibition increases FoxO1 phosphorylation and cytosolic localization in CD4<sup>+</sup> T cells**

**(a)** Primary CD4<sup>+</sup> T cells were negatively selected from the lymph nodes of 6-8 week old mice by magnetic cell sorting. CD4<sup>+</sup> T cells were treated with the indicated dosages of okadaic acid for up to 48 hours in cultures supplemented with 1 $\mu$ g/mL anti-CD3.

**(b)** Western blot analysis of FoxO1 phosphorylation at Thr24 and Akt at Ser 473.

**(c)** Western blot analysis of FoxO1 localization in fractionated CD4 cells. Beta-actin and HDAC were used as cytoplasmic and nuclear controls respectively.

**(d)** Viability of CD4<sup>+</sup> T cells in culture after 48 hours with the indicated concentrations of okadaic acid.

**(e)** Western blot analysis of in vitro phosphatase assay. Immunoprecipitated FoxO1 was treated with PP2A +/- 100nM okadaic acid. **b, c and d** are representative data from 3 individual experiments; **e** is representative of 2 experiments.

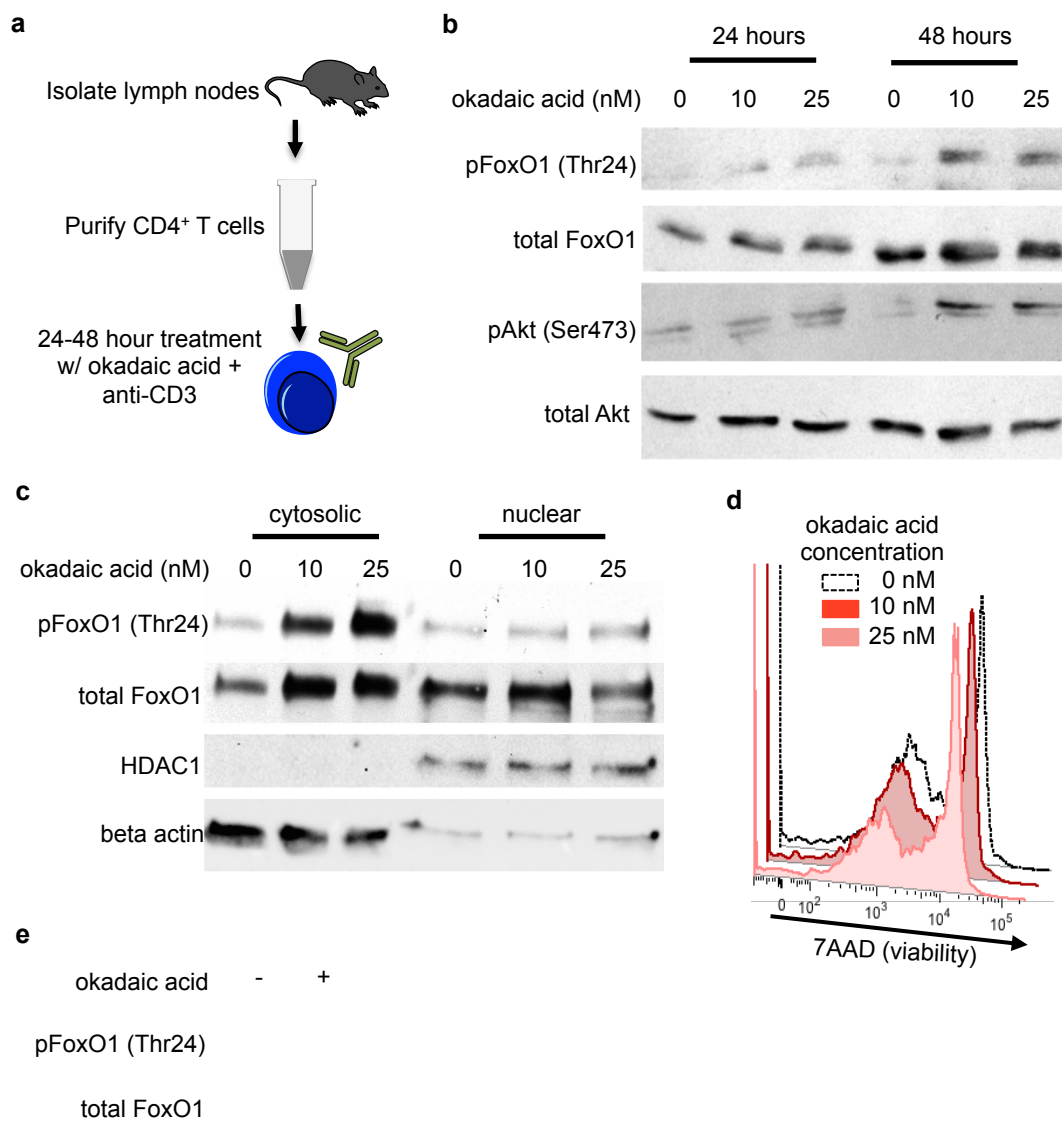
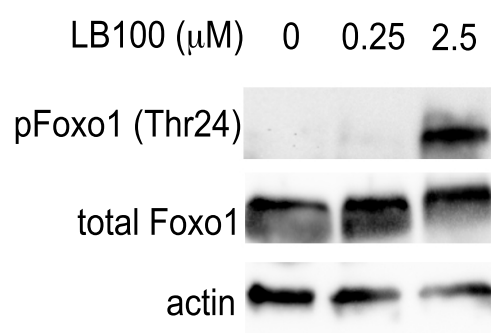


**Figure 3.4: Phosphatase inhibitor LB100 enhances  
FoxO1 phosphorylation**

Primary CD4<sup>+</sup> T cells were isolated from the lymph nodes of WT mice and serum starved for 2 hours in the presence of 0  $\mu$ M, 0.25  $\mu$ M and 2.5  $\mu$ M LB100. After 2 hours, whole cell lysates were collected and FoxO1 phosphorylation was analyzed by western blot. Data are representative of 3 independent experiments.



### 3.4.5 Okadaic acid promotes FoxO1 phosphorylation in Treg cells

We then tested whether okadaic acid was capable of promoting FoxO1 phosphorylation in Treg cells. Since the Treg cell population in a naïve mouse is approximately 10% of the total CD4<sup>+</sup> T cell population, we differentiated Treg cells from naïve CD4<sup>+</sup> T cells *ex vivo* to have enough cells for protein isolation and immunoblotting. Naïve CD4<sup>+</sup> T cells were isolated from the lymph nodes of FoxP3-GFP mice and stimulated with anti-CD3 and anti-CD28 in the presence of TGFβ to elicit FoxP3 expression. As FoxO1 transcriptional activity is critical for the early induction of FoxP3, we waited 24 hours before adding okadaic acid or vehicle control (DMSO) to the culture (**Figure 3.5a**) [229,234,330]. After 72 hours of culture, we confirmed the induction of FoxP3 expression by assessing GFP signal. Furthermore, we determined that treatment with okadaic acid did not diminish FoxP3 induction as measured by GFP signal (**Figure 3.5b**). Analysis of the cell lysates from these Treg cells revealed that okadaic acid treated Treg cells had increased FoxO1 phosphorylation (**Figure 3.5c**) and increased cytosolic localization of FoxO1 (**Figure 3.5d**). These data suggest that okadaic acid promotes FoxO1 phosphorylation and causes its cytosolic sequestration in Treg cells.

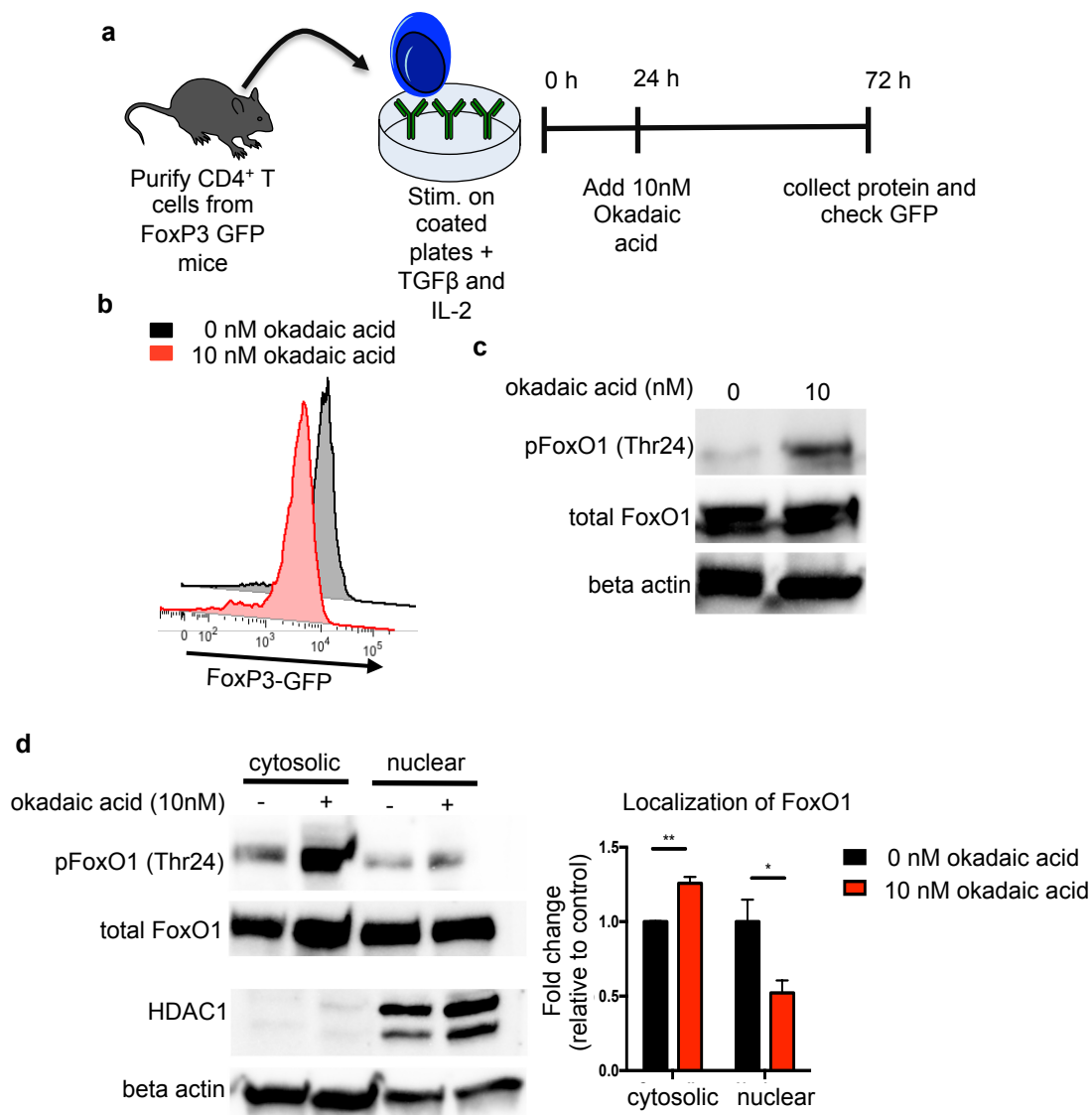
**Figure 3.5: Okadaic acid increases phosphorylation and cytosolic localization of FoxO1 in T regulatory cells**

**(a)** Primary CD4<sup>+</sup> T cells were isolated by negative magnetic selection from the lymph nodes of FoxP3-GFP mice. Cells were cultured on plates coated with anti-CD3 and anti-CD28 and treated with TGF $\beta$  to initiate Treg skewing. Okadaic acid was added after 24 hours in culture. After 72 hours in culture, cells were removed from TCR stimulus for 2 hours prior to protein isolation.

**(b)** Treg differentiation was assessed at the end of the assay by GFP expression.

**(c)** Representative western blot of FoxO1 phosphorylation at Thr24 in Treg cells. Data are representative of 3 independent experiments.

**(d)** Representative western blot of FoxO1 in fractionated Treg cells. Beta actin and HDAC were used as cytosolic and nuclear controls respectively. Bar graph shows summary localization data from 3 experiments as measured by band density and normalized to cytosolic control.



### 3.4.6 Okadaic acid does not impair Treg differentiation ex vivo

To test whether okadaic acid-induced changes in FoxO1 localization had downstream effects on Treg cell physiology, we chose to assess whether okadaic acid impaired Treg cell differentiation when added at the start of the skewing. Since FoxO1 transcriptional activity is essential for the induction of FoxP3 expression [223,256,327,328,330], we used assays of *ex vivo* Treg cell differentiation to assess whether okadaic acid impaired FoxP3 induction. Naïve CD4<sup>+</sup> T cells were isolated from FoxP3-GFP mice and treated with either okadaic acid or vehicle in a Treg cell differentiation assay. In these assays, TGFβ, IL-2, TCR stimulus and okadaic acid were added concomitantly (**Figure 3.6a**). Interestingly, when we assessed GFP expression after 72 hours, we observed that okadaic acid did not impair FoxP3 induction (**Figure 3.6b**). Furthermore, okadaic acid did not affect CD25 expression on either the GFP positive (Treg cells) or GFP negative cells from the culture (**Figure 3.6c**).

One possible explanation for the lack of an effect of okadaic acid on Treg cell differentiation is that okadaic acid requires 48 hours to achieve maximum enhancement of FoxO1 phosphorylation in culture (**Figure 3.3b**). Since FoxO1 is essential for opening the FoxP3 locus (but not maintaining its open state) [217,218,329,346], we hypothesized that pre-treatment of CD4<sup>+</sup> T cells with okadaic acid may be necessary to observe okadaic acid-induced defects in Treg cell differentiation. Therefore, naïve CD4<sup>+</sup> T cells from FoxP3-GFP mice were treated with okadaic acid and CD3 for 48 hours prior to the addition of TGFβ, IL-

2, and CD28. Once the Treg skewing stimuli were applied, we assessed FoxP3 expression by measuring GFP signal (**Figure 3.6d**). Again, okadaic acid pre-treatment did not diminish FoxP3 induction (**Figure 3.6e**). These data indicate that okadaic acid does not influence Treg differentiation *in vitro*, despite increasing cytosolic localization of FoxO1.

**Figure 3.6: Okadaic acid does not impair T regulatory cell differentiation in vitro**

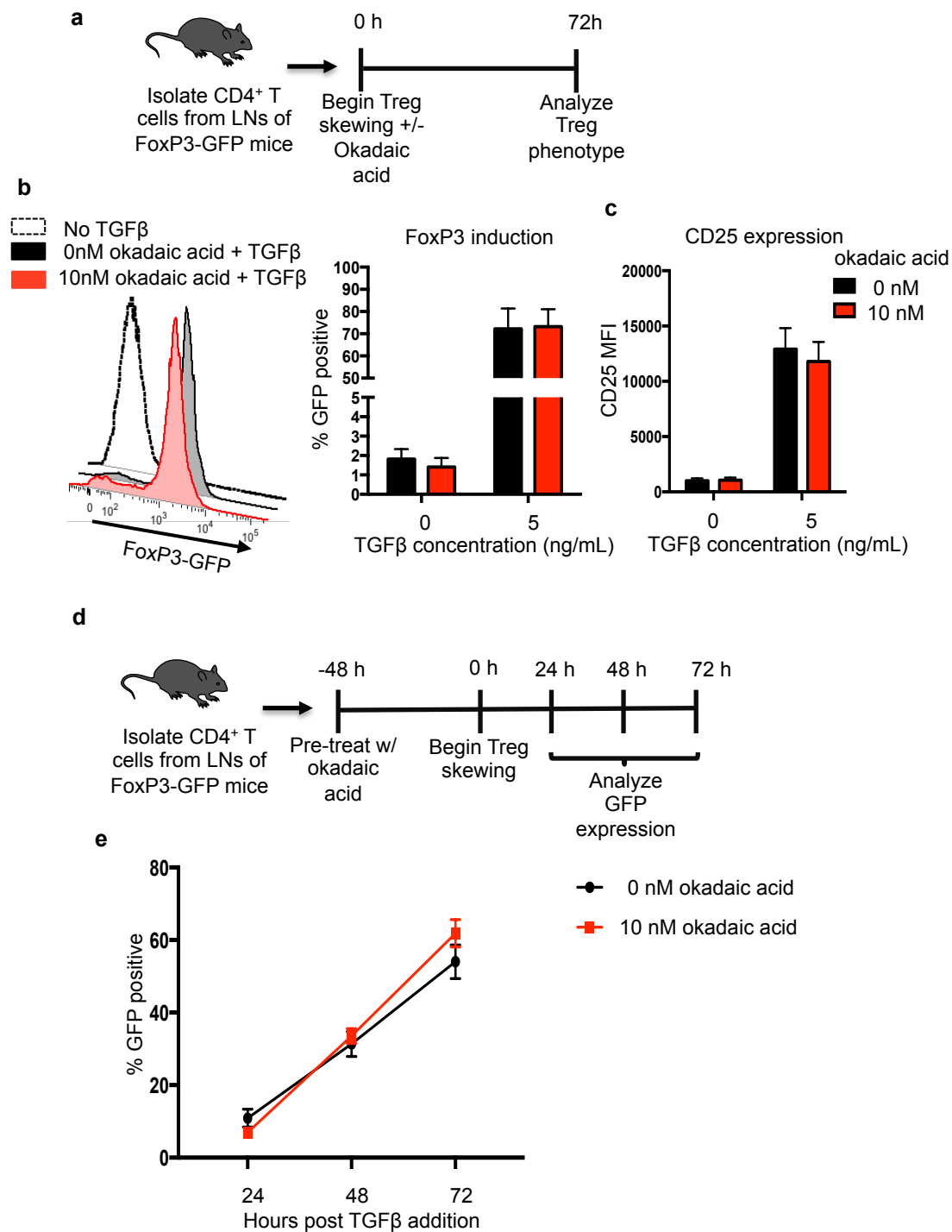
**(a)** Naïve CD4 cells were isolated from the lymph nodes of FoxP3-GFP mice and differentiated in to Tregs for 72 hours.

**(b)** GFP and

**(c)** CD25 expression were assessed by flow cytometry after 72 hours of Treg skewing. Data were compiled from 3 independent experiments with a total n=6 mice per group.

**(d)** Primary CD4 cells were isolated from the lymph nodes of FoxP3 GFP mice and pre-treated with okadaic acid for 48 hours prior to Treg differentiation.

**(e)** GFP expression was assessed by flow cytometry at 24, 48 and 72 hours after the initiation of skewing. Data were compiled from 3 independent experiments with n=6 mice per group. Statistical analysis of **b** and **c** was performed using a two-tailed students' T-test – comparison of vehicle control and okadaic acid treated conditions: FoxP3 p=0.7; CD25 p=0.12. Statistical analysis of **e** was performed by 2-way ANOVA – p-interaction =0.19.



### 3.4.7 Okadaic acid does not affect the phenotype of Treg cells differentiated ex vivo

Mice that lack FoxO1 in Treg cells (FoxP3-cre FoxO1<sup>fl/fl</sup>) mice exhibit severe autoimmune disease that is reminiscent of the disease found in FoxP3-deficient *scurfy* mice [218,223,330,331,347]. However, the lack of FoxO1 does not affect the number of CD4<sup>+</sup>FoxP3<sup>+</sup> cells in these animals. Instead, the Treg cells from these mice adopt a pro-inflammatory phenotype and produce the pro-inflammatory cytokine IFN $\gamma$  [217,218,220]. Therefore, we hypothesized that Treg cells differentiated in the presence of okadaic acid would exhibit increased IFN $\gamma$  production. However, when we assessed IFN $\gamma$  expression by flow cytometry we observed that okadaic acid did not cause IFN $\gamma$  up regulation in Treg cells (**Figure 3.7a**).

It had also been reported that ‘graded’ changes in FoxO1 activity influenced lymph node homing signatures on Treg cells [220,229]. FoxO1 promotes expression of the lymph node homing molecules CD62L and CCR7 [218,219,229,332]. In Treg cells from mice that express increasing levels of constitutively active FoxO1, the expression of these lymph node homing molecules similarly increases [218,220]. Since okadaic acid treatment did not cause complete cytosolic localization of FoxO1 (**Figure 3.5d**), we hypothesized that we might only see effects associated with ‘graded’ changes in FoxO1 localization. However, when we assessed CCR7 and CD62L expression on Treg

cells differentiated in the presence of okadaic acid, we did not observe changes in the expression of these molecules (**Figure 3.7b**).

During the course of our studies, a study utilizing an elegant *in vivo* genetic deletion model for the assessment of PP2A function in Treg cells demonstrated that PP2A was essential for Treg cell function [218,333]. The researchers deleted the dominant catalytic sub-unit of PP2A in Treg cells (FoxP3-cre PP2A $\alpha^{fl/fl}$ ) and observed that these Treg cells produced inflammatory cytokines, including IFN $\gamma$  and IL-17. In light of these findings, we also evaluated IL-17 production in Treg cells that were differentiated in the presence of okadaic acid. Surprisingly, we observed that okadaic acid did not affect IL-17 production by Treg cells (**Figure 3.7a**).

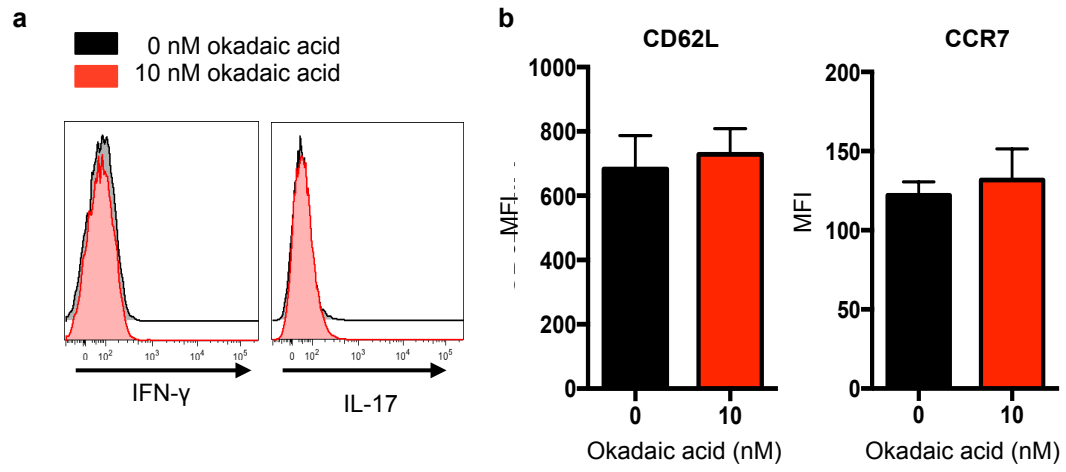
**Figure 3.7: Okadaic acid does not induce a pro-inflammatory phenotype or affect lymph node homing signatures in Treg cells**

Primary CD4<sup>+</sup> T cells were differentiated into Tregs in the presence of okadaic acid for 72 hours.

**(a)** After differentiation, IFN $\gamma$  and IL-17 production and

**(b)** CCR7 and CD62L expression were measured by flow cytometry. Flow panels of cytokine expression are representative data from 3 independent experiments.

Surface marker expression was compiled from 2 independent experiments with n=3 mice total. Data in **b** was analyzed by non-parametric students' T-test: CD62L p=0.5; CCR7 p=0.77.



### 3.4.8 Okadaic acid treatment of Treg cells does not influence Treg suppression *ex vivo*

Treg cells that lack the alpha catalytic sub-unit of PP2A have a decreased suppressive capacity [218,333]. Therefore, we assessed whether okadaic acid would influence the suppressive capacity of Treg cells *ex vivo*. We utilized a standard suppression assay in which co-cultured Treg cells and Teff cells were treated with okadaic acid (**Figure 3.8a**). First, we assessed whether okadaic acid influenced Teff proliferation *ex vivo* and observed that okadaic acid treated Teff cells proliferated to the same extent as vehicle treated controls (**Figure 3.8b**). In addition, we confirmed that okadaic acid retained its activity for the duration of the assay as okadaic acid treated CD4<sup>+</sup> T cells still exhibited increased FoxO1 phosphorylation at 96 hours (**Figure 3.8c**). We then went on to assess the effect of okadaic acid on Treg cell suppression of Teff proliferation. Interestingly, okadaic acid did not affect Treg cell suppressive capacity in these assays (**Figure 3.8d**). Collectively, these data indicate that okadaic acid, despite inhibiting PP2A activity and promoting FoxO1 phosphorylation, does not influence Treg cell phenotype and function *in vitro*.

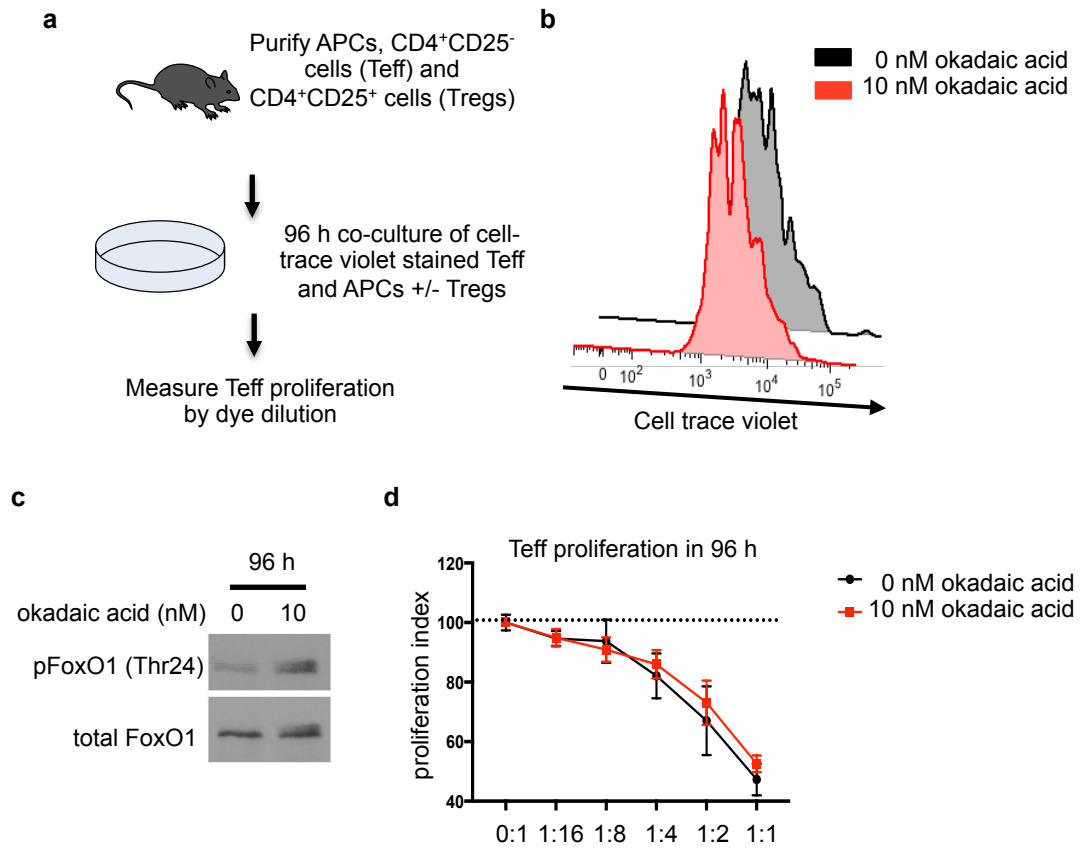
**Figure 3.8: Okadaic acid does not impair T regulatory cell mediated suppression of CD4 effector cells**

(a) Teff and Tregs were isolated from the lymph nodes and spleen of FoxP3-GFP mice. Cells were co-cultured at indicated ratios in the presence of antigen presenting cells and 0.15  $\mu\text{g}/\text{mL}$  anti-CD3 for 96 hours +/- okadaic acid.

(b)  $\text{CD4}^+$  T cell proliferation in the presence of okadaic acid was measured by cell-trace violet dye dilution. Data is representative of 4 independent experiments.

(c) Western blot of FoxO1 phosphorylation at Thr24 in  $\text{CD4}^+$  T cells treated with okadaic acid for 96 hours. Data is representative of 2 independent experiments.

(d) Proliferation index of Teff cells in the presence of increasing numbers of Tregs was assessed by cell-trace violet dye dilution. Data is compiled from 4 independent experiments – statistical analysis was performed by 2-way ANOVA;  $p\text{-interaction}=0.44$ .



### 3.5 Discussion

Allergic airway inflammation and asthma occur due to a breakdown in host immune tolerance to harmless foreign antigens or allergens. In normal individuals, allergens elicit an anti-inflammatory response. However, in patients and experimental animal models with severe allergic airway inflammation and airway hyper-reactivity, a maladaptive inflammatory response develops [232,314-316,334-336]. Treg cell dysfunction has been proposed as a possible reason for the breakdown in tolerance and the subsequent inflammatory response [215,318,319,333]. However, it is unclear how Treg physiology could be subtly altered in a specific inflammatory setting without leading to a broader defect. The purpose of this study was to investigate whether the phenomenon of decreased PP2A expression in asthmatics might be linked to Treg cell dysfunction.

In a mouse model of house dust mite-induced allergic airway inflammation, we observed severe airway inflammation characterized by eosinophilia, Teff cell infiltration, and increased mucus production. These animals also had high numbers of Treg cells in their lungs and mediastinal lymph nodes, yet had no significant increase in IL-10 levels in their airways. As IL-10 is a cytokine often associated with peripheral Treg cells, we hypothesized that these mice could be exhibiting Treg cell dysfunction. Interestingly, these inflamed mice exhibited decreased PP2A expression, a feature previously observed in glucocorticoid resistant asthmatics [234,256,318]. This was of particular interest

as PP2A was previously shown to regulate activity of the critical Treg cell transcription factor, FoxO1 [229,338].

FoxO1 expression is essential for Treg cell differentiation as well as the Treg cell anti-inflammatory phenotype [218,222,223,322,326,339,340]. Deletion of FoxO1 in Treg cells causes them to adopt a pro-inflammatory phenotype and produce IFN $\gamma$ . Interestingly, increased levels of IFN $\gamma$  are observed in patients with severe, glucocorticoid-resistant asthma - the same category of patients that have decreased PP2A expression. We hypothesized that FoxO1 function could become perturbed under conditions with decreased PP2A expression, as PP2A promotes FoxO1 nuclear localization. To determine whether changes in PP2A activity could alter Treg cell phenotypes, we utilized the PP2A inhibitor okadaic acid in a series of *in vitro* assays to test Treg cell differentiation and function.

Surprisingly, we did not observe any perturbations of the Treg cell phenotype in the presence of okadaic acid. Okadaic acid treated Treg cells did not produce inflammatory cytokines, such as IL-17 or IFN $\gamma$ , both of which have been reported in Treg cells deficient in PP2A and FoxO1 [218,333]. Additionally, we observed that the suppressive function of Treg cells on Teff cell proliferation was unaffected by okadaic acid-mediated PP2A inhibition, in contrast to Treg cells lacking PP2A $\alpha$  [333]. From these data we conclude that *in vitro* administration of okadaic acid is an unsuitable experimental system for further dissecting the role of phosphatases in Treg function.

While *in vivo* studies, including genetic deletion of phosphatases, provide valuable information, complementary *ex vivo* assays are critical for mechanistic studies, and for assessing potential therapeutic options prior to testing in an organismal context. Therefore, while we carefully analyzed multiple parameters to ensure that okadaic acid blocked phosphatases and affected FoxO1 phosphorylation status, okadaic acid did not recapitulate the functional deficiencies of Treg cells that have been reported in Treg cells that lack FoxO1 and Treg cells that lack the catalytic subunit of PP2A. This could be due to at least two possibilities. First, the loss of FoxO1 or PP2A achieved genetically occurs throughout the 'life' of the Treg cells prior to their analysis. In our *ex vivo* assays, this is done via acute inhibition of PP2A, and whether the acute versus chronic loss of PP2A function differentially affects Treg phenotype remains to be seen. Second, the function of Treg cells is likely complex and precisely how Treg cells regulate Teff cells *in vivo* is still incompletely understood. Therefore, it is possible that acute inhibition of PP2A activity and subsequent alteration of FoxO1 phosphorylation might lead to subtle changes in Treg cell function that cannot be observed in *ex vivo* systems. Given the *in vivo* findings from other groups regarding the importance of FoxO1 and PP2A in Treg cells, our work suggests that caution should be used in interpreting the *ex vivo* assays of Treg cell function as they correlate to Treg cell functionality *in vivo*.

While our *in vitro* systems were unable to recapitulate the recent *in vivo* observations regarding the importance of PP2A in Treg cell function [333], it is an

intriguing possibility that the decrease in PP2A expression observed in the mediastinal lymph nodes of mice with allergic airway inflammation, and in the peripheral blood monocytes of patients with glucocorticoid resistant asthma, might be associated with Treg cell dysfunction. We hope that further use of genetic models, ideally with temporal manipulation of gene expression, might elucidate how PP2A and FoxO1 function and regulation might influence various acquired inflammatory states.

### **3.6 Acknowledgements and co-author contributions**

#### **Author contributions**

KKP, MWB, SA and KSR designed experiments. KKP performed experiments. KKP and KSR wrote the manuscript. KKP, MWB, SA and KSR edited the manuscript.

#### **Acknowledgements**

We thank the members of the Ravichandran Laboratory for their helpful advice. We thank Ignacio Juncadella for initial help with the HDM model, Emily Mercadante for help with the Treg suppression assay. We also thank Ewa Kubicka and David Brautigan for their assistance with the phosphatase assay and for providing purified PP2A. We thank the UVA Research Histology Core for their preparation of tissue specimens.

## Chapter IV

### Summary and Future Directions

The project described in Chapter III of this dissertation was pursued to its logical conclusion while the project detailed in Chapter II has produced multiple findings that spawned important future directions. The summary and future directions for Chapter II are detailed here.

#### 4.1 Summary

The findings presented in Chapter II make several important contributions to our understanding of PtdSer receptors and their role in coordinating apoptotic cell clearance. First, the *Bai1<sup>Tg</sup>* is capable of rescuing the phagocytic defects in *Mertk<sup>-/-</sup>* Sertoli cells. Second, unlike in Sertoli cells, the *Bai1<sup>Tg</sup>* is unable to rescue the phagocytic defects in *Mertk<sup>-/-</sup>* RPE. Furthermore, the *Bai1<sup>Tg</sup>* does not prevent retinal degeneration in a *Mertk<sup>-/-</sup>* background. Third, the absence of *Mertk* perturbed the visual cycle, as manifested by decreased retinyl ester accumulation. Lastly, *Mertk* deficient RPE exhibited a dysregulated gene expression profile, with changes in genes related to phagocytosis, metabolism and retinal disease.

Prior to this work, PtdSer receptors had been clustered in two broad categories: 'tethering' and signaling. Tethering receptors were thought to simply bind the target but not signal. Signaling PtdSer receptors, while being an exceedingly broad category, have been (erroneously) considered a single cohesive group. We assessed the ability of BAI1 to compensate in the absence

of another PtdSer receptor, MerTK. We assessed functional rescue in two specialized phagocytes *in vivo*: the Sertoli cell and the RPE. Intriguingly, BAI1 overexpression did in fact rescue the defective Sertoli cell-mediated clearance of apoptotic cells in the *Mertk*<sup>-/-</sup> background. Testicular torsion, which increases the amount of germ cell death in the seminiferous tubules, lead to a large accumulation of apoptotic germ cells in the testes in *Mertk*<sup>-/-</sup> mice. In contrast, *Mertk*<sup>-/-</sup>*Bai1*<sup>Tg</sup> mice had significantly fewer corpses in their testes such that the degree of corpse accumulation resembled that observed in wild-type mice.

Like the Sertoli cells, RPE are specialized phagocytes. However, unlike Sertoli cells, which phagocytose apoptotic germ cells, RPE cells phagocytose pieces of the photoreceptors in order to promote photoreceptor survival. Assessment of phagocytic clearance of outer segments by the RPE revealed that (as anticipated) *Mertk*<sup>-/-</sup> mice had decreased outer segment clearance. However, this defect was not reversed in *Mertk*<sup>-/-</sup>*Bai1*<sup>Tg</sup> mice. In addition, the retinal degeneration that occurs as a result of defective outer segment clearance was not rescued or slowed by BAI1 over expression.

These data suggested that MerTK was uniquely critical for RPE function and suggested that BAI1's ability to promote phagocytosis might in fact be tissue or context dependent. In addition to mediating phagocytosis, specialized phagocytes play a multitude of roles in their respective tissues. One of the most important functions of the RPE is converting all-*trans*-retinol to the chromophore

11-*cis*-retinal. Analysis of visual cycle intermediates revealed that *Mertk*<sup>-/-</sup> mice have decreased retinyl esters, which are the precursors of 11-*cis*-retinal. This phenotype was observed in mice at 21 days of age, prior to the onset of retinal degeneration. The decreased retinyl ester accumulation suggested that the absence of MerTK perturbs RPE processes beyond phagocytosis.

To expand our understanding of how RPE expression of MerTK affects RPE functions beyond phagocytosis, we used the unbiased approach of RNAseq to analyze the transcriptome of RPE from *Mertk*<sup>-/-</sup> and *Mertk*<sup>+/+</sup> mice. The RNAseq dataset revealed 60 genes that were differentially regulated in *Mertk*<sup>-/-</sup> RPE. From this dataset, two crucial clusters of genes were identified: genes linked to phagocytosis and genes linked to metabolism. The dysregulation of genes associated with phagocytosis was not only fascinating, it also provided an explanation for why BAI1 is unable to rescue phagocytosis in *Mertk*<sup>-/-</sup> RPE. The dysregulation of metabolic genes was also of significant interest and we considered two possible interpretations of these data. First, the dysregulation of metabolic genes could lead to phagocytic dysregulation since phagocytosis is a metabolically demanding process. However, it is also possible that these metabolic findings might in fact be the result of defective phagocytosis and not the cause. This prospect was particularly fascinating as several genes related to cholesterol metabolism were identified in this dataset and cholesterol export is regulated downstream of phagocytosis in certain cell types. Furthermore,

cholesterol export is an important RPE function and is necessary for the maintenance of retinal homeostasis.

In the following section, I outline the major questions raised by our findings and discuss how these questions might be answered with future studies.

## 4.2 Future Directions

### 4.2.1 Why doesn't BAI1 expression rescue defects in RPE phagocytosis?

We found that BAI1 over expression was capable of rescuing deficient Sertoli cell phagocytosis in *Mertk*<sup>-/-</sup> mice yet we did not see a similar rescue of RPE phagocytosis. The context-dependent nature of BAI1 function is particularly puzzling but there are key differences between the two cell types and modes of clearance that were analyzed, any of which could explain why BAI1 functions in one phagocyte but not the other. I have outlined four possibilities below.

#### **The role for BAI1 in cell pruning:**

First, the phagocytic events that occur in the RPE differ greatly from what occurs in Sertoli cells. POS clearance, unlike apoptotic germ cell clearance, is a cell 'pruning' process. Sertoli cells engulf apoptotic corpses while RPE prune the photoreceptor. The mechanics underlying these processes might differ greatly and it is possible that BAI1 is unsuited to mediating cell pruning despite functioning in corpse-clearance. Thankfully, there are at least two other instances of phagocytic 'pruning' of live cells that we can use as models to investigate this question: synaptic pruning in the central nervous system and residual-body removal in the testis.

Residual body removal during spermatogenesis has been linked to the apoptotic cell clearance machinery via studies in *C. elegans* [348]. Additionally, microscopic analysis of this process in situ suggests that it is a true 'pruning' process [349]. Impaired residual body phagocytosis can lead to abnormal

morphology of the mature sperm due to excessive cytoplasm and/or abnormal accumulation of multinucleate cells in the seminiferous tubules [350]. Additionally, residual body removal can be monitored in situ by quantifying lipid body accumulation in Sertoli cells in stage VIII tubules (the stage when spermiation occurs) and by looking for multinucleate giant cells / large residual bodies in testicular sections [134,349]. To determine if BAI1 promotes residual body 'pruning', we can begin by evaluating *Bai1*<sup>-/-</sup> mice as BAI1 is expressed endogenously by Sertoli cells. We can evaluate oil-red-O staining in stage VIII tubules to quantify residual body uptake. In addition we can evaluate sperm morphology and sperm counts in the seminiferous fluid of *Bai1*<sup>-/-</sup> mice. Should we find that *Bai1*<sup>-/-</sup> mice do not have a phenotype with regard to residual body pruning, we can also evaluate *Mertk*<sup>-/-</sup> and *Mertk*<sup>-/-</sup>*Bai1*<sup>Tg</sup> mice to see if the absence of MerTK causes impaired residual body removal and determine whether BAI1 is capable of rescuing this defect as it did with apoptotic cell clearance.

The functionality of BAI1 in pruning events could also be investigated in a model of synaptic pruning. While synaptic pruning has not been definitively linked to PtdSer exposure, astrocytes have been shown to prune synapses in a MerTK-dependent manner [351]. Additionally, these investigations can be performed *in vitro*, making live monitoring of pruning possible. By using the *in vitro* pruning assays, we could evaluate whether BAI1 overexpression enhances pruning in

MerTK-deficient astrocytes and further test whether BAI1 plays a role endogenously by evaluating BAI1-deficient astrocytes.

**BAI1-mediated clearance in the setting of inflammation:**

Another possible explanation for BAI1's inability to enhance phagocytosis by the RPE is that BAI1 only functions under inflammatory conditions. The *in vivo* studies on the role of BAI1 in apoptotic cell clearance have largely utilized inflammatory models: colitis, testicular torsion, thymic death and atherosclerosis [86,131]. While *Bai1*<sup>-/-</sup> mice have exacerbated apoptotic corpse accumulation in the testes following torsion and in the thymus following dexamethasone injection, they do not have any apparent corpse accumulation at baseline. Conversely, *Mertk*<sup>-/-</sup> mice do exhibit apoptotic corpse accumulation in the testes at baseline [52]. Importantly, this dissertation demonstrates that BAI1 over expression does not reduce the corpse accumulation in *Mertk*<sup>-/-</sup> testes at baseline, though rescue does occur in the inflammatory context of torsion.

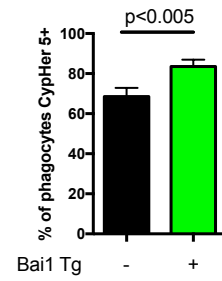
RPE phagocytosis, as assessed in this work, does not occur in a setting of acute inflammation. However, the RPE can also clear debris and apoptotic cells in settings of acute inflammation, such as with N-methyl-N-nitrosurea (MNU) administration [352] Intraperitoneal administration of MNU causes selective death of photoreceptors that occurs between 3 and 7 days post-injection [353]. The RPE clear dead photoreceptors in the setting of acute photoreceptor death induced by MNU [352]. Therefore, we can use a system of MNU injury to evaluate whether BAI1 over expression enhances RPE clearance. Similarly, we

can assess if BAI1 over expression can rescue defective RPE-mediated clearance in *Mertk*<sup>-/-</sup> mice.

The role for BAI1 in the setting of inflammation can be further dissected *in vitro*. Previous studies have shown that over expression of BAI1 enhances phagocytosis in multiple cell types *in vitro* [42,86,131]. To determine whether these enhancements might be more pronounced under inflammatory conditions, we can perform similar phagocytosis assays in the presence of inflammatory cytokines such as TNF $\alpha$  and IL-1. Alternatively, it is possible that the inflammatory environment itself may not enhance BAI1 function directly. Rather, BAI1 might only promote phagocytosis in settings with large numbers of apoptotic cells, which arise in the context of inflammation. To address this possibility *in vitro*, we can titrate apoptotic 'target' ratios to determine whether the enhancement observed in macrophages overexpressing BAI1 (**Figure 4.1**) diminishes when fewer targets are applied to phagocytes.

**Figure 4.1: Peritoneal macrophages over expressing  
BAI1 exhibit enhanced apoptotic cell clearance**

Peritoneal macrophages were isolated from 6-10 week old mice and cultured for 48 h. Apoptotic cells stained with a pH sensitive dye (CypHer 5e) were added to peritoneal macrophages at a 1:10 (phagocyte-to-target) ratio. After 30 minutes of co-culture, peritoneal macrophages were detached and CypHer 5e signal was quantified by flow cytometry.

**Peritoneal macrophage engulfment**

### **BAI1 function in phagocytosis requires the presence of an unknown co-factor**

Our data suggest that BAI1 over expression is capable of rescuing phagocytic defects in Sertoli cells, which express BAI1 endogenously. Furthermore, the current *in vivo* data suggests that endogenous BAI1 is important for apoptotic cell clearance in the testes, even if only in the setting of testicular torsion. Unlike Sertoli cells, RPE do not appear to express BAI1. Therefore, it is possible that we observed rescue in Sertoli cells but not the RPE because Sertoli cells express a previously unidentified co-factor that is essential for BAI1 function.

BAI1 was originally identified as an ELMO interacting partner in a yeast-2-hybrid screen [42]. By using the same yeast-2-hybrid approach, we might identify other potential BAI1 interacting partners and potentially a co-factor involved in promoting BAI1 function. Should BAI1 possess a co-factor that promotes signaling downstream of PtdSer binding, BAI1 might only interact with its co-factor in the context of PtdSer recognition. If the yeast-2-hybrid screen fails to yield any potential co-factors, we could instead over express a tagged version of BAI1 in a cell line. This tagged version of BAI1 would allow us to readily perform co-immunoprecipitations in the presence of apoptotic or simple PtdSer-exposing targets, such as liposomes. BAI1 interacting partners could then be identified by mass spectrometry. These studies, even if they fail to identify a true co-factor,

could reveal other BAI1 interacting partners and illuminate other pathways that are activated downstream of BAI1.

### **GTPase mediation of RPE phagocytosis**

BAI1 elicits cytoskeletal rearrangement via downstream activation of the small GTPase, Rac. While the majority of engulfment pathways converge on Rac, it is not the only GTPase capable of mediating cytoskeletal rearrangement in phagocytic events (**Figure 4.2**). Thus, if RPE phagocytosis is mediated by a different GTPase, BAI1 would be unable to enhance this process as it promotes cytoskeletal rearrangement via Rac.

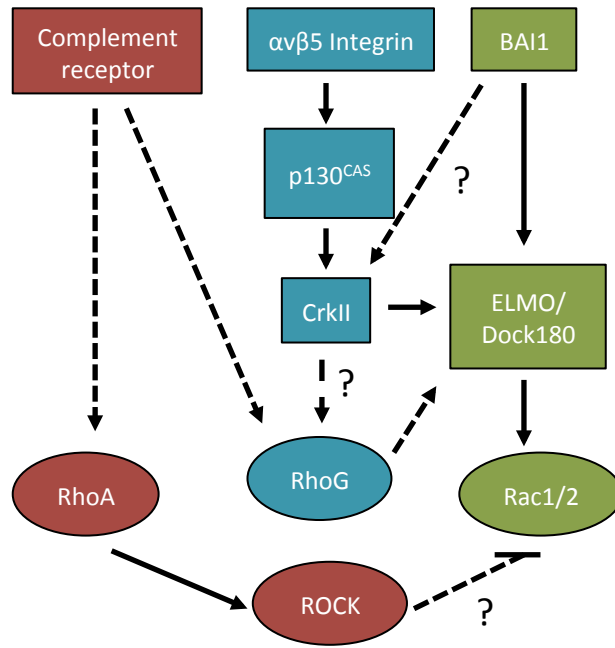
One candidate GTPase for the regulation of RPE phagocytosis is RhoA. While classically considered a negative regulator of apoptotic cell clearance, RhoA functions in other phagocytic pathways including complement receptor-mediated phagocytosis [259]. RhoA inhibits Rac activity via ROCK. In fact, during Rac-mediated phagocytic events, phagocytosis can be enhanced via ROCK inhibition, as this alleviates endogenous Rac suppression [57] (**Figure 4.2**). A potential role for RhoA in RPE phagocytosis is supported by the finding that genetic deletion of the endogenous RhoA inhibitor p27, enhances RPE phagocytosis [352]. Currently our *in vitro* RPE phagocytosis assay contradicts the hypothesis that Rac does not function in this pathway as ROCK inhibition enhanced RPE phagocytosis in culture (**Figure 2.9d**). However, in the same system, *Mertk*<sup>-/-</sup> RPE do not exhibit a phagocytic defect, which potentially

invalidates the finding that ROCK inhibition enhances RPE phagocytosis (**Figure 2.9e**).

In order to rigorously test whether Rac promotes RPE phagocytosis, we can delete *Rac1* in RPE by crossing *Rac1*<sup>Flox</sup> mice to *Best1*-cre mice. *Best1*-cre is driven by the promoter for Bestrophin1, an RPE specific gene [354]. By assessing RPE phagocytosis in *Best1*-cre *Rac1*<sup>Flox</sup> mice, we can evaluate whether Rac1 is essential for phagocytosis of POS. As with our assessment of RPE phagocytosis in *Mertk*<sup>-/-</sup> mice, phagocytosis can be monitored *in situ* by timed analysis of rhodopsin staining in eyecups. Should we find that RPE phagocytosis is not affected by the absence of *Rac1*, it would suggest that BAI1 is unable to rescue RPE phagocytosis in *Mertk*<sup>-/-</sup> mice as it does not elicit the correct phagocytic pathway.

## **Figure 4.2: Phagocytic pathways involve multiple small Rho GTPases**

A network of signaling shows how multiple engulfment pathways intersect and influence each other. Apoptotic cell engulfment via integrins and BAI1 utilize Rac1 to facilitate actin re-arrangement. The integrin pathway can elicit ELMO/Dock180 activation via cooperation with CrkII while BAI1 elicits Rac activation directly by recruiting ELMO. Complement receptor mediated phagocytosis relies on activation of the small GTPase RhoA. This pathway inhibits other engulfment pathways by activating Rho kinase (ROCK). The small GTPase RhoG promotes activity of multiple engulfment pathways. *Dashed arrows indicate indirect or less clearly defined interaction (s).*



#### **4.2.2 Does phagocytosis by specialized phagocytes regulate their non-phagocytic functions?**

Specialized phagocytes play a multitude of roles within their respective tissues including: maintenance of immunological privilege, vitamin A metabolism, cholesterol transport, and glucose transport. Interestingly, almost all of these processes have been linked either directly or indirectly to phagocytosis. This raises the fascinating hypothesis that phagocytosis by specialized phagocytes orchestrates and/or promotes their other functions. This hypothesis is supported by several important findings reported in Chapter II. First, *Mertk*<sup>-/-</sup> mice exhibit reduced retinyl ester accumulation prior to the onset of retinal degeneration. Furthermore, multiple metabolic genes, including several related to cholesterol transport and metabolism, were differentially regulated in *Mertk*<sup>-/-</sup> RPE (**Figure 2.11, Figure 4.3**). These findings support the need for a more in depth investigation of how phagocytosis regulates other functions of specialized phagocytes. Here, I detail several lines of investigation to elucidate the importance of phagocytosis in specialized phagocyte function.

#### **Phagocytosis by specialized phagocytes is necessary for the maintenance of immunological privilege**

Sertoli cells and the RPE play two crucial roles in the maintenance of immunological privilege within their respective tissues. Both cells form physical barriers that prevent infiltration of immune cells and release of certain auto-antigenic material [110,113,164]. In addition, both Sertoli cells and RPE promote

local immune privilege by producing TGF $\beta$  and promoting Treg differentiation. Importantly, TGF $\beta$  is produced by phagocytes following apoptotic cell recognition and clearance, creating a clear link between phagocytosis and immunomodulation [13].

To investigate whether phagocytosis by RPE and Sertoli cells contributes to immunological privilege within the eye and testes respectively, we can first investigate the integrity of the blood-retinal-barrier (BRB) and blood-testes-barrier (BTB) in mice with defective phagocytosis. Importantly, mice lacking all 3 TAM receptors have reduced BTB integrity and abnormal immune cell infiltration in their testes [93,109]. Additionally, unpublished data from our lab suggests that the BTB is impaired both by the loss of Rac1 and by blockade of PtdSer with soluble thrombospondin repeats from BAI1 (BAI1-TSR). These data collectively support a role for phagocytosis in maintaining the BTB. A similar assessment of the BRB can be performed in *Mertk*<sup>-/-</sup> mice, which have profoundly impaired RPE phagocytosis. Barrier integrity in the RPE layer can be assessed by looking for continuous ZO-1 staining in RPE flat mounts. Furthermore, we can assess physiological changes in barrier function using Evan's Blue Dye, which binds to albumin and therefore only extravasates into tissues exhibiting capillary leak.

To assess whether phagocytosis by either Sertoli cells or RPE influences their anti-inflammatory properties, we can utilize *in vitro* culture systems to evaluate TGF $\beta$  production by RPE and Sertoli cells exposed to POS and apoptotic germ cells, respectively. Using this *in vitro* system, we can evaluate

how primary RPE derived from *Mertk*<sup>-/-</sup> mice respond to POS as well as how primary Sertoli cells from *Mertk*<sup>-/-</sup>, *Elmo1*<sup>-/-</sup>, and *Amh1-cre Rac1*<sup>fllox</sup> (Sertoli cell specific deletion of Rac) mice respond to apoptotic germ cells. In addition to assessing TGFβ production, the supernatants from RPE and Sertoli cells that have been exposed to apoptotic or PtdSer-exposing targets, can be applied to primary CD4 T cell cultures to assess whether these supernatants promote Treg differentiation [114,144]. It would also be interesting to address whether supernatants from engulfment deficient Sertoli cells and RPE (e.g. *Mertk*<sup>-/-</sup>) are equally capable of inducing Treg differentiation, both in the presence and absence of PtdSer-exposing targets. These assays would help address whether the loss of engulfment genes influences the ability of RPE and Sertoli cells to regulate immunological barrier function by promoting Treg differentiation.

The immunological privilege maintained by the RPE and Sertoli cells prevents autoimmune inflammation in the eye and testes respectively. To determine if engulfment deficits in RPE and Sertoli cells influence the immunological barriers in their respective tissues, we can evaluate the susceptibility of mice with engulfment deficits in Sertoli cells and RPE to experimental autoimmune orchitis and uveitis. Autoimmune orchitis can be induced with subcutaneous injection of viable germ cells while autoimmune uveitis can be induced by immunization with interphotoreceptor retinoid binding protein [355,356]. Following immunization, we can monitor immune cell infiltrate

and local IgG deposition in both tissues. Interestingly, mice lacking two of the TAM receptors, Axl and MerTK, have increased susceptibility to autoimmune orchitis [357]. This finding supports the hypothesis that impaired phagocytosis leads to impairments in immunological privilege. However, this study was performed with global deletion of both genes (Axl and MerTK) and MerTK was previously shown to promote negative selection of autoreactive T cells and simultaneously promote peripheral T cell tolerance [358,359]. Thus, this finding cannot be directly linked to local engulfment deficits. To properly demonstrate that phagocytosis by Sertoli cells and the RPE contributes to local immune privilege, we will utilize Sertoli cell and RPE specific knock-outs of engulfment genes to ensure that homeostasis of the immune system is not perturbed globally.

### **Phagocytosis by specialized phagocytes influences local vitamin A storage**

Vitamin A storage is a critical feature of both RPE and Sertoli cells. Vitamin A is sequestered in cells for storage by esterification to fatty acids. These retinyl esters are not cell-permeable and are stored in both RPE and Sertoli cells for future use in the retina and testes, respectively [273]. Vitamin A has a well-documented role in the visual cycle where it is required in the form of 11-*cis*-retinal for light recognition [269]. In the testes, Vitamin A is critical for spermatogenesis as retinoid acid signaling in germ cells initiates meiosis [360]. Data presented here show that *Mertk*<sup>-/-</sup> mice exhibit decreased retinyl ester accumulation in the RPE (**Figure 2.10**). This finding is supported by an earlier

observation in *Mertk* deficient RCS rats, which have a defect in vitamin A esterification that was so severe it was (erroneously) proposed to be the cause of retinal degeneration in these animals [361]. These perturbations in vitamin A esterification could be the result of the altered metabolic gene expression profile in *Mertk*<sup>-/-</sup> RPE (**Figure 2.11**) or decreased expression of the enzyme LRAT, which esterifies vitamin A (**Figure 4.3**). While altered LRAT expression seems like an obvious underlying cause of decreased retinyl ester levels, the change in LRAT expression was not significant by adjusted p-value.

As impaired vitamin A esterification has already been observed in *Mertk*<sup>-/-</sup> RPE, the next step is to evaluate retinyl ester accumulation in Sertoli cells of engulfment-deficient mice. As with retinyl ester analysis in the eye, we can use HPLC to quantify retinyl esters in the testes of multiple strains of mice with impaired Sertoli cell phagocytosis including *Mertk*<sup>-/-</sup>, *Elmo1*<sup>-/-</sup>, and *Amh1-cre Rac1<sup>flox</sup>* mice. In addition, phagocytosis in the testes can be blocked by direct injection of annexin V and/or BAI1-TSR. By blocking phagocytosis in this way, we can evaluate whether acute perturbations of Sertoli cell phagocytosis affect retinyl ester accumulation or if phagocytic defects must be life-long. Should we see altered accumulation of retinyl esters in the testes of mice with impaired Sertoli cell phagocytosis, we will perform a similar investigation of the metabolic gene profile and LRAT expression in Sertoli cells. Changes in either LRAT expression or the metabolic gene profile could point to the mechanism by which phagocytosis influences vitamin A esterification in specialized phagocytes.

## **Phagocytosis by specialized phagocytes regulates cholesterol homeostasis in the eye and testes**

Both the retina and seminiferous tubules require complex regulation of cholesterol. Cholesterol in the testes is utilized for generation of steroid hormones while in the retina cholesterol is necessary for daily regeneration of POS. However, accumulation of cholesterol in either tissue impairs function. Importantly, both Sertoli cells and RPE mediate reverse cholesterol transport, which prevents cholesterol accumulation in the testes and eye respectively [130,161]. Deletion of *Abca1*, causes lipid accumulation in Sertoli cells, decreased sperm count, and lower levels of intratesticular testosterone [130]. On the other hand, perturbation of cholesterol metabolism by deletion of *Cyp27a1* causes abnormalities of the retinal vasculature, oxidative stress in photoreceptors and cholesterol deposits on the apical and basolateral sides of the RPE [304,305]. Interestingly, *Abca1* expression is upregulated in macrophages following PtdSer recognition and phagocytosis of apoptotic cells. Furthermore, RNAseq of *Mertk*<sup>-/-</sup> RPE revealed a significant change in the cholesterol regulator *Cyp27a1* (**Figure 4.3**). Additionally, *Mertk*<sup>-/-</sup> RPE exhibited a change (though not statistically significant) in expression of *Abca1* (**Figure 4.3**). These observations support the hypothesis that phagocytosis by specialized phagocytes might regulate cholesterol homeostasis.

To further investigate the role of phagocytosis in cholesterol homeostasis within Sertoli cells and RPE, we can utilize *in vitro* systems to monitor *Abca1*

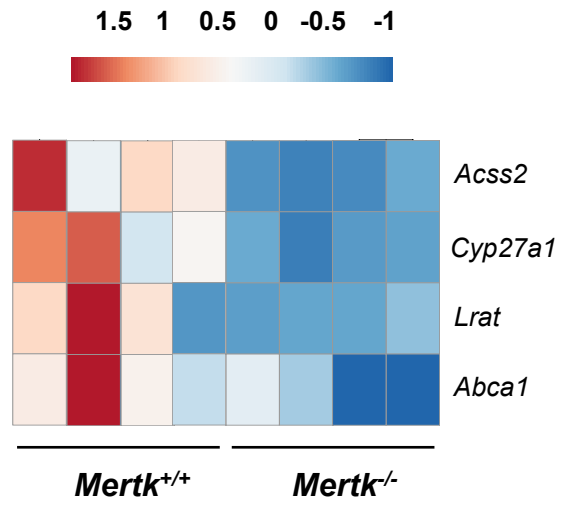
upregulation and cholesterol transport in response to apoptotic germ cells and POS respectively. In addition, we can evaluate *Abca1* expression and localization in Sertoli cells and RPE *in situ* under conditions in which phagocytosis is impaired, such as with genetic mutants or with PtdSer blockade with annexin V or the BAI1-TSR. Importantly, this would enable us to analyze the expression of this critical cholesterol regulator on mature cells. Another interesting approach would be to monitor *Abca1* expression in RPE cells at different times of day since RPE phagocytosis is temporally regulated. Should we find that *Abca1* expression peaks after light onset and wanes overnight, it would support the notion that RPE phagocytosis regulates the cholesterol export machinery in the RPE.

If we see altered expression of *Abca1* in our *in vitro* and *in situ* analyses, it would be informative to assess cholesterol accumulation in the testes and retina in engulfment-deficient mouse lines. Cholesterol levels can be assessed both by staining and direct quantification. Staining of cholesterol in tissue sections is done with oil-red-O and filipin dyes. Importantly, oil-red-O will also pick up retinyl esters [362]. Therefore, direct quantification of cholesterol in perfused tissues will be more informative regarding true cholesterol accumulation. Monitoring ocular cholesterol accumulation in *Mertk*<sup>-/-</sup> mice may prove particularly informative, as almost no RPE phagocytosis should be occurring past 3 months of age.

Collectively, the analyses proposed in this section will provide insight as to whether phagocytosis by specialized phagocytes is necessary for the execution of their other functions.

**Figure 4.3: Genes related to cholesterol metabolism and vitamin A esterification are dysregulated in *Mertk*<sup>-/-</sup> RPE**

Heat map shows genes metabolic genes that are differentially regulated in *Mertk*<sup>-/-</sup> RPE. *Cyp27a1* and *Acss2* are significantly different in *Mertk*<sup>-/-</sup> RPE. *Cyp27a1* is involved in cholesterol metabolism and *Acss2* expression is regulated by sterol responsive binding proteins. *Abca1* mediates reverse cholesterol transport and the difference in expression was not significantly different by adjusted p value ( $p_{adj}=0.76$ ) but raw p value revealed a significant difference ( $p=0.02$ ). *Lrat* promotes vitamin A esterification. Expression in *Mertk*<sup>-/-</sup> RPE was not significantly different by adjusted p value ( $p_{adj}=0.50$ ) but was significantly different by raw p value ( $p=0.008$ )



### 4.2.3 What is the role of RPE-produced insulin?

The photoreceptors of the neural retina are perhaps the most highly glycolytic cells in a healthy mammal. In fact, the astounding level of aerobic glycolysis in the retina was observed by Otto Warburg in 1925 [363]. In order to acquire the large amount of glucose required to sustain this level of glycolysis, the photoreceptors, like muscle, liver and adipose tissue, are insulin-responsive [364,365]. The insulin-response in photoreceptors upregulates the high-affinity glucose transporter, GLUT4 [366]. It has previously been assumed that systemic, circulating insulin is transported across the BRB so that it can act directly on the photoreceptors. However, one of the most surprising transcripts that we identified in our RNAseq screen of RPE was insulin (**Figure 4.4a**). According to the RNAseq dataset, the gene for insulin, *Ins2* was downregulated in *Mertk*<sup>-/-</sup> RPE relative to WT. While the change in expression in *Mertk*<sup>-/-</sup> mice did not repeat when additional animals were analyzed by qRT-PCR, we did observe astonishingly high levels of *Ins2* transcript in the RPE (**Figure 4.4b**). Furthermore, we not only observed insulin expression, we also found that multiple genes previously linked to insulin release are highly expressed in RPE, including *Rhoq*, *Slc4a4*, *Ano1*, and *Slc30a5* (**Figure 4.4a, 4.4b**) [287,367,368].

These observations prompted us to consider that retinal insulin might in fact originate in the RPE, not the systemic circulation. While extra-pancreatic sources of insulin have been reported, this finding would be unprecedented as extra-pancreatic insulin (excluding thymic insulin expression) has only been

reported in mouse models of diabetes [369,370]. The possibility of local insulin production in the eye raises several fascinating questions regarding the regulation of this insulin production and its role in retinal function. To further investigate these observations I have outlined several future directions regarding RPE-produced insulin.

### **Confirm production of insulin by the RPE**

First it will be necessary to confirm that the RPE are in fact producing and releasing insulin. While the RPE preparations for gene expression analysis are considered pure, there is still a possibility of contamination from other cells. To confirm that the RPE are transcribing *Ins2*, we can use RNA FISH or insulin-reporter mice to localize *Ins2* transcript *in situ*. Furthermore, we can stain retinal sections for the insulin protein product. Lastly, we can perfuse mice and quantify the amount of insulin within the eye. Combined, these methods will establish which cells in the retina are expressing/producing insulin and will determine how much insulin is present in the eye under normal conditions. Lastly, it would be interesting to determine how much circulating insulin contributes to the pool of ocular insulin. This could be performed by intravenously injecting mice with radiolabelled insulin. These mice would be euthanized and perfused shortly following injection and radioactive signal could be assessed in eye or retinal homogenates.

### **Regulation of RPE insulin production and release**

The  $\beta$  cells of the pancreas are considered to be the main (and potentially only) source of insulin in healthy animals [369,370]. In pancreatic  $\beta$  cells, insulin production is regulated at the transcriptional and translational levels in response to circulating glucose. Under fasting conditions, insulin expression is downregulated and upon glucose exposure,  $\beta$  cells upregulate production and release of insulin to instruct peripheral tissues to absorb circulating glucose [371]. Unlike muscle, adipose and hepatic tissues, which are also insulin responsive, the photoreceptors rely almost solely on glycolytic metabolism. Considering the metabolic demand of the photoreceptors, the near-exclusive use of glycolysis in these cells necessitates high levels of glucose. Thus, it might be advantageous for photoreceptors to continuously express the insulin-regulated GLUT4 transporter on their surface, so as to ensure consistent glucose absorption. Should photoreceptors continuously express surface GLUT4, they would theoretically require a continuous source of insulin. Thus, we hypothesize that insulin production by the RPE is not affected by circulating glucose levels. To investigate this hypothesis, we can evaluate fasting expression of *Ins2* in the RPE. In addition, we can investigate whether ocular insulin levels change during fasting, when circulating insulin levels drop.

### **Importance of RPE-derived insulin for visual function**

Ultimately, the goal of this line of investigation is to determine whether insulin produced by the RPE is crucial for retinal homeostasis and visual function.

Thus, the most crucial experiment is to eliminate RPE expression of insulin and monitor visual function. Unfortunately, there are no inducible or tissue specific methods to delete insulin. However, the eye is uniquely suited for tissue-specific deletion. The RPE are amenable to *in vivo* methods of gene delivery, including lentiviral and adenoviral transduction systems. In fact, viral gene transfer of *Mertk* to RCS rats and mice has successfully prevented retinal degeneration [188,372]. Thus, we can inducibly delete insulin in the RPE by viral delivery of shRNA against *Ins2*. Of note, rodents express two isoforms of insulin, *Ins1* and *Ins2* [373]. Importantly, *Ins2* is the homolog of insulin that is expressed by other species. Our RNAseq data indicates that *Ins1* is not expressed by the RPE, making shRNA-mediated knockdown of insulin by targeting *Ins2* feasible.

Following *Ins2* knockdown, changes in retinal function and architecture can be monitored in live animals over time. Electrical impulses in the retina are monitored by electroretinogram recordings, which can discern the electrical activity in the photoreceptors from the interneurons and ganglion cells. Optical coherence tomography can also be used in live mice to assess retinal degeneration and any potential retinal detachment and sub-retinal fluid accumulation that might result from long-term insulin deficits. By using these non-invasive techniques, we can monitor mice with insulin-deficient RPE over long periods of time. In addition to monitoring these mice at baseline, we can also assess retinal electrical activity in fasting mice.

### **Assessment of insulin production in Sertoli cells**

In Otto Warburg's original work on the glycolytic metabolism of cancer cells, he mentions the high level of aerobic glycolysis in the retina and the testes. In keeping with the line of investigation proposed in **4.2.2**, it would be informative to evaluate whether Sertoli cells also produce insulin to support the developing germ cells. Indeed, a preliminary analysis of *Ins2* gene expression in Sertoli cells revealed that they expressed low levels of *Ins2* (**Figure 4.3c**). Since Sertoli cells are kept in culture for several days prior to analysis, it is possible that *Ins2* expression is more robust *in vivo*. Therefore, *Ins2* expression should be evaluated *in situ*, using either Insulin-reporter mice or RNA FISH. Furthermore, insulin protein staining and quantification should be evaluated in the testes, as with the retinas.

Should we find that Sertoli cells express and produce insulin, we can perform similar analyses as detailed above. Testicular insulin levels can be monitored in fasting mice in order to determine whether testicular insulin production is dependent upon circulating glucose levels. Unfortunately, viral gene transfer in the testes will not specifically affect Sertoli cells, making it difficult to monitor the effects of tissue-specific deletion on testicular function.

Collectively, these proposed experiments will confirm whether RPE and Sertoli cells are extra-pancreatic sources of insulin. Furthermore, should we determine that RPE and Sertoli cells produce insulin, these studies will help us to understand how that insulin production is regulated and what role it plays in the

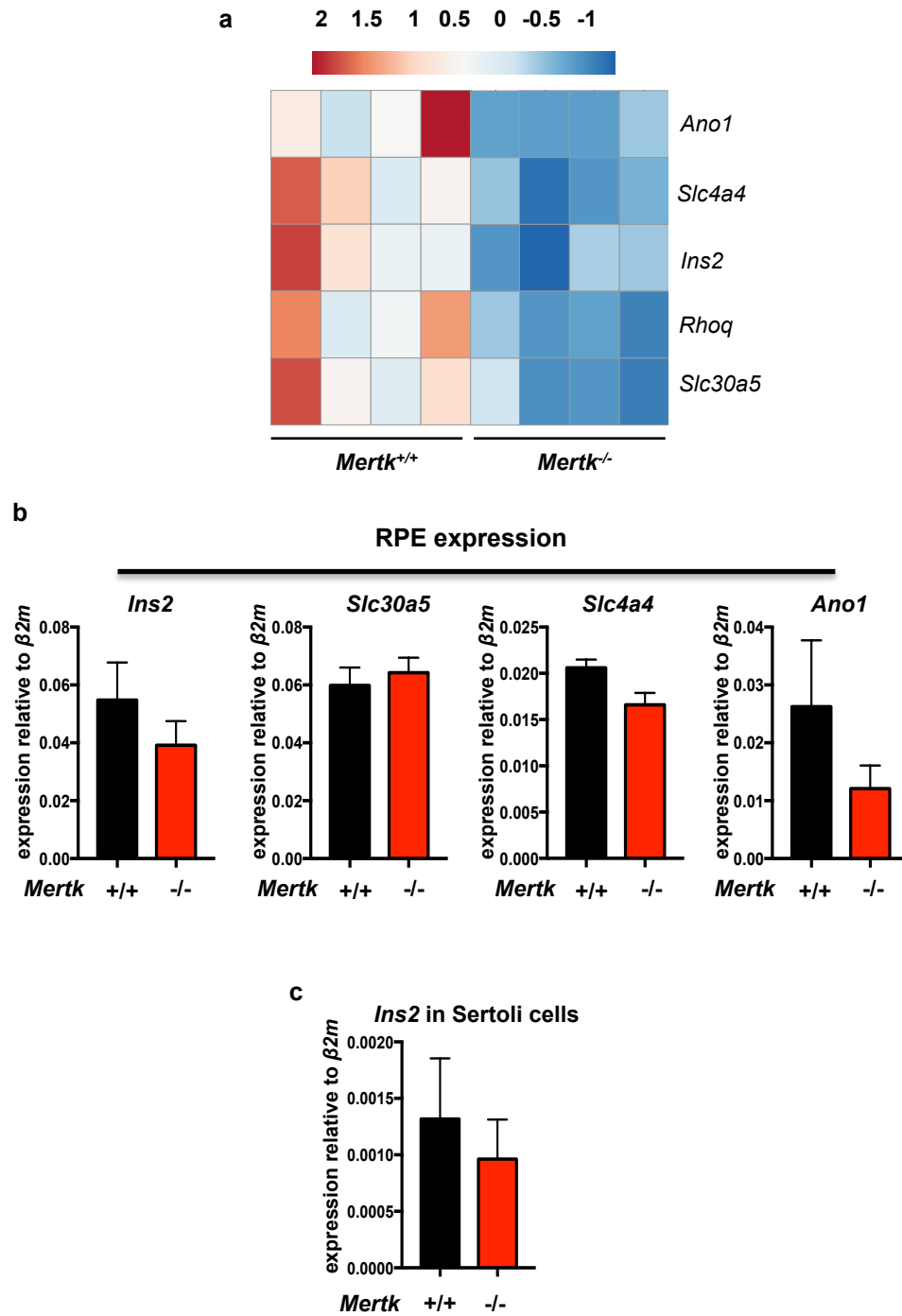
local tissue-environment. Should we uncover extra-pancreatic sources of insulin in healthy mice, it would be a profoundly interesting discovery.

**Figure 4.4: RPE express insulin and multiple genes related to insulin release**

(a) Heat map of genes related to insulin production and release that were differentially regulated according to RNAseq analysis of *Mertk*<sup>+/+</sup> and *Mertk*<sup>-/-</sup> RPE.

(b) Genes related to insulin production and release that were identified in the RNAseq analysis were analyzed in the original library prep and a fresh set of RPE samples by qRT-PCR (WT n=8; KO n=9). Values graphed are  $2^{\Delta\text{CT}}$  and  $\beta 2$  microglobulin was used as a housekeeping control gene. Analysis of *Ins2* and *Slc30a5* revealed that there was no difference between *Mertk*<sup>+/+</sup> and *Mertk*<sup>-/-</sup> mice. While *Slc4a4* and *Ano1* showed no significant differences by  $2^{\Delta\text{CT}}$  values, normalization revealed differences (**Figure 2.11**).

(c) *Ins2* expression was analyzed in Sertoli cells that harvested from P14 mice. Sertoli cells were cultured for 5 days to expand them prior to isolating RNA.



## Appendix I

### Evaluation of *Tim4*<sup>-/-</sup> mice in pristane-induced autoimmune disease

#### A1.1 Introduction

Failure to clear apoptotic cells has been implicated in the development of autoimmune diseases such as systemic lupus erythematosus (SLE) [257]. Patients with SLE are reported to have circulating apoptotic endothelial cells in their sera and apoptotic corpses attached to (but uncleared by) tingible body macrophages in the spleen [374-376]. The defective apoptotic cell clearance in these patients has been attributed to lower concentrations of serum complement proteins relative to healthy controls, suggesting that the defective clearance is not intrinsic to phagocytes [377]. However, PtdSer receptor knock-out mice have been reported to mimic certain features of SLE and this has been hypothesized to result from defective apoptotic cell clearance in these animals [41,90,257,378].

In the original manuscript identifying TIM4 as PtdSer receptor, it was reported that *in vivo* blockade of TIM4 led to an increase in anti-dsDNA antibodies and anti-cardiolipin antibodies [41]. Characterization of a *Tim4*<sup>-/-</sup> mouse supported a crucial role of TIM4 in preventing auto-antibody production as these mice exhibited anti-dsDNA antibodies as early as 8 weeks of age [379]. However, more recent reports contradict these original findings, as auto-antibodies were not found to develop spontaneously in *Tim4*<sup>-/-</sup> mice, but did develop when both TIM4 and MFG-E8 were absent [90]. In considering these

conflicting reports, we hypothesized that *Tim4*<sup>-/-</sup> mice might be more susceptible to autoimmune disease, but spontaneous development of autoimmunity might depend upon a variety of factors, including microbiota differences from one facility to another [380]. Therefore, we attempted to induce autoimmune disease in *Tim4*<sup>-/-</sup> mice by injecting them with pristane.

Pristane is a hydrocarbon that induces chronic inflammation when injected in to the peritoneum of mice [381]. While this method of inducing SLE-like autoimmune disease might be considered artificial, occupational exposure to hydrocarbon oils has been linked to SLE and rheumatoid arthritis [382,383]. C57Bl/6 mice injected with pristane tend to develop a milder course of autoimmune disease than more autoimmune-prone strains such as BALB/c mice. However, pristane-treated C57Bl/6 mice do exhibit increased titers of anti-smRNP auto-antibodies, which are considered pathognomonic for pristane-induced-lupus autoimmune disease. Interestingly, pristane-treated C57Bl6 mice (but less commonly BALB/c) exhibit another feature of SLE, diffuse alveolar hemorrhage resulting from pulmonary capillaritis [384]. Alveolar hemorrhage is a devastating complication of SLE and few mouse models of SLE exhibit alveolar this phenomenon.

Analysis of pristane-treated *Tim4*<sup>-/-</sup> mice led to two surprising observations. First, *Tim4*<sup>-/-</sup> mice treated with pristane do not develop more severe autoimmune disease than WT animals as measured by autoantibody titers and renal pathology. Second, *Tim4*<sup>-/-</sup> mice exhibited increased survival in

the 30 days following pristane-treatment, the time frame in which diffuse alveolar hemorrhage typically develops in C57Bl/6 mice [384]. Recently, the alveolar hemorrhage phenotype in pristane-induced lupus was linked to macrophage activation [385]. Given the reported importance of TIM4 in macrophage production of inflammatory cytokines and nitric oxide [378,386], our data could indicate a role for TIM4 in the pathogenesis of pristane-induced alveolar hemorrhage.

## **A1.2 Experimental procedures**

### **A1.2.1 Mice**

*Tim4*<sup>-/-</sup> mice were generously provided by Vijay Kuchroo [379] at Harvard University. These mice were crossed to C57Bl/6J mice to generate heterozygous animals. *Tim4*<sup>-/-</sup> and *Tim4*<sup>+/+</sup> mice derived from crossing heterozygotes were used for experiments. Mice were maintained under specific pathogen free conditions. 500  $\mu$ L of pristane was administered to 8 week-old mice by IP injection to induce autoimmune disease. Day 0 serum samples were collected by retro-orbital bleed prior to injection. Subsequent serum samples were collected by retro-orbital bleed at the indicated time-post injection of pristane. Retro-orbital bleeds were performed in mice anesthetized with isoflurane. Mice were euthanized 6 months post-pristane administration by CO<sub>2</sub> asphyxiation. Kidneys were collected for histology.

### **A1.2.2 Autoantibody ELISA**

ELISA plates were coated overnight with antigen: dsDNA (Sigma) or smRNP (Immunovision) in pH 9.6 carbonate buffer. Following coating, plates were blocked with PBS 5% FBS (Gemini) for 2 h. Plates were washed and serum samples were diluted 1:50 in PBS and added to the plate. Serum was incubated on shaking plate for 2 h at RT. Anti-mouse IgG conjugated to HRP (Thermo Fisher) was used to detect bound serum antibodies.

**A1.2.3. Glomerular measurement**

Kidneys were fixed in Bouin's fixative solution for 6 hours. Following fixation, kidneys were transferred to 70% EtOH and then paraffin embedded, sectioned and stained with PAS by the UVA Histology Core. Kidney sections were imaged at 20x magnification and images containing glomeruli were captured for analysis. Glomerular diameter was measured in ImageJ (NIH). A total of 20 glomeruli were measured per mouse.

## A1.3 Results

### A1.3.1 *Tim4*<sup>-/-</sup> mice do not exhibit exacerbated pristane-induced autoimmune disease relative to WT mice

In order to evaluate susceptibility of *Tim4*<sup>-/-</sup> mice to autoimmune disease, we elected to use the hydrocarbon oil pristane to induce autoimmune disease. 8-week old *Tim4*<sup>-/-</sup> and *Tim4*<sup>+/+</sup> mice received IP-injections of pristane on Day 0. Prior to injection, serum was collected by retro-orbital bleed in order to determine circulating autoantibody titers at baseline (**Figure A1.1a**). Importantly, *Tim4*<sup>-/-</sup> mice did not exhibit increased total IgG, anti-dsDNA, or anti-smRNP antibodies at baseline (**Figure A1.1b**). This finding contradicts the original characterization of *Tim4*<sup>-/-</sup> mice, which reported that elevated anti-dsDNA titers developed as early as 8 weeks of age [379]. However, our data is in agreement with a more recent report that indicates TIM4 deficiency only leads to autoimmunity when MFG-E8 is simultaneously deleted [90].

After pristane-administration, serum was collected at 30-day intervals for 6 months for measurement of serum autoantibody titers (**Figure A1.1a**). As expected, pristane administration led to detectable titers of anti-smRNP antibodies in approximately 25% of treated-mice and no increase in anti-dsDNA antibodies (**Figure A1.1c**) [381]. However, we were surprised to find that *Tim4*<sup>-/-</sup> mice did not exhibit an increased incidence in autoantibody titers nor did they exhibit higher autoantibody titers relative to *Tim4*<sup>+/+</sup> mice (**Figure A1.1c**). Furthermore, analysis of kidney pathology 6 months-post-pristane administration

revealed no difference in glomerular pathology, as measured by glomerular size (**Figure A1.1d**).

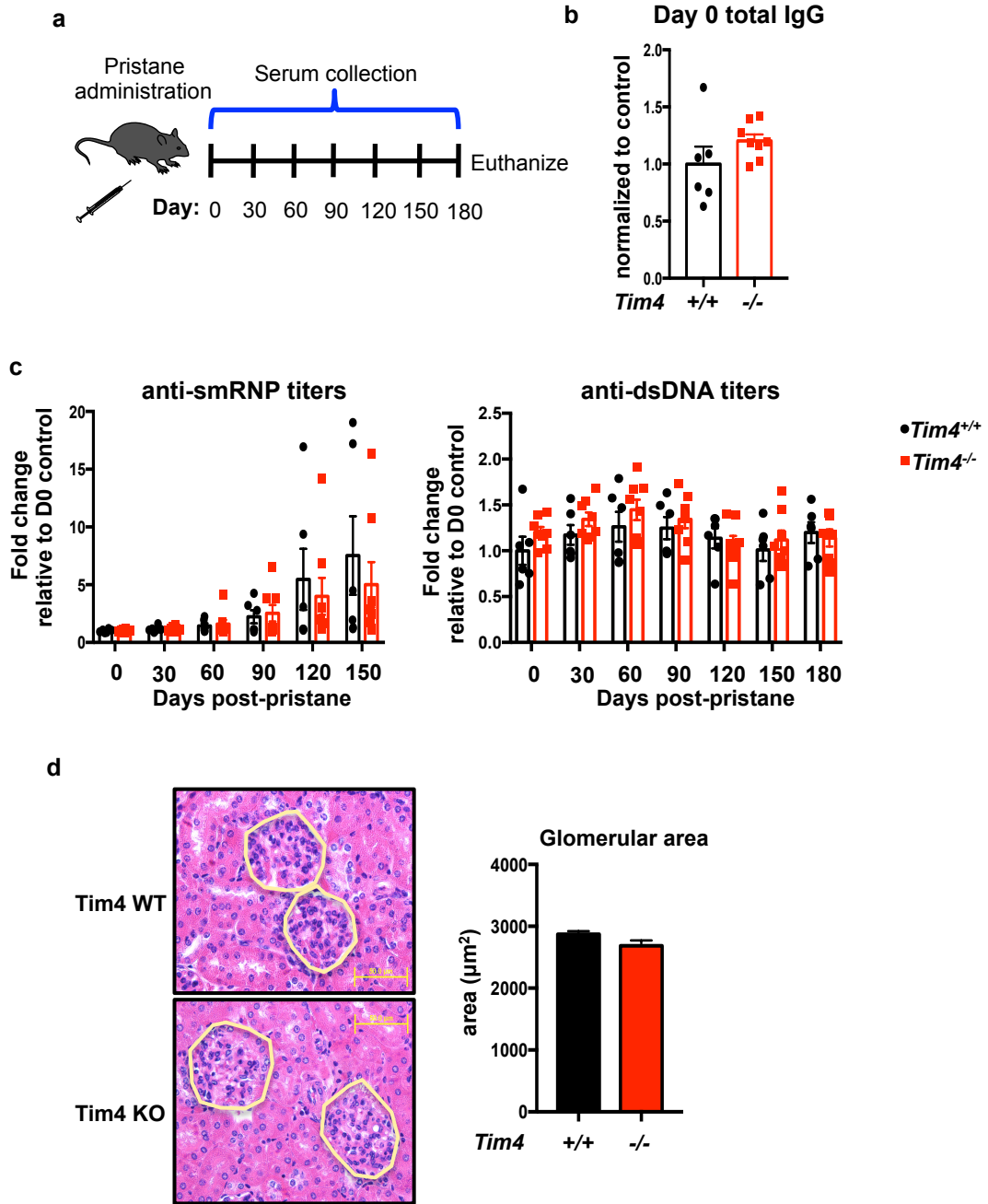
**Figure A1.1: *Tim4*<sup>-/-</sup> mice do not exhibit symptoms of autoimmune disease following pristane administration**

(a) Schematic of disease model. Mice receive an IP injection of pristane on D0. Serum was collected prior to pristane injection on D0 and every 30 days thereafter. Mice were euthanized at D180.

(b) Day 0 measurement of total IgG. Values reported are normalized to WT control. Only mice that survived to the end of the experiment were analyzed (*Tim4*<sup>+/+</sup> n=6; *Tim4*<sup>-/-</sup> n=8).

(c) Anti-smRNP and anti-dsDNA antibody titers were measured by ELISA. Values were normalized to Day 0 *Tim4*<sup>+/+</sup> (*Tim4*<sup>+/+</sup> n=6; *Tim4*<sup>-/-</sup> n=8).

(d) Kidneys isolated from *Tim4*<sup>+/+</sup> and *Tim4*<sup>-/-</sup> upon euthanasia at Day 180. Images were captured at 20x magnification. Glomerular areas were measured in ImageJ. Yellow outlines encircle glomeruli and scale bars are 50  $\mu$ m. Average glomerular measurements are based on n=3 WT and n=2 *Tim4*<sup>-/-</sup>. Measured at least 6 glomeruli per mouse. Error bars are SEM.



### **A1.3.2 *Tim4*<sup>-/-</sup> mice have increased survival following pristane-administration**

Pristane treatment of C57Bl/6 mice leads to substantial mortality in the 30 days following pristane injection. This has been attributed to the development of diffuse alveolar hemorrhage that occurs between 10 and 30 days following pristane injection [384]. Indeed, 10 days post-pristane administration, mice began to exhibit symptoms of severe illness, including labored breathing, poor cutaneous perfusion and lethargy. The vast majority of mice exhibiting these symptoms died within 48 h of symptom-onset. Necropsy of these animals revealed profound pulmonary hemorrhage, supporting the original reports of diffuse alveolar hemorrhage following pristane-administration (**Figure A1.2a**). However, we were surprised to find that *Tim4*<sup>-/-</sup> mice had significantly lower mortality rates than their WT counterparts (**Figure A1.2b**). The development of pulmonary capillaritis following pristane-administration was recently reported to be dependent upon macrophage activation [385]. TIM4 is highly expressed on the surface of macrophages, and reportedly suppresses macrophage TNF $\alpha$  and nitric oxide production [378,386]. Thus, it is possible that the reduced-mortality in *Tim4*<sup>-/-</sup> mice reflects an altered macrophage phenotype.

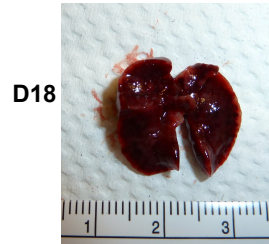
**Figure A1.2: *Tim4*<sup>-/-</sup> mice are resistant to death after pristane administration**

**(a)** Lungs isolated from *Tim4*<sup>+/+</sup> mice during necropsy. Day of death post-pristane administration is noted. Images are representative.

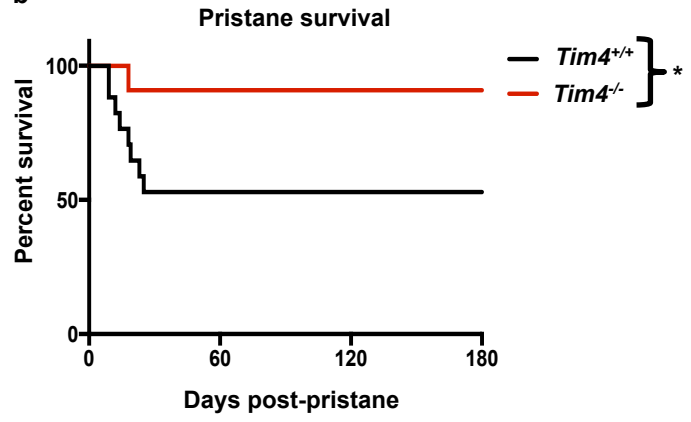
**(b)** Survival curves of *Tim4*<sup>+/+</sup> and *Tim4*<sup>-/-</sup> mice following pristane administration.

*Tim4*<sup>+/+</sup> n=17 ; *Tim4*<sup>-/-</sup> n=11. \*p<0.05.

a



b



## A1.4 Discussion

Impaired apoptotic cell clearance has been touted as an important underlying cause of autoimmune disease [387]. While many PtdSer receptor knockout mice, with impaired apoptotic cell clearance, have been identified, few exhibit signs of overt, spontaneous autoimmune disease. However, mice deficient in TIM4 and MerTK have been reported to develop spontaneous autoimmune disease, though these reports are inconsistent from one research group to the next [52,90,257,378]. One possible explanation for these differences is that while PtdSer receptor knockout animals are more susceptible to autoimmune disease, differences in mouse-facilities dictate whether disease develops spontaneously. Therefore, we hypothesized that inducing autoimmune disease via introduction of pristane, would reveal the susceptibility to autoimmune disease in mice lacking specific PtdSer receptors. To test this hypothesis, we treated *Tim4*<sup>-/-</sup> mice with pristane and monitored the development of autoimmune disease.

We were surprised to find that *Tim4*<sup>-/-</sup> mice did not exhibit greater susceptibility to autoimmune disease, nor did the mice that developed disease exhibit greater disease severity. However, we were surprised to find that *Tim4*<sup>-/-</sup> mice had increased survival relative to WT animals. This increase in survival appeared to be reduced susceptibility to diffuse alveolar hemorrhage. Alveolar hemorrhage due to pulmonary capillaritis is a devastating complication of SLE [388,389]. Our data could indicate a role for TIM4 in the pathogenesis of alveolar

capillaritis. As we did not observe increased susceptibility or severity of autoimmune disease in *Tim4*<sup>-/-</sup> mice, TIM4 might represent a unique target for the treatment or prevention of alveolar hemorrhage in SLE patients.

## Appendix II

### Characterization of colonic epithelial cells and inflammatory infiltrates in *Bai1*<sup>-/-</sup> and *Bai1*<sup>Tg</sup> mice with DSS-colitis

*The experiments described in this section were partially incorporated in to a manuscript: Chang Sup Lee, Kristen K Penberthy, Karen M Wheeler, Ignacio J Juncadella, Peter Vandenabeele, Jeffrey J Lysiak, Kodi S Ravichandran. Boosting apoptotic cell clearance by colonic epithelial cells attenuates inflammation in vivo. Immunity. 2016*

#### A2.1 Introduction

The GPCR BAI1 is a bona fide PtdSer receptor and promotes clearance of apoptotic cells [42]. The original identification and analysis of BAI1 was conducted *in vitro*. In order to evaluate the importance of BAI1 to maintaining the health and homeostasis of an organism, two mouse lines were generated: mice lacking BAI1 (*Bai1*<sup>-/-</sup>) and mice that conditionally overexpress BAI1 in cre-driven manner (*Bai1*<sup>Tg</sup>) [86,131,390]. Analysis of *Bai1*<sup>-/-</sup> revealed only one phenotype at baseline: reduced diameter of muscle fibers [390]. However, there was no clear accumulation of apoptotic cells in any tissues analyzed (thymus, testes, colon).

Therefore, *Bai1*<sup>-/-</sup> mice were subjected to multiple disease models to determine how the absence of BAI1 influenced disease states. Two important findings in *Bai1*<sup>-/-</sup> mice were made based on these studies. First, *Bai1*<sup>-/-</sup> mice that consumed a high-fat, atherogenic diet had larger necrotic cores in their atherosclerotic plaques. This was linked to a role for BAI1 in cholesterol

homeostasis. Second, when subjected to DSS-colitis, *Bai1*<sup>-/-</sup> mice had more severe colitis relative to their wild-type counterparts. Furthermore, when mice globally over expressing BAI1 (*E2a-cre Bai1*<sup>Tg</sup>) or mice over expressing BAI1 in their colonic epithelial cells (*villin-cre Bai1*<sup>Tg</sup>) were studied in DSS-colitis, they were observed to have less severe disease than their wild-type counterparts. Surprisingly, overexpression of BAI1 in macrophages (*LysM-cre Bai1*<sup>Tg</sup>) did not reduce disease. These data suggested that BAI1 expression in colonic epithelial cells dampens DSS-colitis but further characterization was required to evaluate colonic inflammation at a cellular level and confirm that BAI1 was being over expressed in the appropriate tissues. Additionally, the notion that apoptotic cell clearance by the colonic epithelial cells was contributing to dampening of colitis was particularly intriguing. Therefore, we were also curious as to which PtdSer receptors were expressed by the epithelial cells.

To address these questions, I adapted several techniques in order to digest colonic tissue and isolate the IEL and LPL for analysis. I designed several staining panels and gating strategies to identify various cell populations from the LPL and IEL by flow cytometry as well as for sorting populations from the LPL and IEL by FACS. Using these techniques, I confirmed appropriate, tissue-specific expression of the *Bai1*<sup>Tg</sup> in multiple cre-lines. I also evaluated and characterized the inflammatory infiltrates in the LPL and determined that *Bai1*<sup>-/-</sup> mice did not exhibit changes in the infiltrating cell populations. Lastly, by purifying

colonic epithelial cells by FACS, we were able to determine that the colonic epithelium express multiple PtdSer receptors.

## **A2.2 Experimental Procedures**

### **A2.2.1 Mice and DSS-induced colitis**

ES cells (GST\_4419\_G3) with a gene-trap mutation between exons 2 and 3 of *Bai1* were obtained from TIGM. To generate conditional BAI1 transgenic mice, HA-tagged human BAI1 cDNAs (encoding wild-type BAI1 and BAI1- AAA mutant) were inserted into the previously described CAG-STOP-eGFP-ROSA26TV (CTV) vector [391]. CTV-BAI1 vectors were transfected into C57BL/6 embryonic stem cells (JM8A3) and screened for homologous recombination into *Rosa26* locus. Transgene-encoded BAI1 and eGFP were confirmed in the ES cells in vitro via cre transfection. Selected ES clones were used to obtain transgenic mice. Tg-BAI1<sup>flox-STOP-flox</sup> mice were crossed with E2A-cre mice (Jackson Laboratory) for global transgene expression [392], Lyz2-cre mice (Jackson Laboratory) [393] for myeloid expression, and Vil1-cre mice (Jackson Laboratory) for intestinal epithelial cell expression [394]. All animal experiments were performed according to protocols approved by the animal care and use committee (ACUC) at the University of Virginia.

Mice (littermates, 8–10 weeks old) were given 3% or 5% dextran sulfate sodium (DSS; MP Biomedicals) in drinking water for 5 or 8 days and analyzed on d5 or d8. Changes in body weight and disease severity index were checked daily. Disease severity was determined based on weight loss, blood in the stool,

and stool consistency, as previously described [395]. The total scores were calculated as follows: weight loss (0, <1%; 1, 1%–5%; 2, 6%–10%; 3, 11%–15%; 4, >15%), stool blood (0, negative; 2, positive; 4, gross bleeding), and stool consistency (0, normal; 2, loose stools; 4, diarrhea). All mice were randomly allocated to experimental groups and not recognized during the experiment.

### **A2.2.2 Epithelial cell and lamina propria layer isolation**

Cleaned colons were opened longitudinally and incubated in 15 mL of IEL isolation media: PBS 1mM EDTA (Gibco), 10mM HEPES (Gibco), 1mM DTT (Sigma), 5% FBS (Gemini) while shaking horizontally in 50 mL conicals at 250 rpm at 37°C for 20 minutes. Supernatants were passed through 100 µm cell strainer and flow through consisted predominantly of epithelial cells (EpCAM<sup>+</sup> 55.6%). Colons were transferred to 25 mL of LPL digestion media: RPMI, 5% FBS, 10mM HEPES, 1mg/mL collagenase D (Roche), 40µg/mL DNase I (Roche), and 1mg/mL dispase (Worthington). Colons were minced with scissors on ice and then incubated while shaking at 250 rpm at 37°C for 30 minutes in horizontal 50 mL conicals. Pieces of colonic tissue remain after digestion and single cell solutions were maintained by filtering supernatant through 40 µm tissue strainer. Supernatants were centrifuged and re-suspended in 40% percoll in a 15mL conical. 2.5 mL of 80% percoll was underlaid in conical. 80/40 percoll gradient was centrifuged at 470 xg for 20 min without a brake. Live cells were collected from the interface and washed in 45 mL of PBS 0.5% BSA (Roche), 2 mM EDTA. This purified fraction consisted of the LPL.

### **A2.2.3 Flow cytometric analysis of IEL and LPL populations**

Flow cytometric analysis of the IEL was designed to identify colonic epithelial cells (EpCAM<sup>+</sup>). Cells were Fc blocked 1:200 (CD16/32 clone 93) Dead cells were excluded by 7AAD staining (1:500 dilution) and singlets were identified based on FSC-A/FSC-H comparison. With these constraints, EpCAM<sup>+</sup> was identified with PeCy7-conjugate eBioscience clone G8.8 and represented approximately 55% of the total IEL population. Importantly, there was a small but significant population of CD11b<sup>+</sup> cells (APC conjugate clone M1/70) within the IEL.

Panels for LPL population analyses were designed to identify macrophages, monocytes/neutrophils and lymphocytes. For all panels, live cells were identified by 7AAD exclusion (1:500 dilution) and singlets were identified by FSC-A/FSC-H comparison. Cells were Fc blocked 1:200 (CD16/32 clone 93).

The panel conjugates used are listed here. Macrophages: CD11b (APC-eFluor780 clone M1/70), F4/80 (PE-Cy7 clone BM8); Monocytes/neutrophils: CD11b (PE-Cy7 clone M1/70), Ly6c (FITC clone AL-21), Ly6G (APC clone RB6-8C5); lymphocytes: CD11b (PE-Cy7 clone M1/70), TCR $\beta$  chain (APC clone H57-597), B220 (FITC clone RA3-6B2).

FACS sorting for CD11b<sup>+</sup> cells and epithelial cells were conducted from the LPL as many epithelial cells were isolated during this second stage of digestion. For sorting, singlets were identified based on FSC-A/FSC-W comparison and dead cells were excluded by 7AAD staining. Epithelial cells

(EpCAM<sup>+</sup>: PE-Cy7 clone G8.8 CD45<sup>-</sup>: APC clone 30-F11) cells were sorted from the live gate. Of the CD45<sup>+</sup> fraction, CD11b<sup>+</sup> (BV421 clone M1/70) cells were sorted. Flow cytometric analysis was performed on a BD Canto I and FACS sorting was done on a BD Influx.

#### **A2.2.4 Cytokine staining in LPL T cells**

Total LPL fraction was re-suspended in 1mL RPMI (Gibco) 10% FBS, 10mM HEPES, 750 ng/mL ionomycin, 50 nM PMA, Brefeldin A (GolgiPlug BD). LPL were incubated in stimulation solution for 3 hours at 37° C. Following stimulation, cells were Fc blocked 1:200 (CD16/32 clone 93) and then surface stained for CD4 (PerCP-Cy5.5 RM4-5). Following surface staining, cells were stained with an amine-reactive, fixable viability dye (eFluor780, eBiosciences). Cells were fixed and permeabilized with IC fixation kit (eBioscience). Cells were then stained for intracellular cytokines: IFN $\gamma$  (APC clone XMG1.2) and IL-17 (PE clone TC11-18H10).

## A2.3 Results

### A2.3.1 Deletion of BAI1 does not influence the size of inflammatory infiltrate

Apoptotic cell clearance promotes production of anti-inflammatory cytokines that can dampen the inflammatory milieu in tissues. As *Bai1*<sup>-/-</sup> mice exhibited increased disease in the setting of DSS-colitis, we went on to analyze how the absence of BAI1 influenced the infiltration of inflammatory monocytes and lymphocytes. To evaluate the inflammatory infiltrate during DSS-colitis, *Bai1*<sup>-/-</sup> and WT mice were euthanized 5 days after the introduction of DSS. The LPL layer was isolated and the population percentages of neutrophils, monocytes, macrophages, CD4<sup>+</sup> T lymphocytes and B220<sup>+</sup> B lymphocytes were analyzed by flow cytometry (**Figure A2.1a**). Surprisingly, despite the heightened disease in *Bai1*<sup>-/-</sup> mice, there was no shift in any population within the lamina propria of *Bai1*<sup>-/-</sup> mice relative to WT animals (**Figure A2.1b**).

We then went on to analyze the activity of the CD4<sup>+</sup> T lymphocytes from the LPL by assessing their production of pro-inflammatory cytokines. Importantly, we evaluated lamina propria lymphocytes at baseline and in DSS-treated animals. As we observed with the population percentages, we did not see any change in the production of either IFN $\gamma$  or IL-17 by CD4<sup>+</sup> T cells (**Figure A2.1c, A2.1 d**).

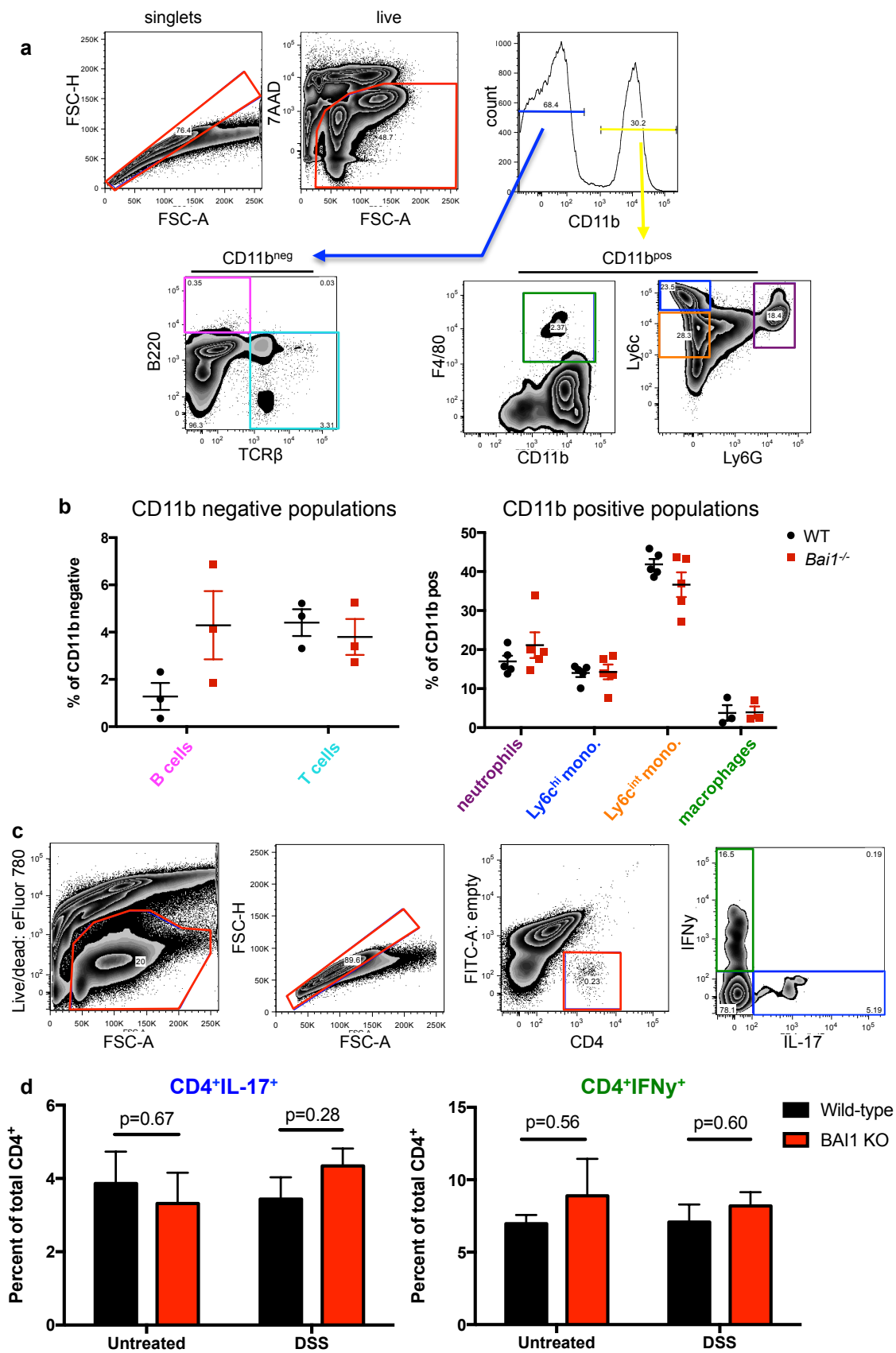
**Figure A2.1: Loss of *Bai1* does not alter the inflammatory population in the lamina propria during DSS-colitis**

**(a)** Gating strategy for identifying neutrophils (purple gate), monocytes (blue and orange gates), macrophages (green gate) and T cells (teal gate) and B cells (magenta gate) populations in the colonic lamina propria. Gates were set based on FMO samples.

**(b)** Population percentage breakdowns of CD11b<sup>+</sup> and CD11b<sup>-</sup> cells from the lamina propria of WT and *Bai1*<sup>-/-</sup> mice. Individual dots are representative of 1 mouse.

**(c)** Gating strategy for analyzing cytokine production in CD4<sup>+</sup> T lymphocytes

**(d)** Analysis of IFN $\gamma$  and IL-17 production by lamina propria CD4<sup>+</sup> lymphocytes in DSS-treated and untreated mice: WT (n=3) and *Bai1*<sup>-/-</sup> (n=4) mice for both treated and untreated. Note that unstimulated cells were analyzed as controls and gates were set based on FMO samples.



### A2.3.2 The *Bai1<sup>Tg</sup>* is expressed in macrophages from the LPL

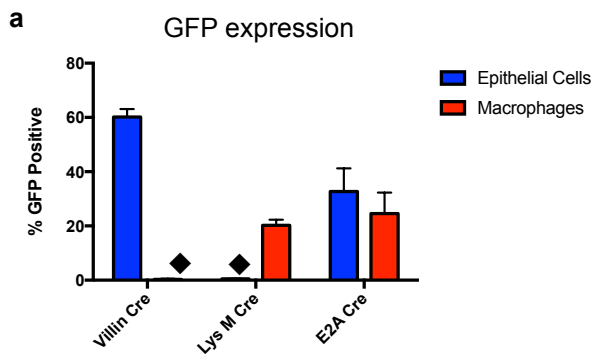
Expression of the *Bai1<sup>Tg</sup>* was driven in multiple cell-types by using a series of cre-drivers including the E2A-cre for global overexpression, villin-cre for overexpression in colonic epithelial cells and LysM-cre for overexpression in macrophages. Interestingly, *E2a-cre Bai1<sup>Tg</sup>* mice and *villin-cre Bai1<sup>Tg</sup>* mice exhibited reduced disease relative to WT mice though the same benefit was not observed in *LysM-cre Bai1<sup>Tg</sup>* mice. This was particularly surprising because monocytes and macrophages produce anti-inflammatory cytokines in response to apoptotic cell clearance, and BAI1 overexpression enhances apoptotic cell clearance by macrophages [131]. In order to confirm that BAI1 overexpression in macrophages truly does not reduce disease, we needed to confirm that lamina propria macrophages were in fact expressing the *Bai1<sup>Tg</sup>* in *LysM-cre Bai1<sup>Tg</sup>* mice. The *Bai1<sup>Tg</sup>* construct was designed with an IRES-GFP to allow detection of BAI1 transcription *in situ*. Indeed, when we isolated lamina propria samples from *E2a-cre Bai1<sup>Tg</sup>* mice and *LysM-cre Bai1<sup>Tg</sup>* mice, we observed GFP expression in LPL macrophages (**Figure A2.2a, A2.2b**). We also confirmed that the *Bai1<sup>Tg</sup>* was being expressed in the colonic epithelium from *villin-cre* mice (**Figure A2.2a, A2.2c**). Importantly, in our analysis of epithelial cells and macrophages from *villin-cre Bai1<sup>Tg</sup>* and *LysM-cre Bai1<sup>Tg</sup>* mice we did not observe the *Bai1<sup>Tg</sup>* firing in inappropriate tissues (**Figure A2.2a**).

**Figure A2.2: *Bai1*<sup>Tg</sup> expression occurs in appropriate tissues**

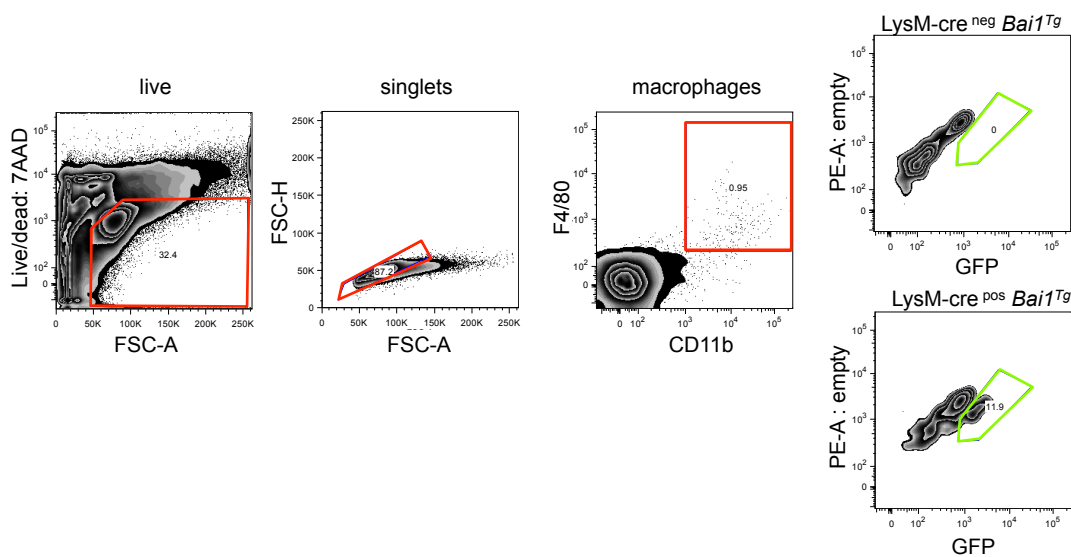
(a) GFP (*Bai1*<sup>Tg</sup>) expression in colonic epithelial cells and LPL macrophages from *E2a-cre Bai1*<sup>Tg</sup> (n=2), *LysM-cre Bai1*<sup>Tg</sup> (n=5) and *villin-cre Bai1*<sup>Tg</sup> (n=5). ◆ labeled bars indicate percentage was 0.5% or less.

(b) Gating strategy for identification of macrophages from lamina propria and GFP expression within lamina propria macrophages.

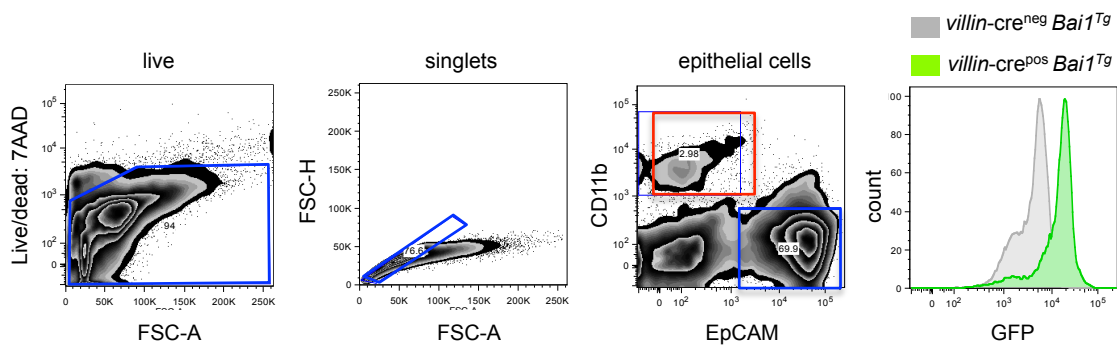
(c) Gating strategy for identification of colonic epithelial cells and GFP within the colonic epithelium. Red gate indicates population of CD11b<sup>+</sup> cells that are isolated with IEL.



**b** LPL macrophage gating strategy



**c** IEL epithelial cell gating strategy



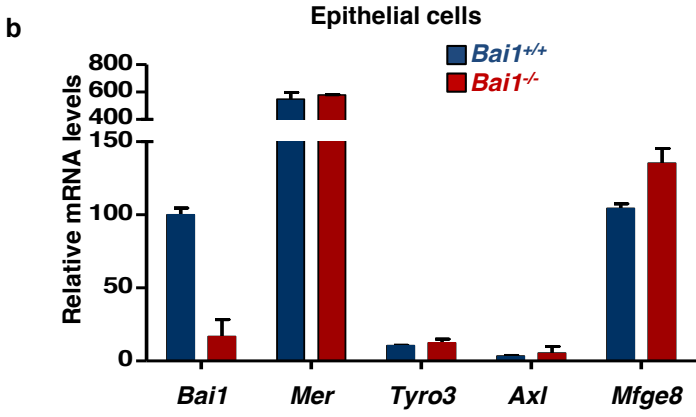
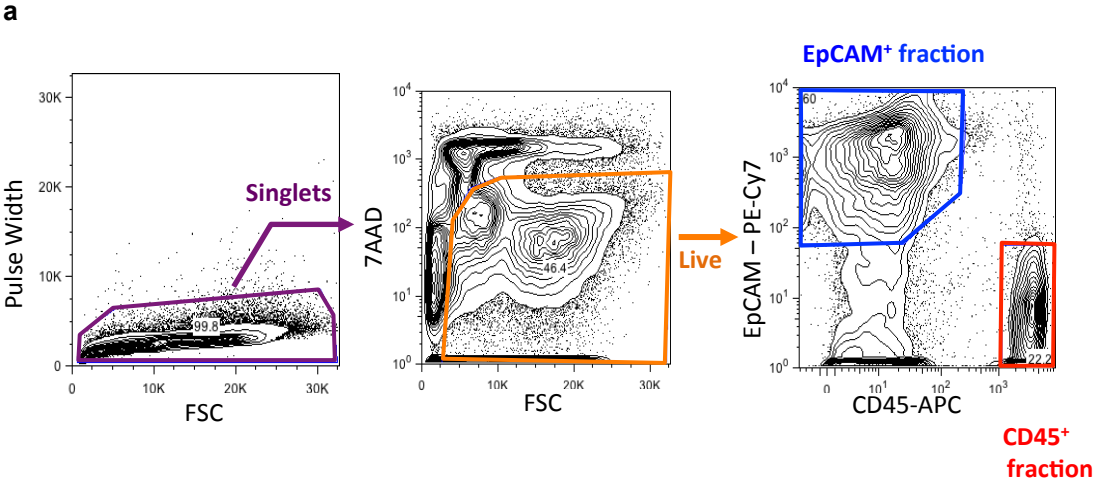
### **A2.3.3 Colonic epithelial cells express multiple PtdSer receptors**

The finding that BAI1 overexpression on the colonic epithelium reduced colitis-severity prompted us to question whether the colonic epithelium express PtdSer receptors endogenously. To assess expression, we chose to use qRT-PCR as the antibodies for many PtdSer receptors, including BAI1, are notoriously poor. However, in order to properly evaluate expression, we needed to obtain a pure population of colonic epithelial cells. The surface protein EpCAM is a reliable marker of epithelial cells. Importantly, crude isolates of colonic epithelial cells are approximately 60% pure (**A2.2c**). To enhance the purity of the epithelial cell preps we sorted colonic epithelial cells by FACS (**Figure A2.3a**). Analysis of colonic epithelial cells from WT and *Bai1*<sup>-/-</sup> mice revealed expression of multiple promoters of phagocytosis, including *Mertk*, *Bai1* and *Mfge8* (**Figure A2.3b**).

**Figure A2.3: Colonic epithelial cells express multiple PtdSer receptors**

**(a)** Sorting strategy for isolation of colonic epithelial cells. Sort was performed on the LPL layer after confirming that a substantial number of epithelial cells were isolated during LPL digestion. Blue gate was sorted as the epithelial population and red gate was the CD45 population.

**(b)** qRT-PCR analysis of isolated epithelial cells from WT and *Bai1*<sup>-/-</sup> mice (n=2).



## A2.4 Discussion

These characterizations of *Bai1*<sup>-/-</sup> and *Bai1*<sup>Tg</sup> mice provided important insight into the role of BAI1 in colitis. It was highly surprising that in spite of exacerbated disease, we did not observe any change in the inflammatory populations in the colon. Disease severity in our model of DSS-colitis was determined by changes in body weight and blood in the stool. As we did not see any changes in the inflammatory population, it is possible that the exacerbated disease in *Bai1*<sup>-/-</sup> mice was mediated at the level of the epithelial cells. Perhaps these mice are more susceptible to epithelial/barrier injury. Additionally, the D5 timepoint for analysis might have prevented us from observing meaningful changes in either B or T lymphocytes, as it may not have been enough time to see an adaptive response.

These experiments also revealed that colonic epithelial cells express multiple PtdSer receptors on their surface. Interestingly, MerTK expression was particularly high. Based on this observation it would be very interesting to evaluate *Mertk*<sup>-/-</sup> mice in the context of DSS-colitis. Additionally, it would be interesting to evaluate apoptotic cell accumulation in the colons of *Mertk*<sup>-/-</sup> mice at baseline.

The observed phenotype of reduced colitis severity in *Bai1*<sup>Tg</sup> mice prompted us to consider whether BAI1 could modify disease states in other tissues, including retinal degeneration in *Mertk*<sup>-/-</sup> mice. Thus these observations provided part of the basis for the line of investigation described in Chapter II.

## References

- [1] Gavrieli Y, Sherman Y, Ben-Sasson SA. Identification of Programmed Cell Death In Situ via Specific Labeling of Nuclear DNA Fragmentation. *Journal of Cell Biology* 1992;119:493–501.
- [2] Duvall E, Wyllie AH, Morris RG. Macrophage recognition of cells undergoing programmed cell death (apoptosis). *Immunology* 1985;56:351–8.
- [3] Goldstein JL, Ho YK, Basu SK, Brown MS. Binding site on macrophages that mediates uptake and degradation of acetylated low density lipoprotein, producing massive cholesterol deposition. *Pnas* 1979;76:333–7.
- [4] Fadok VA, Bratton DL, Konowal A, Freed PW, Westcott JY, Henson PM. Macrophages that have ingested apoptotic cells in vitro inhibit proinflammatory cytokine production through autocrine/paracrine mechanisms involving TGF- $\beta$ , PGE<sub>2</sub>, and PAF. *Journal of Clinical Investigation* 1998;101:890–8.
- [5] Voll R, Herrmann M, Roth EA, Stach C, Kalden JR, Girkontaite I. Immunosuppressive effects of apoptotic cells. *Nature* 1997;390:350–1.
- [6] Fadok VA, Voelker DR, Campbell PA, Cohen JJ, Bratton DL, Henson PM. Exposure of phosphatidylserine on the surface of apoptotic lymphocytes triggers specific recognition of removal by macrophages. *The Journal of Immunology* 1992;148:2207–16.
- [7] Fadok VA, Savill J, Haslett C, Bratton DL, Doherty DE, Campbell PA, et al. Different populations of macrophages use either the vitronectin receptor or the phosphatidylserine receptor to recognize and remove apoptotic cells. *The Journal of Immunology* 1992;149:4029–35.
- [8] Martin SJ, Reutelingsperger CPM, McGahoh AJ, Rader JA, van Schie RCAA, LaFace DM, et al. Early Redistribution of Plasma Membrane Phosphatidylserine Is a General Feature of Apoptosis Regardless of the Initiating Stimulus: Inhibition by Overexpression of Bcl-2 and Abl. *Journal of Experimental Medicine* 1995;182:1545–56.
- [9] Ipseiz N, Uderhardt S, Scholtyssek C, Steffen M, Schabbauer G, Bozec A, et al. The Nuclear Receptor Nr4a1 Mediates Anti-Inflammatory Effects of Apoptotic Cells. *The Journal of Immunology* 2014;192:4852–8. doi:10.4049/jimmunol.1303377.
- [10] Reddy SM, Hsiao KHK, Abernethy VE, Fan H, Longacre A, Lieberthal W, et al. Phagocytosis of Apoptotic Cells by Macrophages Induces Novel Signaling Events Leading to Cytokine-Independent Survival and Inhibition of Proliferation: Activation of Akt and Inhibition of Extracellular Signal-Regulated Kinases 1 and 2. *The Journal of Immunology* 2002;169:702–13. doi:10.4049/jimmunol.169.2.702.
- [11] Grau A, Tabib A, Grau I, Reiner I, Mevorach D. Apoptotic Cells Induce NF- $\kappa$ B and Inflammasome Negative Signaling. *Plos ONE*

- 2015;10:e0122440. doi:10.1371/journal.pone.0122440.s001.
- [12] Freire-de-Lima CG, Xiao Y-Q, Gardai SJ, Bratton DL, Schiemann WP, Henson PM. Apoptotic Cells, through Transforming Growth Factor-, Coordinately Induce Anti-inflammatory and Suppress Pro-inflammatory Eicosanoid and NO Synthesis in Murine Macrophages. *Journal of Biological Chemistry* 2006;281:38376–84.
- [13] McDonald PP, Fadok VA, Bratton DL, Henson PM. Transcriptional and Translational Regulation of Inflammatory Mediator Production by Endogenous TGF- $\beta$  in Macrophages that Have Ingested Apoptotic Cells. *The Journal of Immunology* 1999;163:6164–72.
- [14] Rosen A, Casciola-Rosen L, Ahearn J. Novel packages of viral and self-antigens are generated during apoptosis. *J Exp Med* 1995;181:1557–61.
- [15] Maderna P, Godson C. Phagocytosis of apoptotic cells and the resolution of inflammation. *Biochimica Et Biophysica Acta* 2003;1639:141–51.
- [16] Vanden Berghe T, Vanlangenakker N, Parthoens E, Deckers W, Devos M, Festjens N, et al. Necroptosis, necrosis and secondary necrosis converge on similar cellular disintegration features. *Cell Death and Differentiation* 2010;17:922–30. doi:10.1038/cdd.2009.184.
- [17] Silva MT. Secondary necrosis: the natural outcome of the complete apoptotic program. *FEBS Letters* 2010;584:4491–9. doi:10.1016/j.febslet.2010.10.046.
- [18] Maeda A, Fadeel B. Mitochondria released by cells undergoing TNF- $\alpha$ -induced necroptosis act as danger signal. *Cell Death and Disease* 2014;5:e1312–9. doi:10.1038/cddis.2014.277.
- [19] Scaffidi P, Misteli T, Bianchi ME. Release of chromatin protein HMGB1 by necrotic cells triggers inflammation. *Nature* 2002;418:191–5. doi:10.1038/nature00858.
- [20] Iyer SS, Pulsikens WP, Sadler JJ, Butter LM, Teske GJ, Ulland TK, et al. Necrotic cells trigger a sterile inflammatory response through the Nlrp3 inflammasome. *Pnas* 2009;106:20388–93. doi:10.1073/pnas.0908698106.
- [21] Sheriff A, Gaipal US, Voll RE, Kalden JR, Herrmann M. Apoptosis and systemic lupus erythematosus. *Rheum Dis Clin North Am* 2004;30:505–27–viii–ix. doi:10.1016/j.rdc.2004.04.006.
- [22] Gaipal US, Voll RE, Sheriff A, Franz S, Kalden JR, Herrmann M. Impaired clearance of dying cells in systemic lupus erythematosus. *Autoimmunity Reviews* 2005;4:189–94. doi:10.1016/j.autrev.2004.10.007.
- [23] Kimani SG, Geng K, Kasikara C, Kumar S, Sriram G, Wu Y, et al. Contribution of defective PS recognition and efferocytosis to chronic inflammation and autoimmunity. *Frontiers in Immunology* 2014;5:1–9. doi:10.3389/fimmu.2014.00566/abstract.

- [24] Ravichandran KS, Lorenz U. Engulfment of apoptotic cells: signals for a good meal. *Nature Reviews Immunology* 2007;7:964–74. doi:10.1038/nri2214.
- [25] Elmore S. Apoptosis: a review of programmed cell death. *Toxicol Pathol* 2007;35:495–516. doi:10.1080/01926230701320337.
- [26] Saelens X, Festjens N, Vande Walle L, van Gurp M, van Loo G, Vandenaabeele P. Toxic proteins released from mitochondria in cell death. *Oncogene* 2004;23:2861–74. doi:10.1038/sj.onc.1207523.
- [27] Porter AG, Jänicke RU. Emerging roles of caspase-3 in apoptosis. *Cell Death and Differentiation* 1999.
- [28] Woo M, Hakem R, Soengas MS, Duncan GS, Shahinian A, Kägi D, et al. Essential contribution of caspase 3/CPP32 to apoptosis and its associated nuclear changes. *Genes and Development* 1998;12:806–19.
- [29] Susin SA, Zamzami N, Castedo M, Hirsch T, Marchetti P, Macho A, et al. Bcl-2 inhibits the mitochondrial release of an apoptogenic protease. *J Exp Med* 1996;184:1331–41.
- [30] Gown AM, Willingham MC. Improved detection of apoptotic cells in archival paraffin sections: immunohistochemistry using antibodies to cleaved caspase 3. *J Histochem Cytochem* 2002;50:449–54. doi:10.1177/002215540205000401.
- [31] Sebbagh M, Renvoizé C, Hamelin J, Riché N, Bertoglio J, Bréard J. Caspase-3-mediated cleavage of ROCK I induces MLC phosphorylation and apoptotic membrane blebbing. *Nature Cell Biology* 2001;3:346–52. doi:10.1038/35070019.
- [32] Chekeni FB, Elliott MR, Sandilos JK, Walk SF, Kinchen JM, Lazarowski ER, et al. Pannexin 1 channels mediate “find-me” signal release and membrane permeability during apoptosis. *Nature* 2010;467:863–7. doi:10.1038/nature09413.
- [33] Sandilos JK, Chiu Y-H, Chekeni FB, Armstrong AJ, Walk SF, Ravichandran KS, et al. Pannexin 1, an ATP release channel, is activated by caspase cleavage of its pore-associated C-terminal autoinhibitory region. *J Biol Chem* 2012;287:11303–11. doi:10.1074/jbc.M111.323378.
- [34] Elliott MR, Chekeni FB, Trampont PC, Lazarowski ER, Kadl A, Walk SF, et al. Nucleotides released by apoptotic cells act as a find-me signal to promote phagocytic clearance. *Nature* 2009;461:282–6. doi:10.1038/nature08296.
- [35] Hankins HM, Baldrige RD, Xu P, Graham TR. Role of flippases, scramblases and transfer proteins in phosphatidylserine subcellular distribution. *Traffic* 2015;16:35–47. doi:10.1111/tra.12233.
- [36] Suzuki J, Imanishi E, Nagata S. Exposure of phosphatidylserine by Xk-related protein family members during apoptosis. *J Biol Chem* 2014;289:30257–67. doi:10.1074/jbc.M114.583419.
- [37] Suzuki J, Denning DP, Imanishi E, Horvitz HR, Nagata S. Xk-related

- protein 8 and CED-8 promote phosphatidylserine exposure in apoptotic cells. *Science* 2013;341:403–6. doi:10.1126/science.1236758.
- [38] Segawa K, Kurata S, Yanagihashi Y, Brummelkamp TR, Matsuda F, Nagata S. Caspase-mediated cleavage of phospholipid flippase for apoptotic phosphatidylserine exposure. *Science* 2014;344:1164–8. doi:10.1126/science.1252809.
- [39] Henson PM, Hume DA. Apoptotic cell removal in development and tissue homeostasis. *Trends in Immunology* 2006;27:244–50. doi:10.1016/j.it.2006.03.005.
- [40] Lemke G, Burstyn-Cohen T. TAM receptors and the clearance of apoptotic cells. *Annals of the New York Academy of Sciences* 2010;1209:23–9. doi:10.1111/j.1749-6632.2010.05744.x.
- [41] Miyanishi M, Tada K, Koike M, Uchiyama Y, Kitamura T, Nagata S. Identification of Tim4 as a phosphatidylserine receptor. *Nature* 2007;450:435–9. doi:10.1038/nature06307.
- [42] Park D, Tosello-Trampont A-C, Elliott MR, Lu M, Haney LB, Ma Z, et al. BAI1 is an engulfment receptor for apoptotic cells upstream of the ELMO/Dock180/Rac module. *Nature* 2007;450:430–4. doi:10.1038/nature06329.
- [43] Albert ML, Kim J-I, Birge RB.  $\alpha$ v $\beta$ 5 integrin recruits the CrkII–Dock180–Rac1 complex for phagocytosis of apoptotic cells. *Nature Cell Biology* 2000;2:899–905.
- [44] Akakura S, Singh S, Spataro M, Akakura R, Kim J-I, Albert ML, et al. The opsonin MFG-E8 is a ligand for the  $\alpha$ v $\beta$ 5 integrin and triggers DOCK180-dependent Rac1 activation for the phagocytosis of apoptotic cells. *Experimental Cell Research* 2004;292:403–16. doi:10.1016/j.yexcr.2003.09.011.
- [45] Park S-Y, Kim S-Y, Kang K-B, Kim I-S. Adaptor protein GULP is involved in stabilin-1-mediated phagocytosis. *Biochemical Journal* 2010;398:467–72. doi:10.1016/j.bbrc.2010.06.101.
- [46] Park SY, Jung MY, Lee SJ, Kang KB, Gratchev A, Riabov V, et al. Stabilin-1 mediates phosphatidylserine-dependent clearance of cell corpses in alternatively activated macrophages. *Journal of Cell Science* 2009;122:3365–73. doi:10.1242/jcs.049569.
- [47] Shi J, Heegaard CW, Rasmussen JT, Gilbert GE. Lactadherin binds selectively to membranes containing phosphatidyl-L-serine and increased curvature. *Biochimica Et Biophysica Acta (BBA) - Biomembranes* 2004;1667:82–90. doi:10.1016/j.bbamem.2004.09.006.
- [48] Hanayama R, Tanaka M, Miwa K, Shinohara A, Iwamatsu A, Nagata S. Identification of a factor that links apoptotic cells to phagocytes. *Nature* 2002;417:182–7.
- [49] Andersen MH, Berglund L, Rasmussen JT, Petersen TE. Bovine PAS-6/7 Binds  $\alpha$ v $\beta$ 5 Integrin and Anionic Phospholipids through Two Domains. *Biochemistry* 1997;36:5441–6.

- [50] Andersen MH, Graversen H, Fedosov SN, Petersen TE, Rasmussen JT. Functional Analyses of Two Cellular Binding Domains of Bovine Lactadherin. *Biochemistry* 2000;39:6200–6. doi:10.1021/bi992221r.
- [51] Burstyn-Cohen T, Lew ED, Través PG, Burrola PG, Hash JC, Lemke G. Genetic Dissection of TAM Receptor-Ligand Interaction in Retinal Pigment Epithelial Cell Phagocytosis. *Neuron* 2012;76:1123–32. doi:10.1016/j.neuron.2012.10.015.
- [52] Lew ED, Oh J, Burrola PG, Lax I, Zagórska A, Través PG, et al. Differential TAM receptor-ligand-phospholipid interactions delimit differential TAM bioactivities. *eLife* 2014;3. doi:10.7554/eLife.03385.018.
- [53] Park D, Hochreiter-Hufford A, Ravichandran KS. The Phosphatidylserine Receptor TIM-4 Does Not Mediate Direct Signaling. *Current Biology* 2009;19:346–51. doi:10.1016/j.cub.2009.01.042.
- [54] Tosello-Tramont A, Brugnera E, Ravichandran KS. Evidence for a conserved role for CRKII and Rac in engulfment of apoptotic cells. *J Biol Chem* 2001;276:13797–802. doi:10.1074/jbc.M011238200.
- [55] Reddien PW, Horvitz HR. CED-2/CrkII and CED-10/Rac control phagocytosis and cell migration in *Caenorhabditis elegans*. *Nature Cell Biology* 2000;2:131–6.
- [56] Kinchen JM, Cabello J, Klingele D, Wong K, Feichtinger R, Schnabel H, et al. Two pathways converge at CED-10 to mediate actin rearrangement and corpse removal in *C. elegans*. *Nature* 2005;434:93–9.
- [57] Tosello-Tramont AC, Nakada-Tsukui K, Ravichandran KS. Engulfment of Apoptotic Cells Is Negatively Regulated by Rho-mediated Signaling. *Journal of Biological Chemistry* 2003;278:49911–9. doi:10.1074/jbc.M306079200.
- [58] Akhtar N, Li W, Mironov A, Streuli CH. Rac1 Controls Both the Secretory Function of the Mammary Gland and Its Remodeling for Successive Gestations. *Developmental Cell* 2016;38:522–35. doi:10.1016/j.devcel.2016.08.005.
- [59] Akakura S, Kar B, Singh S, Cho L, Tibrewal N, Sanokawa-Akakura R, et al. C-terminal SH3 domain of CrkII regulates the assembly and function of the DOCK180/ELMO Rac-GEF. *J Cell Physiol* 2005;204:344–51. doi:10.1002/jcp.20288.
- [60] Kaibuchi K, Kuroda S, Amano M. Regulation of the cytoskeleton and cell adhesion by the Rho family GTPases in mammalian cells. *Annual Reviews of Biochemistry* 1999;68:459–86.
- [61] Erickson JW, Cerione RA. Structural Elements, Mechanism, and Evolutionary Convergence of Rho Protein–Guanine Nucleotide Exchange Factor Complexes. *Biochemistry* 2004;43:837–42. doi:10.1021/bi036026v.

- [62] Hart MJ, Eva A, Evans T, Aaronson SA, Cerione RA. Catalysis of guanine nucleotide exchange on the CDC42Hs protein by the *dbl* oncogene product. *Nature* 1991;354:311–4.
- [63] Ron D, Zannini M, Lewis M, Wickner RB, Hunt LT, Graziani G, et al. A region of proto-*dbl* essential for its transforming activity shows sequence similarity to a yeast cell cycle gene, *CDC24*, and the human breakpoint cluster gene, *bcr*. *The New Biologist* 1991;3:372–9.
- [64] Hart MJ, Eva A, Zangrilli D, Aaronson SA, Evans T, Cerione RA, et al. Cellular Transformation and Guanine Nucleotide Exchange Activity are Catalyzed by a Common Domain on the *dbl* Oncogene Product. *Journal of Biological Chemistry* 1994;269:62–5.
- [65] Kiyokawa E, Hashimoto Y, Kobayashi S, Sugimura H, Kurata T, Matsuda M. Activation of Rac1 by a Crk SH3-binding protein, DOCK180. *Genes and Development* 1998;12:3331–6.
- [66] Gumienny TL, Brugnera E, Tosello-Trampont A-C, Kinchen JM, Haney LB, Nishiwaki K, et al. CED-12/ELMO, a Novel Member of the CrkII/Dock180/ Rac Pathway, Is Required for Phagocytosis and Cell Migration. *Cell* 2001;107:27–41.
- [67] Brugnera E, Haney L, Grimsley C, Lu M, Walk SF, Tosello-Trampont A-C, et al. Unconventional Rac-GEF activity is mediated through the Dock180–ELMO complex. *Nature Cell Biology* 2002;4:574–82. doi:10.1038/ncb824.
- [68] Côté J-F, Vuori K. Identification of an evolutionarily conserved superfamily of DOCK180-related proteins with guanine nucleotide exchange activity. *Journal of Cell Science* 2002;115:4901–13. doi:10.1242/jcs.00219.
- [69] Grimsley CM, Kinchen JM, Tosello-Trampont AC, Brugnera E, Haney LB, Lu M, et al. Dock180 and ELMO1 Proteins Cooperate to Promote Evolutionarily Conserved Rac-dependent Cell Migration. *Journal of Biological Chemistry* 2004;279:6087–97. doi:10.1074/jbc.M307087200.
- [70] Abu-Thuraia A, Gauthier R, Chidiac R, Fukui Y, Screatton RA, Gratton J-P, et al. Axl Phosphorylates Elmo Scaffold Proteins To Promote Rac Activation and Cell Invasion. *Molecular and Cellular Biology* 2014;35:76–87. doi:10.1128/MCB.00764-14.
- [71] Wu Y, Singh S, Georgescu M-M, Birge RB. A role for Mer tyrosine kinase in avb5 integrin-mediated phagocytosis of apoptotic cells. *Journal of Cell Science* 2005;118:539–53. doi:10.1242/jcs.01632.
- [72] Shah PP, Fong MY, Kakar SS. PTTG induces EMT through integrin  $\alpha$ V $\beta$ 3-focal adhesion kinase signaling in lung cancer cells. *Oncogene* 2011;31:3124–35. doi:10.1038/onc.2011.488.
- [73] Hamann J, Aust G, Araç D, Engel FB, Formstone C, Fredriksson R, et al. International Union of Basic and Clinical Pharmacology. XCIV. Adhesion G protein-coupled receptors. *Pharmacol Rev* 2015;67:338–67. doi:10.1124/pr.114.009647.

- [74] Nishimori H, Shiratsuchi T, Urano T, Kimura Y, Kiyono K, Tatsumi K, et al. A novel brain-specific p53-target gene, BAI1, containing thrombospondin type 1 repeats inhibits experimental angiogenesis. *Oncogene* 1997;15:2145–50. doi:10.1038/sj.onc.1201542.
- [75] Manodori AB, Barabino GA, Lubin BH, Kuypers FA. Adherence of phosphatidylserine-exposing erythrocytes matrix thrombospondin. *Blood* 2000;95:1293–300.
- [76] Gayen Betal S, Setty BNY. Phosphatidylserine-positive erythrocytes bind to immobilized and soluble thrombospondin-1 via its heparin-binding domain. *Translational Research* 2008;152:165–77. doi:10.1016/j.trsl.2008.07.007.
- [77] Caberoy NB, Zhou Y, Li W. Tubby and tubby-like protein 1 are new MerTK ligands for phagocytosis. *Embo J* 2010;29:3898–910. doi:10.1038/emboj.2010.265.
- [78] Tibrewal N, Wu Y, D'mello V, Akakura R, George TC, Varnum B, et al. Autophosphorylation Docking Site Tyr-867 in Mer Receptor Tyrosine Kinase Allows for Dissociation of Multiple Signaling Pathways for Phagocytosis of Apoptotic Cells and Down-modulation of Lipopolysaccharide-inducible NF- $\kappa$ B Transcriptional Activation. *Journal of Biological Chemistry* 2008;283:3618–27.
- [79] Todt JC, Hu B, Curtis JL. The receptor tyrosine kinase MerTK activates phospholipase C gamma2 during recognition of apoptotic thymocytes by murine macrophages. *Journal of Leukocyte Biology* 2004;75:705–13. doi:10.1189/jlb.0903439.
- [80] Ellis RE, Jacobson DM, Horvitz HR. Genes Required for the Engulfment of Cell Corpses During Programmed Cell Death in *Caenorhabditis elegans*. *Genetics* 1991;129:79–94.
- [81] Feller SM. Crk family adaptors - signalling complex formation and biological roles. *Oncogene* 2001;20:6348–71.
- [82] Wu Y-C, Horvitz HR. *C. elegans* phagocytosis and cell-migration protein CED-5 is similar to human DOCK180. *Nature* 1998;392:501–4.
- [83] Nolan KM, Barrett K, Lu Y, Hu K-Q, Vincent S, Settleman J. Myoblast city, the *Drosophila* homolog of DOCK180/CED-5, is required in a Rac signaling pathway utilized for multiple developmental processes. *Genes and Development* 1998;12:3337–42.
- [84] Hasegawa H, Kiyokawa E, Tanaka S, Nagashima K, Gotoh N, Shibuya M, et al. DOCK180, a Major CRK-Binding Protein, Alters Cell Morphology upon Translocation to the Cell Membrane. *Molecular and Cellular Biology* 1996;16:1–7.
- [85] Wu Y-C, Tsai M-C, Cheng L-C, Chou C-J, Weng N-Y. CED-12 Acts in the Conserved CrkII/DOCK180/Rac Pathway to Control Cell Migration and Cell Corpse Engulfment. *Developmental Cell* 2001;1:491–502.
- [86] Lee CS, Penberthy KK, Wheeler KM, Juncadella IJ, Vandenabeele P,

- Lysiak JJ, et al. Boosting Apoptotic Cell Clearance by Colonic Epithelial Cells Attenuates Inflammation In Vivo. *Immunity* 2016;44:807–20. doi:10.1016/j.immuni.2016.02.005.
- [87] Nishi C, Toda S, Segawa K, Nagata S. Tim4- and MerTK-Mediated Engulfment of Apoptotic Cells by Mouse Resident Peritoneal Macrophages. *Molecular and Cellular Biology* 2014;34:1512–20. doi:10.1128/MCB.01394-13.
- [88] Seitz HM, Camenisch TD, Lemke G, Earp HS, Matsushima GK. Macrophages and Dendritic Cells Use Different Axl/Mertk/Tyro3 Receptors in Clearance of Apoptotic Cells. *The Journal of Immunology* 2007;178:5635–42. doi:10.4049/jimmunol.178.9.5635.
- [89] Kim S, Park SY, Kim SY, Bae DJ, Pyo JH, Hong M, et al. Cross Talk between Engulfment Receptors Stabilin-2 and Integrin  $\alpha$ v $\beta$ 5 Orchestrates Engulfment of Phosphatidylserine-Exposed Erythrocytes. *Molecular and Cellular Biology* 2012;32:2698–708. doi:10.1128/MCB.06743-11.
- [90] Miyanishi M, Segawa K, Nagata S. Synergistic effect of Tim4 and MFG-E8 null mutations on the development of autoimmunity. *International Immunology* 2012;24:551–9. doi:10.1093/intimm/dxs064.
- [91] Sexton DW, Al-Rabia M, Blaylock MG, Walsh GM. Phagocytosis of apoptotic eosinophils but not neutrophils by bronchial epithelial cells. *Clin Exp Allergy* 2004;34:1514–24. doi:10.1111/j.1365-2222.2004.02054.x.
- [92] Vollrath D, Yasumura D, Benchorin G, Matthes MT, Feng W, Nguyen NM, et al. Tyro3 Modulates Mertk-Associated Retinal Degeneration. *PLoS Genet* 2015;11:e1005723. doi:10.1371/journal.pgen.1005723.
- [93] Lu Q, Gore M, Zhang Q, Camenisch T, Boast S, Casagrande F, et al. Tyro-3 family receptors are essential regulators of mammalian spermatogenesis. *Nature* 1999;398:723–8.
- [94] Arandjelovic S, Ravichandran KS. Phagocytosis of apoptotic cells in homeostasis. *Nature Immunology* 2015;16:907–17. doi:10.1038/ni.3253.
- [95] Karl J, Capel B. Sertoli cells of the mouse testis originate from the coelomic epithelium. *Development* 1998;203:323–33. doi:10.1006/dbio.1998.9068.
- [96] Nakagawa A, Shiratsuchi A, Tsuda K, Nakanishi Y. In vivo analysis of phagocytosis of apoptotic cells by testicular Sertoli cells. *Mol Reprod Dev* 2005;71:166–77. doi:10.1002/mrd.20278.
- [97] Tamai M, O'Brien PJ. Retinal dystrophy in the RCS rat: in vivo and in vitro studies of phagocytic action of the pigment epithelium on the shed rod outer segments. *Experimental Eye Research* 1979;28:399–411.
- [98] CREAMER B, SHORTER RG, BAMFORTH J. The turnover and shedding of epithelial cells: Part II The shedding in the small intestine. *Gut* 1961;2:117–8.

- [99] Rawlins EL, Hogan BLM. Ciliated epithelial cell lifespan in the mouse trachea and lung. *Am J Physiol Lung Cell Mol Physiol* 2008;295:L231–4. doi:10.1152/ajplung.90209.2008.
- [100] Miceli MV, Liles MR, Newsome DA. Evaluation of oxidative processes in human pigment epithelial cells associated with retinal outer segment phagocytosis. *Experimental Cell Research* 1994;214:242–9. doi:10.1006/excr.1994.1254.
- [101] Tate DJ, Miceli MV, Newsome DA. Phagocytosis and H<sub>2</sub>O<sub>2</sub> induce catalase and metallothionein gene expression in human retinal pigment epithelial cells. *Investigative Ophthalmology & Visual Science* 1995;36:1271–9.
- [102] Sharpe RM, McKinnell C, Kivlin C, Fisher JS. Proliferation and functional maturation of Sertoli cells, and their relevance to disorders of testis function in adulthood. *Reproduction* 2003;125:769–84.
- [103] Juncadella IJ, Kadl A, Sharma AK, Shim YM, Hochreiter-Hufford A, Borish L, et al. Apoptotic cell clearance by bronchial epithelial cells critically influences airway inflammation. *Nature* 2012;493:547–51. doi:10.1038/nature11714.
- [104] Nakanishi Y, Shiratsuchi A. Phagocytic removal of apoptotic spermatogenic cells by Sertoli cells: mechanisms and consequences. *Biological and Pharmaceutical Bulletin* 2004;27:13–6.
- [105] LaVail MM. Rod outer segment disk shedding in rat retina: relationship to cyclic lighting. *Science* 1976;194:1071–4.
- [106] Griswold MD. The central role of Sertoli cells in spermatogenesis. *Semin Cell Dev Biol* 1998;9:411–6. doi:10.1006/scdb.1998.0203.
- [107] Zhao S, Zhu W, Xue S, Han D. Testicular defense systems: immune privilege and innate immunity. *Cell Mol Immunol* 2014;11:428–37. doi:10.1038/cmi.2014.38.
- [108] Silva CA, Cocuzza M, Carvalho JF, Bonfá E. Diagnosis and classification of autoimmune orchitis. *Autoimmunity Reviews* 2014;13:431–4. doi:10.1016/j.autrev.2014.01.024.
- [109] Zhang Y, Li N, Chen Q, Yan K, Liu Z, Zhang X, et al. Breakdown of immune homeostasis in the testis of mice lacking Tyro3, Axl and Mer receptor tyrosine kinases. *Immunology and Cell Biology* 2013;91:416–26. doi:10.1038/icb.2013.22.
- [110] Dym M. The fine structure of the monkey (*Macaca*) Sertoli cell and its role in maintaining the blood-testis barrier. *Anat Rec* 1973;175:639–56. doi:10.1002/ar.1091750402.
- [111] Pelletier RM, Byers SW. The blood-testis barrier and Sertoli cell junctions: structural considerations. *Microsc Res Tech* 1992;20:3–33. doi:10.1002/jemt.1070200104.
- [112] Pelletier RM, Friend DS. The Sertoli cell junctional complex: structure and permeability to filipin in the neonatal and adult guinea pig. *Am J Anat* 1983;168:213–28. doi:10.1002/aja.1001680208.

- [113] Tung KSK, Harakal J, Qiao H, Rival C, Li JCH, Paul AGA, et al. Egress of sperm autoantigen from seminiferous tubules maintains systemic tolerance. *J Clin Invest* 2017;127:1046–60. doi:10.1172/JCI89927.
- [114] Campese AF, Grazioli P, de Cesaris P, Riccioli A, Bellavia D, Pelullo M, et al. Mouse Sertoli cells sustain de novo generation of regulatory T cells by triggering the notch pathway through soluble JAGGED1. *Biology of Reproduction* 2014;90:53. doi:10.1095/biolreprod.113.113803.
- [115] Suarez-Pinzon W, Korbitt GS, Power R, Hooton J, Rajotte RV, Rabinovitch A. Testicular sertoli cells protect islet beta-cells from autoimmune destruction in NOD mice by a transforming growth factor-beta1-dependent mechanism. *Diabetes* 2000;49:1810–8.
- [116] Dal Secco V, Riccioli A, Padula F, Ziparo E, Filippini A. Mouse Sertoli cells display phenotypical and functional traits of antigen-presenting cells in response to interferon gamma. *Biology of Reproduction* 2008;78:234–42. doi:10.1095/biolreprod.107.063578.
- [117] Fallarino F, Luca G, Calvitti M, Mancuso F, Nastruzzi C, Fioretti MC, et al. Therapy of experimental type 1 diabetes by isolated Sertoli cell xenografts alone. *Journal of Experimental Medicine* 2009;206:2511–26. doi:10.1084/jem.20090134.
- [118] Selawry HP, Cameron DF. Sertoli cell-enriched fractions in successful islet cell transplantation. *Cell Transplantation* 1992.
- [119] Skinner MK, Griswold MD. Sertoli cells synthesize and secrete transferrin-like protein. *J Biol Chem* 1980;255:9523–5.
- [120] Sylvester SR, Griswold MD. The testicular iron shuttle: a “nurse” function of the Sertoli cells. *J Androl* 1994;15:381–5.
- [121] Livera G, Rouiller-Fabre V, Pairault C, Levacher C, Habert R. Regulation and perturbation of testicular functions by vitamin A. *Reproduction* 2002;124:173–80.
- [122] Hogarth CA, Griswold MD. The key role of vitamin A in spermatogenesis. *J Clin Invest* 2010;120:956–62. doi:10.1172/JCI41303.
- [123] Bishop PD, Griswold MD. Uptake and metabolism of retinol in cultured Sertoli cells: evidence for a kinetic model. *Biochemistry* 1987;26:7511–8.
- [124] Riera MF, Meroni SB, Schteingart HF, Pellizzari EH, Cigorraga SB. Regulation of lactate production and glucose transport as well as of glucose transporter 1 and lactate dehydrogenase A mRNA levels by basic fibroblast growth factor in rat Sertoli cells. *J Endocrinol* 2002;173:335–43.
- [125] Oliveira PF, Alves MG, Rato L, Laurentino S, Silva J, Sá R, et al. Effect of insulin deprivation on metabolism and metabolism-associated gene transcript levels of in vitro cultured human Sertoli cells. *Biochimica Et*

- Biophysica Acta 2012;1820:84–9.  
doi:10.1016/j.bbagen.2011.11.006.
- [126] Riera MF, Meroni SB, Gómez GE, Schteingart HF, Pellizzari EH, Cigorraga SB. Regulation of lactate production by FSH, iL1beta, and TNFalpha in rat Sertoli cells. *Gen Comp Endocrinol* 2001;122:88–97. doi:10.1006/gcen.2001.7619.
- [127] T Zeuthen SHMLC. Cotransport of H<sup>+</sup>, lactate and H<sub>2</sub>O by membrane proteins in retinal pigment epithelium of bullfrog. *The Journal of Physiology* 1996;497:3.
- [128] Mullaney BP, Rosselli M, Skinner MK. Developmental regulation of Sertoli cell lactate production by hormones and the testicular paracrine factor, PModS. *Mol Cell Endocrinol* 1994;104:67–73.
- [129] Setchell BP. The secretion of fluid by the testes of rats, rams and goats with some observations on the effect of age, cryptorchidism and hypophysectomy. *J Reprod Fertil* 1970;23:79–85.
- [130] Selva DM, Hirsch-Reinshagen V, Burgess B, Zhou S, Chan J, Mclsaac S, et al. The ATP-binding cassette transporter 1 mediates lipid efflux from Sertoli cells and influences male fertility. *J Lipid Res* 2004;45:1040–50. doi:10.1194/jlr.M400007-JLR200.
- [131] Fond AM, Lee CS, Schulman IG, Kiss RS, Ravichandran KS. Apoptotic cells trigger a membrane-initiated pathway to increase ABCA1. *Journal of Clinical Investigation* 2015. doi:10.1172/JCI80300DS1.
- [132] Kim S-Y, Lim E-J, Yoon Y-S, Ahn Y-H, Park E-M, Kim H-S, et al. Liver X receptor and STAT1 cooperate downstream of Gas6/Mer to induce anti-inflammatory arginase 2 expression in macrophages. *Sci Rep* 2016;6:571. doi:10.1084/jem.20062293.
- [133] Carr I, Clegg EJ, Meek GA. Sertoli cells as phagocytes: an electron microscopic study. *J Anat* 1968;102:501–9.
- [134] Wang H, Wang H, Xiong W, Chen Y, Ma Q, Ma J, et al. Evaluation on the phagocytosis of apoptotic spermatogenic cells by Sertoli cells in vitro through detecting lipid droplet formation by Oil Red O staining. *Reproduction* 2006;132:485–92. doi:10.1530/rep.1.01213.
- [135] Shiratsuchi A, Umeda M, Ohba Y, Nakanishi Y. Recognition of phosphatidylserine on the surface of apoptotic spermatogenic cells and subsequent phagocytosis by Sertoli cells of the rat. *J Biol Chem* 1997;272:2354–8.
- [136] Elliott MR, Zheng S, Park D, Woodson RI, Reardon MA, Juncadella IJ, et al. Unexpected requirement for ELMO1 in clearance of apoptotic germ cells in vivo. *Nature* 2011;467:333–7. doi:10.1038/nature09356.
- [137] Maeda Y, Shiratsuchi A, Namiki M, Nakanishi Y. Inhibition of sperm production in mice by annexin V microinjected into seminiferous tubules: possible etiology of phagocytic clearance of apoptotic spermatogenic cells and male infertility. *Cell Death and Differentiation* 2002;9:742–9. doi:10.1038/sj.cdd.4401046.

- [138] Bharti K, Miller SS, Arnheiter H. The new paradigm: retinal pigment epithelium cells generated from embryonic or induced pluripotent stem cells. *Pigment Cell Melanoma Res* 2011;24:21–34. doi:10.1111/j.1755-148X.2010.00772.x.
- [139] Cunha-Vaz JG. The blood-retinal barriers. *Doc Ophthalmol* 1976;41:287–327.
- [140] Georgiadis A, Tschernutter M, Bainbridge JWB, Balaggan KS, Mowat F, West EL, et al. The tight junction associated signalling proteins ZO-1 and ZONAB regulate retinal pigment epithelium homeostasis in mice. *Plos ONE* 2010;5:e15730. doi:10.1371/journal.pone.0015730.
- [141] Ning N, Wen Y, Li Y, Li J. Meclofenamic acid blocks the gap junction communication between the retinal pigment epithelial cells. *Hum Exp Toxicol* 2013;32:1164–9. doi:10.1177/0960327112472997.
- [142] McKay BS, Irving PE, Skumatz CM, Burke JM. Cell-cell adhesion molecules and the development of an epithelial phenotype in cultured human retinal pigment epithelial cells. *Experimental Eye Research* 1997;65:661–71. doi:10.1006/exer.1997.0374.
- [143] Sugita S, Kamao H, Iwasaki Y, Okamoto S, Hashiguchi T, Iseki K, et al. Inhibition of T-cell activation by retinal pigment epithelial cells derived from induced pluripotent stem cells. *Investigative Ophthalmology & Visual Science* 2015;56:1051–62. doi:10.1167/iovs.14-15619.
- [144] Horie S, Sugita S, Futagami Y, Yamada Y, Mochizuki M. Human retinal pigment epithelium-induced CD4+CD25+ regulatory T cells suppress activation of intraocular effector T cells. *Clin Immunol* 2010;136:83–95. doi:10.1016/j.clim.2010.03.001.
- [145] Sugita S, Horie S, Nakamura O, Futagami Y, Takase H, Keino H, et al. Retinal pigment epithelium-derived CTLA-2alpha induces TGFbeta-producing T regulatory cells. *The Journal of Immunology* 2008;181:7525–36.
- [146] Kvant A. Expression and secretion of transforming growth factor-beta in transformed and nontransformed retinal pigment epithelial cells. *Ophthalmic Res* 1994;26:361–7.
- [147] Kawazoe Y, Sugita S, Keino H, Yamada Y, Imai A. Retinoic acid from retinal pigment epithelium induces T regulatory cells. *Experimental Eye Research* 2012;94:32–40.
- [148] Heckenlively JR, Ferreyra HA. Autoimmune retinopathy: a review and summary. *Semin Immunopathol* 2008;30:127–34. doi:10.1007/s00281-008-0114-7.
- [149] Goel M, Picciani RG, Lee RK, Bhattacharya SK. Aqueous Humor Dynamics: A Review. *The Open Ophthalmology Journal* 2010;4:52–9. doi:10.2174/1874364101004010052.
- [150] Marmor MF. Control of subretinal fluid: experimental and clinical studies. *Eye (Lond)* 1990;4 ( Pt 2):340–4. doi:10.1038/eye.1990.46.
- [151] Stamer WD, Bok D, Hu J, Jaffe GJ, McKay BS. Aquaporin-1 channels in

- human retinal pigment epithelium: role in transepithelial water movement. *Investigative Ophthalmology & Visual Science* 2003;44:2803–8.
- [152] Juuti-Uusitalo K, Delporte C, Grégoire F, Perret J, Huhtala H, Savolainen V, et al. Aquaporin Expression and Function in Human Pluripotent Stem Cell–Derived Retinal Pigmented Epithelial Cells. *Investigative Ophthalmology & Visual Science* 2013;54:3510–9. doi:10.1167/iovs.13-11800.
- [153] Chihara E, Nao-i N. Resorption of subretinal fluid by transepithelial flow of the retinal pigment epithelium. *Graefes Arch Clin Exp Ophthalmol* 1985;23:202–4. doi:10.1007/BF02174060.
- [154] Hughes BA. Effects of cyclic AMP on fluid absorption and ion transport across frog retinal pigment epithelium. Measurements in the open-circuit state. *The Journal of General Physiology* 1984;83:875–99. doi:10.1085/jgp.83.6.875.
- [155] Ng SK, Wood JPM, Chidlow G, Han G, Kittipassorn T, Peet DJ, et al. Cancer-like metabolism of the mammalian retina. *Clin Experiment Ophthalmol* 2015;43:367–76. doi:10.1111/ceo.12462.
- [156] Bergersen L, Johannsson E, Veruki ML, Nagelhus EA, Halestrap A, Sejersted OM, et al. Cellular and subcellular expression of monocarboxylate transporters in the pigment epithelium and retina of the rat. *Neuroscience* 1999;90:319–31.
- [157] Takata K, Kasahara T, Kasahara M, Ezaki O, Hirano H. Ultracytochemical localization of the erythrocyte/HepG2-type glucose transporter (GLUT1) in cells of the blood-retinal barrier in the rat. *Investigative Ophthalmology & Visual Science* 1992;33:377–83.
- [158] Kumagai AK, Glasgow BJ, Pardridge WM. GLUT1 glucose transporter expression in the diabetic and nondiabetic human eye. *Investigative Ophthalmology & Visual Science* 1994;35:2887–94.
- [159] Hamann S, la Cour M, Lui GM, Bundgaard M, Zeuthen T. Transport of protons and lactate in cultured human fetal retinal pigment epithelial cells. *Pflugers Arch - Eur J Physiol* 2000;440:84–92. doi:10.1007/s004249900236.
- [160] Poitry-Yamate CL, Poitry S, Tsacopoulos M. Lactate released by Müller glial cells is metabolized by photoreceptors from mammalian retina. *J Neurosci* 1995;15:5179–91.
- [161] Fliesler SJ, Bretillon L. The ins and outs of cholesterol in the vertebrate retina. *J Lipid Res* 2010;51:3399–413. doi:10.1194/jlr.R010538.
- [162] Fliesler SJ, Schroepfer GJ. Sterol composition of bovine retinal rod outer segment membranes and whole retinas. *Biochimica Et Biophysica Acta (BBA)- ...* 1982;711:138–48.
- [163] Tserentsoodol N, Sztein J, Campos M, Gordiyenko NV. Uptake of cholesterol by the retina occurs primarily via a low density lipoprotein

- receptor-mediated process. *Mol Vis* 2006.
- [164] Strauss O. The retinal pigment epithelium in visual function. *Physiol Rev* 2005;85:845–81. doi:10.1152/physrev.00021.2004.
- [165] Sundaralingam M, Beddell C. Structures of the visual chromophores and related pigments: a conformational basis of visual excitation. *Proc Natl Acad Sci USA* 1972;69:1569–73.
- [166] Kühn H, Mommertz O, Hargrave PA. Light-dependent conformational change at rhodopsin's cytoplasmic surface detected by increased susceptibility to proteolysis. *Biochimica Et Biophysica Acta (BBA)- ...* 1982;679:95–100.
- [167] Rattner A, Smallwood PM, Nathans J. Identification and characterization of all-trans-retinol dehydrogenase from photoreceptor outer segments, the visual cycle enzyme that reduces all-trans-retinal to all-trans-retinol. *J Biol Chem* 2000;275:11034–43.
- [168] O'Byrne SM, Wongsiriroj N, Libien J, Vogel S, Goldberg IJ, Baehr W, et al. Retinoid Absorption and Storage Is Impaired in Mice Lacking Lecithin:Retinol Acyltransferase (LRAT). *Journal of Biological Chemistry* 2005;280:35647–57. doi:10.1074/jbc.M507924200.
- [169] Orban T, Palczewska G, Palczewski K. Retinyl ester storage particles (retinosomes) from the retinal pigmented epithelium resemble lipid droplets in other tissues. *J Biol Chem* 2011;286:17248–58. doi:10.1074/jbc.M110.195198.
- [170] Imanishi Y, Batten ML, Piston DW, Baehr W, Palczewski K. Noninvasive two-photon imaging reveals retinyl ester storage structures in the eye. *The Journal of Cell Biology* 2004;164:373–83. doi:10.1083/jcb.200311079.
- [171] Kim TS, Maeda A, Maeda T, Heinlein C, Kedishvili N, Palczewski K, et al. Delayed dark adaptation in 11-cis-retinol dehydrogenase-deficient mice: a role of RDH11 in visual processes in vivo. *J Biol Chem* 2005;280:8694–704. doi:10.1074/jbc.M413172200.
- [172] Redmond TM, Yu S, Lee E, Bok D, Hamasaki D, Chen N, et al. Rpe65 is necessary for production of 11-cis-vitamin A in the retinal visual cycle. *Nature Genetics* 1998;20:344–51. doi:10.1038/3813.
- [173] Cai X, Conley SM, Naash MI. RPE65: role in the visual cycle, human retinal disease, and gene therapy. *Ophthalmic Genet* 2009;30:57–62. doi:10.1080/13816810802626399.
- [174] Kevany BM, Palczewski K. Phagocytosis of Retinal Rod and Cone Photoreceptors. *Physiology* 2010;25:8–15. doi:10.1152/physiol.00038.2009.
- [175] Young RW, Bok D. Participation of the retinal pigment epithelium in the rod outer segment renewal process. *The Journal of Cell Biology* 1969;42:392–403.
- [176] Roddy GW, Rosa RH, Youn Oh J, Ylostalo JH, Bartosh TJ, Choi H, et al. Stanniocalcin-1 Rescued Photoreceptor Degeneration in Two Rat

- Models of Inherited Retinal Degeneration. *Mol Ther* 2012;20:788–97. doi:10.1038/mt.2011.308.
- [177] Boesze-Battaglia K, Albert AD. Phospholipid distribution among bovine rod outer segment plasma membrane and disk membranes. *Experimental Eye Research* 1992;54:821–3.
- [178] Ruggiero L, Connor MP, Chen J, Langen R, Finnemann SC. Diurnal, localized exposure of phosphatidylserine by rod outer segment tips in wild-type but not *Itgb5*<sup>-/-</sup> or *Mfge8*<sup>-/-</sup> mouse retina. *Pnas* 2012;109:8145–8. doi:10.1073/pnas.1121101109/-/DCSupplemental/pnas.201121101SI.pdf.
- [179] Feng W, Yasumura D, Matthes MT, LaVail MM, Vollrath D. Mertk triggers uptake of photoreceptor outer segments during phagocytosis by cultured retinal pigment epithelial cells. *J Biol Chem* 2002;277:17016–22. doi:10.1074/jbc.M107876200.
- [180] Finnemann SC, Silverstein RL. Differential Roles of CD36 and avb5 Integrin in Photoreceptor Phagocytosis by the Retinal Pigment Epithelium. *Journal of Experimental Medicine* 2001;194:1289–98.
- [181] Nandrot EF, Anand M, Almeida D, Atabai K, Sheppard D, Finnemann SC. Essential role for MFG-E8 as ligand for avb5 integrin in diurnal retinal phagocytosis. *Pnas* 2007;104:12005–10.
- [182] Nandrot EF, Finnemann SC. Lack of  $\alpha$ v $\beta$ 5 Integrin Receptor or Its Ligand MFG-E8: Distinct Effects on Retinal Function. *Ophthalmic Res* 2008;40:120–3. doi:10.1159/000119861.
- [183] D'Cruz PM, Yasumura D, Weir J, Matthes MT, Abderrahim H, LaVail MM, et al. Mutation of the receptor tyrosine kinase gene Mertk in the retinal dystrophic RCS rat. *Hum Mol Genet* 2000;9:645–51.
- [184] Daiger SP, Sullivan LS, Bowne SJ. Genes and mutations causing retinitis pigmentosa. *Clinical Genetics* 2013.
- [185] Margherita Cotonio Bourne DACKT. Hereditary Degeneration of the Rat Retina. *Br J Ophthalmol* 1938;22:613.
- [186] Mullen RJ, LaVail MM. Inherited retinal dystrophy: primary defect in pigment epithelium determined with experimental rat chimeras. *Science* 1976;192:799–801.
- [187] Edwards RB, Szamier RB. Defective phagocytosis of isolated rod outer segments by RCS rat retinal pigment epithelium in culture. *Science* 1977;197:1001–3.
- [188] Vollrath D, Feng W, Duncan JL, Yasumura D, D'Cruz PM, Chappelow A, et al. Correction of the retinal dystrophy phenotype of the RCS rat by viral gene transfer of Mertk. *Proc Natl Acad Sci USA* 2001;98:12584–9. doi:10.1073/pnas.221364198.
- [189] Duncan JL, LaVail MM, Yasumura D, Matthes MT, Yang H, Trautmann N, et al. An RCS-like retinal dystrophy phenotype in mer knockout mice. *Investigative Ophthalmology & Visual Science* 2003;44:826–38. doi:10.1167/iovs.02.

- [190] Ostergaard E, Duno M, Batbayli M, Vilhelmsen K, Rosenberg T. A novel MERTK deletion is a common founder mutation in the Faroe Islands and is responsible for a high proportion of retinitis pigmentosa cases. *Molecular Vision* 2011;17:1485–92.
- [191] Mackay DS, Henderson RH, Sergouniotis PI, Li Z, Moradi P, Holder GE, et al. Novel mutations in MERTK associated with childhood onset rod-cone dystrophy. *Molecular Vision* 2010;16:369–77.
- [192] Prasad D, Rothlin CV, Burrola P, Burstyn-Cohen T, Lu Q, Garcia de Frutos P, et al. TAM receptor function in the retinal pigment epithelium. *Molecular and Cellular Neuroscience* 2006;33:96–108. doi:10.1016/j.mcn.2006.06.011.
- [193] Robinson DS, Larché M, Durham SR. Tregs and allergic disease. *Journal of Clinical Investigation* 2004;114:1389–97. doi:10.1172/JCI200423595.
- [194] Lloyd CM, Hawrylowicz CM. Regulatory T Cells in Asthma. *Immunity* 2009;31:438–49. doi:10.1016/j.immuni.2009.08.007.
- [195] Holgate ST. Innate and adaptive immune responses in asthma. *Nat Med* 2012;18:673–83. doi:10.1038/nm.2731.
- [196] Gaffin JM, Phipatanakul W. The role of indoor allergens in the development of asthma. *Current Opinion in Allergy and Clinical Immunology* 2009;9:128–35. doi:10.1097/ACI.0b013e32832678b0.
- [197] Agrawal DK, Shao Z. Pathogenesis of Allergic Airway Inflammation. *Curr Allergy Asthma Rep* 2009;10:39–48. doi:10.1007/s11882-009-0081-7.
- [198] de Lafaille MAC, Lafaille JJ, Graça L. Mechanisms of tolerance and allergic sensitization in the airways and the lungs. *Current Opinion in Immunology* 2010;22:616–22. doi:10.1016/j.coi.2010.08.014.
- [199] Bilate AM, Lafaille JJ. Induced CD4<sup>+</sup>Foxp3<sup>+</sup> Regulatory T Cells in Immune Tolerance. *Annual Review of Immunology* 2012;30:733–58. doi:10.1146/annurev-immunol-020711-075043.
- [200] Cools N, Ponsaerts P, Van Tendeloo VFI, Berneman ZN. Regulatory T Cells and Human Disease. *Clinical and Developmental Immunology* 2007;2007:1–10. doi:10.1084/jem.194.6.823.
- [201] Hall BM, Verma ND, Tran GT, Hodgkinson SJ. Distinct regulatory CD4<sup>+</sup>T cell subsets; differences between naïve and antigen specific T regulatory cells. *Current Opinion in Immunology* 2011;23:641–7. doi:10.1016/j.coi.2011.07.012.
- [202] Fujio K, Okamura T, Yamamoto K. Chapter 4 - The Family of IL-10-Secreting CD4<sup>+</sup> T Cells. vol. 105. 1st ed. *Advances in Immunology*; 2010. doi:10.1016/S0065-2776(10)05004-2.
- [203] Josefowicz SZ, Lu L-F, Rudensky AY. Regulatory T Cells: Mechanisms of Differentiation and Function. *Annual Review of Immunology* 2012;30:531–64. doi:10.1146/annurev.immunol.25.022106.141623.
- [204] Shevach EM. Mechanisms of Foxp3. *Immunity* 2009;30:636–45.

- doi:10.1016/j.immuni.2009.04.010.
- [205] Venken K, Thewissen M, Hellings N, Somers V, Hensen K, Rummens J-L, et al. A CFSE based assay for measuring CD4+CD25+ regulatory T cell mediated suppression of auto-antigen specific and polyclonal T cell responses. *Journal of Immunological Methods* 2007;322:1–11. doi:10.1016/j.jim.2007.01.025.
- [206] Moore KW, Malefyt R de W, Coffman RL, O'Garra A. Interleukin-10 and the Interleukin-10 Receptor. *Annual Reviews of Immunology* 2001;19:683–765.
- [207] Rubtsov YP, Rasmussen JP, Chi EY, Fontenot J, Castelli L, Ye X, et al. Regulatory T Cell-Derived Interleukin-10 Limits Inflammation at Environmental Interfaces. *Immunity* 2008;28:546–58. doi:10.1016/j.immuni.2008.02.017.
- [208] Akbari O, Freeman GJ, Meyer EH, Greenfield EA, Chang TT, Sharpe AH, et al. Antigen-specific regulatory T cells develop via the ICOS–ICOS-ligand pathway and inhibit allergen-induced airway hyperreactivity. *Nature Medicine* 2002;8:1024–32. doi:10.1038/nm745.
- [209] Borish L, Aarons A, Rumblyrt J, Cvietusa P, Negri J, Wenzel S. Interleukin-10 regulation in normal subjects and patients with asthma. *J Allergy Clin Immunol* 1996:1–9.
- [210] Nguyen KD, Vanichsarn C, Nadeau KC. TSLP directly impairs pulmonary Treg function: association with aberrant tolerogenic immunity in asthmatic airway. *Allergy Asthma Clin Immunol* 2010;6:1–11. doi:10.1186/1710-1492-6-4.
- [211] Nayyar A, Dawicki W, Huang H, Lu M, Zhang X, Gordon JR. Induction of Prolonged Asthma Tolerance by IL-10-Differentiated Dendritic Cells: Differential Impact on Airway Hyperresponsiveness and the Th2 Immunoinflammatory Response. *The Journal of Immunology* 2012;189:72–9. doi:10.4049/jimmunol.1103286.
- [212] Huang H, Dawicki W, Zhang X, Town J, Gordon JR. Tolerogenic Dendritic Cells Induce CD4+CD25hiFoxp3+ Regulatory T Cell Differentiation from CD4+CD25-/loFoxp3- Effector T Cells. *The Journal of Immunology* 2010;185:5003–10. doi:10.4049/jimmunol.0903446.
- [213] Kearley J, Barker JE, Robinson DS, Lloyd CM. Resolution of airway inflammation and hyperreactivity after in vivo transfer of CD4+CD25+ regulatory T cells is interleukin 10 dependent. *Journal of Experimental Medicine* 2005;202:1539–47. doi:10.1084/jem.20051166.
- [214] Lei L, Zhang Y, Yao W, Kaplan MH, Zhou B. Thymic Stromal Lymphopoietin Interferes with Airway Tolerance by Suppressing the Generation of Antigen-Specific Regulatory T Cells. *The Journal of Immunology* 2011;186:2254–61. doi:10.4049/jimmunol.1002503.
- [215] Nguyen KD, Vanichsarn C, Nadeau KC. TSLP directly impairs pulmonary Treg function: association with aberrant tolerogenic immunity in asthmatic airway. *Allergy Asthma Clin Immunol* 2010;6:4.

- doi:10.1186/1710-1492-6-4.
- [216] Kousteni S. FoxO1: A molecule for all seasons. *J Bone Miner Res* 2011;26:912–7. doi:10.1002/jbmr.306.
- [217] Ouyang W, Beckett O, Flavell RA, Li MO. An Essential Role of the Forkhead-Box Transcription Factor Foxo1 in Control of T Cell Homeostasis and Tolerance. *Immunity* 2009;30:358–71. doi:10.1016/j.immuni.2009.02.003.
- [218] Ouyang W, Liao W, Luo CT, Yin N, Huse M, Kim MV, et al. Novel Foxo1-dependent transcriptional programs control Treg cell function. *Nature* 2012;491:554–9. doi:10.1038/nature11581.
- [219] Kerdiles YM, Beisner DR, Tinoco R, Dejean AS, Castrillon DH, DePinho RA, et al. Foxo1 links homing and survival of naive T cells by regulating L-selectin, CCR7 and interleukin 7 receptor. *Nature Immunology* 2009;10:176–84. doi:10.1038/ni.1689.
- [220] Luo CT, Liao W, Dadi S, Toure A, Li MO. Graded Foxo1 activity in Treg cells differentiates tumour immunity from spontaneous autoimmunity. *Nature* 2016;529:532–6. doi:10.1038/nature16486.
- [221] Cabarocas J, Cassan C, Magnusson F, Piaggio E, Mars L, Derbinski J, et al. Foxp3+ CD25+ regulatory T cells specific for a neo-self-antigen develop at the double-positive thymic stage. *Pnas* 2006;103:8453–8.
- [222] Ouyang W, Beckett O, Ma Q, Paik J-H, DePinho RA, Li MO. Foxo proteins cooperatively control the differentiation of Foxp3+ regulatory T cells. *Nature Immunology* 2010;11:618–27. doi:10.1038/ni.1884.
- [223] Kerdiles YM, Stone EL, Beisner DL, McGargill MA, Ch'en IL, Stockmann C, et al. Foxo Transcription Factors Control Regulatory T Cell Development and Function. *Immunity* 2010;33:890–904. doi:10.1016/j.immuni.2010.12.002.
- [224] Martelli AM, Tabellini G, Bressanin D, Ognibene A, Goto K, Cocco L, et al. The emerging multiple roles of nuclear Akt. *BBA - Molecular Cell Research* 2012;1823:2168–78. doi:10.1016/j.bbamcr.2012.08.017.
- [225] Peng SL. Foxo in the immune system. *Oncogene* 2008;27:2337–44. doi:10.1038/onc.2008.26.
- [226] Cyster JG, Schwab SR. Sphingosine-1-Phosphate and Lymphocyte Egress from Lymphoid Organs. *Annual Review of Immunology* 2012;30:69–94. doi:10.1146/annurev-immunol-020711-075011.
- [227] Burgess DJ. Apoptosis: Refined and lethal. *Nature Reviews Cancer* 2013;13:79–9. doi:10.1038/nrc3462.
- [228] Yu CR, Kim SH, Mahdi RM, Egwuagu CE. SOCS3 Deletion in T Lymphocytes Suppresses Development of Chronic Ocular Inflammation via Upregulation of CTLA-4 and Expansion of Regulatory T Cells. *The Journal of Immunology* 2013;191:5036–43. doi:10.4049/jimmunol.1301132.
- [229] Yan L, Lavin VA, Moser LR, Cui Q, Kanies C, Yang E. PP2A regulates the pro-apoptotic activity of FOXO1. *J Biol Chem* 2008;283:7411–20.

- doi:10.1074/jbc.M708083200.
- [230] Janssens V, Goris J. Protein phosphatase 2A: a highly regulated family of serine/threonine phosphatases implicated in cell growth and signalling. *Journal of Biochemical Society* 2001;353:417–39.
- [231] Shi Y. Serine/Threonine Phosphatases: Mechanism through Structure. *Cell* 2009;139:468–84. doi:10.1016/j.cell.2009.10.006.
- [232] Kurimchak A, Graña X. PP2A holoenzymes negatively and positively regulate cell cycle progression by dephosphorylating pocket proteins and multiple CDK substrates. *Gene* 2012;499:1–7. doi:10.1016/j.gene.2012.02.015.
- [233] Baharians Z, Schonthal AH. Autoregulation of Protein Phosphatase Type 2A Expression. *Journal of Biological Chemistry* 1998;273:19019–24. doi:10.1074/jbc.273.30.19019.
- [234] Kobayashi Y, Mercado N, Barnes PJ, Ito K. Defects of Protein Phosphatase 2A Causes Corticosteroid Insensitivity in Severe Asthma. *Plos ONE* 2011;6:e27627. doi:10.1371/journal.pone.0027627.s002.
- [235] Verhagen J, Blaser K, Akdis CA, Akdis M. Mechanisms of allergen-specific immunotherapy: T-regulatory cells and more. *Immunol Allergy Clin North Am* 2006;26:207–31–vi. doi:10.1016/j.iac.2006.02.008.
- [236] Soyer OU, Akdis M, Ring J, Behrendt H, Cramer R, Lauener R, et al. Mechanisms of peripheral tolerance to allergens. *Allergy* 2013;68:161–70. doi:10.1111/all.12085.
- [237] Wills-Karp M. Immunological Basis of Antigen-Induced Airway Hyperresponsiveness. *Annual Review of Immunology* 1999;17:255–81.
- [238] Hammad H, Chieppa M, Perros F, Willart MA, Germain RN, Lambrecht BN. House dust mite allergen induces asthma via Toll-like receptor 4 triggering of airway structural cells. *Nature Medicine* 2009;15:410–6. doi:10.1038/nm.1946.
- [239] Kauffman HF, Tamm M, Timmerman JAB, Borger P. House dust mite major allergens Der p 1 and Der p 5 activate human airway-derived epithelial cells by protease-dependent and protease-independent mechanisms. *Clin Mol Allergy* 2006;4:5. doi:10.1186/1476-7961-4-5.
- [240] Trompette A, Divanovic S, Visintin A, Blanchard C, Hegde RS, Madan R, et al. Allergenecity resulting from functional mimicry of a Toll-like receptor complex protein. *Nature* 2009;457:585–8. doi:10.1038/nature07548.
- [241] D CM, Wünschmann S, Pommès A. Proteases as Th2 Adjuvants. *Allergens* 2007;7:363–7.
- [242] Herbert CA, King CM, Ring PC, Holgate ST, Stewart GA, Thompson PJ, et al. Augmentation of permeability in the bronchial epithelium by the house dust mite allergen Der p1. *Am J Respir Cell Mol Biol* 1995;12:369–78. doi:10.1165/ajrcmb.12.4.7695916.
- [243] Holgate ST. The Sentinel Role of the Airway Epithelium in Asthma Pathogenesis. *Immunological Reviews* 2011;242:205–19.

- [244] Kim HY, Chang Y-J, Subramanian S, Lee H-H, Albacker LA, Matangkasombut P, et al. Innate lymphoid cells responding to IL-33 mediate airway hyperreactivity independently of adaptive immunity. *Journal of Allergy and Clinical Immunology* 2012;129:216–6. doi:10.1016/j.jaci.2011.10.036.
- [245] Stumbles PA, Upham JW, Holt PG. Airway dendritic cells: Co-ordinators of immunological homeostasis and immunity in the respiratory tract. *Apmis* 2003;111:741–55.
- [246] Hammad H, Lambrecht BN. Dendritic cells and epithelial cells: linking innate and adaptive immunity in asthma. *Nature Reviews Immunology* 2008;8:193–204. doi:10.1038/nri2275.
- [247] Ingram JL, Kraft M. IL-13 in asthma and allergic disease: Asthma phenotypes and targeted therapies. *Journal of Allergy and Clinical Immunology* 2012;130:829–42. doi:10.1016/j.jaci.2012.06.034.
- [248] Agrawal DK, Shao Z. Pathogenesis of Allergic Airway Inflammation. *Curr Allergy Asthma Rep* 2009;10:39–48. doi:10.1007/s11882-009-0081-7.
- [249] Broide DH. Molecular and cellular mechanisms of allergic disease ☆ ☆ ☆. *Journal of Allergy and Clinical Immunology* 2001;108:S65–S71. doi:10.1067/mai.2001.116436.
- [250] Akbari O, DeKruyff RH, Umetsu DT. Pulmonary dendritic cells producing IL-10 mediate tolerance induced by respiratory exposure to antigen. *Nature Immunology* 2001;2:725–31.
- [251] Van Hove CL, Maes T, Joos GF, Tournoy KG. Prolonged Inhaled Allergen Exposure Can Induce Persistent Tolerance. *Am J Respir Cell Mol Biol* 2007;36:573–84. doi:10.1165/rcmb.2006-0385OC.
- [252] Akinbami LJ, Moorman JE, Bailey C, Zahran HS, King M, Johnson CA, et al. Trends in Asthma Prevalence, Health Care Use, and Mortality in the United States, 2001–2010 2012;94:1–8.
- [253] Gaffin JM, Phipatanakul W. The role of indoor allergens in the development of asthma. *Current Opinion in Allergy and Clinical Immunology* 2009;9:128–35. doi:10.1097/ACI.0b013e32832678b0.
- [254] National Heart Lung and Blood Institute. Expert Panel Report 3: Guidelines for the Diagnosis and Management of Asthma. *National Asthma Education and Prevention Program* 2007:1–440.
- [255] Karagiannidis C, Akdis M, Holopainen P, Woolley NJ, Hense G, Rückert B, et al. Glucocorticoids upregulate FOXP3 expression and regulatory T cells in asthma. *J Allergy Clin Immunol* 2004;114:1425–33. doi:10.1016/j.jaci.2004.07.014.
- [256] Xystrakis E, Kusumakar S, Boswell S, Peek E, Urry Z, Richards DF, et al. Reversing the defective induction of IL-10-secreting regulatory T cells in glucocorticoid-resistant asthma patients. *Journal of Clinical Investigation* 2005;116:146–55. doi:10.1172/JCI21759DS1.
- [257] Cohen PL, Caricchio R, Abraham V, Camenisch TD, Jennette JC,

- Roubey RAS, et al. Delayed Apoptotic Cell Clearance and Lupus-like Autoimmunity in Mice Lacking the c-mer Membrane Tyrosine Kinase. *Journal of Experimental Medicine* 2002;196:135–40. doi:10.1084/jem.20012094.
- [258] Poon IKH, Lucas CD, Rossi AG, Ravichandran KS. Apoptotic cell clearance: basic biology and therapeutic potential. *Nature Reviews Immunology* 2014;14:166–80. doi:10.1038/nri3607.
- [259] Penberthy KK, Ravichandran KS. Apoptotic cell recognition receptors and scavenger receptors. *Immunological Reviews* 2016;269:44–59. doi:10.1111/imr.12376.
- [260] Breucker H, Schäfer E, Holstein AF. Morphogenesis and fate of the residual body in human spermiogenesis. *Cell Tissue Res* 1985;240:303–9.
- [261] Mattapallil MJ, Wawrousek EF, Chan CC, Zhao H, Roychoudhury J, Ferguson TA, et al. The Rd8 Mutation of the Crb1 Gene Is Present in Vendor Lines of C57BL/6N Mice and Embryonic Stem Cells, and Confounds Ocular Induced Mutant Phenotypes. *Investigative Ophthalmology & Visual Science* 2012;53:2921–7. doi:10.1167/iovs.12-9662.
- [262] Gibbs D, Williams DS. Isolation and Culture of Primary Mouse Retinal pigmented epithelial cells. In: LaVail MM, Hollyfield JG, Anderson RE, editors. *Retinal Degenerations*, vol. 533, Springer US; 2003, pp. 347–52. doi:10.1007/978-1-4615-0067-4\_44.
- [263] Lysiak JJ, Turner SD, Turner TT. Molecular pathway of germ cell apoptosis following ischemia/reperfusion of the rat testis. *Biology of Reproduction* 2000;63:1465–72.
- [264] Smith-Harrison LI, Koontz WW. Torsion of the testis: changing concepts. *AUA update Series*; 1990.
- [265] Zhu D, Li C, Swanson AM, Villalba RM, Guo J, Zhang Z, et al. BAI1 regulates spatial learning and synaptic plasticity in the hippocampus. *Journal of Clinical Investigation* 2015;125:1497–508. doi:10.1172/JCI74603DS1.
- [266] Duman JG, Tzeng CP, Tu Y-K, Munjal T, Schwechter B, Ho TS-Y, et al. The adhesion-GPCR BAI1 regulates synaptogenesis by controlling the recruitment of the Par3/Tiam1 polarity complex to synaptic sites. *Journal of Neuroscience* 2013;33:6964–78. doi:10.1523/JNEUROSCI.3978-12.2013.
- [267] Sethna S, Finnemann SC. Analysis of Photoreceptor Rod Outer Segment Phagocytosis by RPE Cells In Situ. *Methods in Molecular Biology*, vol. 935, Totowa, NJ: Humana Press; 2012, pp. 245–54. doi:10.1007/978-1-62703-080-9\_17.
- [268] Nakaya M, Tanaka M, Okabe Y, Hanayama R, Nagata S. Opposite Effects of Rho Family GTPases on Engulfment of Apoptotic Cells by Macrophages. *Journal of Biological Chemistry* 2006;281:8836–42.

- [269] Kiser PD, Palczewski K. Retinoids and Retinal Diseases. *Annu Rev Vis Sci* 2016;2:197–234. doi:10.1146/annurev-vision-111815-114407.
- [270] Palczewska G, Maeda A, Golczak M, Arai E, Dong Z, Perusek L, et al. Receptor MER Tyrosine Kinase Proto-oncogene (MERTK) Is Not Required for Transfer of Bis-retinoids to the Retinal Pigmented Epithelium. *J Biol Chem* 2016;291:26937–49. doi:10.1074/jbc.M116.764563.
- [271] Tian N. Visual experience and maturation of retinal synaptic pathways. *Vision Res* 2004;44:3307–16. doi:10.1016/j.visres.2004.07.041.
- [272] Dorrell MI, Aguilar E, Weber C, Friedlander M. Global gene expression analysis of the developing postnatal mouse retina. *Investigative Ophthalmology & Visual Science* 2004;45:1009–19.
- [273] O'Byrne SM, Blamer WS. Retinol and retinyl esters: Biochemistry and physiology Thematic Review Series: Fat-soluble vitamins: vitamin A. *J Lipid Res* 2013.
- [274] Batten ML, Imanishi Y, Maeda T, Tu DC, Moise AR, Bronson D, et al. Lecithin-retinol acyltransferase is essential for accumulation of all-trans-retinyl esters in the eye and in the liver. *J Biol Chem* 2004;279:10422–32. doi:10.1074/jbc.M312410200.
- [275] Lamb TD, Pugh EN Jr. Phototransduction, Dark Adaptation, and Rhodopsin Regeneration The Proctor Lecture. *Investigative Ophthalmology & Visual Science* 2006;47:5138–52. doi:10.1167/iovs.06-0849.
- [276] Sarangi P, Wahl L, Vega S. Fibulin-7, a member of the extracellular matrix fibulin family, regulates immune cell migration and function (P5124). *The Journal of Immunology* 2013.
- [277] de Vega S, Hozumi K, Suzuki N, Nonaka R, Seo E, Takeda A, et al. Identification of Peptides Derived from the C-terminal Domain of Fibulin-7 Active for Endothelial Cell Adhesion and Tube Formation Disruption. *Biopolymers* 2015. doi:10.1002/bip.22754.
- [278] de Vega S, Iwamoto T, Nakamura T, Hozumi K, McKnight DA, Fisher LW, et al. TM14 is a new member of the fibulin family (fibulin-7) that interacts with extracellular matrix molecules and is active for cell binding. *J Biol Chem* 2007;282:30878–88. doi:10.1074/jbc.M705847200.
- [279] Sardell RJ, Bailey JNC, Courtenay MD, Whitehead P, Laux RA, Adams LD, et al. Whole exome sequencing of extreme age-related macular degeneration phenotypes. *Molecular Vision* 2016;22:1062–76.
- [280] Barrett T, Wilhite SE, Ledoux P, Evangelista C, Kim IF, Tomashevsky M, et al. NCBI GEO: archive for functional genomics data sets--update. *Nucleic Acids Res* 2013;41:D991–5. doi:10.1093/nar/gks1193.
- [281] Kinchen JM, Ravichandran KS. Phagosome maturation: going through the acid test. *Nat Rev Mol Cell Biol* 2008;9:781–95.

- doi:10.1038/nrm2515.
- [282] Steinberg BE, Huynh KK, Brodovitch A, Jabs S, Stauber T, Jentsch TJ, et al. A cation counterflux supports lysosomal acidification. *The Journal of Cell Biology* 2010;189:1171–86. doi:10.1083/jcb.200911083.
- [283] Swanson J. CFTR: helping to acidify macrophage lysosomes. *Nature Cell Biology* 2006;8:908–9. doi:10.1038/ncb0906-908.
- [284] Yang YD, Cho H, Koo JY, Tak MH, Cho Y, Shim W-S, et al. TMEM16A confers receptor-activated calcium-dependent chloride conductance. *Nature* 2008;455:1210–5. doi:10.1038/nature07313.
- [285] Zhang L, Hui Y-N, Wang Y-S, Ma JX, Wang J-B, Ma L-N. Calcium overload is associated with lipofuscin formation in human retinal pigment epithelial cells fed with photoreceptor outer segments. *Eye (Lond)* 2011;25:519–27. doi:10.1038/eye.2011.7.
- [286] Aalkjaer C, Boedtkjer E, Choi I, Lee S. Cation-coupled bicarbonate transporters. *Compr Physiol* 2014;4:1605–37. doi:10.1002/cphy.c130005.
- [287] Hanzu FA, Gasa R, Bulur N, Lybaert P, Gomis R, Malaisse WJ, et al. Expression of TMEM16A and SLC4A4 in human pancreatic islets. *Cellular Physiology and Biochemistry* 2012;29:61–4. doi:10.1159/000337587.
- [288] Borregaard N, Herlin T. Energy metabolism of human neutrophils during phagocytosis. *Journal of Clinical Investigation* 1982;70:550–7.
- [289] Biswas SK, Mantovani A. Orchestration of metabolism by macrophages. *Cell Metabolism* 2012;15:432–7. doi:10.1016/j.cmet.2011.11.013.
- [290] Dotti MT, Rufa A, Federico A. Cerebrotendinous xanthomatosis: heterogeneity of clinical phenotype with evidence of previously undescribed ophthalmological findings. *J Inherit Metab Dis* 2001;24:696–706.
- [291] Gabriel LAR, Sachdeva R, Marcotty A, Rockwood EJ, Traboulsi EI. Oculodentodigital dysplasia: new ocular findings and a novel connexin 43 mutation. *Arch Ophthalmol* 2011;129:781–4. doi:10.1001/archophthalmol.2011.113.
- [292] Davis AP, Murphy CG, Saraceni-Richards CA, Rosenstein MC, Wiegers TC, Mattingly CJ. Comparative Toxicogenomics Database: a knowledgebase and discovery tool for chemical-gene-disease networks. *Nucleic Acids Res* 2009;37:D786–92. doi:10.1093/nar/gkn580.
- [293] Davis AP, Grondin CJ, Lennon-Hopkins K, Saraceni-Richards C, Sciaky D, King BL, et al. The Comparative Toxicogenomics Database's 10th year anniversary: update 2015. *Nucleic Acids Res* 2015;43:D914–20. doi:10.1093/nar/gku935.
- [294] Alvarez BV, Vithana EN, Yang Z, Koh AH, Yeung K, Yong V, et al. Identification and Characterization of a Novel Mutation in the Carbonic Anhydrase IV Gene that Causes Retinitis Pigmentosa. *Investigative Ophthalmology & Visual Science* 2007;48:3459–68.

- [295] Li S, Lee J, Zhou Y, Gordon WC, Hill JM, Bazan NG, et al. Fatty acid transport protein 4 (FATP4) prevents light-induced degeneration of cone and rod photoreceptors by inhibiting RPE65 isomerase. *Journal of Neuroscience* 2013;33:3178–89. doi:10.1523/JNEUROSCI.2428-12.2013.
- [296] Li MJ, Wang P, Liu X, Lim EL, Wang Z, Yeager M, et al. GWASdb: a database for human genetic variants identified by genome-wide association studies. *Nucleic Acids Res* 2012;40:D1047–54. doi:10.1093/nar/gkr1182.
- [297] Chan W-M, Ohji M, Lai TYY, Liu DTL, Tano Y, Lam DSC. Choroidal neovascularisation in pathological myopia: an update in management. *Br J Ophthalmol* 2005;89:1522–8. doi:10.1136/bjo.2005.074716.
- [298] Grossniklaus HE, Green WR. Pathologic findings in pathologic myopia. *Retina (Philadelphia, Pa)* 1992;12:127–33.
- [299] Batioğlu F, Ozdek S, Hasanreisoglu B. An unusual macular involvement in pathological myopia. *Eye (Lond)* 2003;17:654–6. doi:10.1038/sj.eye.6700416.
- [300] Paznekas WA, Boyadjiev SA, Shapiro RE, Daniels O, Wollnik B, Keegan CE, et al. Connexin 43 (GJA1) mutations cause the pleiotropic phenotype of oculodentodigital dysplasia. *Am J Hum Genet* 2003;72:408–18. doi:10.1086/346090.
- [301] Kojima A, Nakahama K-I, Ohno-Matsui K, Shimada N, Mori K, Iseki S, et al. Connexin 43 contributes to differentiation of retinal pigment epithelial cells via cyclic AMP signaling. *Biochemical Journal* 2008;366:532–8. doi:10.1016/j.bbrc.2007.11.159.
- [302] Malfait M, Gomez P, van Veen TA, Parys JB, De Smedt H, Vereecke J, et al. Effects of hyperglycemia and protein kinase C on connexin43 expression in cultured rat retinal pigment epithelial cells. *J Membr Biol* 2001;181:31–40. doi:10.1007/s002320010008.
- [303] Verrips A, Hoefsloot LH, Steenbergen GC, Theelen JP, Wevers RA, Gabreëls FJ, et al. Clinical and molecular genetic characteristics of patients with cerebrotendinous xanthomatosis. *Brain* 2000;123 ( Pt 5):908–19.
- [304] Saadane A, Mast N, Charvet CD, Omarova S, Zheng W, Huang SS, et al. Retinal and nonocular abnormalities in *Cyp27a1(-/-)Cyp46a1(-/-)* mice with dysfunctional metabolism of cholesterol. *The American Journal of Pathology* 2014;184:2403–19. doi:10.1016/j.ajpath.2014.05.024.
- [305] Omarova S, Charvet CD, Reem RE, Mast N, Zheng W, Huang S, et al. Abnormal vascularization in mouse retina with dysregulated retinal cholesterol homeostasis. *J Clin Invest* 2012;122:3012–23. doi:10.1172/JCI63816.
- [306] Pletscher-Frankild S, Pallejà A, Tsafou K, Binder JX, Jensen LJ. DISEASES: text mining and data integration of disease-gene

- associations. *Methods* 2015;74:83–9. doi:10.1016/j.ymeth.2014.11.020.
- [307] Rebello G, Ramesar R, Vorster A, Roberts L, Ehrenreich L, Oppon E, et al. Apoptosis-inducing signal sequence mutation in carbonic anhydrase IV identified in patients with the RP17 form of retinitis pigmentosa. *Proc Natl Acad Sci USA* 2004;101:6617–22. doi:10.1073/pnas.0401529101.
- [308] Datta R, Waheed A, Bonapace G, Shah GN, Sly WS. Pathogenesis of retinitis pigmentosa associated with apoptosis-inducing mutations in carbonic anhydrase IV. *Pnas* 2009;106:3437–42. doi:10.1073/pnas.0813178106.
- [309] Liles MR, Newsome DA, Oliver PD. Antioxidant enzymes in the aging human retinal pigment epithelium. *Arch Ophthalmol* 1991;109:1285–8.
- [310] Rex TS, Tsui I, Hahn P, Maguire AM, Duan D, Bennett J, et al. Adenovirus-mediated delivery of catalase to retinal pigment epithelial cells protects neighboring photoreceptors from photo-oxidative stress. *Hum Gene Ther* 2004;15:960–7. doi:10.1089/hum.2004.15.960.
- [311] Meyers KJ, Mares JA, Igo RP, Truitt B, Liu Z, Millen AE, et al. Genetic evidence for role of carotenoids in age-related macular degeneration in the Carotenoids in Age-Related Eye Disease Study (CAREDS). *Investigative Ophthalmology & Visual Science* 2014;55:587–99. doi:10.1167/iovs.13-13216.
- [312] Stoffel W, Holz B, Jenke B, Binczek E, Günter RH, Kiss C, et al. Delta6-desaturase (FADS2) deficiency unveils the role of omega3- and omega6-polyunsaturated fatty acids. *Embo J* 2008;27:2281–92. doi:10.1038/emboj.2008.156.
- [313] Mukherjee S, King JL, Guidry C. Phenotype-associated changes in retinal pigment epithelial cell expression of insulin-like growth factor binding proteins. *Investigative Ophthalmology & Visual Science* 2009;50:5449–55. doi:10.1167/iovs.09-3383.
- [314] Umetsu DT, McIntire JJ, Akbari O, Macaubas C, DeKruyff RH. Asthma: an epidemic of dysregulated immunity. *Nature Immunology* 2002;3:715–20.
- [315] Lambrecht BN, Hammad H. Asthma: The importance of dysregulated barrier immunity. *European Journal of Immunology* 2013;43:3125–37. doi:10.1002/eji.201343730.
- [316] Kennedy JL, Heymann PW, Platts-Mills TAE. The role of allergy in severe asthma. *Clinical & Experimental Allergy* 2012;42:659–69. doi:10.1111/j.1365-2222.2011.03944.x.
- [317] Provoost S, Maes T, van Durme YM, Gevaert P, Bachert C, Schmidt-Weber CB, et al. Decreased FOXP3 protein expression in patients with asthma. *Allergy* 2009;64:1539–46. doi:10.1111/j.1398-9995.2009.02056.x.
- [318] Lin YL, Shieh CC, Wang JY. The functional insufficiency of human CD4<sup>+</sup>CD25<sup>high</sup> T-regulatory cells in allergic asthma is subjected to

- TNF- $\alpha$  modulation. *Allergy* 2007;63:67–74. doi:10.1111/j.1398-9995.2007.01526.x.
- [319] Nadeau K, McDonald-Hyman C, Noth EM, Pratt B, Hammond SK, Balmes J, et al. Ambient air pollution impairs regulatory T-cell function in asthma. *Journal of Allergy and Clinical Immunology* 2010;126:845–852.e10. doi:10.1016/j.jaci.2010.08.008.
- [320] Mamessier E, Nieves A, Lorec A-M, Dupuy P, Pinot D, Pinet C, et al. T-cell activation during exacerbations: a longitudinal study in refractory asthma. *Allergy* 2008;63:1202–10. doi:10.1111/j.1398-9995.2008.01687.x.
- [321] Hartl D, Koller B, Mehlhorn AT, Reinhardt D, Nicolai T, Schendel DJ, et al. Quantitative and functional impairment of pulmonary CD4+CD25hi regulatory T cells in pediatric asthma. *Journal of Allergy and Clinical Immunology* 2007;119:1258–66. doi:10.1016/j.jaci.2007.02.023.
- [322] Böhm L, Maxeiner J, Meyer-Martin H, Reuter S, Finotto S, Klein M, et al. IL-10 and regulatory T cells cooperate in allergen-specific immunotherapy to ameliorate allergic asthma. *The Journal of Immunology* 2015;194:887–97. doi:10.4049/jimmunol.1401612.
- [323] Chen W, Jin W, Hardegen N, Lei K-J, Li L, Marinos N, et al. Conversion of peripheral CD4+CD25- naive T cells to CD4+CD25+ regulatory T cells by TGF- $\beta$  induction of transcription factor Foxp3. *J Exp Med* 2003;198:1875–86. doi:10.1084/jem.20030152.
- [324] Hori S, Nomura T, Sakaguchi S. Control of regulatory T cell development by the transcription factor Foxp3. *Science* 2003;299:1057–61. doi:10.1126/science.1079490.
- [325] Lewkowich IP, Herman NS, Schleifer KW, Dance MP, Chen BL, Dienger KM, et al. CD4+CD25+ T cells protect against experimentally induced asthma and alter pulmonary dendritic cell phenotype and function. *J Exp Med* 2005;202:1549–61. doi:10.1084/jem.20051506.
- [326] Borish L, Aarons A, Rumblyrt J, Cvietusa P, Negri J, Wenzel S. Interleukin-10 regulation in normal subjects and patients with asthma. *J Allergy Clin Immunol* 1996;97:1288–96.
- [327] Raundhal M, Morse C, Khare A, Oriss TB, Milosevic J, Trudeau J, et al. High IFN- $\gamma$  and low SLPI mark severe asthma in mice and humans. *J Clin Invest* 2015;125:3037–50. doi:10.1172/JCI80911.
- [328] Kumar RK, Webb DC, Herbert C, Foster PS. Interferon-gamma as a possible target in chronic asthma. *Inflamm Allergy Drug Targets* 2006;5:253–6.
- [329] Du X, Shi H, Li J, Dong Y, Liang J, Ye J, et al. Mst1/Mst2 Regulate Development and Function of Regulatory T Cells through Modulation of Foxo1/Foxo3 Stability in Autoimmune Disease. *The Journal of Immunology* 2014;192:1525–35. doi:10.4049/jimmunol.1301060/-/DCSupplemental.
- [330] Harada Y, Harada Y, Elly C, Ying G, Paik J-H, DePinho RA, et al.

- Transcription factors Foxo3a and Foxo1 couple the E3 ligase Cbl-b to the induction of Foxp3 expression in induced regulatory T cells. *Journal of Experimental Medicine* 2010;207:1381–91. doi:10.1084/jem.20100004.
- [331] Hsu P, Santner-Nanan B, Hu M, Skarratt K, Lee CH, Stormon M, et al. IL-10 Potentiates Differentiation of Human Induced Regulatory T Cells via STAT3 and Foxo1. *The Journal of Immunology* 2015;195:3665–74. doi:10.4049/jimmunol.1402898.
- [332] Puthanveetil P, Wan A, Rodrigues B. FoxO1 is crucial for sustaining cardiomyocyte metabolism and cell survival. *Cardiovascular Research* 2013;97:393–403. doi:10.1093/cvr/cvs426.
- [333] Apostolidis SA, Rodríguez-Rodríguez N, Suárez-Fueyo A, Dioufa N, Ozcan E, Crispín JC, et al. Phosphatase PP2A is requisite for the function of regulatory T cells. *Nature Immunology* 2016;17:556–64. doi:10.1038/ni.3390.
- [334] Van Hoof C, Goris J. PP2A fulfills its promises as tumor suppressor: Which subunits are important? *Cancer Cell* 2004;5:105–6.
- [335] Kim SI, Kwak JH, Wang L, Choi ME. Protein Phosphatase 2A Is a Negative Regulator of Transforming Growth Factor-1-induced TAK1 Activation in Mesangial Cells. *Journal of Biological Chemistry* 2008;283:10753–63. doi:10.1074/jbc.M801263200.
- [336] Bengtsson L, Schwappacher R, Roth M, Boergermann JH, Hassel S, Knaus P. PP2A regulates BMP signalling by interacting with BMP receptor complexes and by dephosphorylating both the C-terminus and the linker region of Smad1. *Journal of Cell Science* 2009;122:1248–57. doi:10.1242/jcs.039552.
- [337] Murata K, Wu J, Brautigan DL. B cell receptor-associated protein alpha4 displays rapamycin-sensitive binding directly to the catalytic subunit of protein phosphatase 2A. *Proc Natl Acad Sci USA* 1997;94:10624–9.
- [338] Robinson DS, Larché M, Durham SR. Tregs and allergic disease. *Journal of Clinical Investigation* 2004;114:1389–97. doi:10.1172/JCI200423595.
- [339] Mays LE, Ammon-Treiber S, Mothes B, Alkhaled M, Rottenberger J, Müller-Hermelink ES, et al. Modified Foxp3 mRNA protects against asthma through an IL-10-dependent mechanism. *Journal of Clinical Investigation* 2013;123:1216–28. doi:10.1172/JCI65351DS1.
- [340] O'Garra A, Vieira PL, Vieira P, Goldfeld AE. IL-10-producing and naturally occurring CD4+ Tregs: limiting collateral damage. *Journal of Clinical Investigation* 2004;114:1372–8. doi:10.1172/JCI23215.
- [341] Zhao X, Gan L, Pan H, Kan D, Majeski M, Adam S, et al. Multiple elements regulate nuclear/cytoplasmic shuttling of FOXO1: characterization of phosphorylation- and 14-3-3-dependent and -independent mechanisms. *Biochemical Journal* 2004;378:839–49.
- [342] Zhang X, Gan L, Pan H, Guo S, He X, Olson ST, et al. Phosphorylation

- of Serine 256 Suppresses Transactivation by FKHR (FOXO1) by Multiple Mechanisms: direct and indirect effects on nuclear/cytoplasmic shuttling and DNA binding. *Journal of Biological Chemistry* 2002;277:45276–84. doi:10.1074/jbc.M208063200.
- [343] Swingle M, Ni L, Honkanen RE. Small-Molecule Inhibitors of Ser/Thr Protein Phosphatases. *Methods in Molecular Biology* 2007;365:23–38.
- [344] Heng TSP, Painter MW, Immunological Genome Project Consortium. The Immunological Genome Project: networks of gene expression in immune cells. *Nature Immunology* 2008;9:1091–4. doi:10.1038/ni1008-1091.
- [345] Lu J, Kovach JS, Johnson F, Chiang J, Hodes R, Lonser R, et al. Inhibition of serine/threonine phosphatase PP2A enhances cancer chemotherapy by blocking DNA damage induced defense mechanisms. *Pnas* 2009;106:11697–702. doi:10.1073/pnas.0905930106.
- [346] Samstein RM, Arvey A, Josefowicz SZ, Peng X, Reynolds A, Sandstrom R, et al. Foxp3 exploits a pre-existent enhancer landscape for regulatory T cell lineage specification. *Cell* 2012;151:153–66. doi:10.1016/j.cell.2012.06.053.
- [347] Chang X, Gao JX, Jiang Q, Wen J, Seifers N, Su L, et al. The Scurfy mutation of FoxP3 in the thymus stroma leads to defective thymopoiesis. *J Exp Med* 2005;202:1141–51. doi:10.1084/jem.20050157.
- [348] Huang J, Wang H, Chen Y, Wang X, Zhang H. Residual body removal during spermatogenesis in *C. elegans* requires genes that mediate cell corpse clearance. *Developmental Cell* 2012;139:4613–22. doi:10.1242/dev.086769.
- [349] O'Donnell L, Nicholls PK, O'Bryan MK, McLachlan RI, Stanton PG. Spermiation: The process of sperm release. *Spermatogenesis* 2011;1:14–35. doi:10.4161/spmg.1.1.14525.
- [350] Chen Y, Wang H, Qi N, Wu H, Xiong W, Ma J, et al. Functions of TAM RTKs in regulating spermatogenesis and male fertility in mice. *Reproduction* 2009;138:655–66. doi:10.1530/REP-09-0101.
- [351] Chung W-S, Clarke LE, Wang GX, Stafford BK, Sher A, Chakraborty C, et al. Astrocytes mediate synapse elimination through MEGF10 and MERTK pathways. *Nature* 2013;504:394–400. doi:10.1038/nature12776.
- [352] Ul Quraish R, Sudou N, Nomura-Komoike K, Sato F, Fujieda H. p27(KIP1) loss promotes proliferation and phagocytosis but prevents epithelial-mesenchymal transition in RPE cells after photoreceptor damage. *Molecular Vision* 2016;22:1103–21.
- [353] Koriyama Y, Furukawa A. HSP70 cleavage-induced photoreceptor cell death caused by N-methyl-N-nitrosourea. *Neural Regen Res* 2016;11:1758–9. doi:10.4103/1673-5374.194721.
- [354] Iacovelli J, Zhao C, Wolkow N, Veldman P, Gollomp K, Ojha P, et al.

- Generation of Cre transgenic mice with postnatal RPE-specific ocular expression. *Investigative Ophthalmology & Visual Science* 2011;52:1378–83. doi:10.1167/iovs.10-6347.
- [355] Naito M, Terayama H, Hirai S, Qu N, Lustig L, Itoh M. Experimental autoimmune orchitis as a model of immunological male infertility. *Med Mol Morphol* 2012;45:185–9. doi:10.1007/s00795-012-0587-2.
- [356] Gery I, Wiggert B, Redmond TM, Kuwabara T, Crawford MA, Vistica BP, et al. Uveoretinitis and pinealitis induced by immunization with interphotoreceptor retinoid-binding protein. *Investigative Ophthalmology & Visual Science* 1986;27:1296–300.
- [357] Li N, Liu Z, Zhang Y, Chen Q, Liu P, Cheng CY, et al. Mice lacking Axl and Mer tyrosine kinase receptors are susceptible to experimental autoimmune orchitis induction. *Immunology and Cell Biology* 2015;93:311–20. doi:10.1038/icb.2014.97.
- [358] Wallet MA, Sen P, Flores RR, Wang Y, Yi Z, Huang Y, et al. MerTK is required for apoptotic cell-induced T cell tolerance. *Journal of Experimental Medicine* 2008;205:219–32. doi:10.1182/blood-2003-12-4302.
- [359] Wallet MA, Flores RR, Wang Y, Yi Z, Kroger CJ, Mathews CE, et al. MerTK regulates thymic selection of autoreactive T cells. *Pnas* 2009;106:4810–5.
- [360] Anderson EL, Baltus AE, Roepers-Gajadien HL, Hassold TJ, de Rooij DG, van Pelt AMM, et al. Stra8 and its inducer, retinoic acid, regulate meiotic initiation in both spermatogenesis and oogenesis in mice. *Pnas* 2008;105:14976–80. doi:10.1073/pnas.0807297105.
- [361] Berman ER, Segal N, Photiou S, Rothman H, Feeney-Burns L. Inherited retinal dystrophy in RCS rats: a deficiency in vitamin A esterification in pigment epithelium. *Nature* 1981;293:217–20.
- [362] Kruth HS, Fry DL. Histochemical detection and differentiation of free and esterified cholesterol in swine atherosclerosis using filipin. *Exp Mol Pathol* 1984;40:288–94.
- [363] Warburg O. The Metabolism of Carcinoma Cells. *The Journal of Cancer Research* 1925;9:148–63. doi:10.1158/jcr.1925.148.
- [364] Reiter CEN, Sandirasegarane L, Wolpert EB, Klinger M, Simpson IA, Barber AJ, et al. Characterization of insulin signaling in rat retina in vivo and ex vivo. *Am J Physiol Endocrinol Metab* 2003;285:E763–74. doi:10.1152/ajpendo.00507.2002.
- [365] Reiter CEN, Gardner TW. Functions of insulin and insulin receptor signaling in retina: possible implications for diabetic retinopathy. *Prog Retin Eye Res* 2003;22:545–62.
- [366] Sánchez-Chávez G, Peña-Rangel MT, Riesgo-Escovar JR, Martínez-Martínez A, Salceda R. Insulin stimulated-glucose transporter Glut 4 is expressed in the retina. *Plos ONE* 2012;7:e52959. doi:10.1371/journal.pone.0052959.

- [367] Crutzen R, Virreira M, Markadieu N, Shlyonsky V, Sener A, Malaisse WJ, et al. Anoctamin 1 (Ano1) is required for glucose-induced membrane potential oscillations and insulin secretion by murine  $\beta$ -cells. *Pflugers Arch - Eur J Physiol* 2015;468:573–91. doi:10.1007/s00424-015-1758-5.
- [368] Kambe T, Narita H, Yamaguchi-Iwai Y, Hirose J, Amano T, Sugiura N, et al. Cloning and characterization of a novel mammalian zinc transporter, zinc transporter 5, abundantly expressed in pancreatic beta cells. *J Biol Chem* 2002;277:19049–55. doi:10.1074/jbc.M200910200.
- [369] Kojima H, Fujimiya M, Matsumura K, Nakahara T, Hara M, Chan L. Extraprostatic insulin-producing cells in multiple organs in diabetes. *Proc Natl Acad Sci USA* 2004;101:2458–63.
- [370] Chen X, Larson CS, West J, Zhang X, Kaufman DB. In vivo detection of extrapancreatic insulin gene expression in diabetic mice by bioluminescence imaging. *Plos ONE* 2010;5:e9397. doi:10.1371/journal.pone.0009397.
- [371] Fu Z, Gilbert ER, Liu D. Regulation of insulin synthesis and secretion and pancreatic Beta-cell dysfunction in diabetes. *Current Diabetes Reviews* 2013.
- [372] LaVail MM, Yasumura D, Matthes MT, Yang H, Hauswirth WW, Deng W-T, et al. Gene Therapy for MERTK-Associated Retinal Degenerations. *Adv Exp Med Biol* 2016;854:487–93. doi:10.1007/978-3-319-17121-0\_65.
- [373] Shiao M-S, Liao B-Y, Long M, Yu H-T. Adaptive evolution of the insulin two-gene system in mouse. *Genetics* 2008;178:1683–91. doi:10.1534/genetics.108.087023.
- [374] Baumann I, Kolowos W, Voll RE, Manger B, Gaipl U, Neuhuber WL, et al. Impaired uptake of apoptotic cells into tingible body macrophages in germinal centers of patients with systemic lupus erythematosus. *Arthritis Rheum* 2002;46:191–201. doi:10.1002/1529-0131(200201)46:1<191::AID-ART10027>3.0.CO;2-K.
- [375] Perniok A, Wedekind F, Herrmann M, Specker C, Schneider M. High levels of circulating early apoptotic peripheral blood mononuclear cells in systemic lupus erythematosus. *Lupus* 1998;7:113–8.
- [376] Kluz J, Kopeć W, Jakobsche-Policht U, Adamiec R. Circulating endothelial cells, endothelial apoptosis and soluble markers of endothelial dysfunction in patients with systemic lupus erythematosus-related vasculitis. *Int Angiol* 2009;28:192–201.
- [377] Bijl M, Reefman E, Horst G, Limburg PC, Kallenberg CGM. Reduced uptake of apoptotic cells by macrophages in systemic lupus erythematosus: correlates with decreased serum levels of complement. *Ann Rheum Dis* 2006;65:57–63. doi:10.1136/ard.2005.035733.
- [378] Wong K, Valdez PA, Tan C, Yeh S, Hongo J-A, Ouyang W. Phosphatidylserine receptor Tim-4 is essential for the maintenance of

- the homeostatic state of resident peritoneal macrophages. *Pnas* 2010;107:8712–7. doi:10.1073/pnas.0910929107/-/DCSupplemental/sm01.avi.
- [379] Rodriguez-Manzanet R, Sanjuan MA, Wu HY, Quintana FJ, Xiao S, Anderson AC, et al. T and B cell hyperactivity and autoimmunity associated with niche-specific defects in apoptotic body clearance in TIM-4-deficient mice. *Pnas* 2010;107:8706–11. doi:10.1073/pnas.0910359107.
- [380] Zhang H, Liao X, Sparks JB, Luo XM. Dynamics of gut microbiota in autoimmune lupus. *Applied and Environmental ...* 2014.
- [381] Reeves WH, Lee PY, Weinstein JS, Satoh M, Lu L. Induction of autoimmunity by pristane and other naturally occurring hydrocarbons. *Trends in Immunology* 2009;30:455–64. doi:10.1016/j.it.2009.06.003.
- [382] Sverdrup B, Källberg H. Association between occupational exposure to mineral oil and rheumatoid arthritis: results from the Swedish EIRA case–control study. *Arthritis ...* 2005.
- [383] Dahlgren J, Takhar H, Anderson-Mahoney P, Kotlerman J, Tarr J, Warshaw R. Cluster of systemic lupus erythematosus (SLE) associated with an oil field waste site: a cross sectional study. *Environ Health* 2007;6:8. doi:10.1186/1476-069X-6-8.
- [384] Chowdhary VR, Grande JP, Luthra HS, David CS. Characterization of haemorrhagic pulmonary capillaritis: another manifestation of Pristane-induced lupus. *Rheumatology* 2007;46:1405–10. doi:10.1093/rheumatology/kem117.
- [385] Zhuang H, Han S, Lee PY, Khaybullin R, Shumyak S, Lu L, et al. Pathogenesis of diffuse alveolar hemorrhage in murine lupus. *Arthritis Rheumatol* 2017. doi:10.1002/art.40077.
- [386] Xu L-Y, Qi J-N, Liu X, Ma H-X, Yuan W, Zhao P-Q, et al. Tim-4 Inhibits NO Generation by Murine Macrophages. *Plos ONE* 2015;10:e0124771. doi:10.1371/journal.pone.0124771.
- [387] Hanayama R, Tanaka M, Miyasaka K, Aozasa K, Koike M, Uchiyama Y, et al. Autoimmune disease and impaired uptake of apoptotic cells in MFG-E8-deficient mice. *Science* 2004;304:1147–50. doi:10.1126/science.1094359.
- [388] Zamora MR, Warner ML, Tuder R, Schwarz MI. Diffuse alveolar hemorrhage and systemic lupus erythematosus. Clinical presentation, histology, survival, and outcome. *Medicine (Baltimore)* 1997;76:192–202.
- [389] Porres-Aguilar M, Mendez-Ramirez J, Eraso LH, Porres-Munoz M, Pema K. Diffuse alveolar hemorrhage as an initial presentation of systemic lupus erythematosus. *J Natl Med Assoc* 2008;100:1485–7.
- [390] Hochreiter-Hufford AE, Lee CS, Kinchen JM, Sokolowski JD, Arandjelovic S, Call JA, et al. Phosphatidylserine receptor BAI1 and apoptotic cells as new promoters of myoblast fusion. *Nature*

- 2013;497:263–7. doi:10.1038/nature12135.
- [391] Xiao C, Calado DP, Galler G, Thai T-H, Patterson HC, Wang J, et al. MiR-150 controls B cell differentiation by targeting the transcription factor c-Myb. *Cell* 2007;131:146–59. doi:10.1016/j.cell.2007.07.021.
- [392] Lakso M, Pichel JG, Gorman JR, Sauer B, Okamoto Y, Lee E, et al. Efficient in vivo manipulation of mouse genomic sequences at the zygote stage. *Proc Natl Acad Sci USA* 1996;93:5860–5.
- [393] Clausen BE, Burkhardt C, Reith W, Renkawitz R, Förster I. Conditional gene targeting in macrophages and granulocytes using LysMcre mice. *Transgenic Research* 1999;8:265–77.
- [394] Madison BB, Dunbar L, Qiao XT, Braunstein K, Braunstein E, Gumucio DL. Cis elements of the villin gene control expression in restricted domains of the vertical (crypt) and horizontal (duodenum, cecum) axes of the intestine. *J Biol Chem* 2002;277:33275–83. doi:10.1074/jbc.M204935200.
- [395] Owen KA, Abshire MY, Tilghman RW, Casanova JE, Bouton AH. FAK regulates intestinal epithelial cell survival and proliferation during mucosal wound healing. *Plos ONE* 2011;6:e23123. doi:10.1371/journal.pone.0023123.